STATICS AND DYNAMICS OF SUSPENSION BRIDGES

WITH NOTES ON SUSPENSION CABLES AND NETS

by

HASSAN IBRAHIM A. HEGAB

B.Sc.(1st Class Hons.), M.Sc.(Struct. Engrg.)

Submitted in fulfilment of the requirements for

the degree of

DOCTOR OF PHILOSOPHY IN CIVIL ENGINEERING

UNIVERSITY OF TASMANIA

HOBART, AUSTRALIA

JULY 1977

I declare that, except as stated therein, the thesis contains no material which has been accepted for the award of any other degree or diploma in any university, and that, to the best of my knowledge and belief, the thesis contains no copy or paraphrase of material previously published or written by any other person, except when due reference is made in the text of the thesis.

H.I.A. Hegab

Hassan Ibrahim A. Hegab

ACKNOWLEDGEMENTS

The writer is greatly indebted to his supervisors, Dr. M. S. Gregory and Dr. F. van der Woude, for their continuous guidance and encouragement.

Thanks are also due to the following persons of the University of Tasmania for their help and advice, and later for reviewing some chapters of the thesis:

Professor A.R. Oliver, head of the civil and mechanical engineering department;

Mr. E. Middleton, Dr. P.E. Doe, Dr. G.J. Walker, and Mr. B.F. Cousins, all senior lecturers in the faculty of engineering;

Mr. C. Wyld, director of the computing centre;

Messrs. I. Baldwin, T. Lucas, and B. Stiberc of the civil engineering workshop.

During almost three years, the writer corresponded with many of the suspension-bridge builders and analysts. Some of them helped by sending publications, others by their useful and constructive comments or by sending data and information without which the work could not have proceeded. Out of these, the writer wishes to record his thanks to the following persons:

Mr. D.W. Smith, of the University of Dundee, U.K.;

Professor T.M. Charlton and Mr. B.K. Drakeley, of the University of Aberdeen, U.K.;

Mr. C. Scruton, of the National Physical Laboratory (now retired), U.K.;

Mr. J.K. Anderson, Consulting Engineer, U.K.;

Emeritus Professor T. Fukuda, of the University of Tokyo, Japan;

Messrs. A. Hedefine, and L.G. Silano, Consulting Engineers, U.S.A.;

Mr. G.J. O'Hara, of the Naval Research Laboratory, U.S.A.

Also during writing the thesis, Professor D.V. Reddy of the Memorial University of Newfoundland, Canada, visited the University of Tasmania and gave valuable advice and comments.

Thanks are also due to Mrs. Stabb for her care in typing the thesis.

Finally, the writer wishes to express his deepest thanks to Dr. M.S. Gregory for offering a scholarship, and to the University of Tasmania for supporting it.

CONTENTS

PREFACE

A designer usually needs

(1) A preliminary design method which must be clear and short, suitable for a small computer; and

(2) A final design method which must be accurate enough and reliable, and usually relevant to the use of big computers.

Research workers are often interested mainly in mathematical aspects, while the designers' main interest is usually in the structural action and the real behaviour of the structure. A research worker uses mathematics, theories, and assumptions, in analysing his mathematical model, but a designer is always tending to use charts, tables, and codes of practice, or what are often called "established methods".

There is, thus, at times a big gap between the two, and it is hoped that this thesis helps in closing the gap and producing some link between the mathematical and the physical view points. This may be achieved by presenting simple methods of analysis for the design office.

* * * *

This thesis deals mainly with the statics and dynamics of suspension bridges. A short chapter on the dynamics of suspension cables and nets is also included.

Suspension bridges have been known, constructed, and used since prehistoric times. A review of the history of suspension bridges is presented in Chapter I.

The great majority of authors analyse the suspension bridge as a plane structure, as if it has a single cable and a very narrow deck with no torsional stiffness. The static analysis of such a "single-cable bridge" is presented in Chapter II, with analytical and experimental application on a laboratory model of a single-cable bridge. The chapter probes rather deeply into the development of methods of analysis, and, by trying out the various methods on the laboratory model, actually making the numerical calculations, brings out forcefully some important points both on the given methods and on the behaviour of suspension bridges. Real suspension bridges have, usually, two or more cables supporting a deck of some width. They act as a plane structure if they are loaded in such a manner that the deck flexes only, without twisting. However, in the case of torsional loadings, i.e. loadings which are asymmetric about the longitudinal centre line of the bridge, the single-cable bridge analysis is not valid.

The dynamic analysis of the "single-cable bridge" is dealt with in Chapter III. To test it out, in some detail, the flexibility matrix of the laboratory model was calculated (and measured), and an iterative procedure was implemented to get the first three modes of vibration for the dead

load, (D.L.), condition and also some live load, (L.L.), conditions. An estimate for the fundamental frequency was evaluated using Rayleigh's quotient. Measurements showed good agreement with calculations in most of the cases.

The iterative procedure is also used in the dynamic analysis of suspension cables and nets in Chapter IV.

In Chapter V, a simple, approximate, but adequate method for the analysis of the suspension bridge as a three-dimensional structure, is derived. It is, actually, an extension to Timoshenko's energy method of 1930. The method ignores the torsional stiffness of the towers, but this does not greatly affect the accuracy of the analytical results of our laboratory model since a separate tower has been provided for each cable. However, the resulting error is almost self-corrected if the extensibility of the main cables (and backstays) is considered.

Under flexural loading, the method reduces, automatically, to Timoshenko's method of 1930 for analysing the so-called "plane suspension bridge". But its use is in analysing the suspension bridges under torsional loads. Results obtained by this method gave reasonable, and rather encouraging agreement with direct measurements on the laboratory model.

Chapter VI gives full details of the results of the method as applied to a fairly realistic laboratory model. The flexibility matrix was calculated for the dead load condition and for two torsional loadings. The natural "flexural" and "torsional" frequencies and modes of vibration were determined. A simple and quick method for eigenvalue exonomization is suggested by the writer. The aim is to help the designer, especially in preliminary design.

Measurements on the model were taken for some of the natural frequencies and modes of vibration. The measurements favourably support the validity of the static and dynamic analyses (of Chapters V and VI), and the eigenvalue economization procedure.

Studies on the Newport bridge, (Ref. 7.7), showed that the torsional stiffness of the towers increases the torsional frequencies of the bridge by about 10%. This means that the present method of analysis is erring on the safe side by ignoring the torsional stiffness of the towers. The reason, as is clear from Chapter VII, is that the 10% increase in the torsional frequencies of the bridge increases the separation between torsional and flexural frequencies, and thus inhibits coupling, and increases the critical wind speed which causes flutter. The aerodynamic behaviour of suspension bridges, in general, is covered (to some extent) in Chapter VII.

* * * *

Chapter VIII presents a study of the design, construction and erection, and the economics of suspension bridges. Some repetition is involved between Chapters I (history) and VIII, and perhaps Chapter VII, for the sake of completeness. A method for the design of laboratory models and real bridges as well is also given in Chapter VIII.

A set of conclusions and recommendations is given in Chapter IX which ends the thesis. The references of the whole thesis are listed in Appendix A1, a list of notation is provided in Appendix A2, and abbreviations are listed in Appendix A3. Appendix A4 comprises some important notes on singular matrices.

CHAPTER I

HISTORICAL INTRODUCTION TO SUSPENSION BRIDGES

1.1 INTRODUCTION

There is much written on the history of suspension bridges.* Among the distinguished writers is Steinman who is one of the famous bridge builders and who played an important role in the development of methods of suspension-bridge analysis since early this century. Pugsley also is among the writers of the history of suspension bridges. He presented a good deal of theoretical (and some experimental) work on the statics and dynamics of suspension bridges, mainly at the middle of this century. A survey of some of his work, as well as some of the work of many others, is presented in his interesting book, (Ref. 1.3).

The following two sections deal with the history of both the construction and erection of, and the literature on, suspension bridges.

1.2 HISTORY OF CONSTRUCTION AND ERECTION

Primitive suspension bridges, made of bamboo, twisted lianas, creepers, or other similar materials, were found in China, India, Africa, and South America. Cables were anchored to posts set in the ground, or were tied round large trees or rock. In some of these primitive bridges, the roadway was directly resting on cables, where branches were cut and placed close together across the cables to form the roadway within a few hours. The result was a shaky structure, but it had sufficient strength and security to serve the needs of a primitive society.

Another type was the basket type, (with only one cable), in which the traveller carries a wooden saddle with a groove in it, and when he comes to a cable bridge, he fixes the cable into the groove, seats himself, and he is transported by natural gravitation to the opposite bank. On his return he is pulled up by ropes.

A third type was the suspended roadway type, provided with handrail cables. This type was similar to modern suspension bridges. The only modification in modern suspension bridges has been the discovery of better materials and the invention of improved machinery, which have rendered

---

* See References 1.1 - 1.7 , Appendix A1.

possible the bridging of spans of a new order of magnitude.

Iron was being made in India earlier than 1500 B.C., and its manufacture had followed the trade routes into China and was well established there by 600 B.C. In China, chain-suspended bridges had been in use since time immemorial. The first metal rope occurred in China when iron chains were used in building suspension bridges with, sometimes, masonry towers. Kircher, in 1667, described a bridge 200 ft span built by the Emperor Ming in A.D. 65 using 20 iron chains.

The Chinese practice of using at least four chains connected together transversely with smaller chains would ensure the continuous life of a bridge because defective links could be replaced when they failed without serious disruption of traffic and without appreciable risk since it would be unlikely that links in two different chains would fail together at the same cross-section, and it would not be catastrophic even if they did.

In 1632 a 200 ft span chain bridge over the Hwa Kiang River in China was built using 16 iron chains, and it is still existing.

Jakkula records that in 1515 a rope bridge was built across the Padus River in Italy. A rope suspension bridge was also built in 1569 across the Clain River.

The first European description of a suspension bridge was published by an Italian, F. Verantius, in 1607. He showed the hangers of wrought iron and described an all-iron suspension bridge.

The earliest reported iron chain bridge in Europe was at Glorywitz where one was built in 1734 across the Oder River. The first chain bridge in England was the Winch Bridge over the River Tees in 1741. It was a footbridge, 2 ft wide and 70 ft span, with the flooring supported directly on the chain cables in the primitive fashion. It stood for 61 years.

The first iron suspension bridge in North America was built in 1769 by Finley across Jacob's Creek in Pennsylvania (U.S.A.) using two iron chains, one on each side, to support a deck, 72 ft span and 13 ft wide. By 1810 the number of suspension bridges in U.S.A. built to the catenary principle, was already considerable. Of these, the 244 ft chain bridge over the Merrimac River (Massachusetts), built by Finley in 1809, is still in existence today, the chains having been replaced by parallel-stranded wires, and the timber towers were replaced by new reinforced concrete ones in 1909.

In 1808 Burr tried out timber cables on Mohawk Bridge (four spans, 225 ft each). The wooden cables were made of two-inch planks of Norway Pine, bolted together. The bridge deflected so much under traffic that it was converted into an eight-span bridge by building additional piers to support the centre of each of the original four spans. It was finally demolished in 1873, after 65 years in service.

* * *

The first cable suspension bridge was built in North America (Philadelphia) in April 1816 with a 408 ft span. It stood for only one year. In November 1816, a foot bridge 111 ft span was built in Scotland using iron wire cables. About the same time, Napier replaced the ropes in an existing suspension bridge with wire cables. In addition, he stiffened this bridge with stays radiating from the tops of the towers. The first major cable bridge in Europe was built at Geneva in 1823 by Dufour and Séguin with two spans 132 ft each. The tests carried out by Dufour revealed that drawn wires have a greater strength than wires of untreated or annealed material.

In 1814, Telford and Brown carried out experiments with chain bridges. In 1817, Brown patented his flat eyebar links, intended to replace the round and square rods then in use. He used modest masts, each of which was stabilised by two straight back-stays. Matching the angles of the back-stays were two more stays radiating from each mast to intermediate points on the main span.

In 1820, Brown built the Union Bridge over the Tweed River in England, 449 ft span and 18 ft wide. It was the first suspension bridge in Great Britain to carry loaded carriages. In this bridge, eyebars were used for the first time for its 12 main chains (six on each side). Its dip-span ratio was 1/15. It was reported, in November 1965, that it is still carrying a good deal of traffic between England and Scotland. At about the same time Messrs Smith built the Dryburgh Abbey suspension bridge over the Tweed, which contained the first use of auxilliary stays. Both these two bridges (over the Tweed) had suspended level floors, a feature of modern suspension bridges which was invented by Finley.

During the early 19th century, 40 bridges of Finley's design were erected throughout the U.S.A. A famous one of them was the Newburyport Bridge (Massachusetts) built in 1809 with 244 ft span, using 10 chains on each side. It stood for 100 years.

In 1823, Sir Marc Brunel used braced chains for the bridges of Bourbon Isle in France.

* * *

Telford became the leader of his age in building suspension bridges. He built the Menai Straits Bridge in Wales in 1826 with a record span of 580 ft and 24 ft wide, using four wrought-iron chains. The deck was of timber and there was no stiffening truss or any diagonal wind stays, and so it was repeatedly damaged by storms. In 1839 a heavier timber deck was built, and in 1893 a steel deck was installed and survived until 1939 when the four old wrought-iron chains were replaced by two chains of high tensile steel eye-bars.

Most of the suspension bridges built during the first decades of the 19th century had no bracing, and not a few of them have failed after a comparatively brief existence owing to the resonance vibrations caused by wind forces. The Union Bridge, for instance, was destroyed during a gale only six months after its completion. The long list of failures of suspension bridge decks raised the important task of devising a structure with stiff enough deck. James Dredge in 1832 was one of the pioneers in stiffening the roadway.

The Fribourg Bridge was built in 1834 by Chaley in Switzerland with a record span of 870 ft. It had four wire cables and stood for 90 years.

The second quarter of the 19th century is considered an era of suspension bridges in France, where an average of about one bridge per month was built in the period 1834- '41. In the year 1834 alone, 16 suspension bridges were built in France. No bridges of bar-iron were built, whereas this was the "golden age" of wire bridges, following Vicat's report of 1830. Vicat patented the air-spinning method in 1829 which has ever since been used, with few exceptions, for all cables made up of parallel wires.

Ellet was the first famous bridge builder to adopt the wire cables. He built the first wire cable bridge in America in 1842 with a span of 358 ft. In 1848 he built the first long-span wire-cable suspension bridge in the world at Wheeling over the Ohio River, 1010 ft main span with 12 wire cables, six at each side. After being destroyed by a storm in 1854 it was repaired and strengthened by Roebling. It is still standing and in use. A wire suspension bridge, 650 ft span, was also built in France in 1836 by Le Blanc.

* * *

The first railway suspension bridge built in England in 1830 over the Tees, with a span of 281 ft, had a very brief life. The deck sagged beneath the weight of the trains and rose in front of them. Within 11 years the bridge was literally torn into pieces by excessive bending. In 1840, Séguin built a railway suspension span of 137 ft in France with wire cables and 8 ft deep stiffening girders.

The first successful railway suspension bridge in the world was built by Roebling in 1855 across the Niagara with 821 ft span. For 43 years thereafter it carried progressively increasing weight, amounting in time to 2.5 times the original design loading. In this bridge, Roebling introduced a new method for constructing the wrought-iron cables with the separate strands consolidated into a compact cylindrical cable and then wrapped with softer wire for protection from the weather. Four main wire cables were used to support the two decks. The upper deck was 24 ft wide and the lower

one was 15 ft wide, and they were connected together on each side by trusses 20 ft deep. These formed, in effect, a stiffened box 24 ft wide by 20 ft deep; a splendid section to resist torsion. 64 diagonal stays were added above the box, mostly radiating down from the tops of the towers to the top deck, but some radiating outwards from the tower, at deck level, up to various points along the cables. Also 56 underfloor stays were anchored to the rocky cliffs.

In 1841, Roebling patented and made his first twisted, or stranded, wire ropes, which ensured uniform tension on all wires and on all strands of a rope. His cables were the first ones to have the continuous spiral wrapping advocated by Vicat. Roebling then conceived the idea of making parallel wire cables, which is used in most of the American suspension bridges today.

In 1847, Roebling said that it cannot be questioned that wire cables, when well made, offer the safest and most economical means for the support of heavy weights. He added that wire-cable bridges, properly constructed, will be found hereafter the most durable and cheapest railway bridges for spans over 100 ft and up to 1500 ft.

In 1851, Serrel built the Lewiston Bridge, 1043 ft span and 20 ft wide, and, in 1855, underfloor stays were added on Roebling's suggestion. The Ohio River Bridge was built by Roebling in 1867 with a span of 1057 ft centre to centre of the 230 ft high massive masonry towers.

In 1869, the first Niagara-Clifton Bridge was built below the falls by Keefer, with a record span of 1268 ft and a wooden deck only 10 ft wide. After a year or two the deck was rebuilt and the wooden stiffening chords and towers replaced by steel. The bridge was widened in 1888 and destroyed in a gale seven months later. It was replaced within a year but it was taken down eight years later as it was found not stiff enough to carry the new electric trolley cars that had come into use.

Steel in bridge-building was first used in constructing a chain suspension span of 312 ft at Vienna in 1828. The chains were fashioned of flat eye-bars of open-hearth steel.

* * *

The Brooklyn Bridge, at New York, is the first great modern suspension bridge. It was built by the Roeblings (father and son) in 1883 with a record span of 1595½ ft, and the radiating stays of John Roebling were also used. The bridge held its record as the longest suspension span for twenty years until it was surpassed in 1903 by the Williamsburg Bridge (1600 ft span), only 4½ ft longer than the Brooklyn Bridge. Then, in 1924, the Bear Mountain

Bridge was completed with a new record span of 1632 ft, which was, in turn, surpassed by the Philadelphia-Camden Bridge in 1926 with 1750 ft span, and, then, the Ambassador Bridge at Detroit in 1929 with a span of 1850 ft.

In one jump, only two years later, Ammann almost doubled the previous record of span with his giant stride of 3500 ft by building the George Washington Bridge (1931) to span the Hudson River at New York City, using four cables with straight backstays, and only 29 ft deep trusses to support the 120 ft wide deck. In 1962 a second deck was added. (Note: The author has been told privately that this famous bridge has proved too flexible and connections are failing by fatigue. Measures are being taken to try to stiffen it, a most formidable task.)

Engineers again pushed their way forward with the Golden Gate Bridge (4200 ft span) in 1937, and then Ammann's Verrazano Bridge in 1964 with 4260 ft span.

* * *

The first Tacoma Bridge was built in 1940, with, at its time, the third longest suspension span in the world (2800 ft). It was only 39 ft wide (1/72 of the span L)*, and plate girders only 8 ft deep (L/350). Being very slender, it was completely destroyed four months later by wind due to its unanticipated "aerodynamic instability", although the wind force was only 10% of the static wind force which was quite safe. In 1950, the second Tacoma Bridge was built with the same span, but using open-web stiffening trusses, 33 ft deep (L/85) instead of the 8 ft solid plate girders used in the former. The width centre to centre of the cables is 60 ft (L/47) compared with 39 ft in the first bridge.

The longest self-anchored suspension bridge ever built was the Cologne-Mülheim Bridge over the Rhine with 1032 ft span. It was built in 1938 and destroyed at the end of the war in 1945. The longest existing self-anchored suspension bridge in the world is the Paseo Bridge, over the Missouri River, at Kansas City. It has a 616 ft main span and two side spans 318 ft each, and it was completed in 1954. In a self-anchored suspension bridge, a strut is built (usually a deck level) between the two anchorages, which relieves them of any horizontal pull.

In Europe, the most famous modern suspension bridges are the Forth Road Bridge in England, built in 1964 with a main span of 3300 ft, and the Severn Bridge (1966) with a main span of 3240 ft and a tubular deck. In Turkey, the Bosporus Bridge was completed in 1973 with a tubular deck and a main span of 1074 m (3524 ft). The huge Humber Bridge is now being built in England with 1.4 km span (7/8 of a mile ≃ 4600 ft).

---

* See Appendix A2: Notation.

In 1894, in a report by the Board of U.S. Engineers the maximum span practicable for a wire suspension bridge was estimated as 4335 ft with a unit stress in the cable of 60,000 psi (=413 Mpa)*. With the discovery of better materials, and the invention of new materials, a working stress of 700 Mpa could be used for the cables of the Severn Bridge in 1966.

In his "Bridges and their Builders", in 1957, Steinman said: "The decades immediately ahead will see the realization and the construction of other bridges of even greater spans. Fifty years ago, the feasibility of a span of 3000 ft was seriously questioned. Now bridge engineers confidently agree that suspension bridge spans as long as 10,000 ft are practically feasible. And such spans will be built"**.

Steinman was the builder of the Mackinac Straights Bridge at Michigan in 1958, with a main span of 3800 ft, which is now the third longest suspension span in the world (exceeded only by the Golden Gate Bridge built in 1937 (4200 ft) and the Verrazano Bridge (4260 ft)built in 1964).

1.3 HISTORY OF LITERATURE AND THEORIES

The first European description of a suspension bridge was published by an Italian, F. Verantius, in 1607. His "Machinae Novae" included a description of a portable suspension bridge with a horizontal floor connected to cables by vertical hangers.

In 1794, Fuss developed the theory of the parabolic cable supporting a load that was uniform along the span.

In an article in "The Portfolio" in 1810, Finley described his stiffened suspension bridge, claiming that "in 1801 I erected the first bridge on this construction over Jacob's Creek". Pope's "Treatise on Bridge Architecture" in 1811 spread Finley's "ingenious invention" all over the world.

In 1823, Navier published in Paris his "Rapport et Mémoire sur les Ponts Suspendus" in which he analysed the effects of changes of temperature and other factors on cables and platforms. This was the pioneer work which dominated the theory of suspension bridges for a long time. It was followed in 1824 by Séguin's "Des Ponts en Fil de Fer". In his "Résumé des Leçons données à l'Ecole des Ponts et Chaussées", published in 1826, Navier initiated the modern theory of arches and applied it to the design of a suspension bridge over the Seine in Paris, partly constructed in 1831 and later abandoned.

In 1826, Provis published a complete report upon the construction of Telford's Menai Bridge. In the same year, D. Gilbert read a paper before the Royal Society "on the Mathematical Theory of Suspension Bridges with

---

* See Ref. 1.8, pp. 10-11.

** See Ref. 1.6, p. 371.

Tables for Facilitating their Construction", which dealt with the ordinary catenary and also the catenary of equal strength.

Vicat completed his masterly report on the air-spinning methods in 1830, and it was published the following year in "Annales des Ponts et Chaussées". In 1834, he published another Report on "The Progressive Lengthening of Iron Wire Submitted to Various Tensions", and he became the first man to notice and investigate creep.

Pasley, in 1839, submitted a memorandum to the Institution of Civil Engineers, ICE*, in which he said: "The injuries to the roadways of suspension bridges, are owing to the violent action of the wind from below". This proved to be true, to some extent, a hundred years later after the failure of the first Tacoma Bridge in 1940. Pasley's memorandum was followed by another paper by Provis in 1841 on repairs to the Menai Bridge, which was followed by a lively discussion at the ICE. In the same year (1841), Rendel delivered his "Memoir of the Montrose Suspension Bridge" to the Institution, in which he described the measures he had adopted.

The first paper "on the Vibration of Suspension Bridges and other Structures; and the Means of Preventing Injury from this Cause", was published in 1841 by John Russel, in the Transactions of the Royal Scottish Society of Arts, in which he discussed "the general nature of the vibrations that destroy suspension bridges and other slender structures".

In 1846, Roebling published his first report on his Ohio River Bridge (of 1867), and in 1856 there followed another report on its practicability and probable cost. In 1855, he presented his final report, on the Niagara Railway Bridge (of 1854), which was a masterly summary of the concepts underlying the success of the first large railway suspension bridge.

* * *

The fact that the response of a heavy suspension cable, without any stiffening girder, under a concentrated load is non-linear was well known in the first half of the 19th century. The mathematical expression of this non-linearity, however, did not appear in general form till the publication of an approximate analysis by an unknown author in 1862, (Ref. 1.9).

In 1868, Bender read a paper to the American Society of Civil Engineers, ASCE, in which he traced successive improvements to suspension bridges. Bender credited Finley with his first regular suspension bridge across Jacob's Creek in 1796, although, in his first article (of 1810), Finley himself said that it was in 1801.

---

* See Appendix A3: Abbreviations.

Rankine's books, on Applied Mechanics (1858) and Civil Engineering (1863), presented the combination of cable (for direct stress) and stiffening girder (for bending). He produced his approximate theory, for two and three-hinged stiffening girders, that has been used so much ever since. By assuming that any concentrated load was spread by the girder uniformly across the whole span on to the cables, he produced the first rational theory of the interaction of cable and girder.

In 1880, Clericetti published a paper in the proceedings of the ICE, on "The Theory of Modern American Suspension Bridges", which was followed in 1881 by another paper by Bender on "The Combined Action of an Elastic Beam Suspended from an Elastic Cable". By 1886, in a paper by Lévy in the Annales des Ponts et Chaussées, the essential ingredients of the approximate elastic theory were crystallised. By 1922, the elastic theory of today was standardised by Steinman, (Ref. 1.7).

* * *

The first non-linear theory of suspension bridges was evolved by Melan in a comprehensive review of existing knowledge, published in 1888, in which the change of shape under a concentrated load and the corresponding change of the tension in the chain were considered. This was refined and presented in practical form in his "Handbuch der Ingenierurwissenschaften" in 1906, which was translated into English by Steinman in 1913, (Ref. 1.10).

The first application of this deflection theory of Melan was, by Moisseiff, in the computations for the Manhattan Bridge which was completed in 1909 with a span of 1470 ft. It was then used in the design of many other American bridges like Ammann's George Washington Bridge in 1931 (3500 ft span) and Strauss's Golden Gate Bridge in 1937 (4200 ft span).

Rankine's method was, of course, itself so simple as to be a direct design method without modification. With the development of the elastic method, however, greater complexity was introduced which Steinman simplified by the diagrams and tables in his standard book, (Ref. 1.7), in which he set a system of coefficients and charts for the design of suspension bridges. He used a non-dimensional stiffness factor, S, in the form

$$S = (1/L).\sqrt{EI/H_o} \qquad (1.1)$$

where L is the span, EI is the bending stiffness of the girder, and H_o is the initial horizontal component of the cable tension (due to the dead load condition). This stiffness factor had been used before at the end of the

last century by Godard, (Ref. 1.11), in the form

$$(1/S) = L. \sqrt{H_o/EI} \qquad (1.2)$$

and, after that, it has been widely used by Southwell, (Ref. 1.12), and many others.

Castigliano's work, in 1879, on arches in terms of his energy theorems, led gradually to the restatement of the arch-like theory of suspension bridges in the energy form given by Johnson, Bryan, and Turneaure in their comprehensive text book on "Modern Framed Structures", (Ref. 1.13), first published in 1893. The first English text-book to include a summary of this elastic theory was by Pippard and Baker in 1936.

In 1894, Godard, (Ref. 1.11), proposed a linearisation of Melan's deflection theory both for its simplification and for the advantages that it gave, by making the use of superposition and influence lines legitimate. With more experience of the deflection theory and its application to bridges of longer and longer spans, the linearised theory became increasingly valuable and relevant.

In 1911, Steinman published his first book "Suspension Bridges and Cantilevers - Their Economic Proportions and Limiting Spans".

In his 1930 paper, (Ref. 1.14), Timoshenko showed how the basic differential equation of the deflection theory could be solved by the use of Fourier trigonometric series, and potential and strain energy analysis. And in 1933, Ammann published a paper in the Transactions of the ASCE describing his George Washington Bridge, in which he pointed out that the stiffening girders had been designed according to Melan's deflection theory which obviated the need for empirical proportioning.

H. Bleich, in 1935, showed that linearisation of Melan's treatment was possible without undue error and led to considerable computative simplification. Accepting this for the large span bridges of today, in which the cable plays the major structural part, Pugsley, (Ref. 1.15), in 1949 suggested the treatment of the suspension bridge in terms of two structures, one the cable and the other the stiffening girder, by matching their deflections, both vertical and horizontal (if necessary), by finite tables of influence or flexibility coefficients. Only nine stations across the span were found adequate to give reasonable accuracy. This method was used for the analysis of the stresses during the erection of both the Forth and Severn bridges, while the Relaxation method has been used for their design, (Ref. 1.3).

In 1939, Hardesty and Wessman produced their preliminary design method for suspension bridges. In the same year (1939), Southwell, (Ref. 1.12), showed how the differential equation of the deflection theory could be

treated using the Relaxation Process. By his process, allowance could be made, for the first time, for the calculations of the horizontal displacements, from vertical, of the hangers. This was followed in 1946 by Crosthwaite's paper, (Ref. 1.16), which showed how the Relaxation Method could be applied in practice (in the preliminary design calculations for the then proposed Severn Bridge).

F. Bleich, following the linearised deflection theory, in 1950, could discuss the natural frequencies and modes of vibration of suspension bridges.

In 1952, '53, '62, Pugsley called the attention of suspension bridge designers to the real structural action of their structures, including its "gravity stiffness", the stiffness produced by its own weight. He succeeded in treating the stiffening girder, approximately, as an elastic beam on a linear foundation provided by the cable. This simple and basic method was analysed by Charlton, (Refs. 1.17 and 1.18), using both potential and complementary energy treatments, the aim being to give designers reliable approximate computations of the main effects. The latter was modified by Hegab in 1975, (Ref. 1.19), to give the same equations of Pugsley's method of 1949, (Ref. 1.15).

The collapse of the first Tacoma Bridge in 1940, as a result of excessive torsional oscillations in transverse wind of only 42 m.p.h., led the engineers to study and understand the aerodynamic instability problems. Large model experiments have been made in England, America, and Japan by many authors, (Refs. 1.20 - 1.24).

As a result, it has been found that the gravest oscillations can be largely prevented by proper aerodynamic measures applied to the deck and girders of the bridge.

The first published torsion analysis of suspension bridges was presented in 1957 by Sih, (Ref. 1.25). This was followed in 1975 by a paper by Fukuda, (Ref. 1.26). A potential energy analysis has been derived by the writer and will be discussed in detail in Chapter V.

In a recent paper, Van der Woude, (Ref. 1.27), analysed the single-cable bridge problem with an energy analysis using the calculus of variations to validate the energy equations.

CHAPTER II

SINGLE-CABLE BRIDGE: STATICS

2.1 INTRODUCTION

The analysis of the suspension bridge as a single-cable bridge dominated the methods of solution of suspension bridges, both in this century and the previous century as well. It has been dealt with by many authors and using several theories and procedures (Refs. 2.1 - 2.7)*. In this chapter, a number of these methods will be applied in the analysis of a realistic laboratory model of a single-cable bridge. The aim is to bring out the history of the development of various theories and simplifications which came into use. This can best be done by making calculations with them and checking the results against measurements. The results are illuminating, and add greatly to appreciation of the action of a suspension bridge. The term "single-cable bridge" means a suspension bridge loaded symmetrically with respect to its longitudinal centre line.

2.2 MODEL DESCRIPTION

Although it could have been a model with two cables loaded symmetrically about its longitudinal centre line, the model used herein was made using only one structural cable to support its narrow deck, by means of nine equidistant vertical hangers, at its longitudinal centre line, Fig. 2.1. The horizontal component of the cable tension, H, for any loading condition is measured by means of a double lever system to which the end of one of the back-stays is anchored. The bending stiffness, EI, of the deck was obtained from a direct bending test on a deck specimen. The effective cable stiffness was measured using a cable specimen loaded and unloaded a few times within the elastic range, (Ref. 2.8). The initial cable shape is assumed to be parabolic under the dead load, D.L., with unstressed deck; i.e. under the action of D.L. only, the deck is assumed to carry no load or bending while all the D.L. is carried by only the main cable. The model was very carefully set up to attain this assumed condition.

---

* See also Refs. (1.7, 1.10, 1.12, 1.14 - 1.18, 1.27).

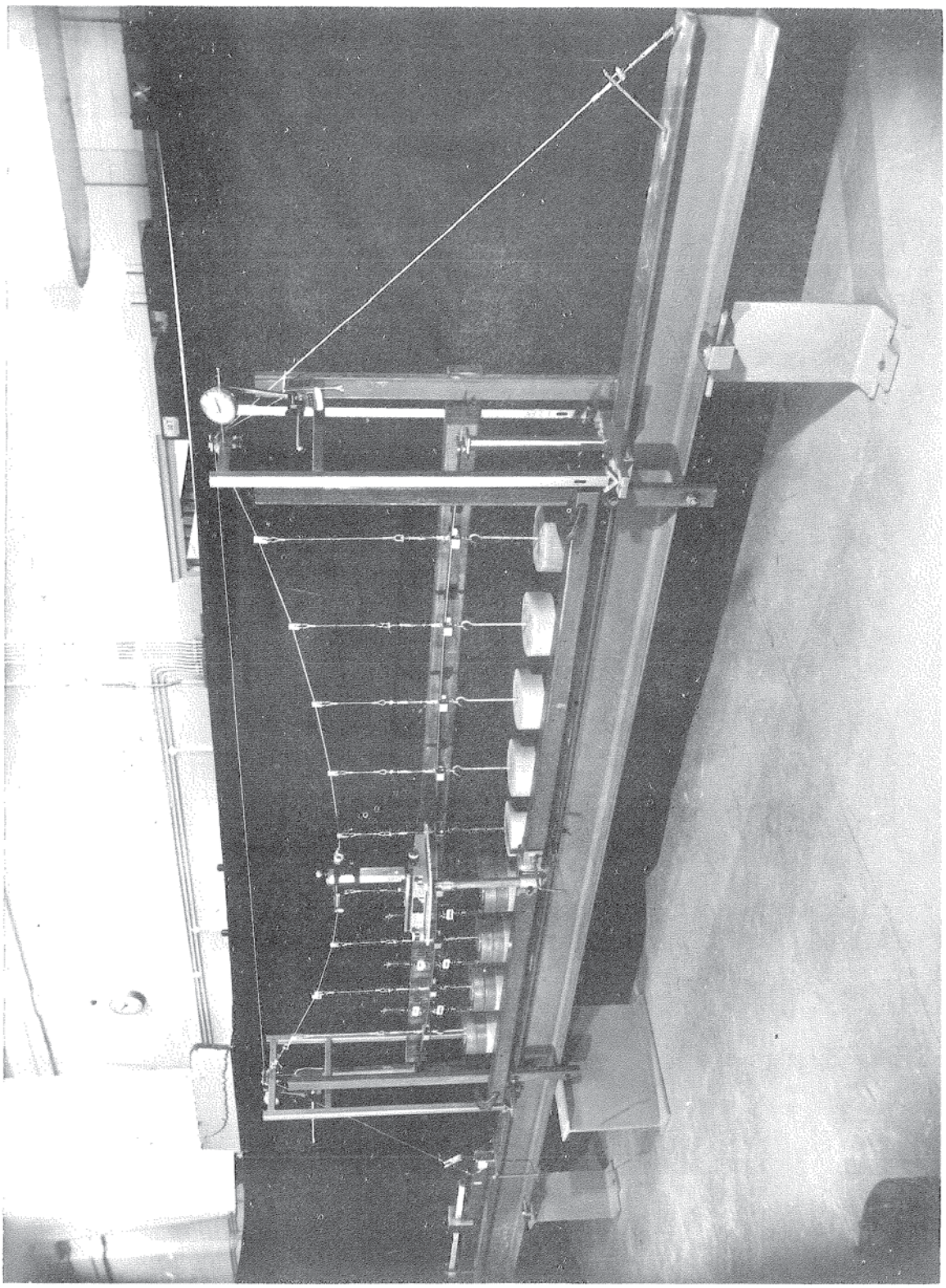

Fig. 2.1 (a) Laboratory Model of the Single-Cable Bridge.

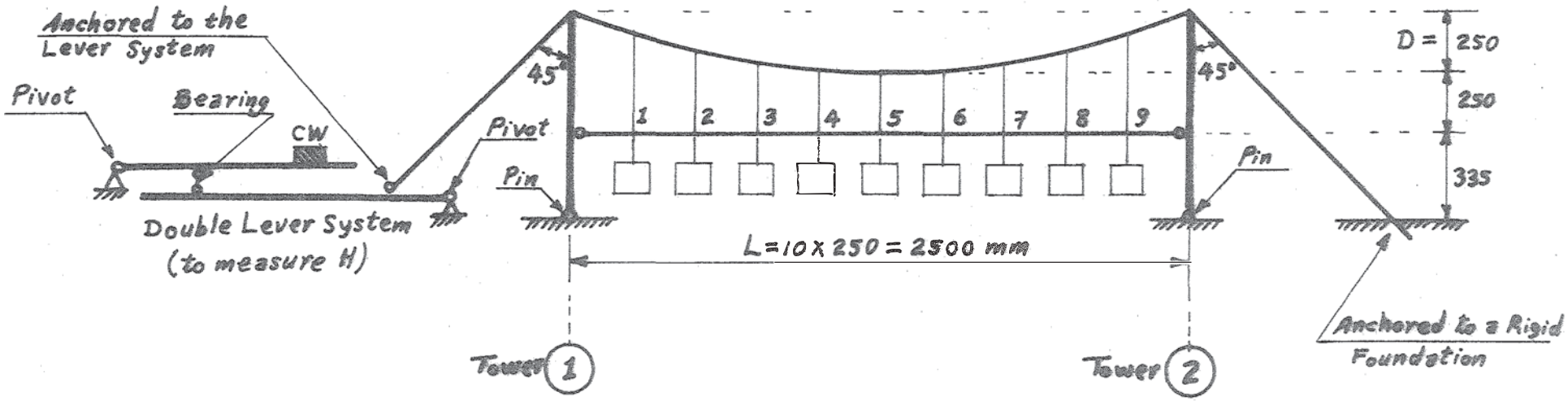

No. of Hangers = 9
D.L. Per Station = 78.5 Newtons
Dip - Span Ratio = 1 : 10
Effective AE = 500×10^3 Newtons

EI = 12.5 $N.m^2$
H_o = 985 Newtons
CW = Counter Weight

Fig. 2.1 (b) Diagrammatic Sketch for the Laboratory Model of the Single-Cable Bridge.

2.3 AN IDEA ABOUT THE BEHAVIOUR OF THE MODEL

Some preliminary tests have been carried out to investigate the response of the model to live load, L.L. Regarding the cable tension, an increasing point-load was applied at various stations, one at a time, (Fig. 2.2-a). Another loading condition was to start by loading station 1 only, and then extend the load to adjacent stations until loading all the stations with an increasing load, (Fig. 2.2-b). Fig. 2.2 shows that the increase in the horizontal component of the cable tension is, nearly, linearly proportional to the live load, an approximation that has been used before by Timoshenko, (Ref. 1.14).

As for the deflections, an increasing point-load was moved on the bridge deck and both the vertical and horizontal deflections of all the stations were measured using a two-way microscope moving across the whole span, close to the cable joints. (Actually, the hangers of the laboratory model are so "rigid" that their extensions are nearly negligible, a case in which it can be said that the vertical deflection of the cable is equal to that of the deck at the same distance in the spanwise direction.) Fig. 2.3 shows plots of the deflections (in both the vertical and the horizontal directions) due to a point-load travelling across the span. The terms v_{ij}, u_{ij} represent respectively the vertical and the horizontal displacement of point i due to a point-load, P, acting vertically at j.

The general conclusions, out of this preliminary study, can be summarized as follows:

(i) The horizontal component of the cable tension, H, is almost linearly proportional to the L.L., whether it is uniformly distributed over the entire span or a part of it, or even if it is a single concentrated load acting at any position.

(ii) The deflections (both vertically and horizontally) are, generally, non-linear with the load, and the structure tends to stiffen as the load increases.

2.4 METHODS OF ANALYSIS

In this section, the single-cable bridge model will be analysed using a few of the previous theories with some modification, by the writer, whenever it seems to be relevant. A comparison between measurements and calculation will accompany each method.

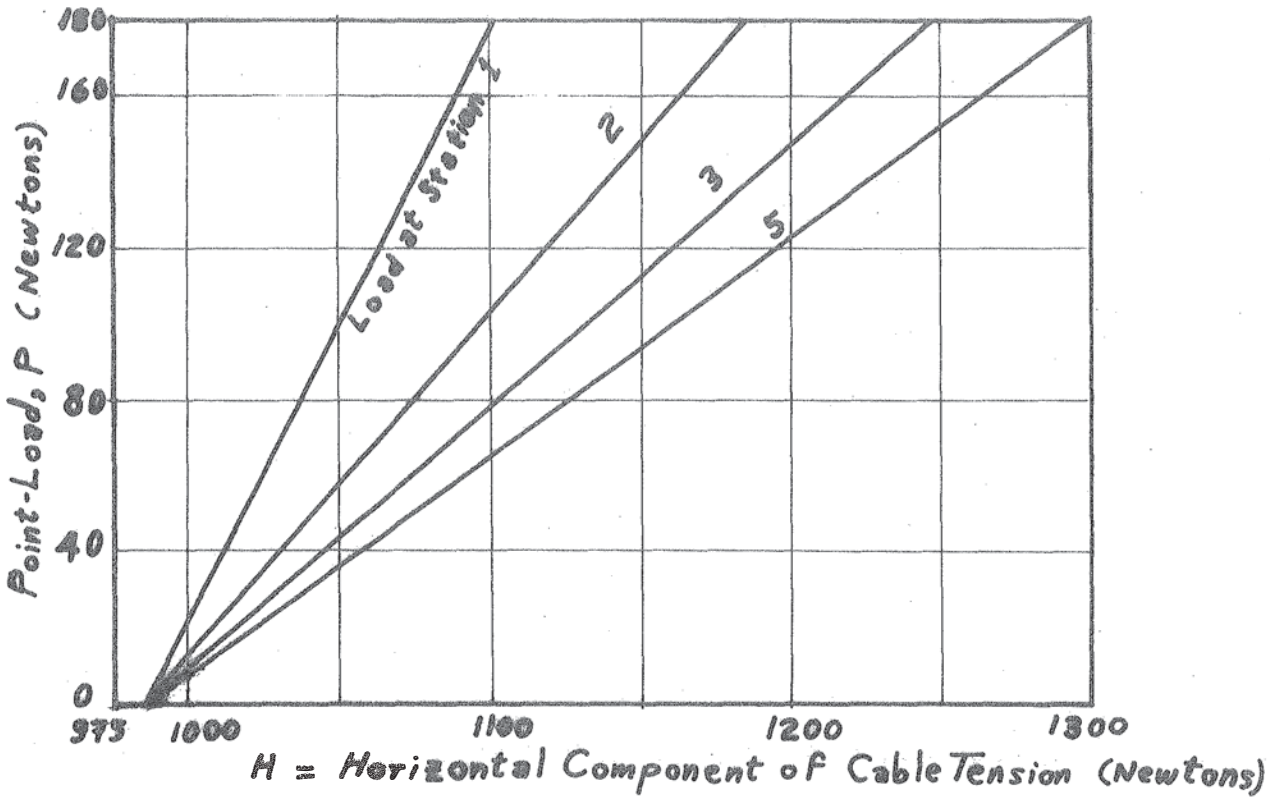

(a) One Point-Load.

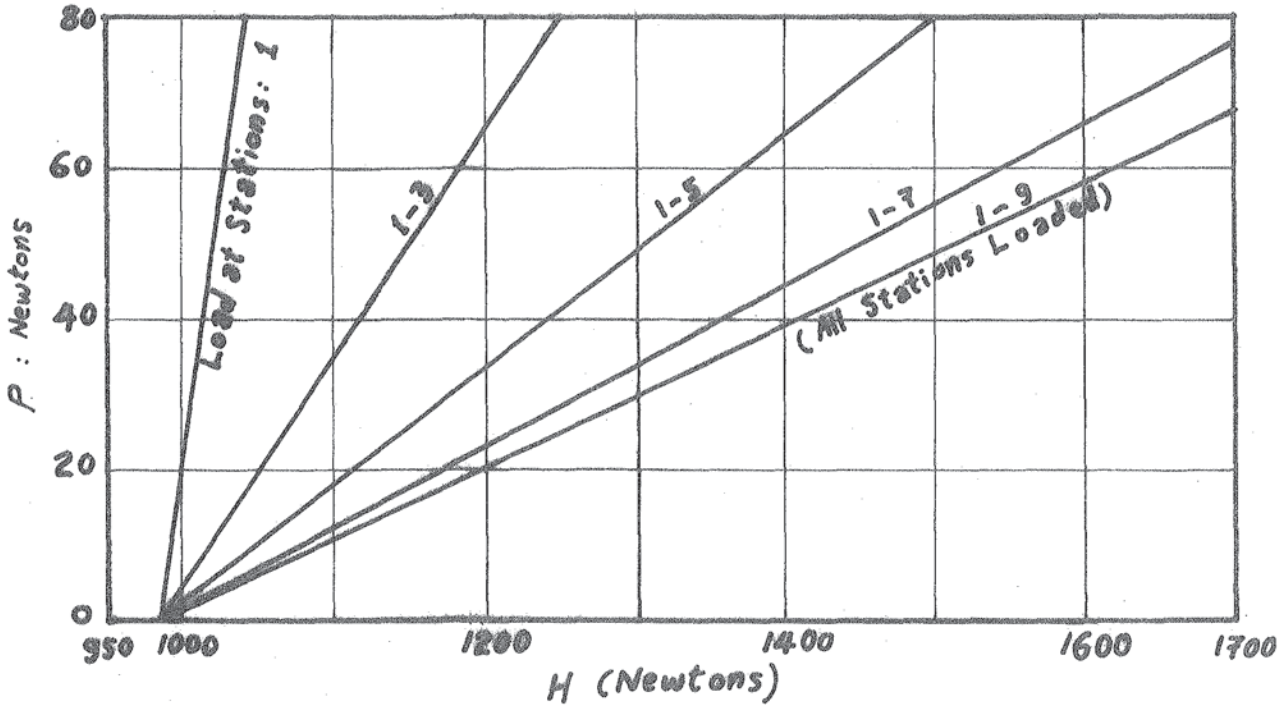

(b) Several Point-Loads.

Fig 2.2.-- Variation of Measured H with Loading.

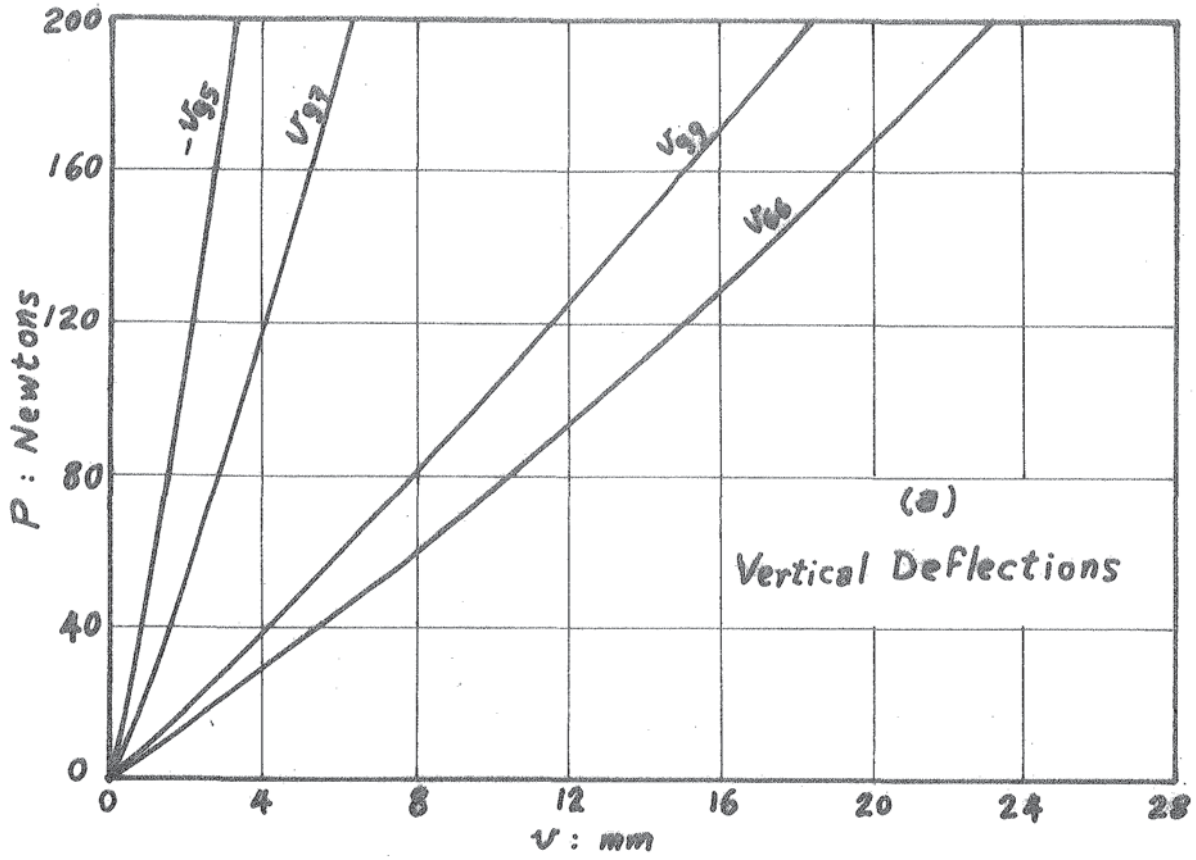

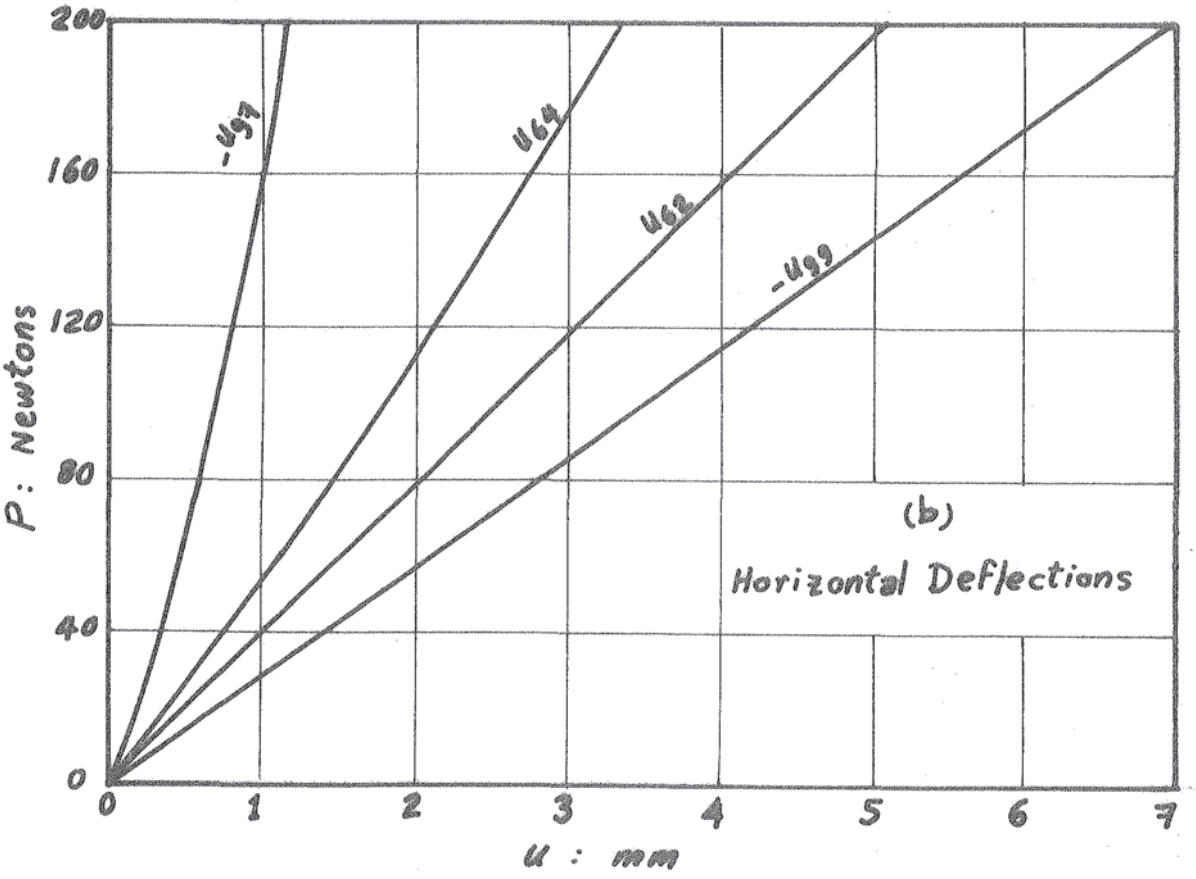

Fig. 2.3.- Variation of Measured Deflections with a Point-Load.

2.4.1 THE DEFLECTION THEORY OF MELAN, (Refs. 1.3, 1.7, 1.10, 1.13)

This is the first non-linear theory of suspension bridges, in which the change of shape under loading, and the corresponding change of the tension in the cable were considered.

The bending moment, M, in the stiffening girder is given by

$$M = m_o - h.y - (H_o + h).v \qquad (2.1)$$

where m_o = bending moment due to the L.L., p, on the girder when treated as isolated and simply supported at its ends;

h = increment, due to the L.L., p, in the horizontal component of the cable tension;

y = the co-ordinate of a cable point, distance x from the left end of the span, with the x-axis being the chord joining the two cable ends, Fig. 2.4;

H_o = horizontal component of the cable tension, D.L. condition; and

v = increment, in y, due to the live load p
= vertical deflection of the cable at distance x.

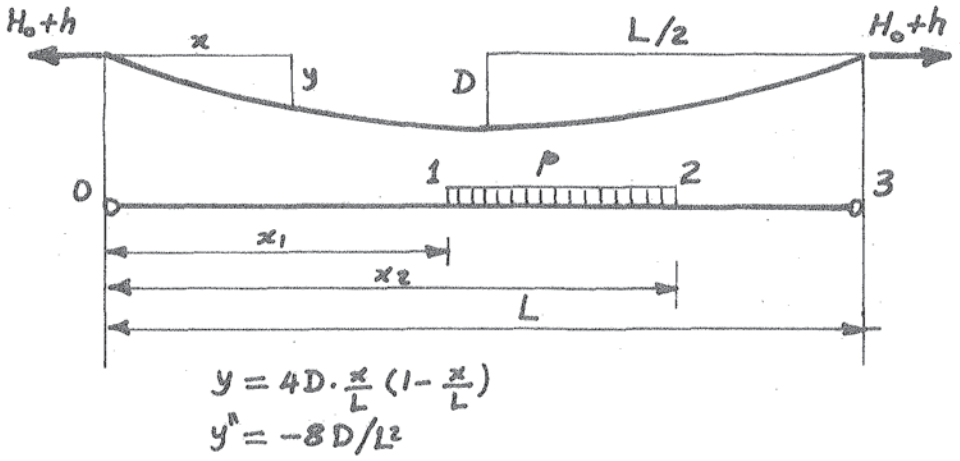

Fig. 2.4.

Using the approximation $d^2v/dx^2 = M/EI$, Eq. 2.1 can be written in the form

$$\frac{d^2v}{dx^2} = \frac{c^2}{H_o + h}(m_o - hy) - c^2v \qquad (2.2a)$$

where $c^2 = \dfrac{H_o + h}{EI}$ (2.2b)

Eq. 2.2a is a second order differential equation, D.E., in v, which may be directly solved provided h is known, or can be found. The solution gives

$$v = \frac{h}{H_o + h}[C.e^{cx} + C'.e^{-cx} + (\frac{m_o}{h} - y) + \frac{1}{c^2} \cdot \frac{d^2}{dx^2}(\frac{m_o}{h} - y)] \qquad (2.3)$$

where C and C' are integration constants which are to be found from the boundary and the continuity conditions.

Substituting Eq. 2.3 in Eq. 2.1, the bending moment M, in the stiffening girder becomes

$$M = -h[C.e^{cx} + C'.e^{-cx} + \frac{1}{c^2}.\frac{d^2}{dx^2}(\frac{m_o}{h} - y)] \qquad (2.4)$$

The D.E. of the suspension bridge can also be written in the form*

$$EI.\frac{d^4v}{dx^4} - (H_o + h).\frac{d^2v}{dx^2} = p + h.\frac{d^2y}{dx^2} \qquad (2.5)$$

which is a 4th order D.E. in v, that can be solved to give the same solution as in Eq. 2.3. It can also be considered as a 2nd order D.E. in M as

$$\frac{d^2M}{dx^2} - c^2M = p + h.\frac{d^2y}{dx^2} \qquad (2.6)$$

which when solved gives the same solution previously given in Eq. 2.4.

We come now to the number of the constants of integration C, and C'. If the whole span is uniformly loaded, all through, by a load, p, the number of these constants is two, namely C_1 and C_1'. If only a part of the span is loaded, or if the span is loaded with loads of different intensities, the span is divided into zones on each of which the load is either uniform or zero. For example, in the case shown in Fig. 2.4, we have three zones, and so we have six constants of integration, for which six boundary, or continuity, conditions are needed.** The boundary conditions are provided by knowing the deflections (or the moments) at both ends of the span if Eq. 2.3 (or Eq. 2.4) is used (respectively). The continuity conditions are provided by matching the deflections and the slopes (or the bending moments and the shear forces) to the left and the right of both points 1 and 2, if Eq. 2.3 (or Eq. 2.4) is used (respectively). Whether Eq. 2.3 or Eq. 2.4 is used, the six constants are the same. These

---

* See Refs. 1.3, 2.9.

** Generally, the number of the constants of integration is always twice the number of zones to which the span is to be divided, i.e. two constants for each zone.

constants have been evaluated by the writer, and by Steinman before (Ref. 1.7). They can be written in the form

(i) For Zone 0-1 $(o \leqslant x \leqslant x_1)$

$$C_1 = \frac{1}{c^2}\left[\frac{\frac{p}{2h}\left[e^{c\{L-(x_1+x_2)\}}+e^{-c\{L-(x_1+x_2)\}}-e^{c(L-x_1)}-e^{-c(L-x_1)}\right]-(8D/L^2)(1-e^{-cL})}{e^{cL}-e^{-cL}}\right] \tag{2.7a}$$

$$C_1' = -C_1 - \frac{1}{c^2}(8D/L^2) \tag{2.7b}$$

(ii) For Zone 1-2 $(x_1 \leqslant x \leqslant x_2)$

$$C_2 = C_1 + \frac{1}{c^2}\cdot\frac{p}{2h}\cdot e^{-cx_1} \tag{2.7c}$$

$$C_2' = -C_1 + \frac{1}{c^2}\left(\frac{p}{2h}\cdot e^{cx_1}-(8D/L^2)\right) \tag{2.7d}$$

(iii) For Zone 2-3 $(x_2 \leqslant x \leqslant L)$

$$C_3 = C_1 + \frac{1}{c^2}\cdot\frac{p}{2h}(1 - e^{-cx_2})\cdot e^{-cx_1} \tag{2.7e}$$

$$C_3' = -C_1\cdot e^{2cL} - \frac{1}{c^2}\left[\frac{p}{2h}\cdot e^{c(2L-x_1)}\cdot(1-e^{-cx_2}) - (8D/L^2)e^{cL}\right] \tag{2.7f}$$

Eqs. 2.7 give the other five constants in terms of the first one, a method that has been used before by Pugsley, (Ref. 1.3), in his four-constants' problem. Steinman, (Ref. 1.7), gives the second constant in each pair in terms of the first one of the same pair, which, in turn, is evaluated using only the dimensions and the properties of the structure.

The constant C_1 seems to be small, and it is, actually, very small for the laboratory model, while the constants C_2 and C_3 are very much smaller. On the other hand, the constants C_2' and C_3' are very big, especially C_3' which is very large. It can thus be noticed from both Eqs. 2.3, 2.4 that the small coefficients C are multiplied by big quantities, e^{cx}, while the big coefficients C' are multiplied by small quantities e^{-cx}.

For our laboratory model, using either Pugsley's or Steinman's method of evaluating the integration constants, it has been found that each pair of constants C and C' has the same sign for both the first and the second zones (negative sign for Zone 0-1, and positive sign for Zone 1-2), while in the third zone (Zone 2-3) they have different signs (C_3 is a very small negative number, and C_3' is a very big positive number).* Here a very serious case of ill-conditioning arises, which makes it impossible to get the solution for the third zone. However, the solution, for the third zone, could be obtained starting from the right (with the origin at the right end of the span), thus having the wanted zone (Zone 2-3) as the first zone which is solved with no problems. The designers of old bridges, like the Manhattan Bridge, for instance, did not face such trouble because of the high stiffness of their decks. The ill-conditioning of the traditional solution of the deflection theory at the third zone is related, actually to two factors:

(i) the stiffness of the deck;

(ii) the form of the integration constants, or the method of their derivation.

Regarding the stiffness of the deck, the laboratory model itself is well-conditioned, because everything could be measured easily and properly. However, it has been found that if the stiffness of the deck is, theoretically, increased by 50% (or more), the analysis becomes well-conditioned. Fig. 2.5 gives a measure of ill-conditioning represented by the ratio $v_{2r}/v_{2\ell}$ versus the non-dimensional parameter $EI/H_o L^2$, where v_{2r} is the vertical deflection of point 2 calculated from Zone 2-3; $v_{2\ell}$ is the vertical deflection of the same point calculated from Zone 1-2; (these two values must be equal as it was put in the continuity condition at point 2 in getting the integration constants).

As for the form of the integration constants, the problem has been carefully investigated by the writer, and the following results were obtained. Steinman's way of writing the constants gives

$$C_3' = -e^{cL}(C_3 \cdot e^{cL} + (8D/c^2L^2)) \qquad (2.7f.1)$$

It has been found that the two terms in brackets in Eq. 2.7f.1 are very close and have opposite signs. Bearing in mind that C_3 is very small and e^{cL} is very big, the product $(C_3 \cdot e^{cL})$ is not, then, reliable.

---

* Thus, it becomes improper to calculate C_3' in terms of C_3 (as Steinman, (Ref. 1.7) did). It is not recommended, even, to calculate C_3' in terms of C_1 (as Pugsley, (Ref. 1.3) did), since C_1 also is small and may be beyond the accuracy of the computing device. However, the best way is to get all the constants, only in terms of the dimensions and the properties of the structure.

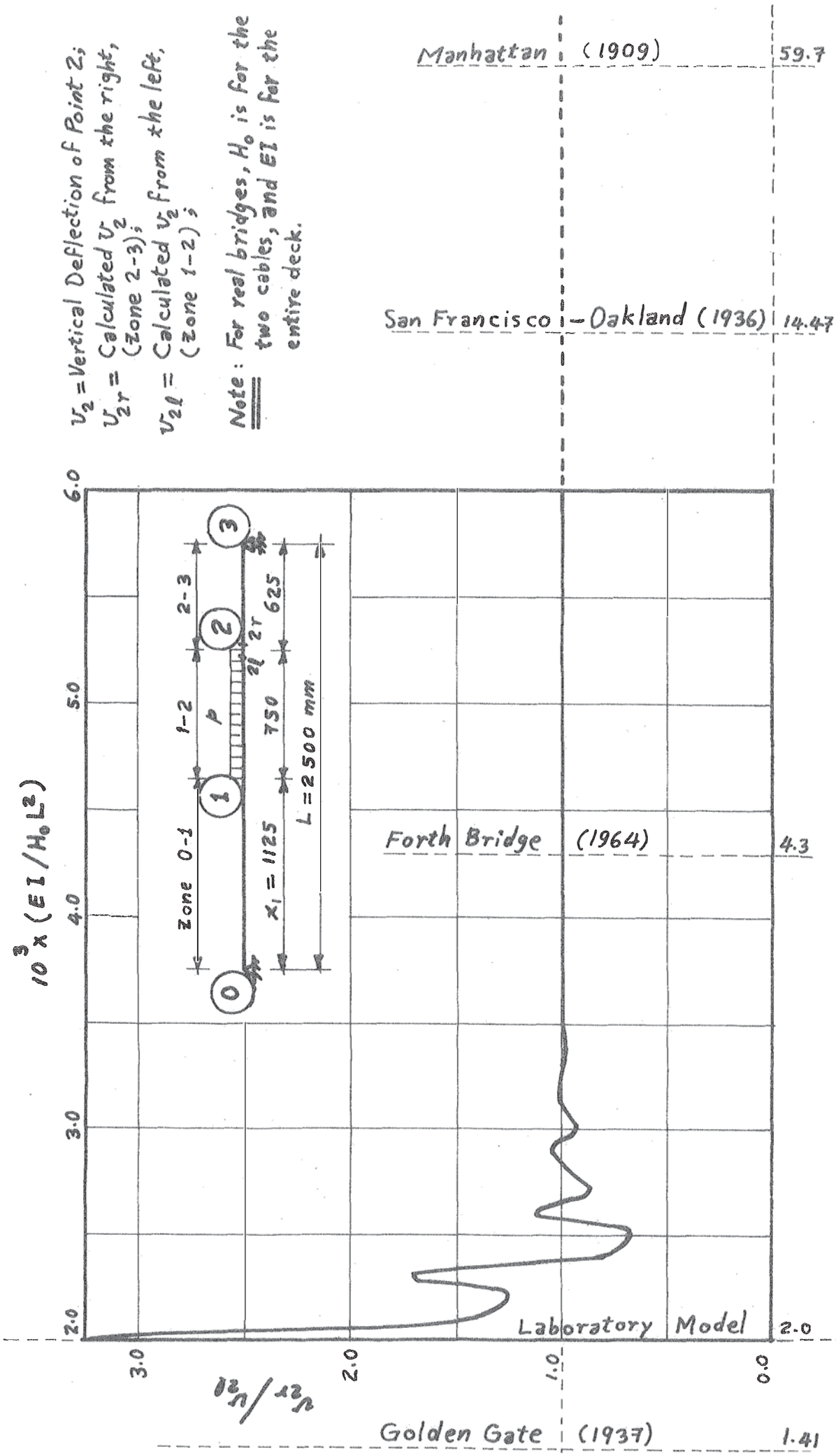

Fig. 2.5. – A Measure of the Ill-Conditioning of the Traditional Solution of the Deflection Theory, in the Third Zone.

The term in brackets becomes then, in turn, a non-reliable small quantity, which is to be multiplied by the very big number, e^{cL}, to give a very big value for C_3'. The sign of this very big C_3' has been proved to be wrong for the laboratory model when Eq. 2.7f.1 was used in the calculations.

Also, Pugsley's way of writing the integration constants gives C_3' as in Eq. 2.7f, which can be rewritten in the form

$$C_3' = -e^{cL} \cdot [C_1 \cdot e^{cL} + \frac{1}{c^2}(\frac{p}{2h} \cdot e^{c(L-x_1)} \cdot (1-e^{-cx_2}) + (8D/L^2))] \qquad (2.7f.2)$$

Again, C_1 is small and when multiplied by the very big number e^{cL}, the result becomes inaccurate. The term $C_1.e^{cL}$ is negative, while the other terms in the square bracket are all positive, and the result between the square brackets in Eq. 2.7f.2 becomes similar to the result in parentheses in Eq. 2.7f.1, both of which being multiplied by the same factor ($-e^{cL}$) which is very big.

The Manhattan Bridge has a relatively stiff deck (as can be seen from Fig. 2.5), but the writer cannot deny that both the George Washington Bridge and the Golden Gate Bridge are a bit more slender than our laboratory model, although they were designed using the deflection theory. Perhaps the three-zone case of loading was not considered in their designs.

However, in order to avoid such trouble, the writer suggests the following forms for the six integration constants.

$$C_1 = \frac{1}{c^2}\left[\frac{\frac{p}{2h}[e^{c\{L-(x_1+x_2)\}}+e^{-c\{L-(x_1+x_2)\}}-e^{c(L-x_1)}-e^{-c(L-x_1)}]-(8D/L^2)(1-e^{-cL})}{e^{cL}-e^{-cL}}\right] \qquad (2.8a)$$

$$C_1' = -\frac{1}{c^2}\left[\frac{\frac{p}{2h}[e^{c\{L-(x_1+x_2)\}}+e^{-c\{L-(x_1+x_2)\}}-e^{c(L-x_1)}-e^{-c(L-x_1)}]+(8D/L^2)(e^{cL}-1)}{e^{cL}-e^{-cL}}\right] \qquad (2.8b)$$

$$C_2 = \frac{1}{c^2}\left[\frac{\frac{p}{2h}[e^{c\{L-(x_1+x_2)\}}+e^{-c\{(L-(x_1+x_2)\}}-e^{c(L-x_1)}-e^{-c(L+x_1)}]-(8D/L^2)(1-e^{-cL})}{e^{cL}-e^{-cL}}\right] \qquad (2.8c)$$

$$C_2' = -\frac{1}{c^2}\left[\frac{\frac{p}{2h}[e^{c\{L-(x_1+x_2)\}}+e^{-c\{L-(x_1+x_2)\}}-e^{c(L-x_1)}-e^{+c(L+x_1)}]+(8D/L)(e^{cL}-1)}{e^{cL}-e^{-cL}}\right] \qquad (2.8d)$$

$$C_3 = \frac{1}{c^2}\left[\frac{\frac{p}{2h}[e^{-c\{L-(x_1+x_2)\}}+e^{-c\{L+(x_1+x_2)\}}-e^{-c(L-x_1)}-e^{-c(L+x_1)}] - (8D/L^2)(1-e^{-cL})}{e^{cL} - e^{-cL}}\right] \tag{2.8e}$$

$$C_3' = -\frac{1}{c^2}\left[\frac{\frac{p}{2h}[e^{c\{L-(x_1+x_2)\}}+e^{c\{L+(x_1+x_2)\}}-e^{c(L-x_1)}-e^{c(L+x_1)}] + (8D/L^2)(e^{cL}-1)}{e^{cL} - e^{-cL}}\right] \tag{2.8f}$$

all of them being in terms of the dimensions and the properties of the structure to minimize the round-off errors. This process succeeded in eliminating, entirely, the ill-conditioning of zone 2-3, when the computations were carried out on a PDP-8 Digital computer (a small laboratory computer).

It remains now to evaluate the value of h, in terms of which the constant c is calculated (Eq. 2.2b). The problem is a bit complicated and needs some approximations in order to get a solution. Several approximations have been used before by many authors (Refs. 1.3, 1.7, 1.13), each of which does not affect much the value of h, but the deflections are remarkably affected.

One of these approximations is to neglect the effect of the cable extensibility on h by putting

$$\int_0^L \mathbf{v} \cdot dx = 0 \tag{2.9}$$

This gives, for the loading condition of Fig. 2.4

$$h = \frac{p}{\frac{16D}{c^3L^2}\left(\frac{e^{cL}-1}{e^{cL}+1}\right) - \frac{8D}{c^2L} + \frac{2}{3}DL}\left[x_2 \cdot \left[\frac{x_1}{4}(L-x_1) + \frac{(x_1+x_2)}{4}\{L-(x_1+x_2)\} + \frac{x_2^2}{12} - \frac{1}{c^2}\right]\right.$$

$$- \frac{1}{c^3(e^{cL}-e^{-cL})}\left[e^{cx_1}+e^{-cx_1}+e^{c\{L-(x_1+x_2)\}}\right.$$

$$\left.+e^{-c\{L-(x_1+x_2)\}}-e^{c(L-x_1)}-e^{-c(L-x_1)}-e^{c(x_1+x_2)}\right.$$

$$\left.\left.-e^{-c(x_1+x_2)}\right]\right] \qquad (2.10)$$

Using this procedure, the laboratory model was analysed for three point loads, each of which equals 98.1 Newtons, acting at stations 5, 6, 7. The results are shown in Fig. 2.6, where the measurements are also plotted.

Corrections, to the deflections, due to the extensions of both the main cable and the back-stays must be added. The latter is represented by the horizontal movements of the tower tops. These corrections are added, by superposition, according to the diagram shown in Fig. 2.7, which is suggested by the writer. A similar procedure has been proposed before, in 1862, (Ref. 1.9). The idea is to get first the deflections considering the cable to be inextensible with fixed ends. A symmetrical parabolic wave caused by the cable stretch is then added, followed by another symmetrical parabolic wave caused by the tower movements which shorten the span and thus increase the sag.

The changes in the central dip of a cable due to changing both its length and span have been evaluated before by Pugsley, (Ref. 1.3). A simplification can be made by the writer as follows

$$\ell \simeq L\left[1 + \frac{8}{3}\left(\frac{D}{L}\right)^2 - \frac{32}{5}\left(\frac{D}{L}\right)^4\right] \qquad (2.11)$$

Where ℓ is the length of the main cable, L is the span, $(\frac{D}{L})$ is the dip-span ratio. Eq. 2.11 is a quadratic equation in $(\frac{D}{L})^2$ from which D + δD can be easily calculated if ℓ becomes (ℓ + $\delta\ell$) and L becomes (L - δL_1 - δL_2) where δD, $\delta\ell$, δL_1 and δL_2 are the changes in the central sag, the length of the main cable, and the horizontal movements of the tower tops, respectively.

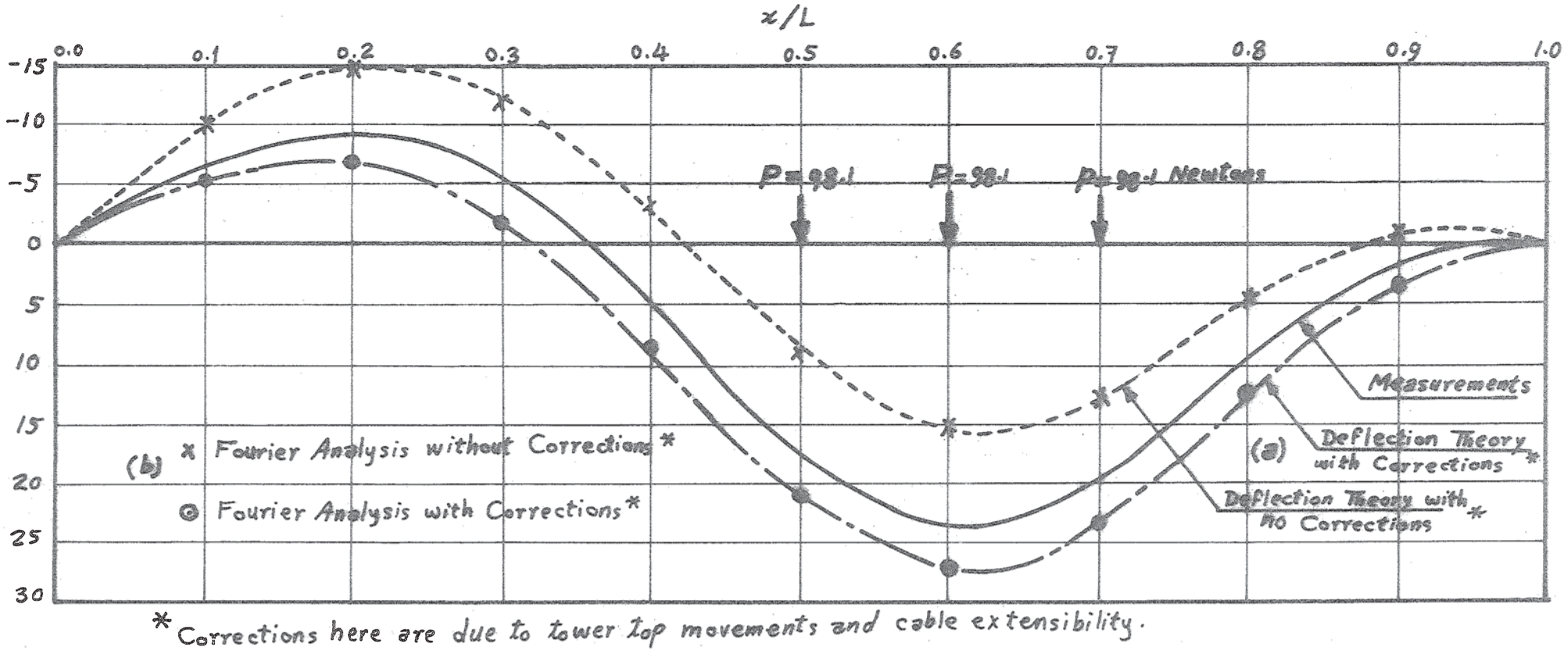

* Corrections here are due to tower top movements and cable extensibility.

Fig. 2.6.— Vertical Deflections Obtained From the Deflection Theory Using:
(a) Direct Solution of the Differential Equation; and
(b) Fourier Series Analysis.
Compared with Measurements taken on Laboratory Model.

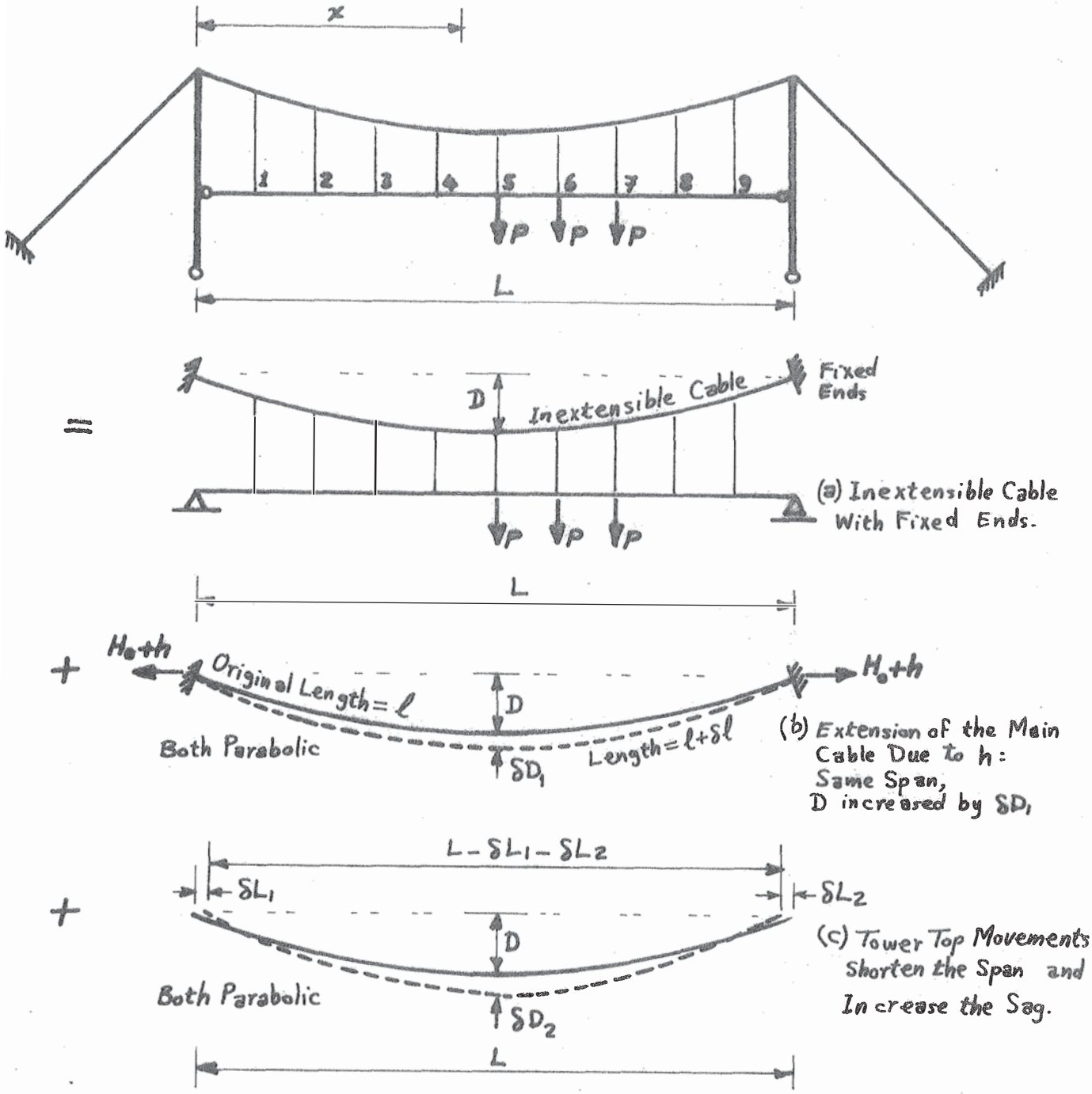

Fig. 2.7.– Corrections Due to Main Cable Extensibility and Tower Top Movements.

Knowing the change of the central sag, δD, the corresponding correction in the vertical deflection at any section, distance x from the left support, becomes

$$\delta v = 4\delta D \cdot \frac{x}{L}\left(1 - \frac{x}{L}\right) \tag{2.12}$$

The main cable extension can be approximately written as

$$\delta \ell = \frac{h.L}{AE} \tag{2.13}$$

Also the tower top movement δL, using Fig. 2.8, can be given as follows:

$$\delta \ell_2 = \frac{(h/\cos 45^\circ) \cdot \ell_2}{AE}$$

$$\delta \ell_2 = \frac{h \cdot \ell_2}{AE.\cos^2 45^\circ} = \frac{2h \cdot \ell_2}{AE}$$

where ℓ_2 is the initial length of back-stay 2, (D.L. condition).

Thus the reduction in the span due to the tower movements becomes

$$\delta L = \delta L_1 + \delta L_2 = \frac{2h}{AE}\ (\ell_1 + \ell_2) \tag{2.14}$$

where ℓ_1 is the initial length of back-stay 1, (D.L. condition).

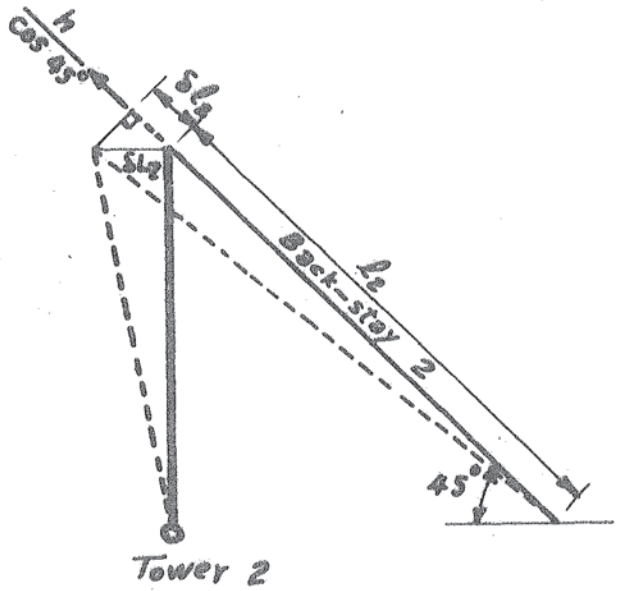

Fig. 2.8.

It can be seen from Fig. 2.6 that the above analysis of the deflection theory agrees with the laboratory measurements within about 15% at the point of maximum deflection, which can be accepted according to the foregoing successive approximations in the analysis, and within the laboratory accuracy in both measuring and modelling.

* * *

A Fourier series analysis has been worked out by the writer in solving the basic D.E. of the deflection theory as follows:

Eq. 2.5 can be rewritten in the form

$$EI.\frac{d^4v}{dx^4} = (p + w) = (H_o + h) \; . \; (y'' + v'') \tag{2.15}$$

where w = intensity of D.L. per unit length of the span; $v'' = d^2v/dx^2$ ≃ the curvature, K, of the deck; $y'' = (d^2y/dx^2) = -(8D/L^2)$.

Eq. 2.15 can, approximately, be solved using a Fourier series technique by multiplying both sides by $(\sin \frac{i\pi x}{L})$ and integrating from 0 to L; thus

$$EI\int_o^L \frac{d^4v}{dx^4}.\sin\frac{i\pi x}{L}\,dx = \int_o^L (p+w).\sin\frac{i\pi x}{L}\,dx + (H_o+h)\int_o^L ((-8D/L^2)+v'').\sin\frac{i\pi x}{L}\,dx \tag{2.16}$$

$$\text{Put} \quad v = \Sigma\, a_n \,.\sin\frac{n\pi x}{L} \tag{2.17a}$$

$$\therefore \; v' = \Sigma\, a_n \,(\frac{n\pi}{L}).\cos\frac{n\pi x}{L} \tag{2.17b}$$

$$v'' = -\Sigma\, a_n \,(\frac{n\pi}{L})^2.\sin\frac{n\pi x}{L} \tag{2.17c}$$

$$\frac{d^4v}{dx^4} = +\Sigma\, a_n \,(\frac{n\pi}{L})^4.\sin\frac{n\pi x}{L} \tag{2.17d}$$

Therefore, the left-hand side, L.H.S., of Eq. 2.16, after some algebra, reduces to

$$EI\,(\frac{i\pi}{L})^4 \; . \; \frac{L}{2} \; . \; a_i$$

For a uniform L.L., p acting from x_1 to x_2 on the span, the first term of the right-hand side, R.H.S., of Eq. 2.16, after manipulation, becomes

$$\frac{L}{i\pi}\left[p\left(\cos\frac{i\pi x_1}{L} - \cos\frac{i\pi x_2}{L}\right) + w(1 - \cos i\pi)\right]$$

The second term of the R.H.S. of Eq. 2.16 also becomes

$$-(H_o + h)\left[(8D/L^2)\left(\frac{L}{i\pi}\right)(1 - \cos i\pi) + \left(\frac{i\pi}{L}\right)^2 .\frac{L}{2} .a_i\right]$$

Rearranging the terms, Eq. 2.16 thus yields

$$a_i = \frac{p\left(\cos\frac{i\pi x_1}{L} - \cos\frac{i\pi x_2}{L}\right) + \{w-(8D/L^2)(H_o+h)\}(1 - \cos i\pi)}{\left(\frac{i\pi}{L}\right)^3 .\frac{L}{2}\left[EI\left(\frac{i\pi}{L}\right)^2 + (H_o+h)\right]} \qquad (2.18)$$

which is exactly the same as that given by Timoshenko, (Ref. 1.14) for the Fourier coefficient given below in Eq. 2.21, noting that $w = H_o.(8D/L^2)$, $h = \beta.H_o$. The value of h can be obtained using the foregoing method or any other relevant method.

The laboratory model was analysed using this Fourier approximation and the above method of evaluating h. The results, using only five Fourier terms, are shown in Fig. 2.6, and are almost coincident with the results of the direct solution of the D.E. This Fourier approximation avoids completely the ill-conditioning which is likely to happen in some cases. We may be sure, of course, that ill-conditioning if it occurs is a property of our method of calculation, not of the actual structural action and deflections of the suspension bridge.

2.4.2 TIMOSHENKO'S ENERGY METHOD, (Ref. 1.14)

In this method the potential energy of the deck, U_1, is evaluated using a Fourier series for the vertical deflections, as previously given in Eq. 2.17a. An expression for the Fourier coefficients a_i is obtainable by imposing the condition of stationary potential energy. It must be noticed here, again, that the coefficient a_i is obtained in terms of h. In this method h is obtained from the equation of the strain and potential energy, U_2 of the cable.

The potential energy U_1 of the deck can be written as

$$U_1 = \int_0^L \int_0^K EIK.dK.dx + \int_0^L \int_0^v qdx.dv - \int_0^L \int_0^v pdx.dv \qquad (2.19)$$

where K = curvature of the deck $\simeq v''$;

q = the intensity of the live load portion carried by the cable
$= \beta w - H_o (1 + \beta).v''$ as given by Timoshenko;

$\beta = h/H_o$;

w = intensity of D.L. on the bridge;

p = L.L. intensity on the bridge acting from x_1 to x_2 as shown in Fig. 2.4.

For a stationary potential energy we can write

$$\frac{\partial U_1}{\partial a_i} = 0 \qquad (2.20a)$$

Thus Eq. 2.19 gives, after substituting for K and q, if EI is constant

$$EI. \int_0^L v''.\frac{\partial v''}{\partial a_i}.dx + \int_0^L [\beta w - H_o(1+\beta).v''].\frac{\partial v}{\partial a_i}.dx - \int_0^L p.\frac{\partial v}{\partial a_i}.dx = 0 \qquad (2.20b)$$

For a uniform L.L., p on the bridge, and after some algebra, Eq.2.20b yields

$$a_i = \frac{p(\cos\frac{i\pi x_1}{L} - \cos\frac{i\pi x_2}{L}) - \beta w(1 - \cos i\pi)}{(\frac{i\pi}{L})^3 . \frac{L}{2} . [EI\ (\frac{i\pi}{L})^2 + H_o(1+\beta)]} \qquad (2.21)$$

which is the value of the Fourier coefficients of the vertical deflections in terms of the parameter β . To evaluate β, the change in the strain and potential energy of the cable, U_2, was given as follows.

The complete change in the strain energy of the cable, U_{2s} may be expressed as

$$U_{2s} = \frac{h(H_o + \frac{1}{2}h)}{AE} \int_0^L (\frac{ds}{dx})^3 \, dx$$

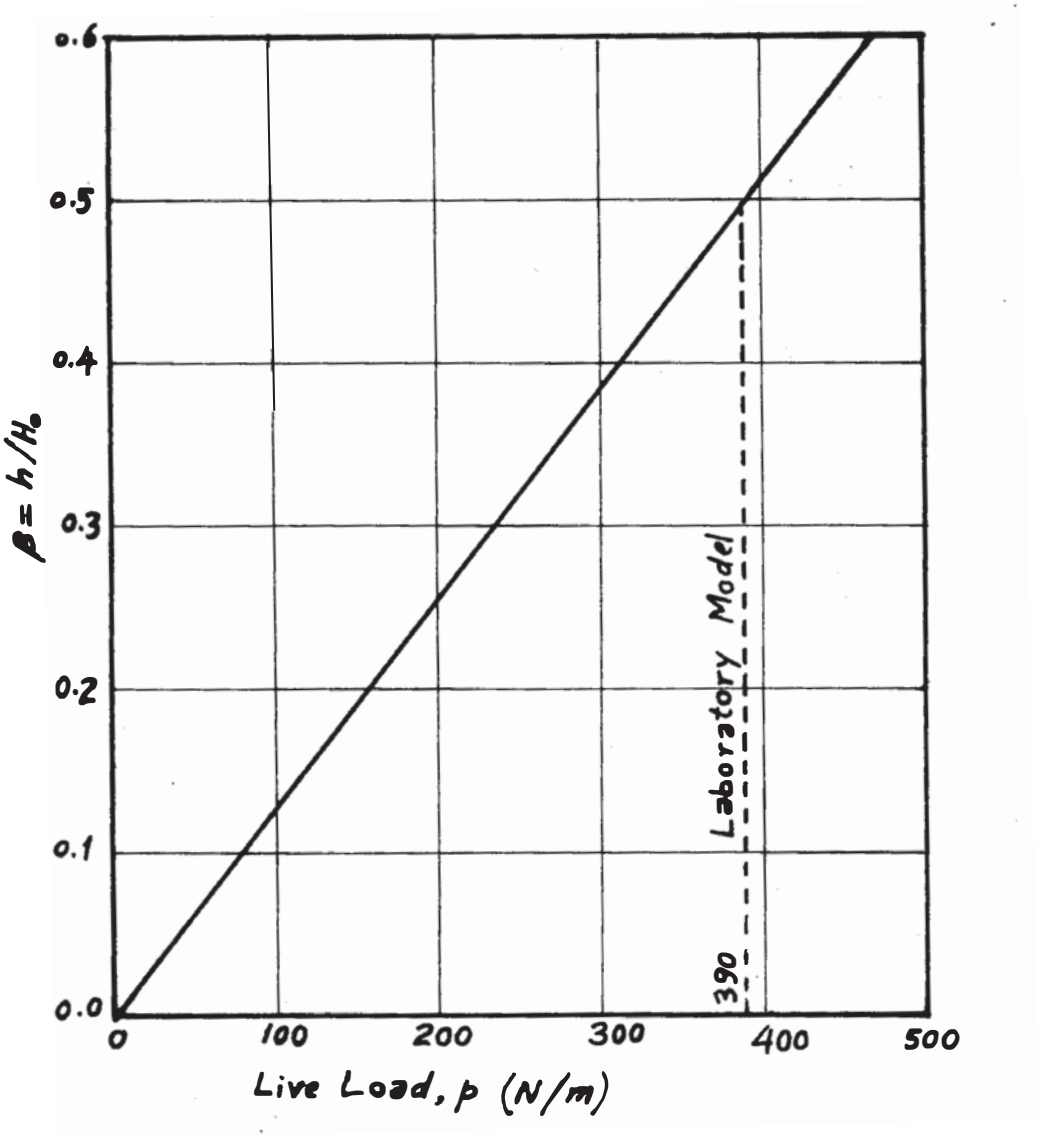
0.6
0.5
0.4
0.3
0.2
0.1
0.0
β = h/H₀
0
100
200
300
400
500
Live Load, p (N/m)
Laboratory Model
390

Fig. 2.9.

$$\simeq \frac{h}{AE}\left(H_o + \frac{h}{2}\right) \cdot L\left[1 + 8\left(\frac{D}{L}\right)^2\right]^* \qquad (2.22a)$$

which is a simpler form than that given by Timoshenko.

Assuming an average intensity of the load on the cable, the work done by that load, U_{2w}, is

$$U_{2w} = \int_o^L \left(w + \frac{q}{2}\right) .v.dx$$

$$= w\left(1+\frac{\beta}{2}\right).\frac{2L}{\pi}\left(a_1 + \frac{a_3}{3} + \frac{a_5}{5} + \ldots\right) + H_o.\frac{\pi^2}{4L}(1+\beta)\left(a_1^2 + 2^2.a_2^2 + 3^2.a_3^2 + \ldots\right) \qquad (2.22b)$$

Equating U_{2s} to U_{2w} yields after some manipulation

$$\frac{H_o}{AE}.\beta L\left(1+\frac{\beta}{2}\right)\left[1+8\left(\frac{D}{L}\right)^2\right] = \frac{16D}{\pi L}\left(1+\frac{\beta}{2}\right)\left(\Sigma\frac{a_n}{n}\right)_{1,3,5..} + \frac{\pi^2}{4L}(1+\beta).\left[\Sigma\left(n^2.a_n^2\right)\right]_{1,2,3...} \qquad (2.23)$$

where a_n are as given by Eq. 2.21 (as a function of β and the L.L., p).

Eqs. 2.21, 2.23 may be solved together to get both the redundants a_i and β. The solution is performed by a trial and error method. A value for β is assumed, and then the corresponding value of p is calculated. Assuming for small fluctuations in cable stress that β is proportional to p, the increase h in the horizontal component of the cable tension can easily be calculated. This assumption is actually confirmed by the measurements shown in Fig. 2.2 given before. However, Fig. 2.9 shows the relationship between the assumed β and the calculated p using Timoshenko's method, from which it can be seen that this relation is truly almost linear.

It has been found that this method is convergent, and only five Fourier terms are quite sufficient for practical cases.

The method was applied to the laboratory model loaded as shown in Fig. 2.4. The results are shown in Fig. 2.10. It can be seen from Eq.2.23 that this method takes the extensibility of the main cable into consideration.

---

* Using the approximations $\frac{ds}{dx} \simeq 1 + \frac{1}{2}\left(\frac{dy}{dx}\right)^2$, $\left(\frac{ds}{dx}\right)^3 \simeq 1 + 1.5\left(\frac{dy}{dx}\right)^2$,

neglecting higher powers of $\left(\frac{dy}{dx}\right)^2$, where $y = 4D.\frac{x}{L}\left(1 - \frac{x}{L}\right)$

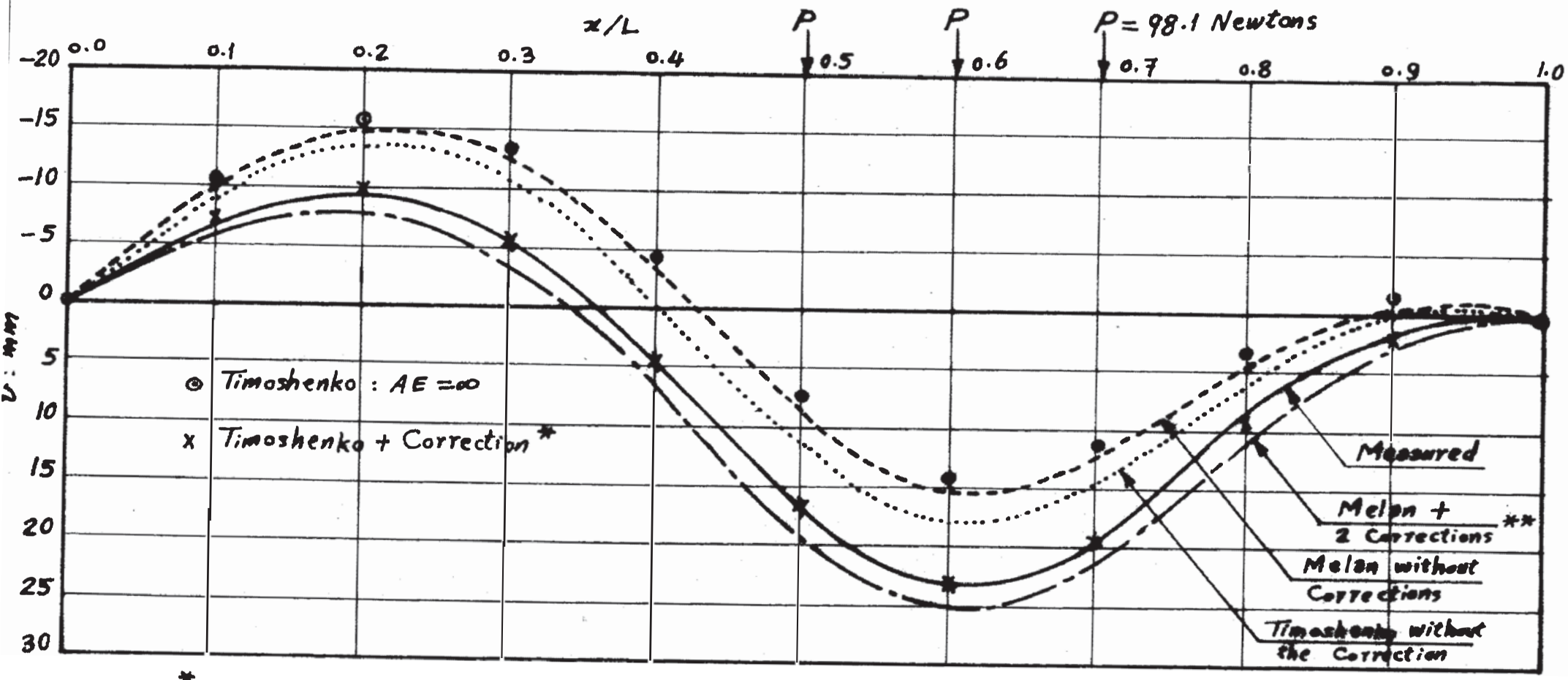

* Correction to Timoshenko is due to tower movements only.

** Corrections to Melan are due to cable extensibility and tower Movements.

Fig. 2.10._ Vertical Deflections Obtained from Timoshenko's Method and Comparison with the Deflection Theory of Melan.

Measurements taken on Laboratory Model are shown by Full-Line.

Thus it remains only to add the corrections due to the tower movements as shown in Fig. 2.7c, i.e. putting $\delta D_1 = \delta \ell = 0$, since their effect has been already included in Eq. 2.23. Thus Eq. 2.11 becomes

$$\ell = (L-\delta L)\left[1+ \frac{8}{3}\left(\frac{D+\delta D_2}{L-\delta L}\right)^2 - \frac{32}{5}\left(\frac{D+\delta D_2}{L-\delta L}\right)^4\right] \qquad (2.24)$$

which can easily be solved in $(D+\delta D_2)^2$ as before. The corrected deflection curve is also shown in Fig. 2.10, from which it can be seen that it is almost coincident with the measurements.

On Fig. 2.10, also, Timoshenko's solution for an inextensible cable ($AE \simeq \infty$) is shown, and compares reasonably with the results of Melan's method.

2.4.3 PUGSLEY'S FLEXIBILITY METHOD, (Ref. 1.15)

This method is based on determining the flexibility coefficients for both the cable and the girder. The span is divided into ten equal segments by nine equidistant stations as shown in Fig. 2.11. The flexibility coefficients of the cable are determined considering that it carries all

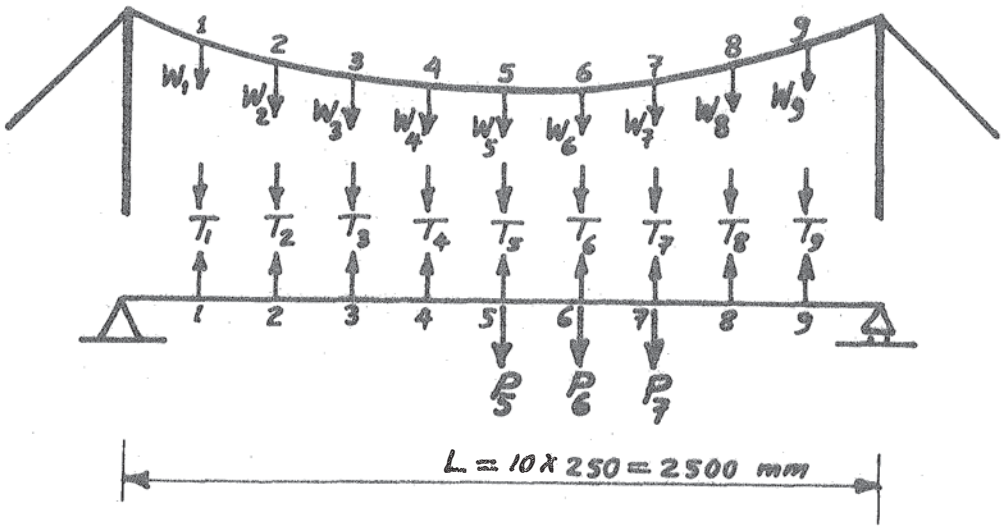

Fig. 2.11.– Cable and Girder.

the D.L., in addition to the moving influence load and the hanger tensions. This can be done using the above-mentioned Timoshenko's method, (Ref. 1.14), assuming a very slender deck with no bending stiffness (EI = 0). It can also be done using the method given by Pugsley in his book, (Ref. 1.3, Ch.3). Fig. 2.12 shows some load-deflection curves using both methods.

Neglecting the extensions of the suspension rods, (because they are very small), the deflections of the cable can be considered identical with the corresponding deflections of the girder. Thus, at any hanger position i we can write

$$v_i = V_i \tag{2.25a}$$

where

$$v_i = \sum_{j=1}^{9} T_j \cdot v_{ij} \tag{2.25b}$$

= cable deflection at i;

$$V_i = \sum_{j=1}^{9} (P_j - T_j) \cdot V_{ij} \tag{2.25c}$$

= girder deflection at i;

T_j = Tension in hanger j;

P_j = Point-Live load acting on the deck at the hanger j;

v_{ij} = deflection of the cable at the hanger i due to a unit load acting on the cable at the hanger j;

V_{ij} = deflection of the girder at the hanger i due to a unit load acting on the girder at the hanger j.

Thus Eq. 2.25a can be written in the form

$$[v_i] \cdot [T] = [V_i] \cdot [P - T] \tag{2.25d}$$

where

$[v_i]$ = row vector of the flexibility coefficients of the cable at the hanger i;

$[T]$ = column vector of the hanger tensions;

$[V_i]$ = row vector of the flexibility coefficients of the girder at the hanger i;

$[P]$ = column vector of the L.L.

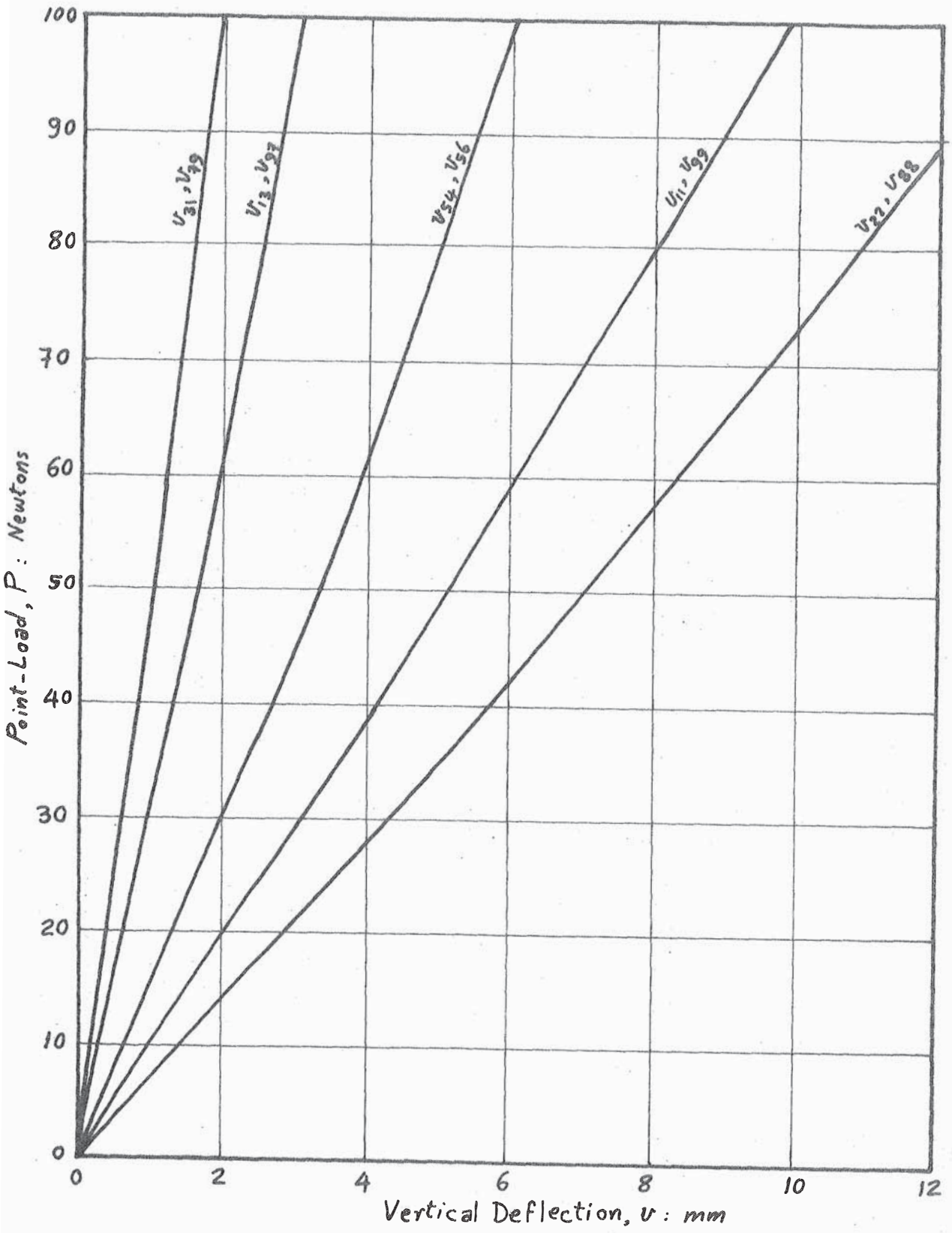

Fig. 2-12.-- Load-Deflection Curves Due to a Single Point-Load:
(a) Timoshenko's Method Applied to the Suspension Cable Only, ($EI_{deck} = 0$).

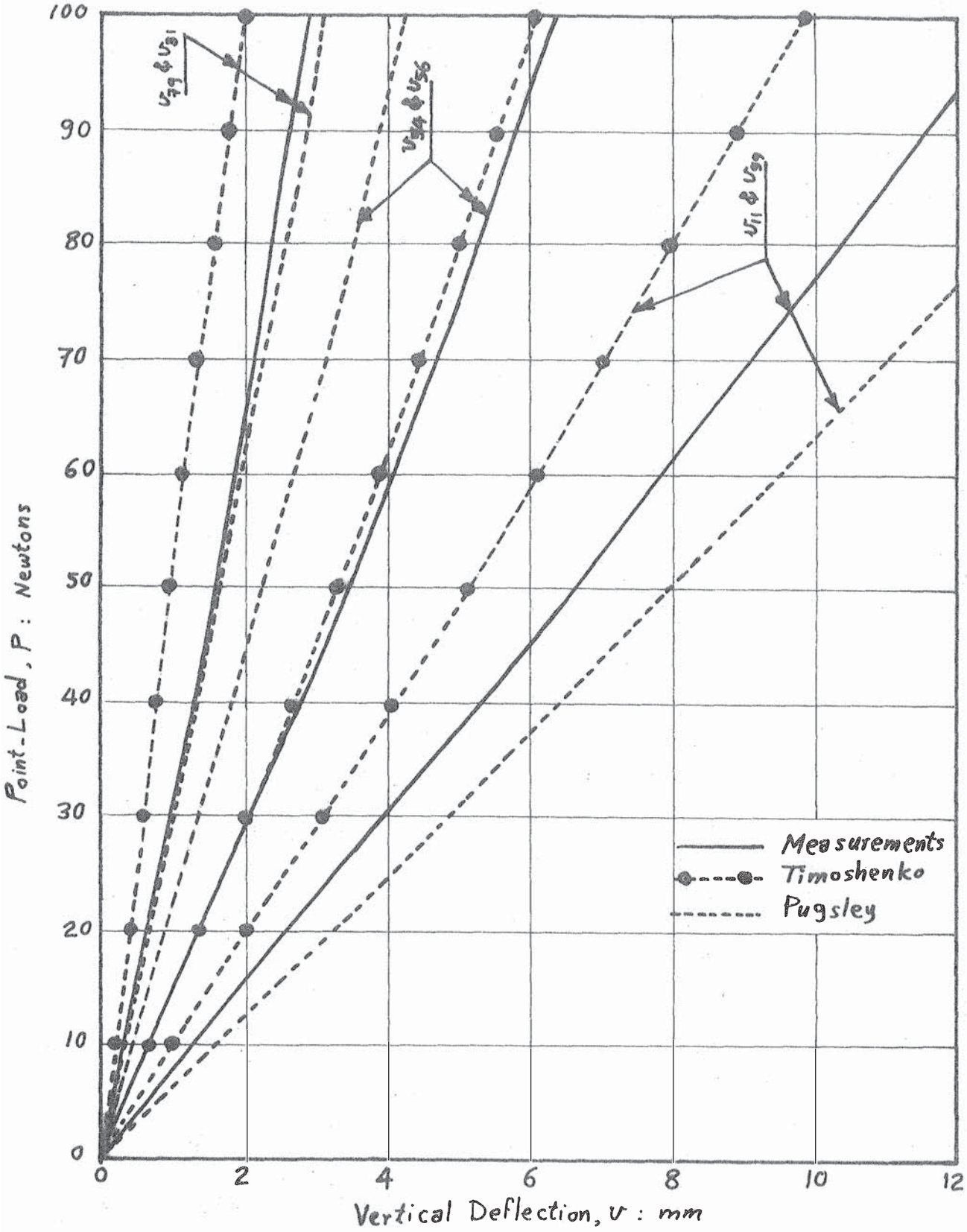

Fig. 2.12.— Load ~ Deflection Curves Due to a Single Point-Load:
(b) Timoshenko and Pugsley's Methods, and Measurements
on the Cable of the Laboratory Model.

For the entire system Eq. 2.25d can be written as

$$[v] \cdot [T] = [V] \cdot [P - T] \qquad (2.26a)$$

where

[v] = flexibility coefficients' matrix for the cable; and

[V] = flexibility coefficients' matrix for the girder.

Eq. 2.26a can be rewritten as follows.

$$[v + V] \cdot [T] = [V] \cdot [P] \qquad (2.26b)$$

in which the elements of the matrix [v + V] are the algebraic sum of the corresponding elements of the two matrices [v] and [V].

Writing Eq. 2.26b in full, thus

$$\begin{bmatrix} v_{11}+V_{11} & v_{12}+V_{12} & \cdots & v_{19}+V_{19} \\ v_{21}+V_{21} & v_{22}+V_{22} & \cdots & v_{29}+V_{29} \\ \vdots & \vdots & & \vdots \\ v_{91}+V_{91} & v_{92}+V_{92} & \cdots & v_{99}+V_{99} \end{bmatrix} \cdot \begin{bmatrix} T_1 \\ T_2 \\ \vdots \\ T_9 \end{bmatrix} = \begin{bmatrix} V_{11} & V_{12} & \cdots & V_{19} \\ V_{21} & V_{22} & \cdots & V_{29} \\ \vdots & \vdots & & \vdots \\ V_{91} & V_{92} & \cdots & V_{99} \end{bmatrix} \cdot \begin{bmatrix} P_1 \\ P_2 \\ \vdots \\ P_9 \end{bmatrix} \qquad (2.26c)$$

The square matrix of the R.H.S. is symmetrical, while that on the L.H.S. is not so, because Maxwell's principle of reciprocal deflections does not hold for cables, (see Figs. 2.12). Again, V_{19} (for example) is the deflection of the girder at station 1 due to a unit load acting at point 9.

Figs. 2.12 show that the cable deflections are not linearly proportional to the acting point loads. So it is essential to linearise the cable deflections at some load values near the expected hanger tensions in order to get convenient flexibility coefficient for the cable. From Figs. 2.12, it is clear that the cable deflections increase, at a diminishing rate, with the increase of the load, and this means that when the cable deflections are linearised at loads less than the hanger tensions, the solution will overestimate the final deflections of the bridge, and vice versa. This is clear in Figs. 2.13, and so, after having an idea about the hanger tensions, the cable flexibility coefficients can be obtained by a linearisation process at an average value of such hanger tensions.

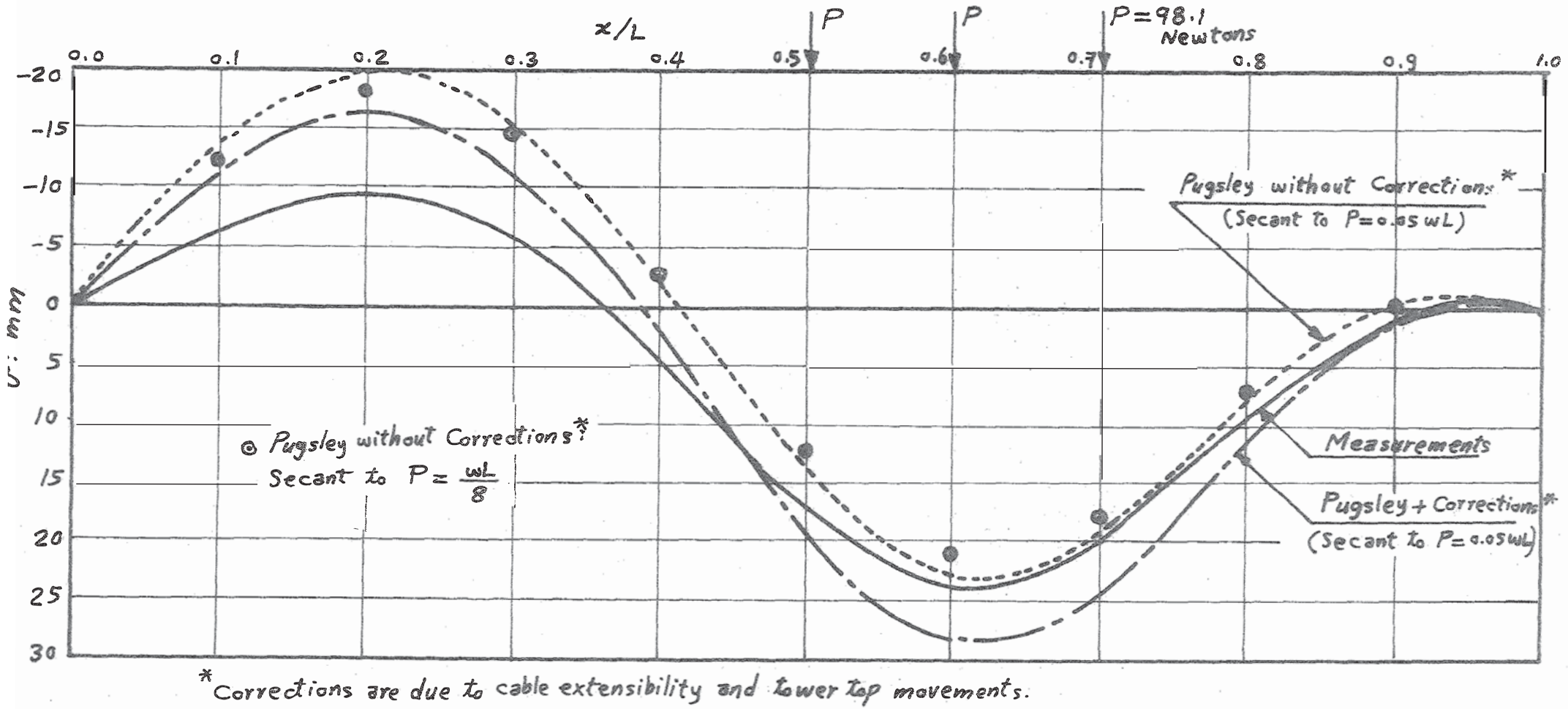

Fig. 2.13.- Vertical Deflections Obtained from Pugsley's Method of Flexibility Coefficients: (a) Flexibility coefficients are determined using Timoshenko's method.

Measurements on the Laboratory Model are Shown by Full-Line.

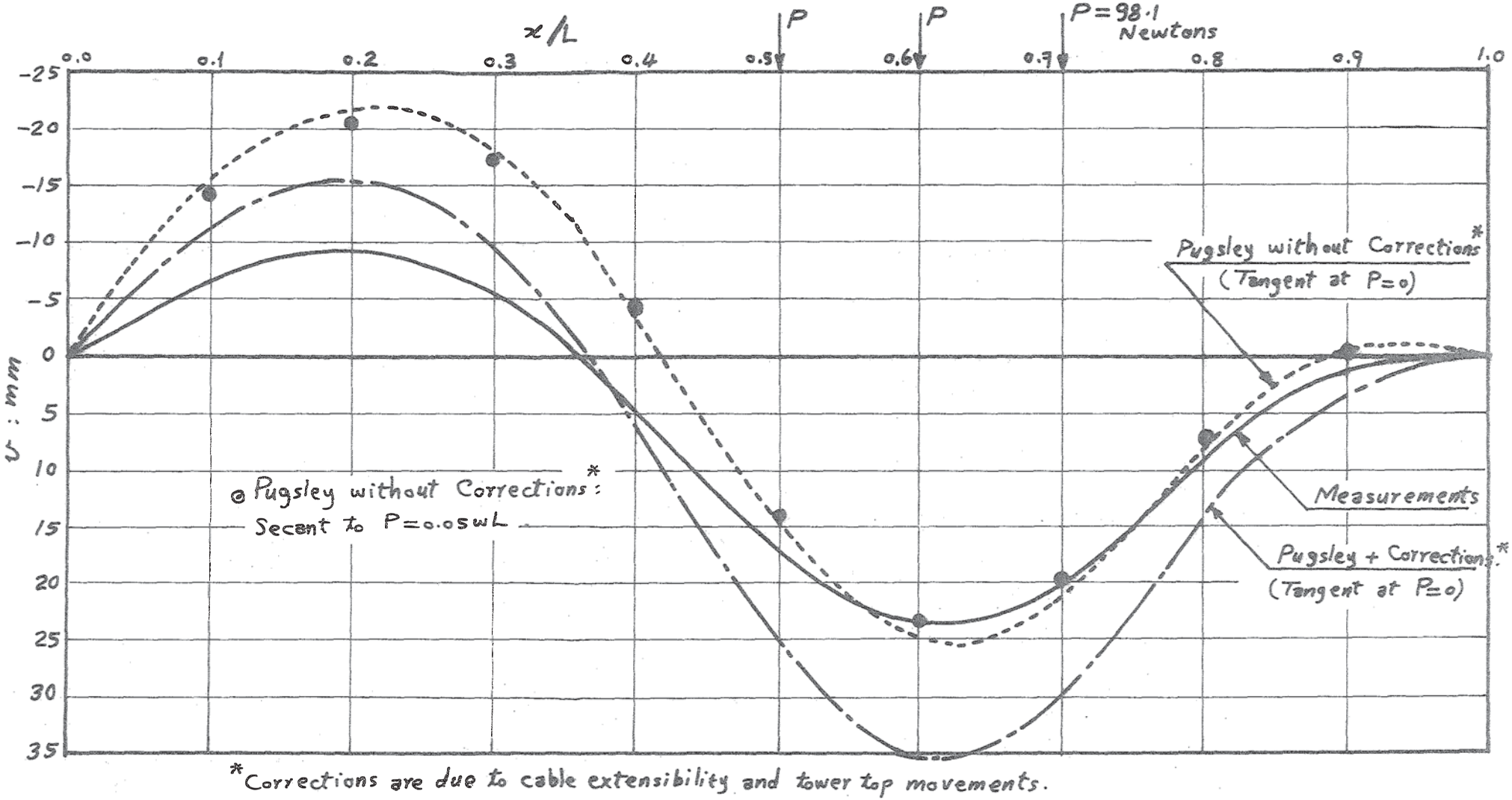

Fig. 2.13.– Vertical Deflections Obtained from Pugsley's Method of Flexibility Coefficients:
(b) Flexibility coefficients are determined using Pugsley's method.
Measurements on Laboratory Model are Shown by Full-Line.

The flexibility coefficients of the cable as evaluated using Timoshenko's energy method already include the effect of the cable extensibility, and so only the correction due to the tower movements is added to the resulting vertical deflections as before. However, the method, as shown in Figs. 2.13, overestimates both the upward and the downward deflections everywhere throughout the entire span of the bridge.

It is obvious that the deflections of the bridge are calculated after solving Eq. 2.26c in the hanger tensions [T] and substituting in either of the Eqs. 2.25b and 2.25c.

2.4.4 CHARLTON'S ENERGY METHOD, (Refs. 1.17, 1.18)

This method is based on Pugsley's flexibility coefficients of the cable (v_{ij}), mentioned in the previous sub-section, but using both potential and complementary energies. The span here also is divided into 10 equal segments by 9 equidistant stations.

The complementary energy procedure, (Ref. 1.17), has been modified by the writer, (Ref. 1.19), and leads to the basic flexibility equation (Eq. 2.26b) of Pugsley, given in the previous sub-section.

Charlton's potential energy equation, (Ref. 1.17), can also be rewritten in the form *

$$U = \int_0^L \int_0^K M dK.dx + \sum_{i=1}^{9} \int_0^{v_i} T_i \cdot dv_i - \sum_{i=1}^{9} \int_0^{v_i} W_i \cdot dv_i \qquad (2.27)$$

where

M = $EIK \simeq EIv''$, for a linear deck;

$T_i = \sum_{j=1}^{9} (s_{ij}\, v_j)$; (s_{ij} is an element in the stiffness matrix of the cable only).

W_i = D.L. on cable at hanger i (as shown in Fig. 2.11).

Putting the deflections v in the form of a Fourier series, as in Eq. 2.17a above, and after some algebra we can write for stationary potential energy $\frac{\partial U}{\partial a_m} = 0$. Thus

$$EI \int_0^L K. \frac{\partial K}{\partial a_m} . dx + \sum_{i=1}^{9} \sum_{j=1}^{9} s_{ij}\, v_j \frac{\partial v_i}{\partial a_m} - \sum_{i=1}^{9} W_i \frac{\partial v_i}{\partial a_m} = 0 \qquad (2.28)$$

---

* See Ref. 2.10.

which, in turn, can be reduced to

$$EI\left(\frac{m\pi}{L}\right)^4 \cdot \frac{L}{2} \cdot a_m + \left[\sum_{i=1}^{9} \sum_{j=1}^{9} s_{ij}\left(\sum a_n \sin\frac{n\pi x}{L}\right) \sin\frac{m\pi x_i}{L}\right] - \sum_{i=1}^{9} W_i \sin\frac{m\pi x_i}{L} = 0 \qquad (2.29)$$

Eq. 2.29 is, actually, a set of equations, the number of which is equal to the number of the Fourier terms used (=n). After obtaining the Fourier coefficients a_n, the deflections can be obtained using Eq. 2.17a.

The matrix of the stiffness coefficients $[s_{ij}]$ is obtained as the inverse of the flexibility coefficients matrix $[a_{ij}]$.

The flexibility matrix obtained by Pugsley's method is symmetrical only if it is calculated using the tangent to the $P \sim v$ graph at $P = 0$. However, it seems to the writer that Charlton got his symmetrical flexibility matrix at $(P/wL) = 0.1$ by taking the average of the off-diagonal elements obtained using the secant to $(P/wL) = 0.1$.

Fig. 2.14 shows the results of this method, which are nearly the same as those given by Pugsley's flexibility method (i.e. overestimating the deflections everywhere along the entire span).

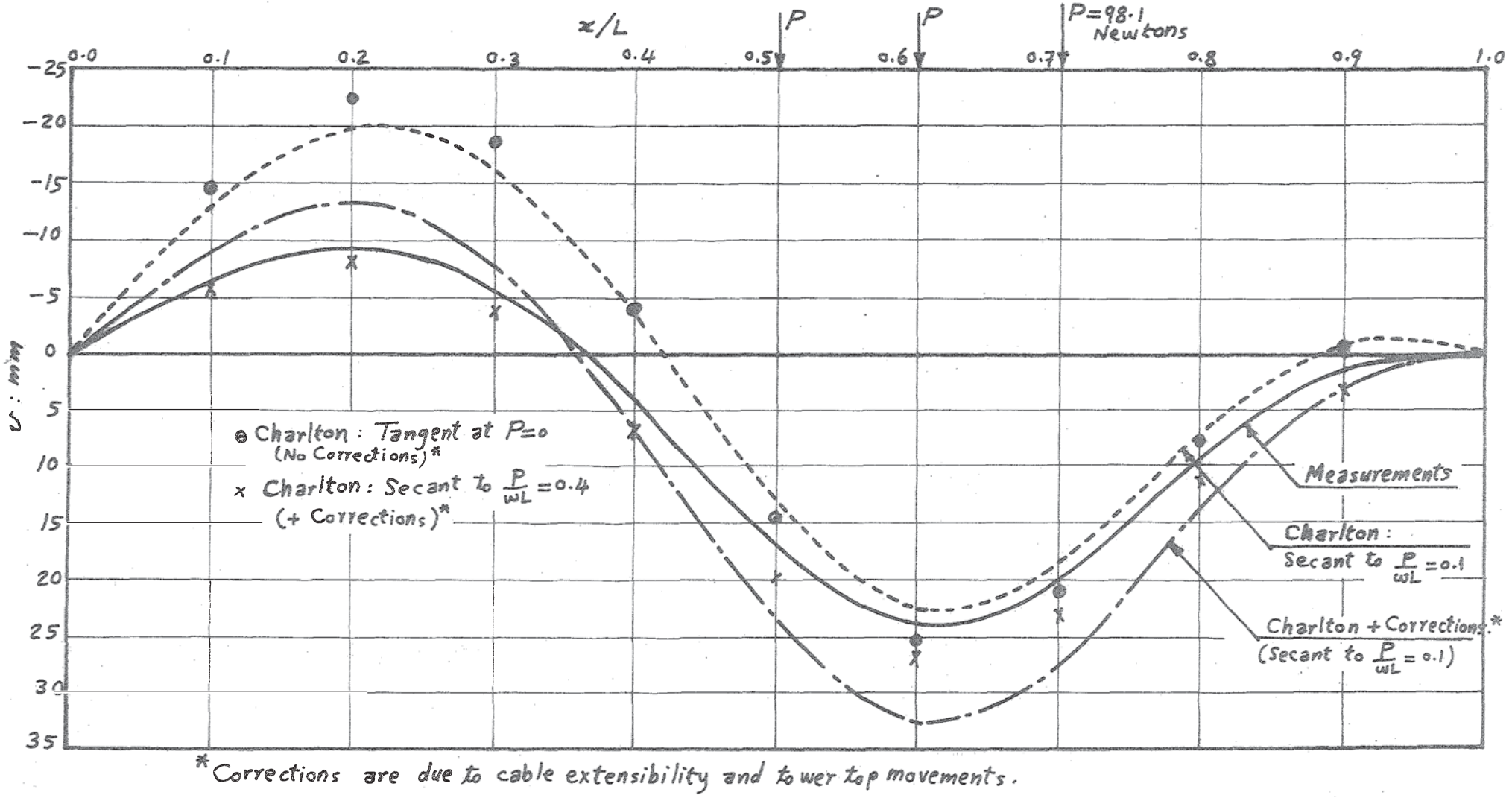

*Corrections are due to cable extensibility and tower top movements.

Fig. 2.14.- Vertical Deflections Obtained from Bowen & Charlton Potential Energy Method. Measurements on the Laboratory Model are Shown by Full-Line.

CHAPTER III

SINGLE-CABLE BRIDGE: DYNAMICS

3.1 INTRODUCTION

The aim of this chapter is to summarize the results of a study of the natural frequencies and modes of vibration of the so-called "single-cable suspension bridge". Being a single-cable bridge, it has only flexural modes of vibration with no twist in the deck.

A real bridge, of course, usually has at least two main cables supporting a wide deck which is able to vibrate both flexurally and torsionally. As a necessary preliminary, the laboratory model of the single-cable bridge was dynamically analysed, and natural modes and frequencies were measured and compared with calculations. The reasons are twofold.

(1) Dynamic analysis must contain all the simplifications and approximations of the static analysis, and, as a further test of their validity or otherwise, the opportunity should not be missed to try out these simplifications and approximations on the simplest possible model, the single-cable bridge.

(2) The flexural vibrations of a real bridge must have much in common with its single-cable representation.

3.2 METHOD OF ANALYSIS

There are several methods of calculating frequencies and modes of vibration of structures. For a single-cable bridge analysis, it is enough to know the first two (or three) natural frequencies and modes of vibration. In this case, the iteration method, (Ref.3.1), is the most relevant procedure as it is simple and attractive to the engineer. It begins with a gussed mode shape and obtains, quickly, reasonable results for the wanted mode shape and its frequency.

The matrix equation of motion of an elastically connected system of masses undergoing free undamped vibrations is given, according to Newton's second law of motion, as

$$[m]\,[\ddot{X}] + [k]\,[X] = 0 \qquad (3.1)$$

where $[X]$ = column vector of displacements;

$[\ddot{X}]$ = column vector of accelerations, $(\ddot{X} = d^2X/dt^2)$;

t = time;

$[0]$ = the zero matrix;

$[k]$ = stiffness matrix of the vibrating system; and

$[m]$ = mass matrix of the vibrating system, which has a diagonal form for lumped mass systems.

Using the assumption of harmonic motion, we have $[\ddot{X}] = -\omega^2[X]$, where ω = angular frequency. Thus, it appears that the problem is an eigenvalue problem. If the stiffness matrix, $[k]$, of the system is easy to obtain, Eq. 3.1 is premultiplied by the inverse $[m]^{-1}$ of the mass matrix to give, after some algebra

$$[X] = \frac{1}{\omega^2} [m]^{-1} \cdot [k] \cdot [X] \tag{3.2}$$

which can be solved by iteration, provided ω^2 is real and positive.

The iterative procedure starts by assuming a mode shape for the R.H.S. of Eq. 3.2 and then calculating an improved mode at the L.H.S. This improved mode shape is normalized and used again on the R.H.S. to get a further improved mode on the L.H.S., and so on.

This iterative procedure converges, usually, to the lowest value of $(1/\omega^2)$, i.e. to the highest angular frequency ω. The sweeping procedure can then be used to get the lower modes, (Ref. 3.1). Alternatively, after getting the highest mode, the lowest mode can be obtained using the parallel shift method, (Ref. 2.10).

* * *

However, for most structures, it may be easier to obtain the flexibility matrix $[k]^{-1}$. In some cases, it may be impossible to get the stiffness matrix, (if the flexibility matrix is singular). Here, Eq. 3.1 is premultiplied by $[k]^{-1}$ to give after some algebra:

$$[X] = \omega^2 [k]^{-1} \cdot [m] \cdot [X] \tag{3.3}$$

which can also be solved by iteration as mentioned above. The iterative procedure converges here to the lowest ω^2, i.e. to the fundamental (=lowest) mode which is more useful. Higher modes can then be obtained using the sweeping procedure. The sweeping matrix of the first mode is given in Ref. 3.1, and that of the first and second modes has been derived by the writer.

Rayleigh's quotient, (Refs. 3.1, 3.2) can be used to check the value of the fundamental frequency.

3.3 ILLUSTRATIVE EXAMPLE

The iterative procedure was applied first to the triple pendulum of Fig. 3.1. This elementary example of wires and masses, without elasticity, is given in order to clarify simple ideas, both analytically and experimentally.

The problem has three degrees of freedom, and so three modes of vibration were calculated and also measured, Fig. 3.2, from which it appears that the calculations agree quite well with the measurements, except perhaps in the modal shape of the second mode.

The solution was carried out using both the stiffness and flexibility matrix procedures. The stiffness matrix procedure converges first to the highest mode, (mode 3), while the flexibility matrix procedure converges first to the fundamental (=first) mode. A check using Rayleigh's quotient was made to get an estimate for the fundamental frequency.

The modes were not easy to excite by hand: the system had to be excited first by starting the wanted mode with its natural frequency. After making some calculations, the system was excited, at the three mass positions simultaneously, in each of the three natural modes, (one mode at a time), and the frequency of each mode was measured using a stop watch.

Again, the iteration method used in this example can give all the modes of a three-degrees-of-freedom system, or, at most, a four-degrees-of freedom system. For a system with more degrees of freedom, the iteration method must not be used to get more than the first three modes to avoid complexity in the sweeping matrices, and also to avoid the inaccuracy in calculating the higher modes due to the accumulation of impurities from the first few modes.

If all the modes, or more than three modes, are wanted, it is better to use some more general computerized procedure, as will be shown in chapters IV and VI.

* * *

The results of the iteration are independent of the first guess of the modal shape, $[X]_o$, for each mode. However, a reasonable guess makes the iterative analysis converge quicker. It also gives a good estimate to the fundamental mode using Rayleigh's quotient. In this example, for all modes, the guessed mode shape was $(X_1:X_2:X_3)_0 = (1:2:3)$, and convergence was achieved rapidly.

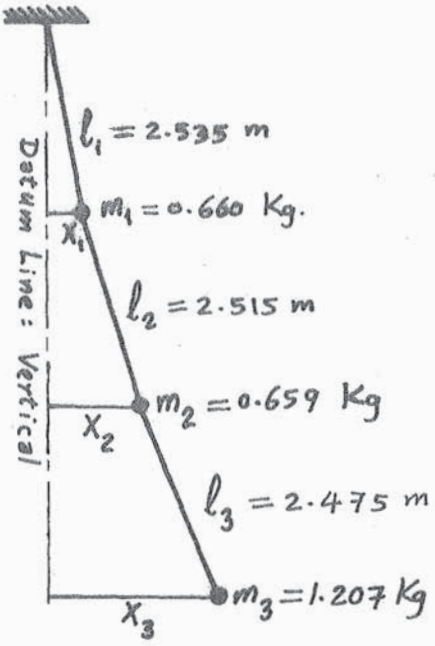

Fig. 3.1.– The Triple Pendulum.

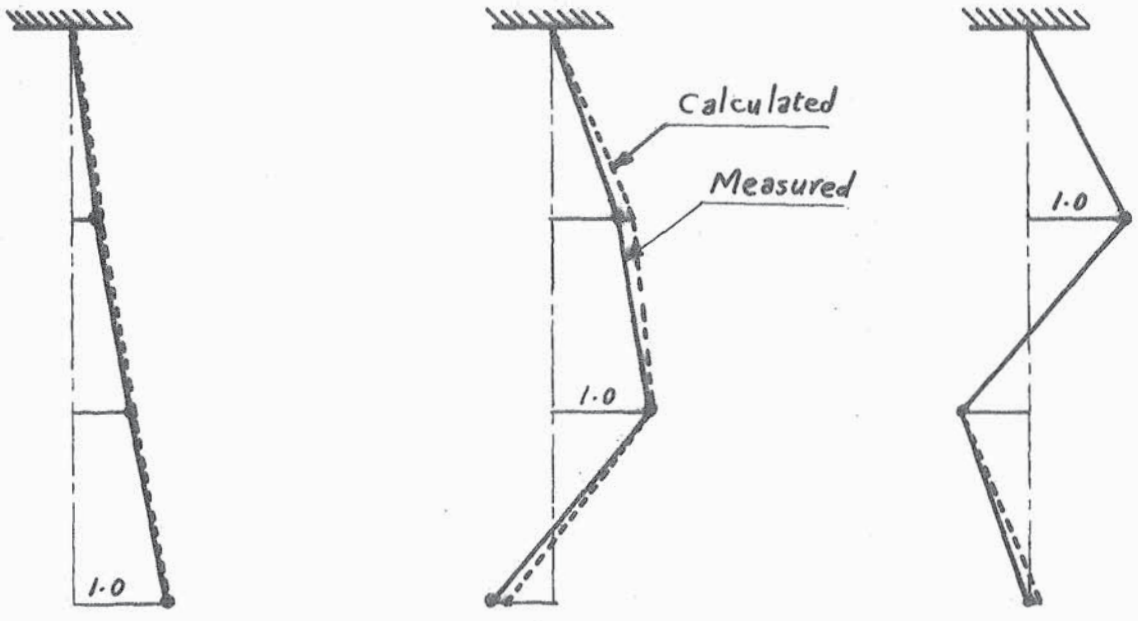

Mode 1 Mode 2 Mode 3

Frequency:			Shape:
Measured:	0.20 Hz.	0.56 Hz.	0.90 Hz. ———
Calculated:	0.196 Hz.	0.563 Hz.	0.929 Hz. - - - - - - -
Rayleigh:	0.196 Hz.		

Fig. 3.2.– Natural Modes of the Triple Pendulum.

3.4 APPLICATION TO THE SINGLE-CABLE BRIDGE MODEL

The above analysis was applied to the laboratory model of the single-cable suspension bridge using the flexibility matrix. For most structures, the flexibility matrix is very much easier to calculate, or to measure, than the stiffness matrix. For the model of the single-cable bridge, as is usual for other suspension structures, it was found that the flexibility matrix is singular, and so it becomes only possible to use the flexibility matrix procedure in the dynamic study. For more information about singular matrices see Appendix A4.

Firstly, the flexibility matrix of the model was calculated using Timoshenko's energy method, (Ref. 1.14), (because it gave the best agreement with the laboratory model measurements). An influence load was placed in turn at nine stations on the span, and the deflected shape calculated.

It was not considered sufficient to just use this calculated flexibility matrix in a subsequent dynamic study without checking it against statical measurements on the laboratory model, even though this required much careful work. The work was systematically done, and measured flexibility matrices for three loading conditions showed good agreement with calculations, as shown in Fig. 3.3. In both calculations and measurements, the influence coefficients, (flexibility matrix elements), were obtained by the secant to an influence load equal to 12.5% of the total D.L. on the bridge, which was applied at one station at a time. It can be said that we have here a satisfactory method of obtaining a flexibility matrix.

The iterative procedure was used to calculate the first three modes of vibration. The model has nine degrees of freedom; in the laboratory, only the first two modes could be excited and measured. The frequencies were measured by direct counting and using a stop-watch, while the amplitudes were measured using dial gauges with some additional accessories, designed by the writer with the aid of technical staff to stay in the position of maximum amplitude, (Fig. 3.4).

A comparison between calculations and measurements is shown in Figs. 3.5, 3.6, for the D.L. condition and for one L.L. condition, from which it can be seen that the agreement is good for the D.L. condition, (Fig. 3.5), for both the frequencies and the mode shapes. For the L.L. condition, (Fig. 3.6), the frequencies agree well but the modes seem to be somewhat shifted.

For the D.L. condition, (Fig. 3.5), the fundamental mode, being anti-symmetric, is what may be called a "non-stretching mode", that is, there is no cable stretch, and there is a good agreement between the measured and calculated frequencies and mode shapes. The second mode is a symmetric "stretching mode", (one involving cable stretch), and also there is a good agreement between measured and calculated frequencies and mode shapes. The

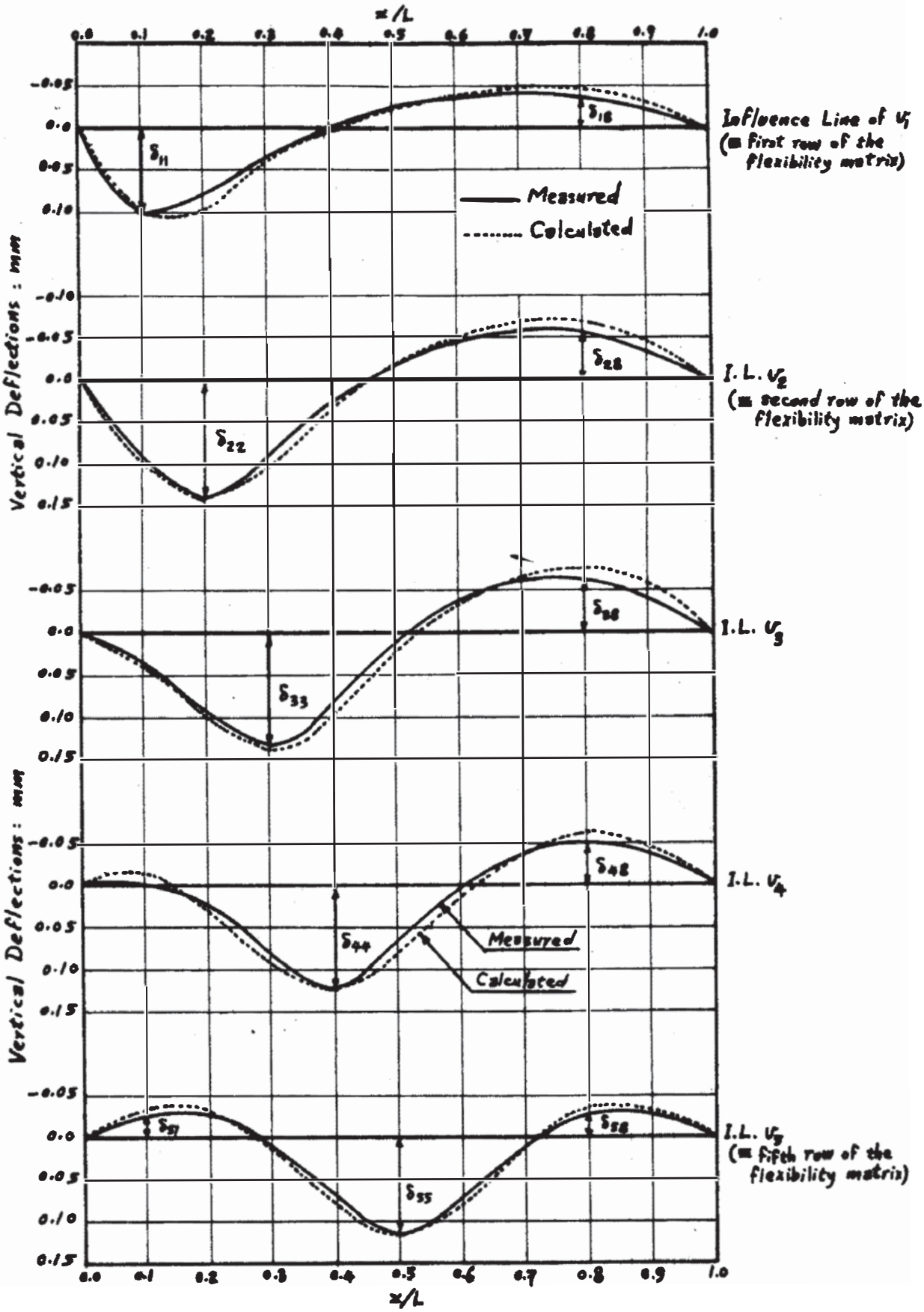

Fig. 3.3.— Secant Flexibility Matrix; Influence Load = $\frac{1}{8}$ of the Total Dead Load on the Laboratory Model.

(a) Dead Load Condition.

Full line = Measurements

Dotted line = Calculated Values

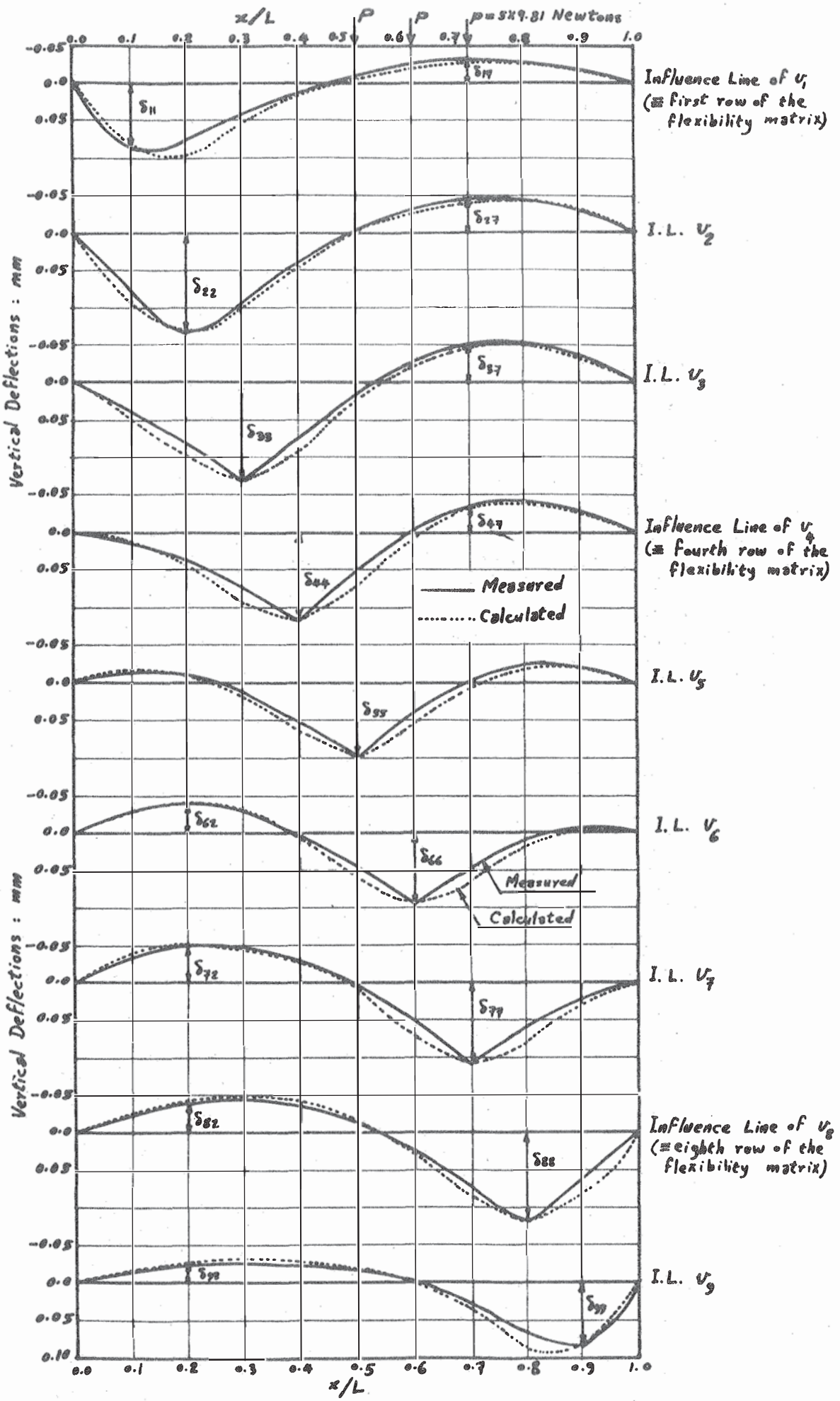

Fig. 3.3.—Secant Flexibility Matrix ; Influence Load = $\frac{1}{8}$ of the Total Dead Load on the Laboratory Model.

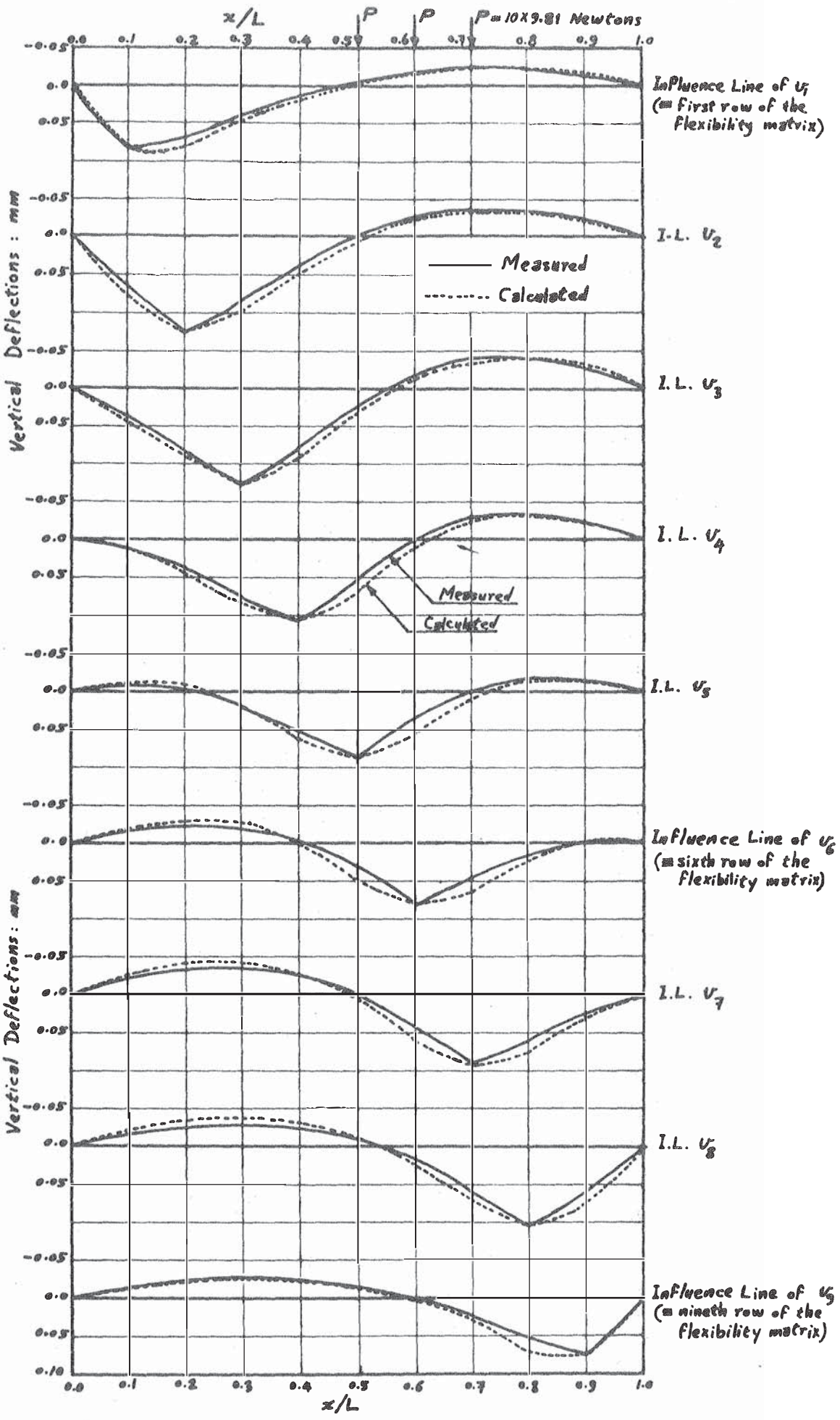

Fig. 3.3.– Secant Flexibility Matrix; Influence Load = $\frac{1}{8}$ of the Total Dead Load on the Laboratory Model.

(c) Live Load: Three Point-Loads as Shown.

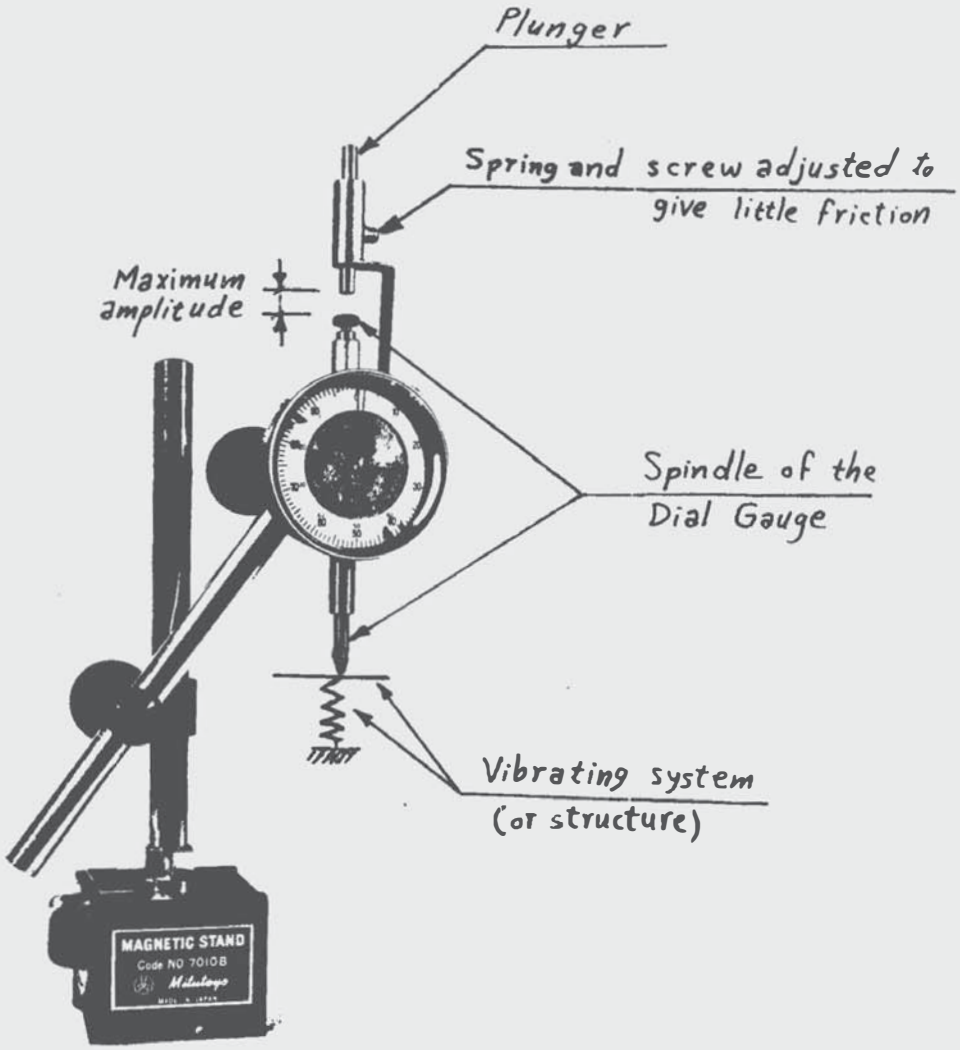

Fig.34.-Dial Gauge With Device To Measure The Maximum Excursion.

The plunger is left behind at the position corresponding to the maximum movement (amplitude) experienced by the spindle of the dial gauge, very much as a dead pointer shows the maximum load in a test carried out in a testing machine. Later, the spindle of the dial gauge is moved so that its top just touches the plunger, and a reading is obtained.

Note:

The wanted harmonic mode of vibration of the structure must be built up slowly and carefully, without transients, for the above method of measurement to be workable. Several such gauges on the structure, conveniently positioned, give the mode.

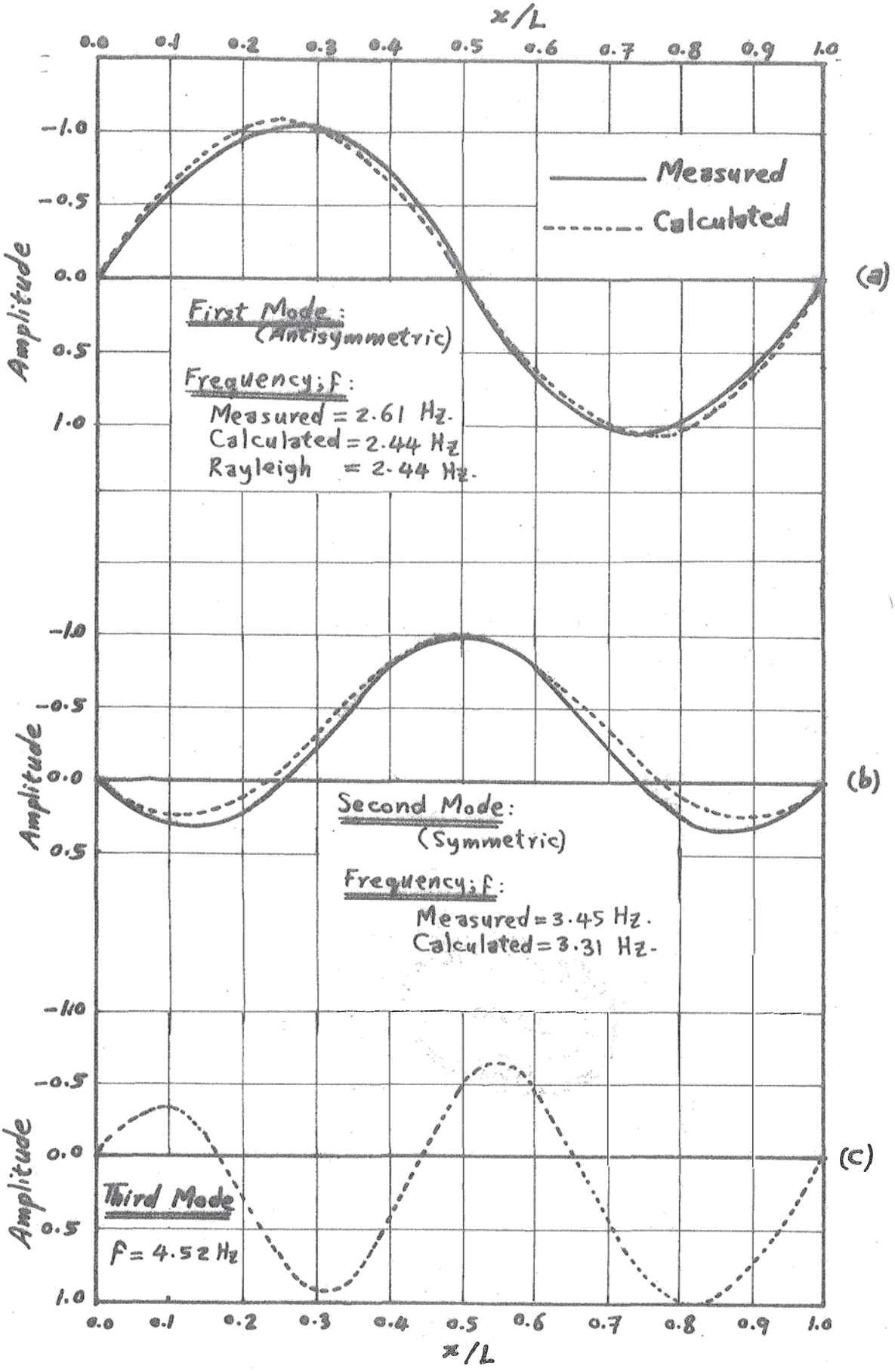

Fig.3.5.- First Three Vibration Modes:

Dead Load Condition.

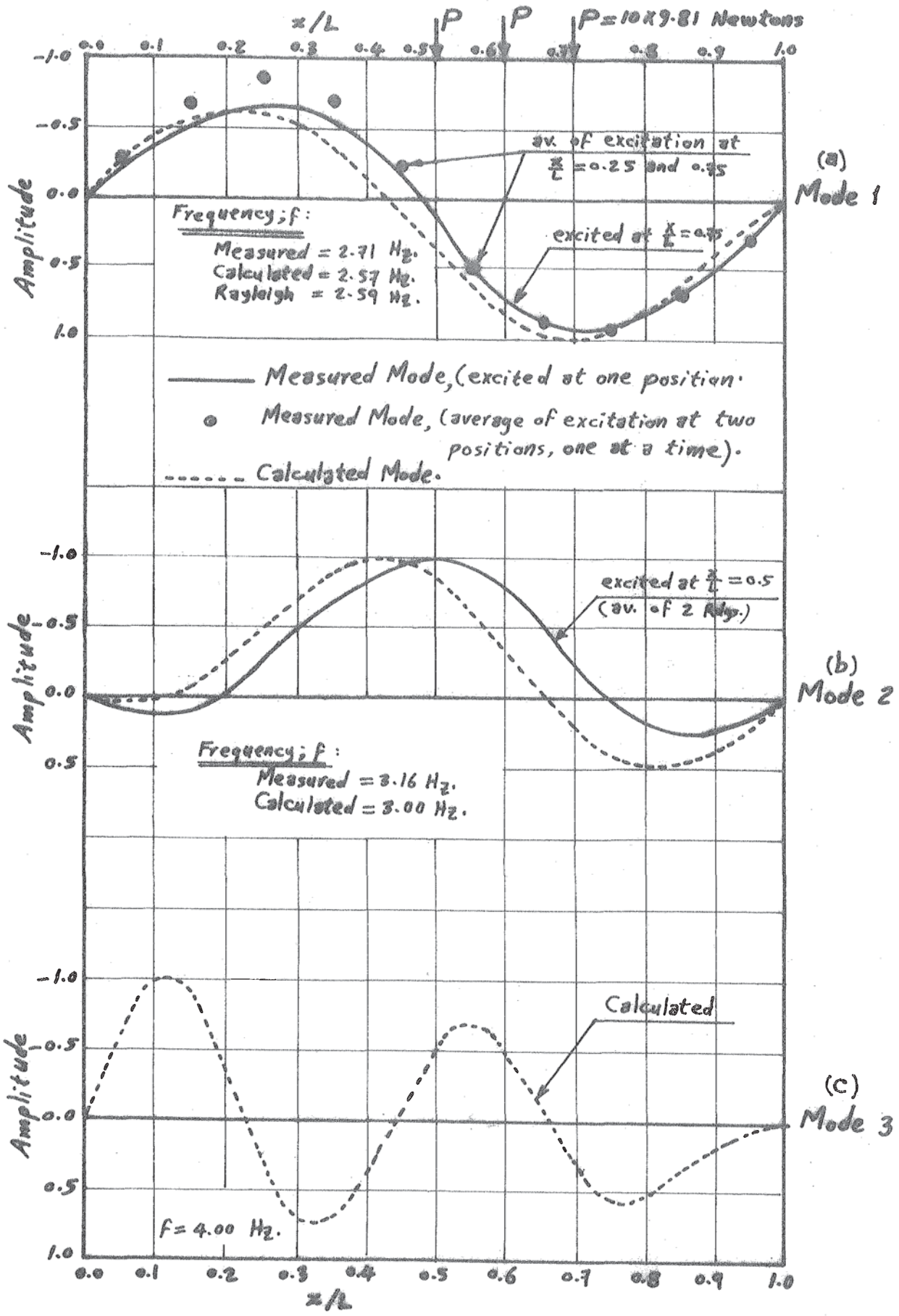

Fig. 3.6.— First Three Vibration Modes.

Live Load: Three Point-Loads as Shown.

third mode was only calculated and could not be measured. It was expected to be antisymmetric with two complete sine waves, but it was not found to be quite so. The reason, perhaps, is the impurities accumulated from the first two modes in the sweeping matrix which is calculated to get the third mode. Although the third mode is not thus accurately calculated, the designer may still be glad to have an estimate of it.

An estimate for the fundamental frequency was obtained using Rayleigh's quotient with a guessed mode having one or two sine waves, which gave nearly the same value as obtained by the iterative procedure. This emphasizes the fact that Rayleigh's quotient gives a good estimate, (an upper bound), for the fundamental frequency for a large margin of guessed modes, (Ref. 2.10, pp. 86-88).

For the L.L. condition, Fig. 3.6, the first three modes were calculated and again only the first two were measured. Reasonable agreement was obtained regarding the measured and the calculated frequencies. In the laboratory, the first mode was excited, (with the hand), as in the D.L. condition, at $\frac{X}{L} = 0.25$ once and $\frac{X}{L} = 0.75$ another time, and the average mode shape was obtained. But, as is clear from the calculations, the mode is not antisymmetric; it has deflections on the loaded side of the span greater than those on the unloaded side, causing some stretch in the cable. It was noticed that exciting a mode from one position only produces larger amplitudes, (or excessive displacements), in the vicinity of the excited position, and so it becomes more suitable to excite each mode at the position of maximum deflection, (or nearly so). For that reason, the mode excited at $\frac{X}{L} = 0.75$ shows better agreement with measurements as in Fig. 3.6a. The maximum deflection seems to be not exactly at $\frac{X}{L} = 0.75$ but shifted a bit to the left, i.e. a little away from the loaded zone. The second mode also has maximum deflection some distance away from the loaded zone.

The third mode, as calculated, seems again to be not reliable; the iteration method is thus not recommended for getting more than the first two modes, especially when the number of the degrees of freedom of the system is more than three or four.

3.5 VARIATION OF FREQUENCY WITH LIVE LOAD

This may be of importance for real suspension bridges. It appears to go unmentioned in the literature.

The influence of imposing L.L. on the bridge, on the frequencies of the first two modes, was investigated. Three point-loads, each equal to P, acting at $\frac{X}{L} = 0.5, 0.6, 0.7$ from the left support were used, varying from P = 0 until P = 16 x 9.81 Newtons in increments of 2 x 9.81 Newtons. The first two frequencies were measured and calculated for each loading condition

and an estimate of the fundamental frequency was also evaluated using Rayleigh's quotient. The results are shown in Fig. 3.7.

Before discussing Fig. 3.7, the following must be realised.

(i) For the usual elastic structure, more mass gives lower frequency if all the other factors are the same, which really means if the stiffness matrix goes unchanged.

(ii) For a suspension structure, more L.L. means greater stiffness, (according to Fig. 3.8), and this gives higher frequency.

(iii) More L.L. gives more cable stretch due to vibrations, and more cable stretch also means more stiffness, (Fig. 3.8), and this yields higher frequency as in (ii) above.

Now Fig. 3.7 can be explained as follows:

(1) The fundamental mode, which is generally a non-stretching mode, (although some stretch happens for high L.L.), has an increasing frequency with increasing L.L. due to increasing the stiffness, (as in (ii) and (iii) above), which seem to dominate over the effect of increasing the mass. This is, actually, seen from measurements and calculations, and also from the application of Rayleigh's quotient.

(2) The second mode, which is a stretching mode, has a frequency which decreases with increasing L.L. according to (i) above. The effect of increasing the mass seems here to dominate over the increase in stiffness due to both the static L.L. and the stretch due to vibration.

It is clear from Fig. 3.7 that the calculated frequencies are less than the measured ones for both the fundamental and the second modes. This is expected since the calculated flexibility coefficients are higher than those measured as shown in Figs. 3.3. The reason of this discrepancy is perhaps due to the inaccuracy in measuring the bridge properties and dimensions like AE, EI, ... etc., which were used in calculations. The difference between measurements and calculations, especially in mode shapes, may be due to the following reasons.

(i) The analysis is based on free-undamped vibrations, while the system was excited by the finger, and has some damping. The dial gauges, which were used in measuring the amplitudes, also participate in damping the oscillations.

(ii) To get correct results, we should excite the system in a natural mode, otherwise we will get a combination of different modes. But actually the model was excited by

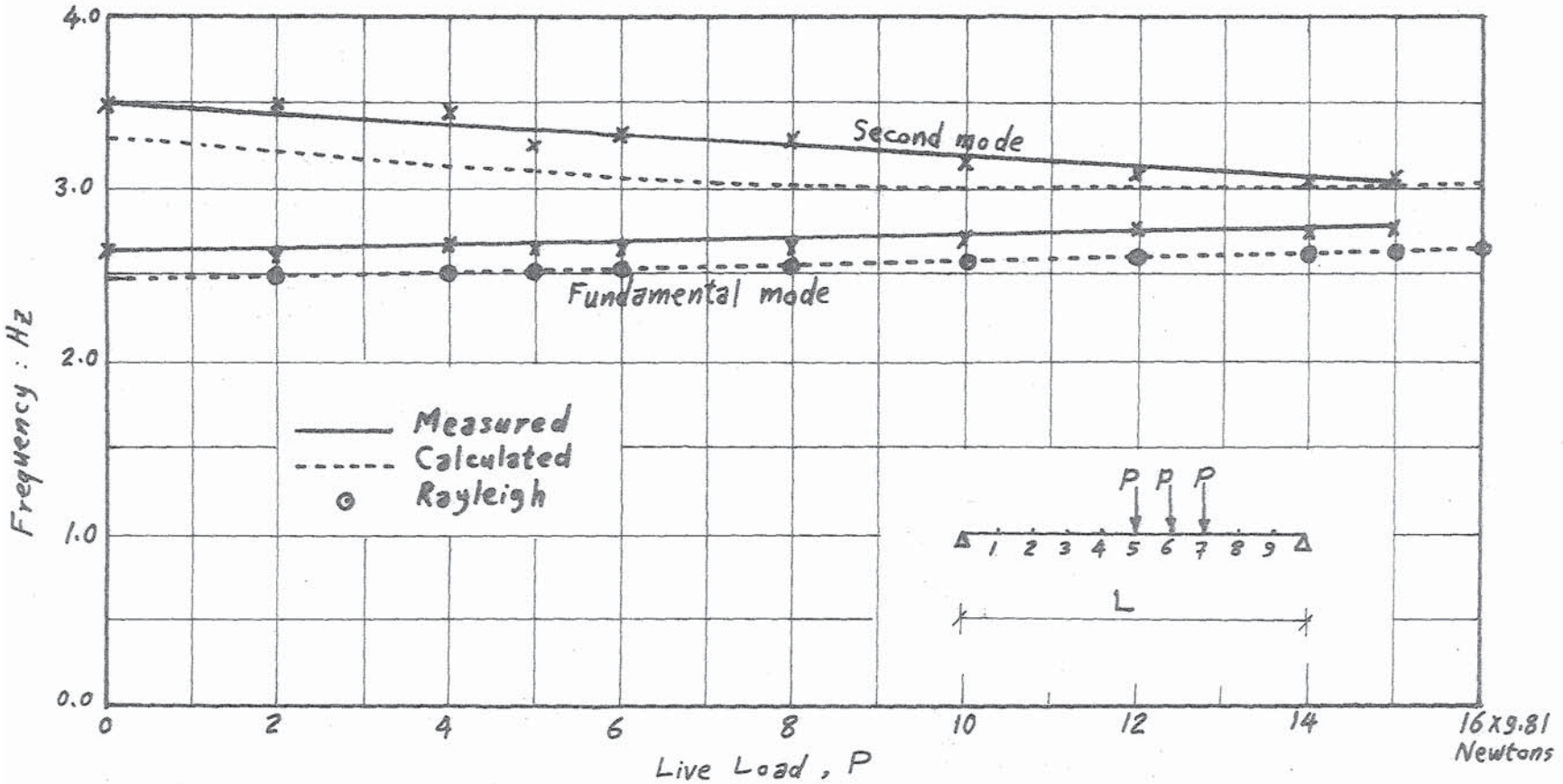

Fig. 3.7.- Variation of Frequency with Live Load.

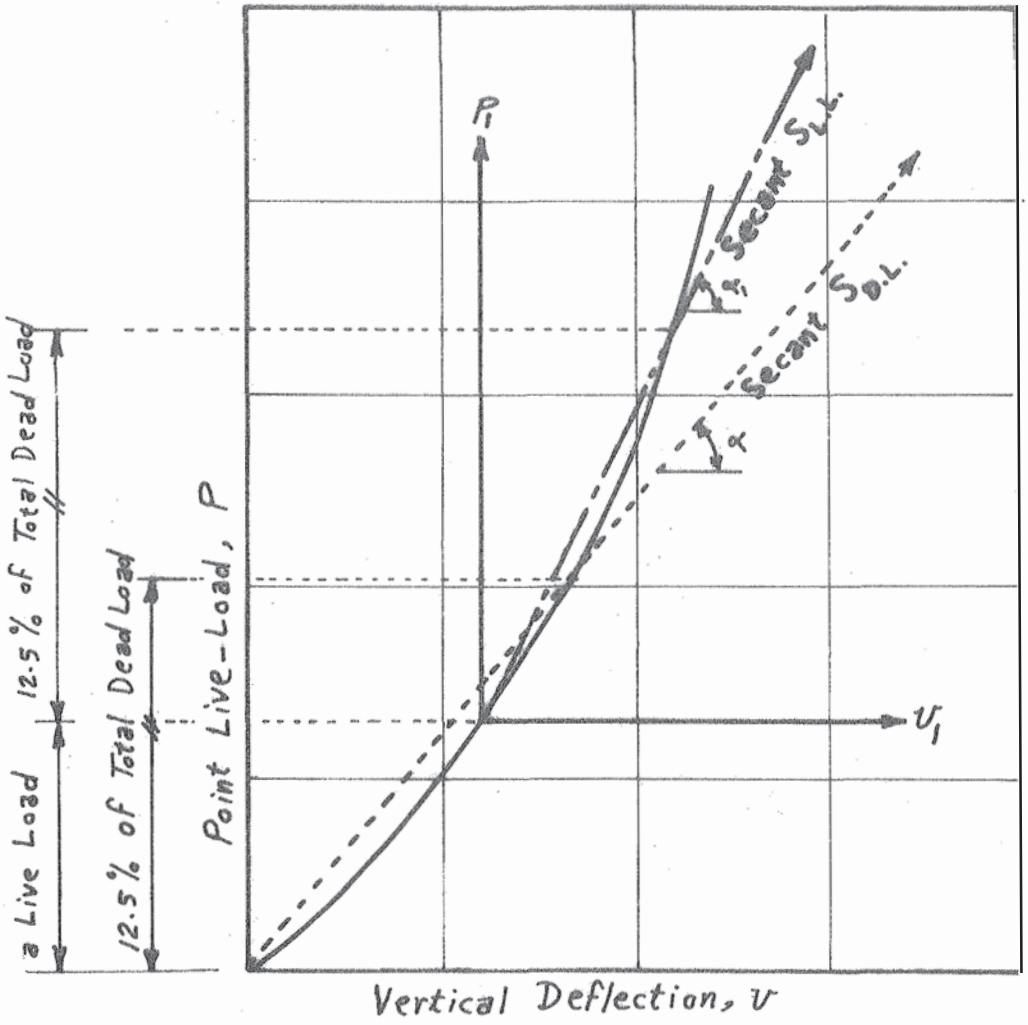

Fig. 3.8.--Typical Load~Deflection Curve for a Suspension Structure.

	Dead Load Condition	Live Load Condition
Axes of Load ~ Deflection Curve	$P \sim v$	$P_1 \sim v_1$
Secant to 12.5% of Dead Load	$S_{D.L.}$	$S_{L.L.}$
"Stiffness Coefficient"	$\tan \alpha$	$\tan \alpha_1$
Flexibility Coefficient	$\cot \alpha$	$\cot \alpha_1$

finger* from one position only** and not from all the stations.

(iii) The iterative procedure is based on using real matrices which have real eigenvalues and eigenvectors, and this can be only guaranteed for symmetric matrices. The flexibility matrix of our model is in the first place a fairly drastic simplification of real non-linear behaviour. Moreover, it is not symmetric, and also it is singular or nearly so. It is though not very far from symmetric, and this is the reason for giving adequate results for the first two modes.

(iv) The model itself is not exactly symmetric since backstay No. 1, (on the double lever side), is shorter than backstay No. 2, (resulting in some difference in the tower top movements and consequently the flexibility coefficients). Also, there is a rigging screw in the first segment of the main cable, (from the double lever side), while there is no such rigging screw on the other side, and this affects the flexibility coefficients.

(v) There may be some inaccuracy in measuring the vibrational mode shapes and frequencies.

3.6 STRESSES DUE TO VIBRATIONS; INTRODUCTORY REMARKS

One may ask: what is the use of studying the vibrations of structural systems and getting their mode shapes and frequencies? The answer is simple: vibration causes alternating displacements and strains, which in turn cause alternating stresses, and these yield the possibility of local fatigue of the structure, or of overall failure. Also, the first Tacoma Bridge was safe against static wind loads, but it was aerodynamically unstable due to ignoring the aerodynamic action of wind, (Ref. 1.6, pp. 362-363).

The foregoing analysis was based on free-undamped vibrations, which is a simplification of the problem of a real suspension bridge, and of our laboratory model as well. Damping may be regarded as small and having little effect on the magnitudes of the natural frequencies of the system, (but large enough to limit the resonant amplitudes to measurable bounds).

In summary, if the exciting forces are ignored, the natural frequencies and the normal modes can be obtained. However, if the exciting forces are

---

* Mechanical excitation could not be used because of the low frequencies of the model.

** Position of maximum displacement.

known, they may be introduced as a column vector on the R.H.S. of Eq. 3.1; the equation can be solved to get the actual magnitudes of the displacements instead of just their ratios to one another, (Ref. 3.3, pp. 86-87).

The magnitudes of the amplitudes are thus calculated from the equation $[m][\ddot{X}] + [k][X] = [F]$, where F is the harmonic forcing.

Once the deflection curve becomes known, it can be differentiated twice to get the curvature diagram,(of the deck), then the bending moment diagram,(or the strains), and finally the stress distribution due to vibrations. This amounts to saying that a mode of vibration, with known amplitudes, determines shape, shape determines strains and therefore stresses.

The above is what the designer needs. He will specify his materials of construction by deciding whether the structure is safe or not against these fluctuating stresses due to vibrations. The Australian Standards of 1968,(Ref. 3.4), for example, limited the maximum working tensile (or compressive) stresses in the case of fatigue,(with equal tensile and compressive stress at each section), to 4.3% to 27.1% of the yield stress of the material of construction, for a life equivalent to 100×10^6 cycles, according to the efficiency and care in construction and erection.

Sometimes, an unwanted or dangerous mode of oscillation can be restrained by ties. This has been done for some bridges.

CHAPTER IV

DYNAMICS OF SUSPENSION CABLES AND NETS

4.1 INTRODUCTION

This chapter contains ideas and methods directly useful for designers of suspension roofs and suspension bridges. The first example represents the suspension cable: a case of a suspension bridge during erection with its cables extending between towers with the deck not yet suspended or not yet connected up. In the second example given, the suspension net, we are concerned with both the gravity stiffness and the elasticity of the cables (since there is no deck). So we are facing the basic action of a set of hanging wires and gravity.

The statics of suspension cables and nets was previously studied by the writer, (Ref. 4.1), as well as by many other authors, (Refs. 4.2-4.7). Their dynamics have also received considerable attention, (Refs. 4.8-4.11). In Ref. 4.11, for example, plane cables only were studied and were assumed to be inextensible in the calculation of the influence coefficients.

The aim of this chapter is to present a quick study of the dynamic behaviour of suspension cables and nets. Measurements of the natural frequencies and modes of vibration are compared with the results of calculations.

4.2 THE SUSPENSION CABLE

The suspension cable only of the laboratory model of the single-cable bridge was first studied briefly using the iteration method. The flexibility matrix was calculated for the cable using Timoshenko's energy method, (Ref. 1.14), by putting the deck stiffness, EI, equal to zero.

A comparison was made between the dynamic response of both the entire bridge and the cable alone, (bridge without deck), carrying the same loads, Figs. 4.1-4.3. It is clear from the graphs that both systems have nearly the same dynamic characteristics. The cable seems to have slightly lower frequencies than the bridge for all cases of loading. This is because the deck, no doubt, increases the stiffness of the structure slightly, and consequently increases the natural frequencies.

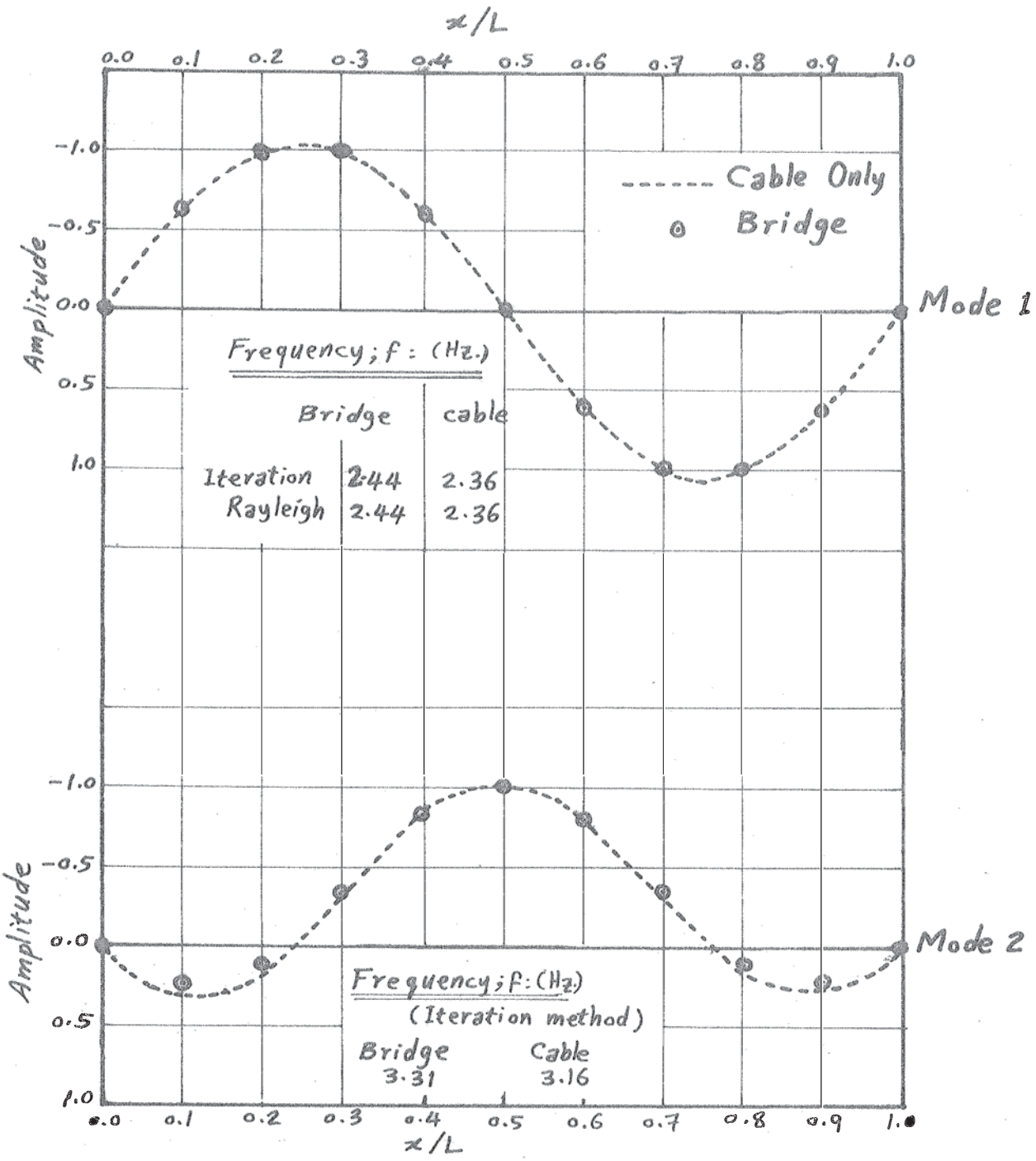

Fig. 4.1.– First Two Modes of Vibration, Calculated, for the Dead Load Condition.

Comparison Between the Single-Cable Bridge and the Cable Only.

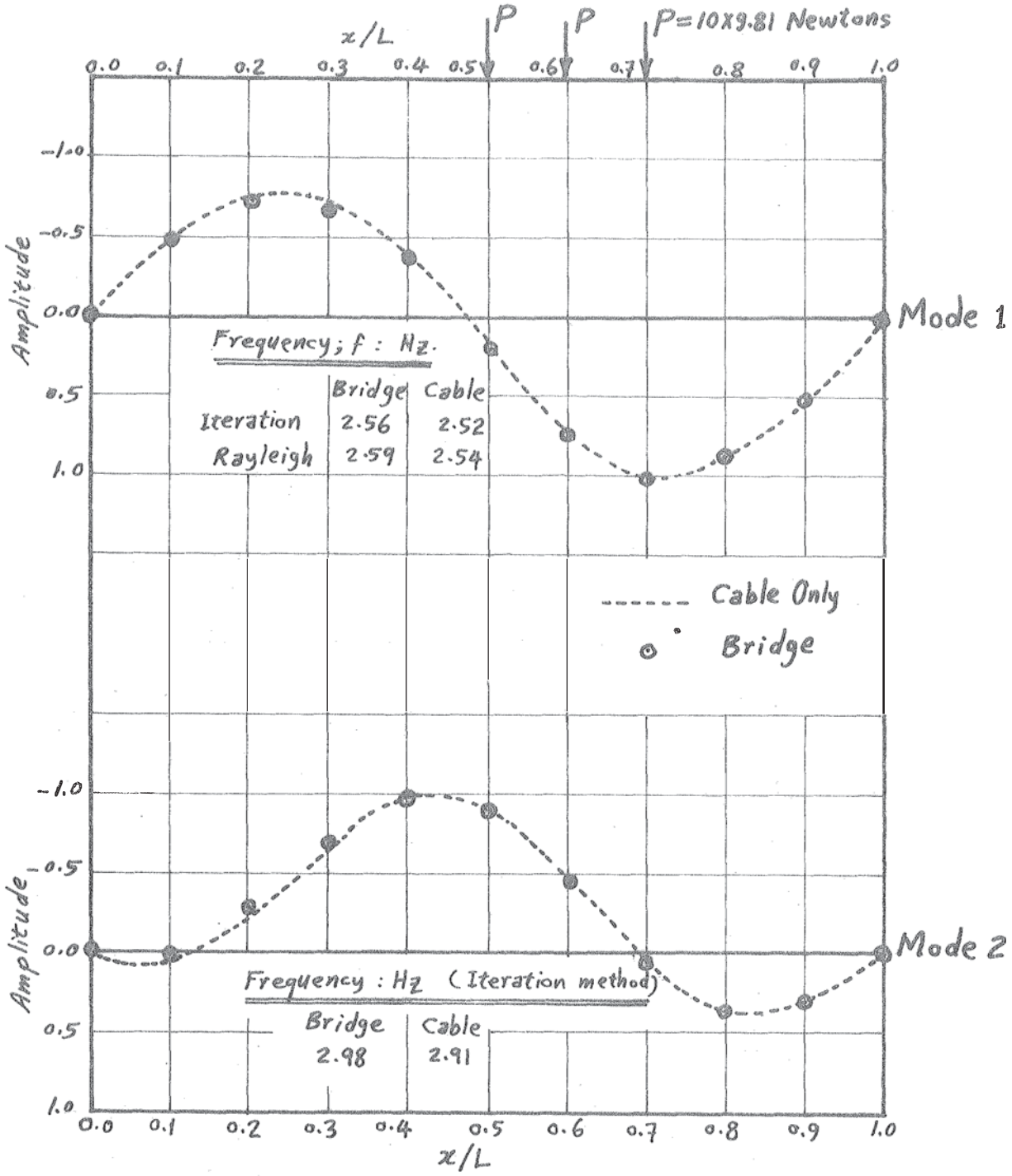

Fig. 4.2.— First Two Modes of Vibration, Calculated, for the Shown Live Load Condition.

Comparison Between the Single-Cable Bridge and the Cable Only.

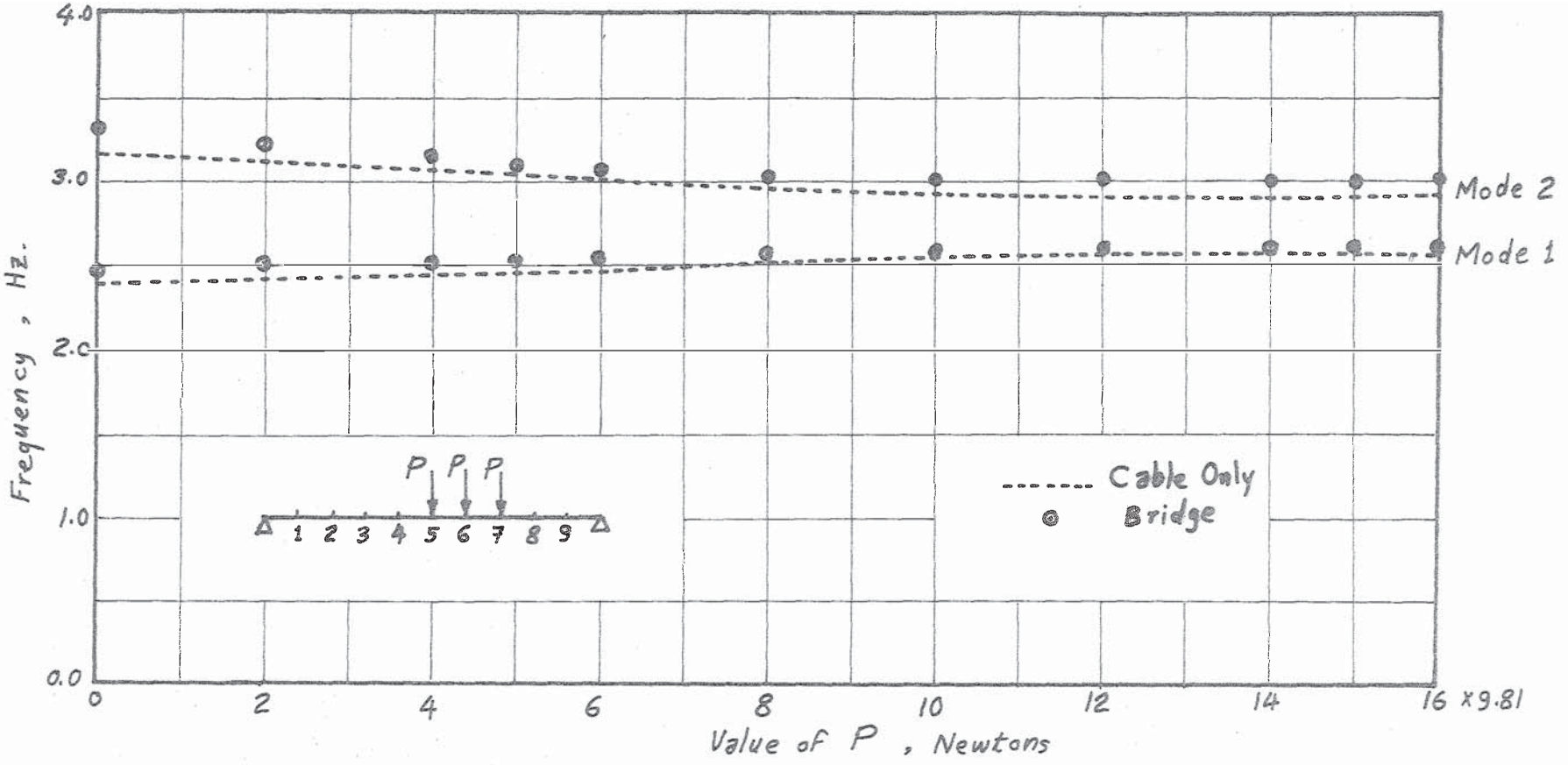

Fig. 4.3.- Variation of Frequency, with Live Load, For Both the Single-Cable Bridge and the Cable Only.

Live Load is Three Point-Loads as Shown.

The mass of our deck is small compared to the masses hanging on the cable, and so it does not lower the frequencies of the bridge considerably. Thus the difference between the frequencies of the bridge and the cable is not considerable because of the low stiffness of the deck.

Fig. 4.4 shows the cable frequency versus the loaded length of a given L.L. It can be seen that maximum frequency for mode 1 and minimum frequency for mode 2 are obtained when the L.L. is spread over half the span. It can also be seen from Fig. 4.5 that moving the load towards the centre of the span increases the fundamental frequency and lowers the frequency of the second mode. Generally it appears from Figs. 4.3-4.5 that any increase in the fundamental frequency, due to any change in the loading conditions, is always associated with a reduction in the frequency of the second mode.

From Fig. 4.6 it can be emphasized, as was noticed in chapter III, that the application of L.L. makes the amplitudes under the L.L. greater than the corresponding amplitudes if the L.L. is absent. Also, it is seen that when a L.L. is covering the entire span, the mode shapes are similar to those of the D.L. condition, with slight reductions in the frequencies due to the increase in the mass which seems to dominate over the rise in the stiffness.

4.3 THE SUSPENSION NET

4.3.1 General

A paraboloid surface, square in plan, was built with rigid boundaries and three high tensile steel wires in each of the two orthogonal directions, normal to the sides of the rigid square boundary. All the wires have positive dip-span ratios of 0.10. The nine intersections of the cables form joints at which the dead and live loads were applied. It is to be noted that the intersections of different cables with each side of the square rigid boundary are located on a parabola similar in shape to the wire shapes, as shown in Figs. 4.7, 4.8.

Wires 0.56 mm in diameter were used with a yield stress = 2000 Mpa ≈ ultimate stress. The D.L. at each joint is 3 x 9.81 Newtons.

Analytical and experimental studies were carried out on the dynamic response of the model for the D.L. condition only. The same procedure can easily be applied to any L.L. condition as previously dealt with in both the single-cable bridge and the suspension cable.

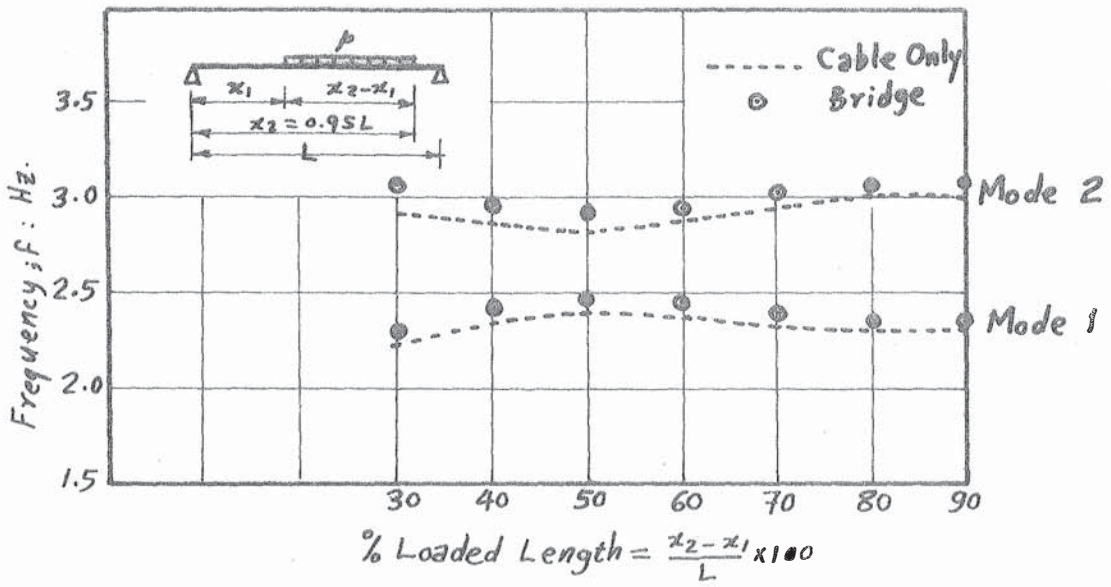

Fig. 4.4.- Effect of Loaded Length on Frequencies.
Total Live Load = $p(x_2 - x_1) = 30 \times 9.81$ Newtons.

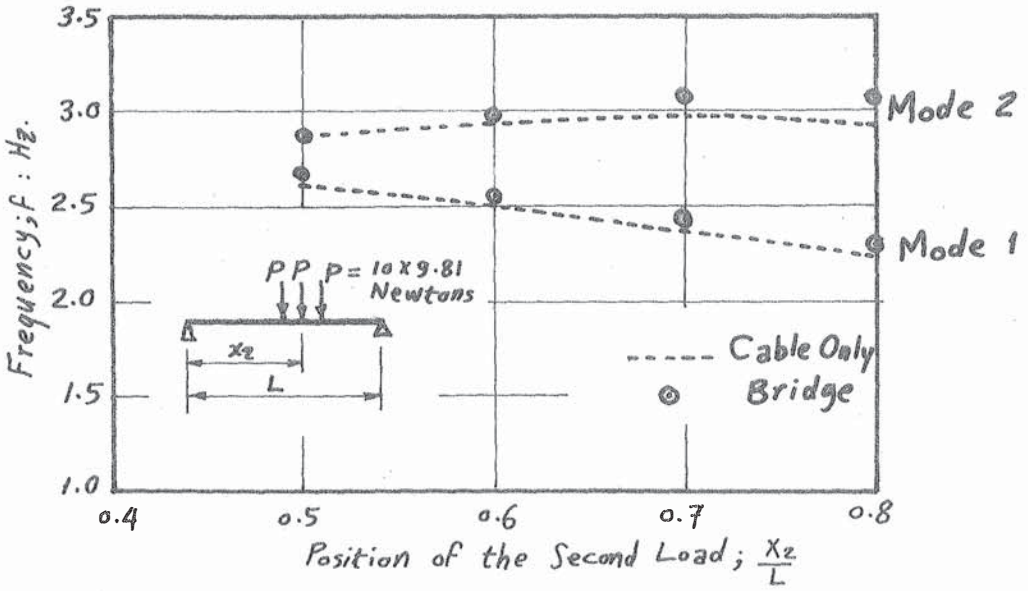

Fig. 4.5.- Effect of Load Position on Frequencies.
Live Load is Three Point-Loads Travelling Across the Span.

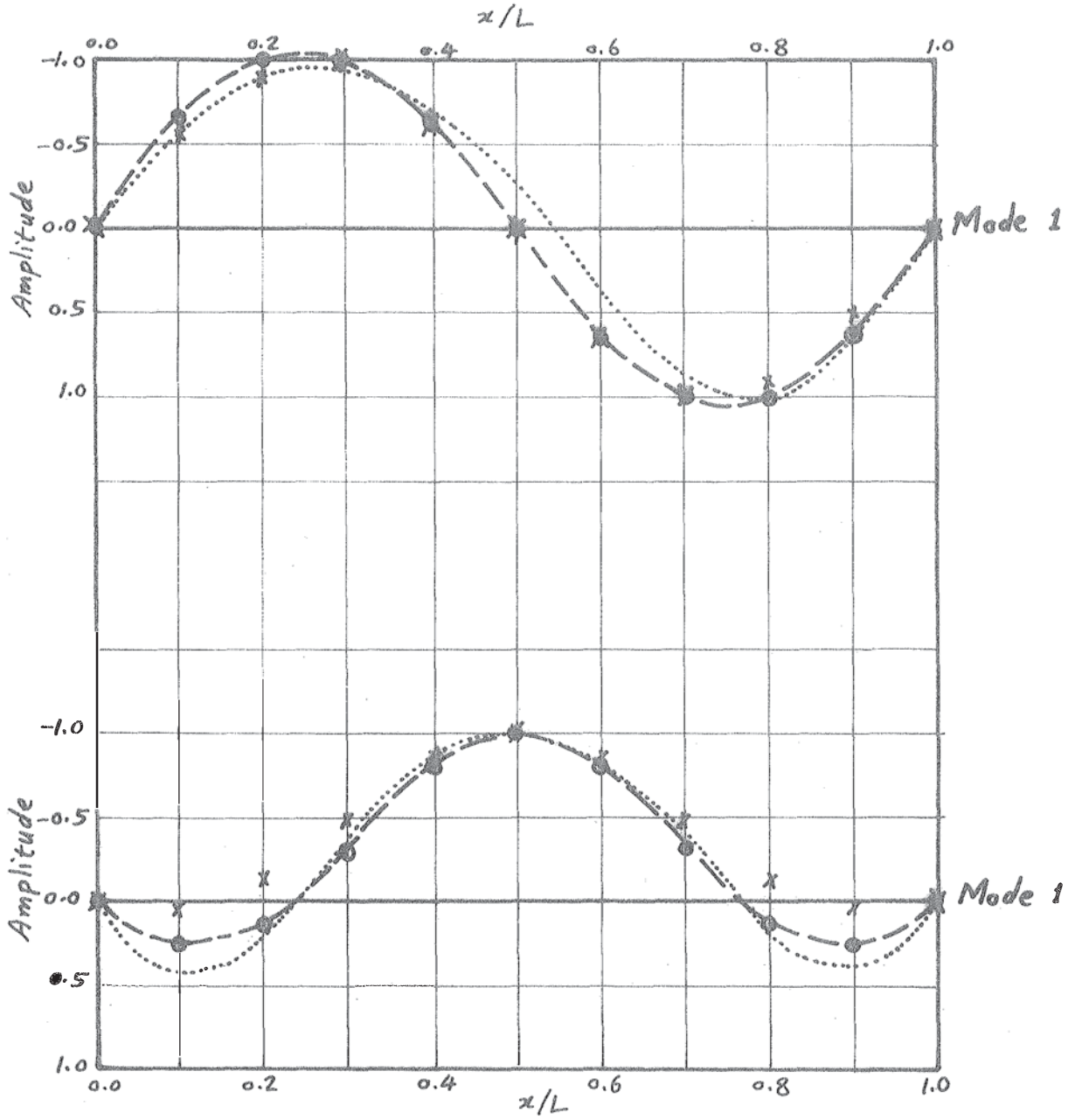

	Loading Condition	Frequency, Hz.		Remarks
		Mode 1	Mode 2	
o	Dead Load Only	2.36	3.15	
— — —	P P P P P P P P P 1 2 3 4 5 6 7 8 9	2.30	3.01	P = 3.33 x 9.81 Newtons
x	P P P 1 2 3 4 5 6 7 8 9	2.61	2.87	P = 10 x 9.81 Newtons
.....	P P P 1 2 3 4 5 6 7 8 9	2.25	2.93	P = 10 x 9.81 Newtons

Fig. 4.6.– First Two Modes, for the Cable Only, for Different Loadings.

(a) General View

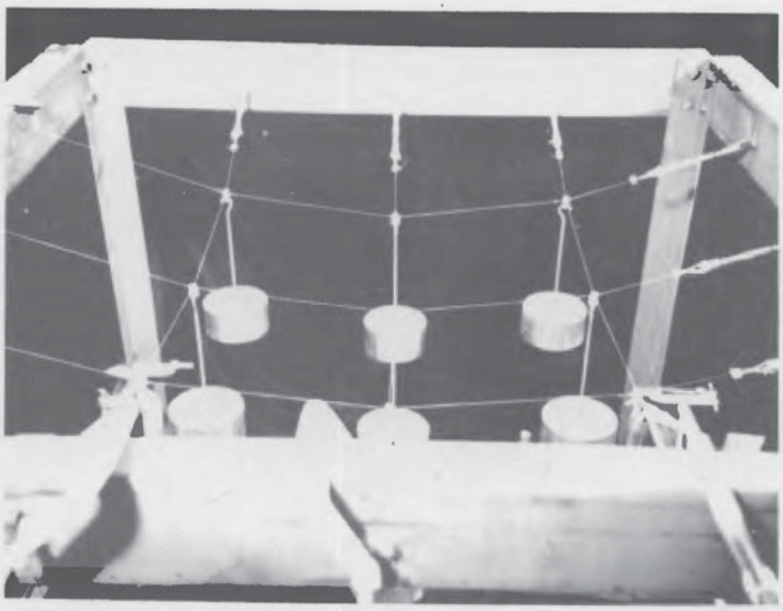

(b) Top View

Fig. 4.7 .- Laboratory Model of the Suspension Net.

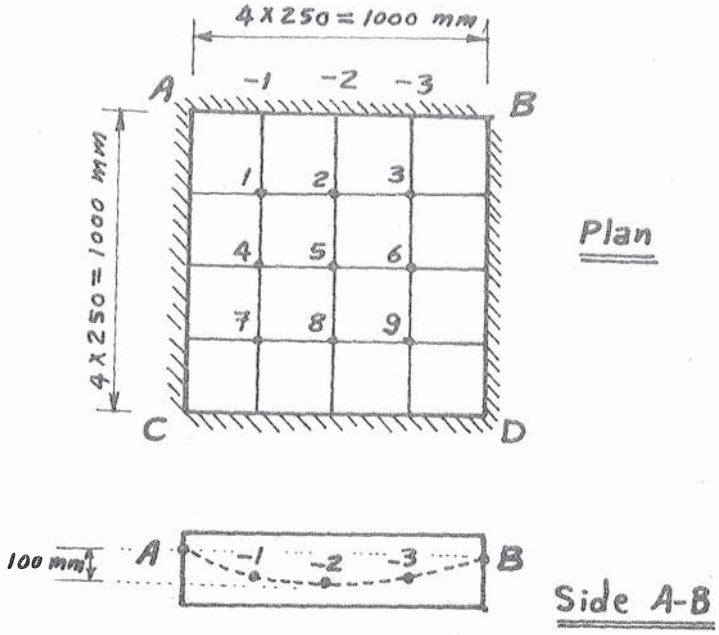

Fig. 4.8

The flexibility matrix of the system was measured and also calculated as the slope of a secant to an influence load = 3 x 9.81 Newtons, which is equal to the D.L. per joint.

The frequencies and modal shapes of the first two modes of vibration were measured using an oscilloscope and the dial gauges with its accessories shown in Fig. 3.4.

Calculations using either the measured or the calculated flexibility matrix showed good agreement with the measured first two modes. Fig. 4.9 shows a summary of the analytical and experimental results.

4.3.2 Measured Flexibility Matrix

The flexibility matrix of the model was measured. It is, as expected for a suspension structure, not symmetric, but yet it is not far from symmetric. A symmetric flexibility matrix gives real latent roots, but our slightly asymmetric flexibility matrix may, or may not, give some complex latent roots.

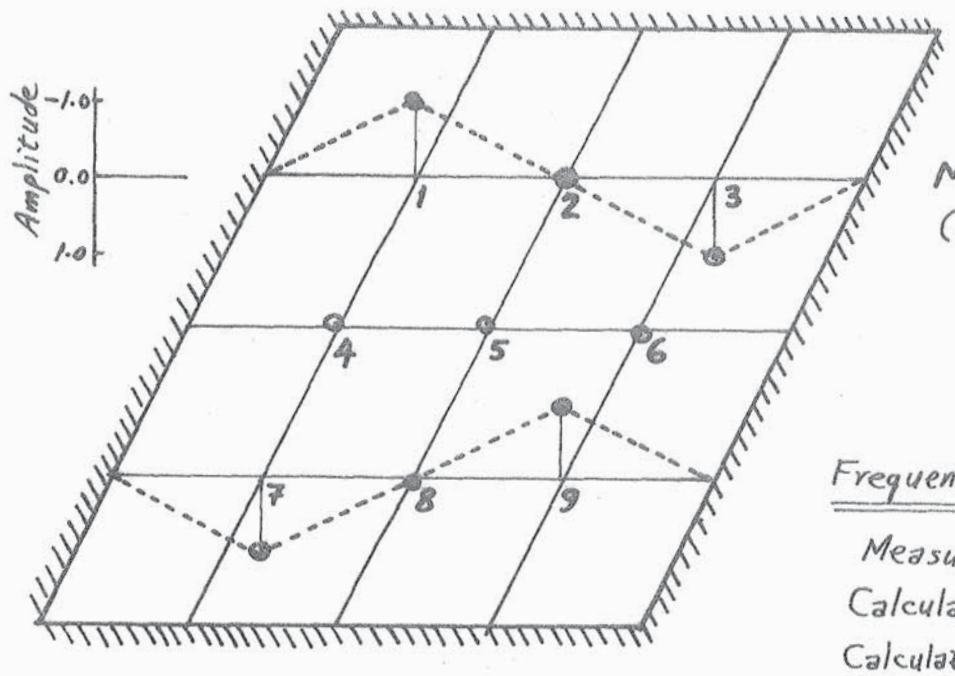

Mode 1
(Antisymmetric, i.e. no cable stretch)

Frequency; f:

Measured: 3.40 Hz.
Calculated*: 3.82 Hz.
Calculated**: 3.34 Hz.

------ Calculated
⊙ Measured

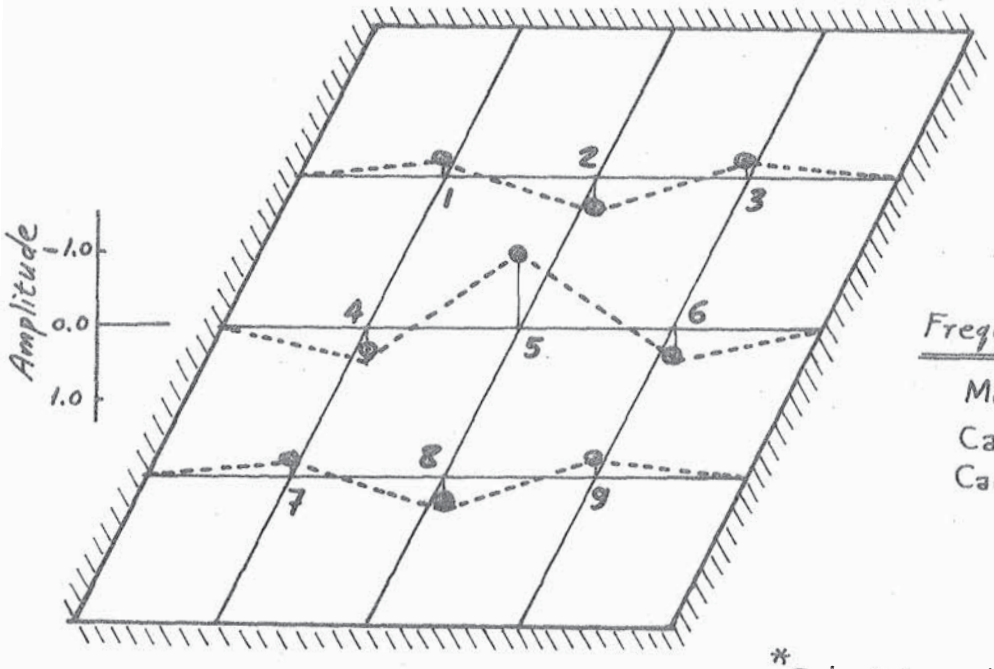

Mode 2
(Symmetric, with perhaps little stretch).

Frequency; f:

Measured: 3.90 Hz.
Calculated*: 4.73 Hz.
Calculated**: 4.65 Hz.

*Calculations based on measured flexibility matrix.
**Calculations based on calculated flexibility matrix.

Fig. 4.9.- First Two Modes of Vibration For the Suspension Net.
Dead Load Condition, Secant Flexibility Matrix,
Influence Load = Dead Load Per Joint.

However, the iteration procedure was carried out to get the first two modes and their frequencies using both: (a) the asymmetric flexibility matrix as it is; and (b) a flexibility matrix made symmetric by taking the average of the off-diagonal elements.

It may be seen, from a first inspection, that the structure has nine degrees of freedom, but if the extensibility of the wires is neglected, the number of degrees of freedom of the system reduces to only three (= 9 joints x 3 deflections per joint - 24 inextensible wire segments).* This means that we can have only three modes of vibration. However, only two "good" modes could be obtained both analytically and experimentally.

The iteration procedure gave nearly the same results for both the asymmetric matrix as it is, and the matrix when made symmetric by taking the average of the off-diagonal elements. Both modes agree well with the measured mode shapes, while the measured frequencies are remarkably less than the calculated ones (by 12% for the fundamental frequency and 20% for the second frequency).

Nearly the same results could be obtained by solving the problem, by computer, by getting the latent roots and latent vectors using the Jacobi method for symmetric matrices, (Ref. 4.12, ch. 10). Even when the asymmetric matrix was solved as it is (without the averaging procedure) it gave, using the Jacobi method, nearly the same solution as when it was made symmetric. It is obvious that the reason is that our flexibility matrix is not very far from symmetric.

However, to check the validity of Jacobi's method as applied to our asymmetric flexibility matrix as it is, the characteristic equation of the system was obtained using the Krylov method, (Ref. 4.12, ch. 10), and the roots of the polynomial were found and showed good agreement with the other methods of calculation mentioned above, (iteration and Jacobi methods).

4.3.3 Simplification of the Solution

The solution of the problem can be greatly simplified making use of symmetry and antisymmetry, as well as some experimental observation. The first mode may be obtained, very quickly, by solving only one equation in one unknown. Similarly, for the second mode, the problem can be reduced to an eigenvalue problem of a 3 x 3 matrix, or to solving three equations in three unknowns, which can also be carried out in almost no time.

This simplification can be done using the symmetric 9 x 9 flexibility matrix. The results of this method are exactly the same as those of the iteration, Jacobi, and Krylov methods, which were used in solving the problem.

---

* It is worthwhile to point out that the flexibility matrix of the suspension net has been also found singular. This is, perhaps, the reason for getting some complex latent roots, (i.e. complex frequencies of vibration).

A description of the method is given below.

Referring to Fig. 4.10, let the flexibility matrix of the net be

$$[\delta_{ij}] = \begin{bmatrix} \delta_{11} & \delta_{12} & \delta_{13} \cdots\cdots & \delta_{19} \\ \delta_{21} & \delta_{22} & \delta_{23} \cdots\cdots & \delta_{29} \\ \vdots & \vdots & \vdots & \vdots \\ \delta_{91} & \delta_{92} & \delta_{93} \cdots\cdots & \delta_{99} \end{bmatrix} = [K]^{-1} \qquad (4.1)$$

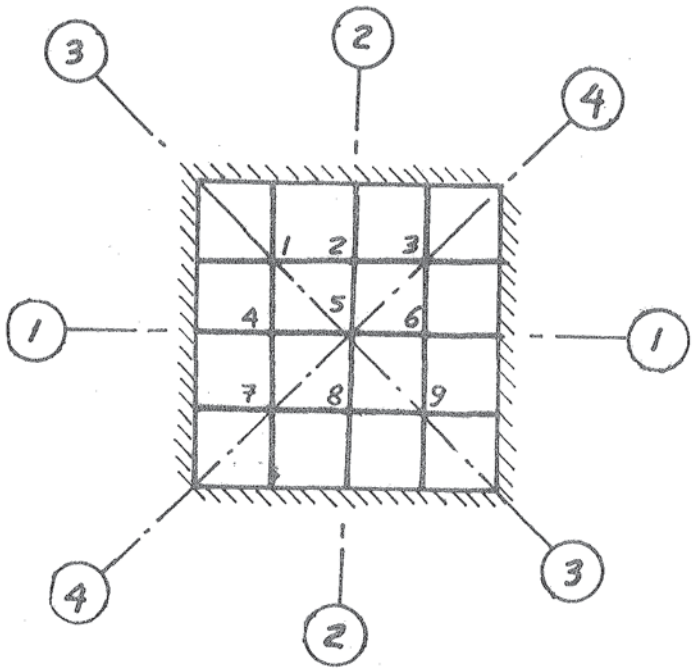

Fig. 4.10.- Symmetry and Antisymmetry.

Making use of reciprocity and symmetry of the influence coefficients about all the axes 1-1, 2-2, 3-3, 4-4, we can write

$$\delta_{11} = \delta_{33} = \delta_{77} = \delta_{99} \tag{4.2.1}$$

$$\delta_{12} = \delta_{14} = \delta_{32} = \delta_{36} = \delta_{74} = \delta_{78} = \delta_{96} = \delta_{98} = \delta_{41} = \delta_{23} = \delta_{63} = \delta_{47} = \delta_{87} = \delta_{69} = \delta_{89} = \delta_{21} \tag{4.2.2}$$

$$\delta_{13} = \delta_{17} = \delta_{93} = \delta_{97} = \delta_{71} = \delta_{39} = \delta_{79} = \delta_{31} \tag{4.2.3}$$

$$\delta_{15} = \delta_{35} = \delta_{75} = \delta_{95} = \delta_{53} = \delta_{57} = \delta_{59} = \delta_{51} \tag{4.2.4}$$

$$\delta_{16} = \delta_{18} = \delta_{34} = \delta_{38} = \delta_{72} = \delta_{76} = \delta_{92} = \delta_{94} = \delta_{81} = \delta_{43} = \delta_{83} = \delta_{27} = \delta_{67} = \delta_{29} = \delta_{49} = \delta_{61} \tag{4.2.5}$$

$$\delta_{19} = \delta_{37} = \delta_{73} = \delta_{91} \tag{4.2.6}$$

$$\delta_{22} = \delta_{44} = \delta_{66} = \delta_{88} \tag{4.2.7}$$

$$\delta_{24} = \delta_{26} = \delta_{84} = \delta_{86} = \delta_{62} = \delta_{48} = \delta_{68} = \delta_{42} \tag{4.2.8}$$

$$\delta_{25} = \delta_{45} = \delta_{65} = \delta_{85} = \delta_{54} = \delta_{56} = \delta_{58} = \delta_{52} \tag{4.2.9}$$

$$\delta_{28} = \delta_{46} = \delta_{64} = \delta_{82} \tag{4.2.10}$$

$$\delta_{55} = \delta_{55} \tag{4.2.11}$$

Thus, the number of the different elements in the flexibility matrix reduces to 11 in place of its 81 elements. The flexibility matrix can, thus, be written in full as

$$[k]^{-1} = \begin{bmatrix} \delta_{11} & \delta_{12} & \delta_{13} & \delta_{12} & \delta_{15} & \delta_{16} & \delta_{13} & \delta_{16} & \delta_{19} \\ \delta_{12} & \delta_{22} & \delta_{12} & \delta_{24} & \delta_{25} & \delta_{24} & \delta_{16} & \delta_{28} & \delta_{16} \\ \delta_{13} & \delta_{12} & \delta_{11} & \delta_{16} & \delta_{15} & \delta_{12} & \delta_{19} & \delta_{16} & \delta_{13} \\ \delta_{12} & \delta_{24} & \delta_{16} & \delta_{22} & \delta_{25} & \delta_{28} & \delta_{12} & \delta_{24} & \delta_{16} \\ \delta_{15} & \delta_{25} & \delta_{15} & \delta_{25} & \delta_{55} & \delta_{25} & \delta_{15} & \delta_{25} & \delta_{15} \\ \delta_{16} & \delta_{24} & \delta_{12} & \delta_{28} & \delta_{25} & \delta_{22} & \delta_{16} & \delta_{24} & \delta_{12} \\ \delta_{13} & \delta_{16} & \delta_{19} & \delta_{12} & \delta_{15} & \delta_{16} & \delta_{11} & \delta_{12} & \delta_{13} \\ \delta_{16} & \delta_{28} & \delta_{16} & \delta_{24} & \delta_{25} & \delta_{24} & \delta_{12} & \delta_{22} & \delta_{12} \\ \delta_{19} & \delta_{16} & \delta_{13} & \delta_{16} & \delta_{15} & \delta_{12} & \delta_{13} & \delta_{12} & \delta_{11} \end{bmatrix} \quad (4.3)$$

The equation of free undamped motion, using the flexibility matrix, (Eq. 3.3), is repeated here again

$$[X] = \omega^2 [k]^{-1} . [m][X] \quad (4.4a)$$

For the D.L. condition, $[m] = 3[I]$, where $[I]$ = the identity matrix; and the D.L. at each joint has a mass of 3 kg. Thus Eq. 4.4a becomes

$$[X] = 3\omega^2 [k]^{-1} . [X] \quad (4.4b)$$

(i) First Mode

For the first mode, it can be noticed from the experimental observations, or from any analytical procedure, that that mode has equal amplitudes at the four corners with each of the two displacements on the same diagonal having opposite signs to the other two (of the other diagonal), while all the other five joints are stationary.* Thus, for the R.H.S. of Eq. 4.4b we can put

---

* This means that the fundamental mode shape takes the form of a hyperbolic-paraboloid, with equal central sagging and hogging rises (= amplitude of a corner joint). The axes of symmetry of the surface are 3-3 and 4-4, (Fig. 4.10), while 1-1 and 2-2 are axes of antisymmetry (on which all points are free from displacement). In the language previously used, it is non-stretching.

$$[X] = \begin{bmatrix} \Delta \\ 0 \\ -\Delta \\ 0 \\ 0 \\ 0 \\ -\Delta \\ 0 \\ \Delta \end{bmatrix} \tag{4.5}$$

Substituting from Eq. 4.5 into the R.H.S. of Eq. 4.4b gives

$$\begin{bmatrix} X_1 \\ X_2 \\ X_3 \\ X_4 \\ X_5 \\ X_6 \\ X_7 \\ X_8 \\ X_9 \end{bmatrix} = 3\omega^2 \, [k]^{-1} \cdot \begin{bmatrix} \Delta \\ 0 \\ -\Delta \\ 0 \\ 0 \\ 0 \\ -\Delta \\ 0 \\ \Delta \end{bmatrix} \tag{4.6}$$

Eqs. 4.6 are, actually, nine equations in the nine amplitudes of the vector [X], which can easily be solved by direct multiplication of the R.H.S. Making use of the simplified matrix $[k]^{-1}$ (of Eq. 4.3), Eq. 4.6 yields

$$X_1 = -X_3 = -X_7 = X_9 = 3\omega^2 \, (\delta_{11} - 2\delta_{13} + \delta_{19}) \, . \, (\Delta) \tag{4.7a}$$

and $$X_2 = X_4 = X_5 = X_6 = X_8 = 0 \tag{4.7b}$$

where Δ is the numerical value of the corner amplitude that can have any value, (e.g. $\Delta = 1$).

Substituting for the measured elements of the flexibility matrix

$$\left.\begin{aligned} \delta_{11} &= 0.2423 \times 10^{-3} \quad \text{m/N} \\ \delta_{13} &= -0.1341 \times 10^{-3} \quad \text{m/N} \\ \delta_{19} &= 0.0696 \times 10^{-3} \quad \text{m/N} \end{aligned}\right) \qquad (4.7c)$$

If the vector [X] of Eq. 4.5 represents the final correct shape of the fundamental mode, it can, thus, be substituted into the L.H.S. of Eq. 4.6. Thus Eq. 4.7a yields

$$\omega = 23.97 \text{ rad./sec.}$$
$$f = 3.815 \text{ Hz}$$

which are the same as the results given by the other analytical methods.

(ii) Second Mode

In the same manner, experimental observation, or analytical study, may lead us to guess the shape of the second mode, making use of symmetry about the four axes of Fig. 4.10. Thus, [X] can be substituted in Eq.4.4b as

$$[X] = \begin{bmatrix} X_1 \\ X_2 \\ X_3 \\ X_4 \\ X_5 \\ X_6 \\ X_7 \\ X_8 \\ X_9 \end{bmatrix} = \begin{bmatrix} \Delta_1 \\ \Delta_2 \\ \Delta_1 \\ \Delta_2 \\ 1 \\ \Delta_2 \\ \Delta_1 \\ \Delta_2 \\ \Delta_1 \end{bmatrix} \qquad (4.8)$$

where, in the second mode, the displacements of the four corners are assumed to be equal and each of which = Δ_1 . Also, the displacements of the four mid-sides are assumed to be equal and each of which = Δ_2 , while the central displacement, X_5, can have any other relative value, say 1.

Substitution from Eq. 4.8 into Eq. 4.4b gives nine equations in which

(a) the 1st, 3rd, 7th, 9th equations, (representing the four corner joints), are identical and yield

$$\Delta_1 = 3\omega^2[(\delta_{11} + 2\delta_{13} + \delta_{19}).\Delta_1 + (2\delta_{12} + 2\delta_{16}).\Delta_2 + \delta_{15}.(1)] \qquad (4.9a)$$

(b) the 2nd, 4th, 6th, 8th equations, (representing the four mid-sides) are identical and yield

$$\Delta_2 = 3\omega^2[(2\delta_{12} + 2\delta_{16}).\Delta_1 + (\delta_{22} + 2\delta_{24} + \delta_{28}).\Delta_2 + \delta_{25}.(1)] \qquad (4.9b)$$

(c) the 5th equation, representing the central joint, yields

$$1 = 3\omega^2[(4\delta_{15}).\Delta_1 + (4\delta_{25}).\Delta_2 + \delta_{55}.(1)] \qquad (4.9c)$$

Thus we have only three equations in the three unknowns, Δ_1, Δ_2, ω. These equations can be rewritten in the form

$$\begin{bmatrix} \alpha_{11} - \lambda & \alpha_{12} & \alpha_{13} \\ \alpha_{21} & \alpha_{22} - \lambda & \alpha_{23} \\ \alpha_{31} & \alpha_{32} & \alpha_{33} - \lambda \end{bmatrix} \cdot \begin{bmatrix} \Delta_1 \\ \Delta_2 \\ 1 \end{bmatrix} = \begin{bmatrix} 0 \\ 0 \\ 0 \end{bmatrix} \qquad (4.10)$$

which is an eigenvalue problem where

$$\alpha_{11} = \delta_{11} + 2\delta_{13} + \delta_{19} \qquad (4.11a)$$

$$\alpha_{12} = 2\delta_{12} + 2\delta_{16} \quad = \alpha_{21} \qquad (4.11b)$$

$$\alpha_{13} = \delta_{15} \quad = \alpha_{31} \div 4 \qquad (4.11c)$$

$$\alpha_{22} = \delta_{22} + 2\delta_{24} + \delta_{28} \qquad (4.11d)$$

$$\alpha_{23} = \delta_{25} \quad = \alpha_{32} \div 4 \qquad (4.11e)$$

$$\alpha_{33} = \delta_{55} \qquad (4.11f)$$

$$\lambda = 1/(3\omega^2) \qquad (4.11g)$$

It can be noticed that the square matrix on the L.H.S. is not symmetric, but, to become symmetric, the third row needs to be divided by 4. This, again, will give us $\lambda/4$ instead of the usual λ of the eigenvalue problems. This is due to the 4:4:1 nature of the assumed mode which leads to a kind of 1:1:4 in the final matrix.

(1) An Approximate Solution

An approximate solution can be obtained using Jacobi's method which solves the case of a symmetric matrix. Although the matrix is not symmetric a good approximate solution could be obtained, using the following information, in addition to those given by Eq. 4.7c.

$$\left.\begin{aligned}
\delta_{12} &= -0.0788 \times 10^{-3} \quad \text{m/N} \\
\delta_{16} &= 0.0381 \times 10^{-3} \quad \text{m/N} \\
\delta_{15} &= 0.0250 \times 10^{-3} \quad \text{m/N} \\
\delta_{22} &= 0.2351 \times 10^{-3} \quad \text{m/N} \\
\delta_{24} &= 0.0248 \times 10^{-3} \quad \text{m/N} \\
\delta_{28} &= -0.1264 \times 10^{-3} \quad \text{m/N} \\
\delta_{25} &= -0.0790 \times 10^{-3} \quad \text{m/N} \\
\delta_{55} &= 0.2263 \times 10^{-3} \quad \text{m/N}
\end{aligned}\right\} \qquad (4.11h)$$

The solution of Eq. 4.10, thus, gives the following three values of λ :

$$\lambda_1 = -0.00635$$

$$\lambda_2 = 0.0563$$

$$\lambda_3 = 0.3784$$

Here, λ_1 gives a complex frequency which is to be refused. Also, λ_2 is not accepted since we must take the highest value of λ(i.e.λ_3) to get the lowest value of the second frequency. Using λ_3 we get

$$f = 4.724 \text{ Hz}$$

which is almost the same as that given by other analytical methods.

Substituting for $\lambda = \lambda_3$ in Eq. 4.10 we get, for the second mode,

$$\begin{bmatrix} \Delta_1 \\ \Delta_2 \\ \Delta_3 \end{bmatrix} = \begin{bmatrix} 0.178 \\ -0.425 \\ 1.000 \end{bmatrix}$$

which is, again, similar to that obtained by other methods of analysis.

(2) Other Solutions

Eq. 4.10 can be solved by writing down the characteristic equation which, after some manipulation, reduces to

$$\lambda^3 - 0.4287\lambda^2 + 0.01858\lambda + 0.000136 = 0 \qquad (4.12)$$

A rough solution to Eq. 4.12 can be obtained very quickly using only the first two terms, which give

$\lambda = 0.4287$

$f = 4.44$ Hz (6% less than the correct value)

A better solution can be obtained using the first three terms of Eq. 4.12, giving

$\lambda_1 = 0.0489$ (to be refused)

$\lambda_2 = 0.380$, $f = 4.714$ Hz (which is nearly equal to the correct value).

The correct value of the second frequency is obtained using all terms of Eq. 4.12 in solving the third order polynomial equation*, getting

$\lambda_1 = -0.00635$)
) to be refused as before
$\lambda_2 = 0.0563$)

$\lambda_3 = 0.378$, $f = 4.726$ Hz which is again close to the foregoing solutions.

---

* See Ref. 4.12, chapter 8.

4.3.4 Calculated Flexibility Matrix

The flexibility matrix of the suspension net can be calculated using any of the methods referred to in section 4.1 for the analysis of suspension nets. A quick approximate method used here by the writer gave good agreement with the measurements of the fundamental mode and the calculations of the second mode.

The method is based, approximately, on considering that an influence load at a joint is only carried by the two cables intersecting at that joint. For the corner joints 1, 3, 7, 9 and the central joint 5, the influence load at a joint is carried equally by the corresponding two cables intersecting therein. For other joints 2, 4, 6, 8, the influence load at a joint is distributed between the two cables intersecting at that joint, such that the joint deflection is identical when calculated from either cable, Fig. 4.7.

Timoshenko's method of 1930, (Ref. 1.14), was again used here for calculating the influence coefficients of each individual cable, putting again EI = 0 in the energy equations. Symmetry of the structure was then made use of, to complete the flexibility matrix of the net, bearing in mind that the influence load at a joint is assumed to be carried only by the two cables intersecting at that joint, while other joints have zero coefficients. So, for our model, we have five non-zero elements and four zeros in each row of the flexibility matrix. Charlton and Drakeley used only the diagonal elements of the stiffness matrix of the suspension bridge in a recent approximate method, (Ref. 1.18).

The so-called flexibility matrix is not symmetric, but it is not far from symmetric. Also, it is an approximate matrix, and so there is no need to keep it asymmetric as it is, but it can be made symmetric by taking the average of the off-diagonal elements to simplify the solution.

The results calculated by this method, using the iterative procedure, are shown in Fig. 4.8. The flexibility matrix used has the following form:

$$[k]^{-1} = \begin{bmatrix} \delta_{11} & \delta_{12} & \delta_{13} & \delta_{12} & 0 & 0 & \delta_{13} & 0 & 0 \\ \delta_{12} & \delta_{22} & \delta_{12} & 0 & \delta_{25} & 0 & 0 & \delta_{28} & 0 \\ \delta_{13} & \delta_{12} & \delta_{11} & 0 & 0 & \delta_{12} & 0 & 0 & \delta_{13} \\ \delta_{12} & 0 & 0 & \delta_{22} & \delta_{25} & \delta_{28} & \delta_{12} & 0 & 0 \\ 0 & \delta_{25} & 0 & \delta_{25} & \delta_{55} & \delta_{25} & 0 & \delta_{25} & 0 \\ 0 & 0 & \delta_{12} & \delta_{28} & \delta_{25} & \delta_{22} & 0 & 0 & \delta_{12} \\ \delta_{13} & 0 & 0 & \delta_{12} & 0 & 0 & \delta_{11} & \delta_{12} & \delta_{13} \\ 0 & \delta_{28} & 0 & 0 & \delta_{25} & 0 & \delta_{12} & \delta_{22} & \delta_{12} \\ 0 & 0 & \delta_{13} & 0 & 0 & \delta_{12} & \delta_{13} & \delta_{12} & \delta_{11} \end{bmatrix} \quad (4.13)$$

in which

$$\delta_{11} = \delta_{33} = \delta_{77} = \delta_{99} \tag{4.14.1}$$

$$\delta_{12} = \delta_{14} = \delta_{32} = \delta_{36} = \delta_{74} = \delta_{78} = \delta_{96} = \delta_{98}$$
$$= \delta_{41} = \delta_{23} = \delta_{63} = \delta_{47} = \delta_{87} = \delta_{69} = \delta_{89} = \delta_{21} \tag{4.14.2}$$

$$\delta_{13} = \delta_{17} = \delta_{93} = \delta_{97}$$
$$= \delta_{71} = \delta_{39} = \delta_{79} = \delta_{31} \tag{4.14.3}$$

$$\delta_{22} = \delta_{44} = \delta_{66} = \delta_{88} \tag{4.14.4}$$

$$\delta_{25} = \delta_{45} = \delta_{65} = \delta_{85}$$
$$= \delta_{54} = \delta_{56} = \delta_{58} = \delta_{52} \tag{4.14.5}$$

$$\delta_{28} = \delta_{46}$$
$$= \delta_{64} = \delta_{82} \tag{4.14.6}$$

$$\delta_{55} = \delta_{55} \tag{4.14.7}$$

i.e. we have only seven different elements in the matrix, while 36 elements are zeros.

4.4 SUMMARY OF RESULTS

The following table summarizes the frequency results of the cable net.

Mode	Calculated Frequencies (Hz)					Measured Frequencies (Hz)
	Measured Flexibility matrix				Calcu.Flex. matrix	
	Iteration	Jacobi	Roots of Ch. Eq.	Simplified Solution	(Iteration)	
Mode 1	3.82	3.82	3.90	3.82	3.34	3.4
Mode 2	4.73	4.73	4.72	4.724 [a] 4.726 [b] 4.714 [c] 4.44 [d]	4.66	3.9
	matrix 9 x 9			matrix 1x1(mode 1) or 3x3(mode 2)	matrix 9x9	

a Solution using Jacobi method for solving eigenvalue problems with symmetric matrices.

b Roots of the characteristic equation using all the four terms.

c Roots of the characteristic equation using only the first three terms.

d Roots of the characteristic equation using only the first two terms.

CHAPTER V

TWO-CABLE BRIDGE: STATICS

5.1 INTRODUCTION

The static structural action of a suspension bridge is three-dimensional. Observation shows that heavy off-centre live load twists the deck. However, there is not much published on the analysis of the suspension bridge as a three-dimensional structure. Nearly all the previous work tackles the problem of the suspension bridge as if it is a plane structure. Only three papers on the torsional analysis of suspension bridges could come to the hands of the writer, (Refs. 1.25, 1.26, 5.1). In Refs. 1.25, 1.26, the authors resolve asymmetric loads into symmetric and antisymmetric components. In Ref. 5.1, the author analyses the bridge under a point torque or a uniformly distributed torque over a part of the span.

Present day designers of the great suspension bridges, and the designers of the past, must have had their methods of torsional analysis as applied to bridge decks and the stiffening girders. Certainly, torsional frequencies of oscillation are quoted, but not the methods of obtaining them. It appears that the static strength of a modern suspension bridge, under static live load, whether designed in America, Japan, U.K., or Europe, is provided by designing with respect to a single-cable analysis. Then aerodynamic stability is achieved by ensuring that aerodynamic excitation by shed vortices or the like is not coincident with a natural frequency in either flexure or torsion. (See also Chapter VII).

* * *

Timoshenko's method of 1930, (Ref. 1.14), is extended by the writer herein to solve the problem of the two-cable bridge, i.e. to allow for the torsional stiffness of the bridge deck. It is recommended as a design procedure, in view of its simplicity, and the way in which design modifications can be incorporated readily. Its main parameters are cable stiffness in tension and deck stiffness in bending and twisting. The writer has checked the method against the detailed measured behaviour of a fairly realistic laboratory model.

5.2 DESIGN OF THE LABORATORY MODEL

For a real bridge, the span is chosen according to the crossing and the geology of the site as well as economical considerations. The width of the bridge depends on the requirements of traffic. So, the choice is nearly limited for both the span and the width. Therefore, the design of the bridge superstructure will include the main cable, the hangers, and the deck cross section (as well as the towers, of course).

(i) First Trial

For our model let

$L = 2.500$ m	(span centre to centre of towers);
$B = 0.250$ m	(total deck width);
$b = 0.200$ m	(width between centres of cables)*;
$t = 2$ mm	(thickness of deck which is a flat plate);
$H_o = 800$ N	(horizontal component of tension in each cable due to D.L.);
$E = 200 \times 10^3$ Mpa	(modulus of elasticity for the deck material);
$G = 0.4E$	(modulus of elasticity in shear for the deck material);
$I \simeq 167$ mm^4	(moment of inertia of the deck $\simeq B.t^3/12$);
$J \simeq 4I$	(torsional modulus of the deck $\simeq B.t^3/3$);
$G.J. \simeq 1.6\ EI$	(for a thin rectangular plate); and

$$\left.\begin{aligned} \frac{2H_o.L^2}{EI} &= 300 \\ \frac{G.J}{EI} \cdot \left(\frac{L}{b}\right)^2 &= 250 \end{aligned}\right\}$$ (two dimensionless parameters).

(ii) Comparison with the Forth Road Bridge

The following parameters for the Forth Road Suspension Bridge were published in Refs. 5.2, 5.3, and are presented here to compare with our model.

---

* L/b = 12.5 which is nearly reasonable compared to real bridges for which L/b ranges usually between 20 and 50. It was made rather small to ensure measurable torsional behaviour.

$L = 1006$ m) $L/b = 42.3$
$b = 23.8$ m)

$H_o = 10290$ tonne (per cable)

$I = 78900$ in^2 ft^2)*
) $J/I = 0.269$
$J = 21200$ in^2 ft^2)

$G = 0.4E$

$$\frac{2H_o.L^2}{EI} = 230$$

$$\frac{G.J}{EI} \cdot \left(\frac{L}{b}\right)^2 = 192$$

(iii) Design of Main Cable and Hangers

(a) Dead Load

Using the well-known equation $H_o = wL^2/8D$, and the above data given in (i), and for a dip-span ratio, $(D/L) = 0.10$, the total dead load for each cable becomes $wL = 640$ Newtons.

Let the self weights of the deck, cable, hangers, joints,..etc. $\simeq 0.15$ wL. Therefore, the dead weights at nine stations $= 0.85$ wL $= 640 \times 0.85 = 544$ Newtons per cable.

Mass per station $= (544 \div 9) \div 9.81 = 6.16$ Kg.

(b) Main Cable

Let $h_{max} = 0.5\ H_o = 400$ Newtons = maximum increase in the horizontal component of the cable tension due to L.L.**

Therefore $H_o + h_{max} = 1200$ Newtons.

Maximum tension in each backstay*** $= (H_o + h_{max}).\sqrt{2} \simeq 1700$ Newtons.

Let the factor of safety = 2.

Therefore yield load for each backstay = 3400 Newtons, say 4000 Newtons.

Yield stress of cable material $\sigma_y = 2000$ Mpa

Therefore cross-sectional area of main cable $= 4000 \div 2000 = 2$ mm^2.

Diameter of main cable $\phi_c \simeq 1.6$ mm.

---

* Ref. 5.2, p.57.

** For the Forth Bridge, $h_{max} = 0.32\ H_o$, (Ref. 5.3).

*** To keep down the overall length of the model, to enable it to be erected in available space, backstays were designed to be 45° to the horizontal which is greater than the slope at any section on the main cable. So the backstay section is the critical section for design.

(c) Hangers

Let maximum L.L. at any station = 120 Newtons.

Therefore maximum hanger force ≃ 60 + 120 = 180 Newtons, (D.L. + L.L.)

Let the factor of safety = 2 (as in the main cable design).

Yield load for a hanger = 360 Newtons, say 400 Newtons.

Using yield stress for the hanger material, σ_y = 2000 Mpa,

Cross-sectional area of a hanger = 400 ÷ 2000 = 0.2 mm^2,

Hanger diameter , ϕ_h = 0.50 mm.

(d) Finalization of the Model Dimensions

The model was constructed and erected, using the available materials, with the following dimensions. Firstly, the deck was horizontal (without camber).

L = 2.500 m

D = 0.250 m (This was altered thereafter to produce some camber).

B = 0.250 m

b = 0.200 m

t = 2 mm

ϕ_c = 1.63 mm

ϕ_h = 0.57 mm

length of backstays: ℓ_1 = 0.95 m, ℓ_2 = 1.05 m, (average = 1.0 m)

height of tower = 0.850 m

spacing between hangers = 0.250 m

height of camber = 0.0

(AE) = 417 x 10^3 Newtons, (Axial stiffness of a main cable)

GJ = 35 $N.m^2$ (Torsional stiffness of the deck section) *

EI = 56.5 $N.m^2$ (Bending stiffness of the deck section) *

Lumped mass hung per station = 6.0 Kg , (for D.L.).

The horizontal component of the cable tension H_o, in each cable (due to D.L.), was measured, for the above profile with no camber, and gave an average value ≃ 800 Newtons, which is the same as the design value.

A real bridge has some camber. To get a camber, either of the following two methods can be used.

(i) Shortening the hangers to get the required deck profile while the cable length and sag, and the length of backstays, are kept unaltered, or

---

* These are the average measured values. For details see Appendix at the end of this chapter.

(ii) Decreasing the sag (and consequently the cable length), while keeping the hangers and backstays unchanged in length. In this case, the deck profile will have a parabolic shape if the cable is also so.

The second method is the one used by the writer. The sag D was reduced to 0.235 m to produce a camber with a central rise = 0.015 m = L/167, Fig. 5.1.* This increased H_o to 846 Newtons (≃ 800 x 250/235).

* * *

The horizontal component of each cable tension is measured by a single-lever system as shown in Figs. 5.1. The tower legs are separate. In other words, each cable is supported at, more or less, a separate tower each side. This makes it possible to ignore the torsional stiffness of the towers in both the analysis and the physical behaviour of the bridge model. This is unlike what happens in real bridges, where the tower legs are braced together, but our model is rather a simplified one.

5.3 METHOD OF ANALYSIS

As previously mentioned, Timoshenko's method is extended herein to evaluate the potential energy of the deck in terms of the increase in the horizontal components of the two cable tensions, h_1 and h_2, using a Fourier series analysis for the vertical deflections of the deck. The strain energies of the cables can then be evaluated, which may give the values of h_1 and h_2 somehow. The method can be outlined as follows:

Total potential (and strain) energy of the deck, U, is:

$$U = \int_0^L \int_0^K M.dK dx + \int_0^L \int_0^{K_{xy}} M_t.dK_{xy}\, dx + \int_0^L \int_0^{v_1} (q_1.dx)dv_1 + \int_0^L \int_0^{v_2} (q_2.dx)dv_2$$

$$- \int_{x_1}^{x_2} \int_0^{v_1} (p_1.dx)dv_1 - \int_{x_3}^{x_4} \int_0^{v_2} (p_2.dx)dv_2 \qquad \cdots\cdots \qquad (5.1)$$

---

* For the Forth Bridge, height of camber = L/220, (Ref. 5.2, p.86).

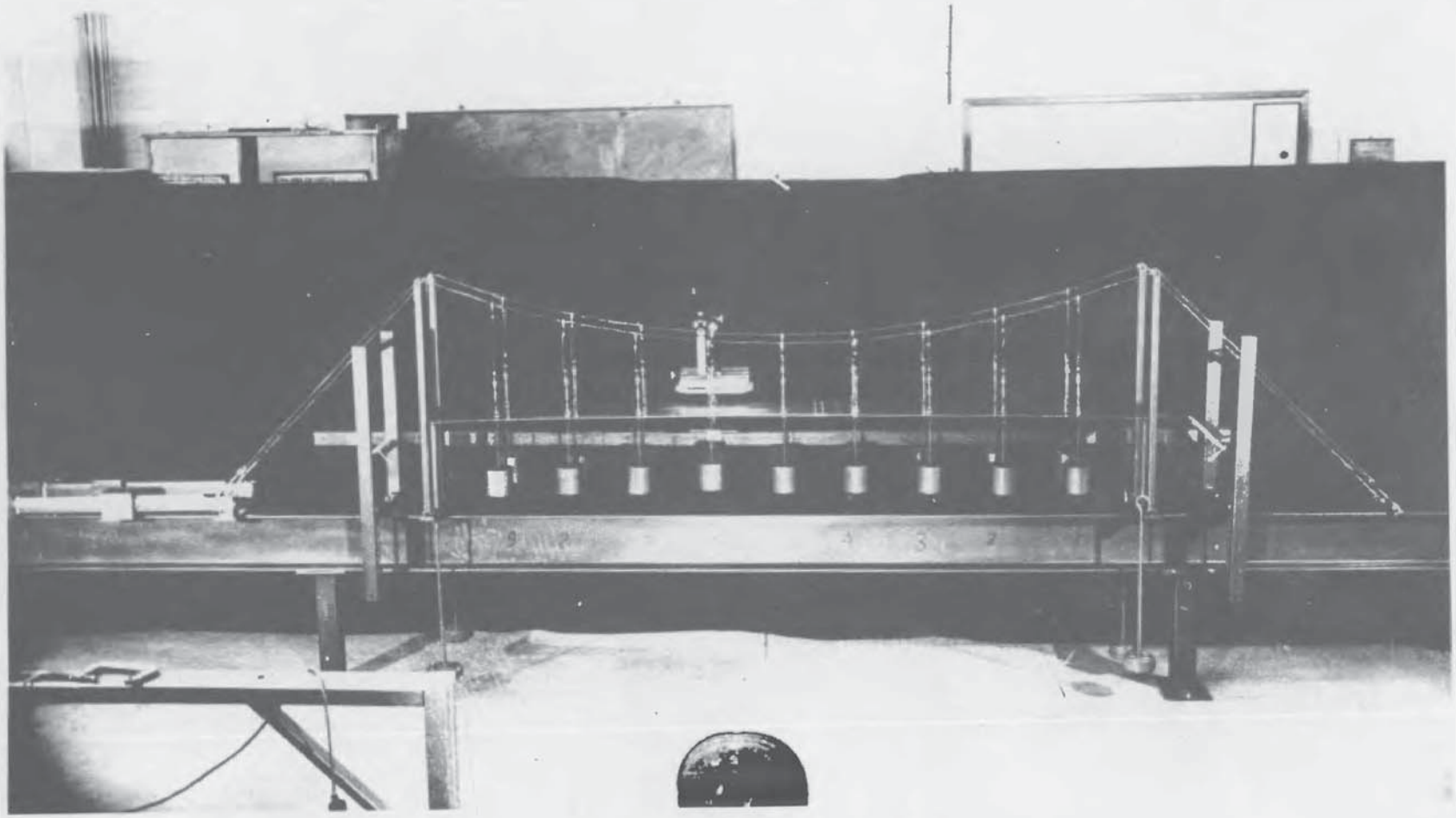

Fig. 5.1 (a) .- Laboratory Model of the Two-Cable Bridge.

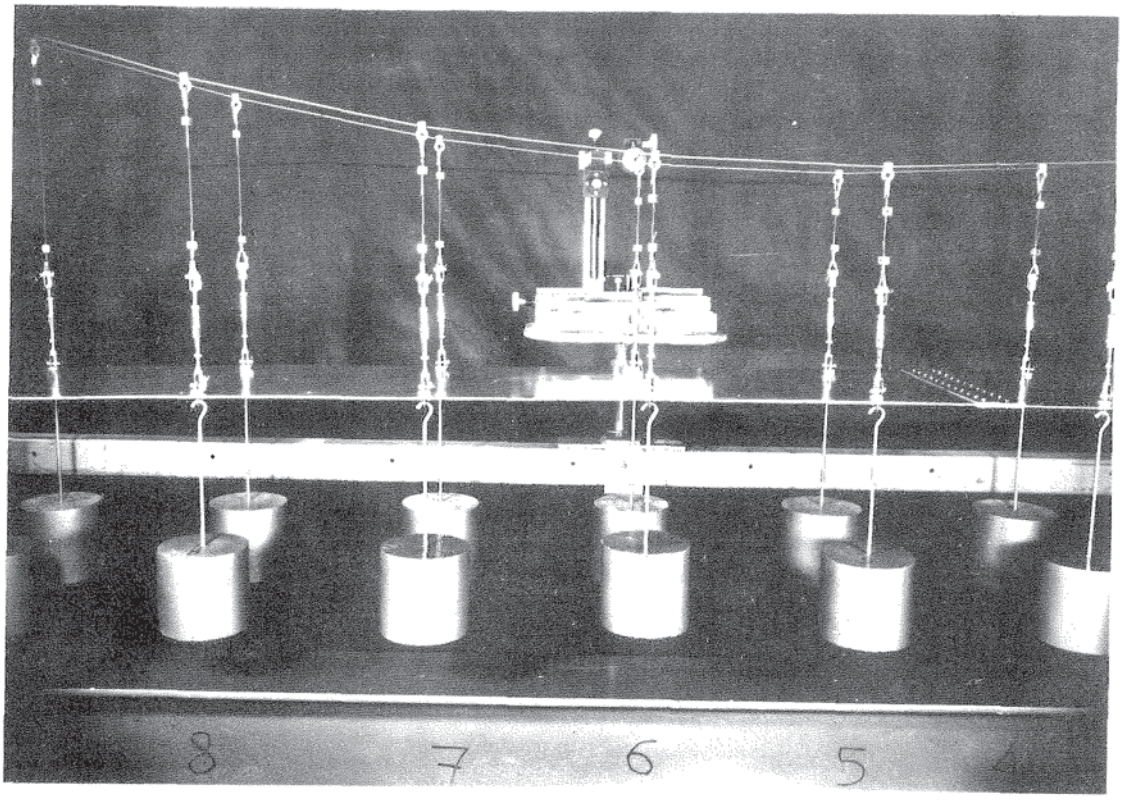

(i)

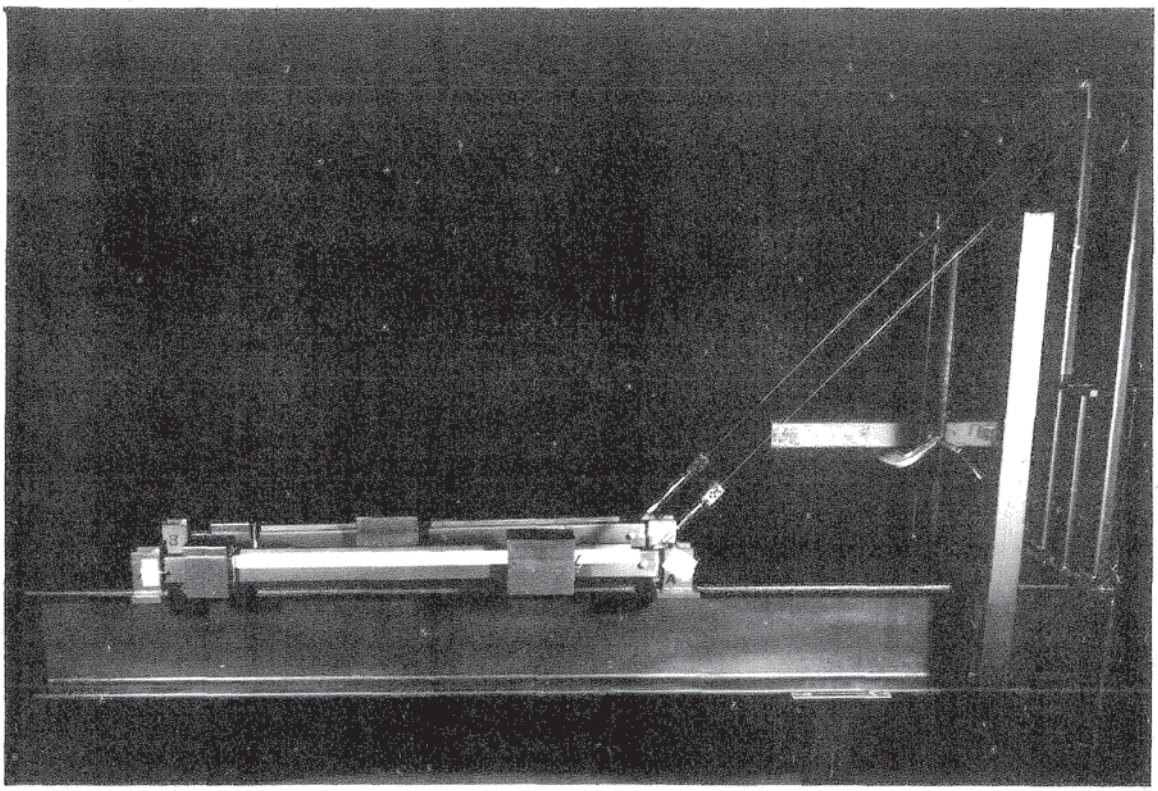

(ii)

Fig. 5.1 (b).- Details of the Laboratory Model of the Two-Cable Bridge:

(i) Cables, Hangers, Deck, Dead Weights, and Two-Way Microscope;
(ii) Towers, Backstays, and Single-Lever Systems.

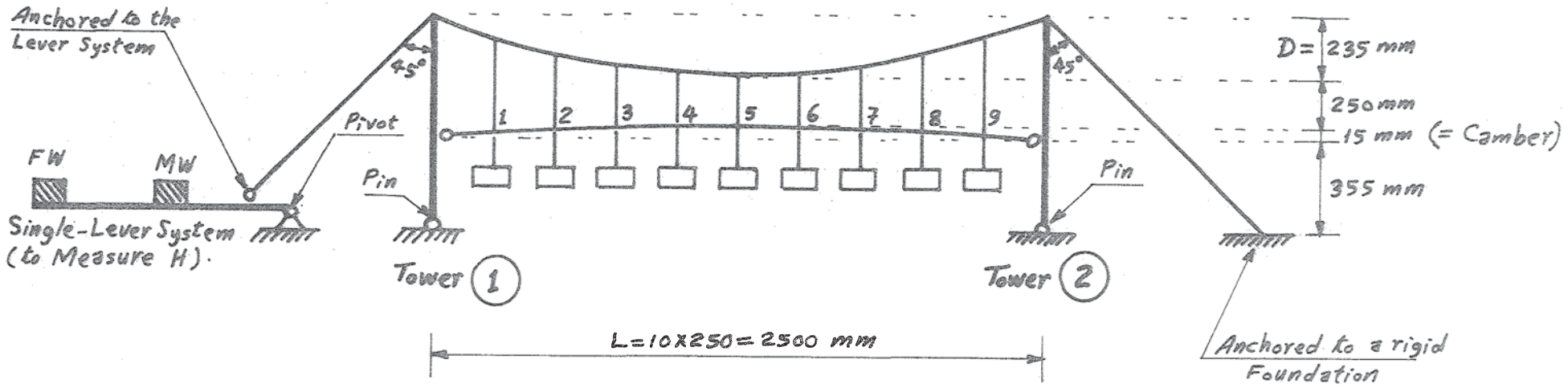

No. of Hangers = 9 (Each Side)
Dead Load = 6 x 9.81 Newtons (Per Station, Each Side)
Dip-Span Ratio = 1 : 10.6
H_o = 846 Newtons (Per Cable)
Effective AE = 417 KN (Per Cable)

$EI = 35\ N.m^2$
$GJ = 56.6\ N.m^2$
FW = Fixed Weight
MW = Movable Weight.

Fig. 5.1(c) Diagrammatic Sketch for the Laboratory Model of the Two-Cable Bridge.

in which v_1, v_2 = vertical deflections of cables 1-1 and 2-2, respectively, neglecting the hanger extensions, due to the live loads p_1, p_2 ;

$v = (v_1 + v_2)/2$ = vertical deflection of the bridge centre line *;

$K \simeq v'' = d^2v/dx^2$ = curvature of the deck centre line in the spanwise direction *;

v_1', $v_2' = dv_1/dx$, dv_2/dx, respectively;

v_1'', $v_2'' = d^2v_1/dx^2$, d^2v_2/dx^2, respectively;

$M = EIK \simeq EIv''$ = bending moment in the deck in the longitudinal direction;

$$K_{xy} = \frac{d}{dx}\left(\frac{dv}{dy}\right) = \frac{d}{dx}\left(\frac{v_1 - v_2}{b}\right) = (v_1' - v_2')/b$$

= twist in the deck assuming no lateral curvature;

$M_t = GJ.K_{xy} = GJ.(v_1' - v_2')/b$ = torsional moment in the deck;

h_1, h_2 = increments in the horizontal pull in cables 1-1, 2-2, respectively, due to live load;

β_1, $\beta_2 = h_1/H_o$, h_2/H_o, respectively;

$q_1 = \beta_1 w - H_o(1 + \beta_1) \cdot v_1''$ = portion of live load, p_1, carried by cable 1-1; and

$q_2 = \beta_2 w - H_o(1 + \beta_2) \cdot v_2''$ = portion of live load, p_2, carried by cable 2-2.

Thus Eq. 5.1 becomes

$$U = EI \int_0^L \int_0^{v''} v''dv''dx + \frac{GJ}{b^2} \cdot \int_0^L \int (v_1' - v_2')d(v_1' - v_2')dx + \int_0^L \int_0^{v_1} (q_1.dx).dv_1$$

$$+ \int_0^L \int_0^{v_2} (q_2.dx).dv_2 - \int_{x_1}^{x_2} \int_0^{v_1} (p_1.dx)dv_1 - \int_{x_3}^{x_4} \int_0^{v_2} (p_2.dx)dv_2 \quad \ldots \quad (5.2)$$

where x_1, x_2, x_3, x_4 are defined as shown in Fig. 5.2.

---

* In the transverse direction, the deck is assumed to be straight, with $v = \frac{v_1 + v_2}{2}$, since the deck is narrow compared to the span. For other cases where the transverse bending of the deck is not negligible, its potential energy must be included in Eq. 5.1.

Put $v_1 = \Sigma a_i \sin \frac{i\pi x}{L}$, $v_2 = \Sigma b_i \sin \frac{i\pi x}{L}$

$$\therefore \quad v_1' = \frac{\pi}{L} \Sigma i a_i \cos \frac{i\pi x}{L} , \quad v_2' = \frac{\pi}{L} \Sigma i b_i \cos \frac{i\pi x}{L}$$

$$v_1'' = - \left(\frac{\pi}{L}\right)^2 \Sigma i^2 a_i \sin \frac{i\pi x}{L} ; \quad v_2'' = - \left(\frac{\pi}{L}\right)^2 \Sigma i^2 b_i \sin \frac{i\pi x}{L}$$

$$\therefore \quad v'' = \frac{v_1'' + v_2''}{2} = - \tfrac{1}{2}\left(\frac{\pi}{L}\right)^2 \left[\Sigma i^2 (a_i + b_i) \cdot \sin \frac{i\pi x}{L} \right]$$

where a_i and b_i are Fourier coefficients.

It is worth stating here that the unknowns in this analysis are the cable deflections v_1 and v_2, which are both Fourier series.

If the potential energy U is differentiated with respect to a Fourier coefficient a_i, Eq. 5.2 gives, for stationary potential energy,

$$0 = \frac{\partial U}{\partial a_i} = EI \int_0^L v'' \cdot \frac{\partial v''}{\partial a_i} dx + \frac{GJ}{b^2} \int_0^L (v_1' - v_2') dx \cdot \frac{\partial}{\partial a_i}(v_1' - v_2') + \int_0^L q_1 dx \cdot \frac{\partial v_1'}{\partial a_i}$$

$$+ \int_0^L q_2 dx \cdot \frac{\partial v_2'}{\partial a_i} - \int_{x_1}^{x_2} p_1 dx \cdot \frac{\partial v_1}{\partial a_i} - \int_{x_3}^{x_4} p_2 dx \cdot \frac{\partial v_2}{\partial a_i} \qquad \ldots\ldots (5.3)$$

where $\frac{\partial v''}{\partial a_i} = - \tfrac{1}{2}\left(\frac{i\pi}{L}\right)^2 \cdot \sin \frac{i\pi x}{L}$;

$$\frac{\partial v_1'}{\partial a_i} = \left(\frac{i\pi}{L}\right) \cdot \cos \frac{i\pi x}{L} \quad ;$$

$$\frac{\partial v_1}{\partial a_i} = \sin \frac{i\pi x}{L} ; \quad \text{and}$$

$$\frac{\partial v_2'}{\partial a_i} = \frac{\partial v_2}{\partial a_i} = 0$$

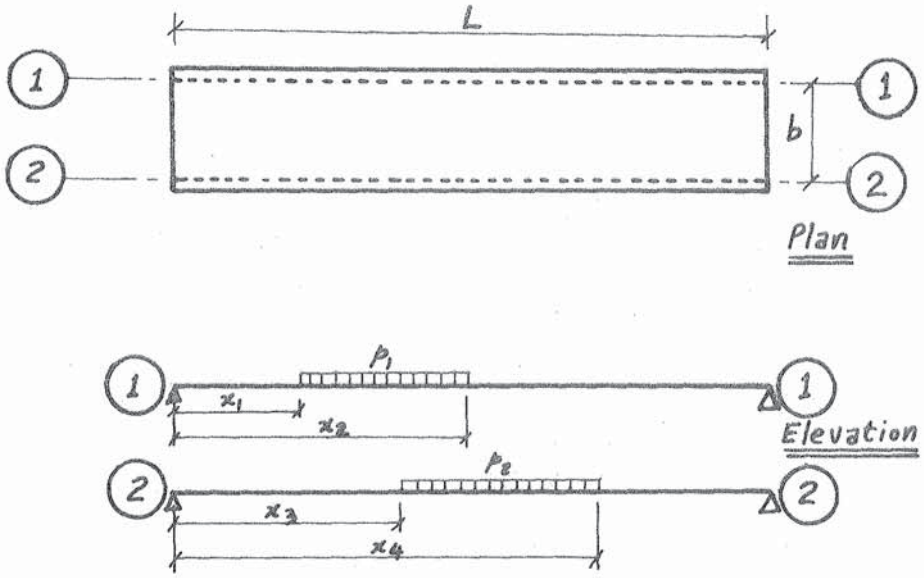

Fig. 5.2.

Thus, after some algebra, Eq. 5.3 reduces to

$$\left(\frac{i\pi}{L}\right)^3 \cdot \frac{L}{2}\left[\left[\frac{EI}{4}\left(\frac{i\pi}{L}\right)^2 + \frac{GJ}{b^2} + H_o(1+\beta_1)\right] \cdot a_i + \left[\frac{EI}{4}\left(\frac{i\pi}{L}\right)^2 - \frac{GJ}{b^2}\right] \cdot b_i\right]$$

$$= \left[p_1\left(\cos\frac{i\pi x_1}{L} - \cos\frac{i\pi x_2}{L}\right) - \beta_1 w\,(1 - \cos i\pi)\right] \qquad \ldots.(5.4)$$

Similarly, using

$$\frac{\partial v''}{\partial b_i} = -\tfrac{1}{2}\left(\frac{i\pi}{L}\right)^2 \cdot \sin\frac{i\pi x}{L} \quad ;$$

$$\frac{\partial v_1'}{\partial b_i} = \frac{\partial v_1}{\partial b_i} = 0 \quad ;$$

$$\frac{\partial v_2'}{\partial b_i} = \left(\frac{i\pi}{L}\right) \cdot \cos\frac{i\pi x}{L} \quad ; \text{ and}$$

$$\frac{\partial v_2}{\partial b_i} = \sin\frac{i\pi x}{L} \,,$$

and for a stationary potential energy, we can write

$$\left(\frac{i\pi}{L}\right)^3 \cdot \frac{L}{2}\left[\left[\frac{EI}{4}\left(\frac{i\pi}{L}\right)^2 - \frac{GJ}{b^2}\right] \cdot a_i + \left[\frac{EI}{4}\left(\frac{i\pi}{L}\right)^2 + \frac{GJ}{b^2} + H_o\,(1+\beta_2)\right] \cdot b_i\right]$$

$$= \left[\, p_2 \left(\cos\frac{i\pi x_3}{L} - \cos\frac{i\pi x_4}{L}\right) - \beta_2 w\,(1 - \cos i\pi)\,\right] \qquad \ldots(5.5)$$

Eqs. 5.4, 5.5 can be written in the form

$$\begin{bmatrix} \alpha_{11} & \alpha_{12} \\ \alpha_{21} & \alpha_{22} \end{bmatrix}_i \cdot \begin{bmatrix} a_i \\ b_i \end{bmatrix} = \begin{bmatrix} \alpha_{10} \\ \alpha_{20} \end{bmatrix}_i \qquad (5.6)$$

which can, easily, be solved in the two unknown Fourier coefficients a_i, b_i, where

$$(\alpha_{11})_i = \left(\frac{i\pi}{L}\right)^3 \cdot \frac{L}{2}\left[\frac{EI}{4}\left(\frac{i\pi}{L}\right)^2 + \frac{GJ}{b^2} + H_o\,(1+\beta_1)\right] \;;$$

$$(\alpha_{12})_i = \left(\frac{i\pi}{L}\right)^3 \cdot \frac{L}{2}\left[\frac{EI}{4}\left(\frac{i\pi}{L}\right)^2 - \frac{GJ}{b^2}\right] = (\alpha_{21})_i \;;$$

$$(\alpha_{22})_i = \left(\frac{i\pi}{L}\right)^3 \cdot \frac{L}{2}\left[\frac{EI}{4}\left(\frac{i\pi}{L}\right)^2 + \frac{GJ}{b^2} + H_o\,(1+\beta_2)\right] \;;$$

$$(\alpha_{10})_i = \left[p_1\left(\cos\frac{i\pi x_1}{L} - \cos\frac{i\pi x_2}{L}\right) - \beta_1 w\,(1 - \cos i\pi)\right] \;;$$

$$(\alpha_{20})_i = \left[p_2\left(\cos\frac{i\pi x_3}{L} - \cos\frac{i\pi x_4}{L}\right) - \beta_2 w\,(1 - \cos i\pi)\right] \;.$$

To summarize the mathematical treatment so far: the shape of each side of the bridge has been written as a Fourier series, one side having the coefficients a_i, the other side having coefficients b_i. These are the unknowns. When the a_i and b_i are known, we have deck curvature and twist everywhere, hence bending moment and torque. The equations involve deck bending stiffness EI and torsional stiffness GJ. They also involve the increase in the horizontal component of both the cable tensions, h_1, h_2, which appear non-dimensionally as $\beta_1 = h_1/H_o$ and $\beta_2 = h_2/H_o$, respectively.

It is obvious from Eq. 5.6 that each pair of the Fourier coefficients a_i, b_i is totally independent of the other pairs, and so any number of the Fourier coefficients can easily be calculated according to the desired accuracy. For practical purposes, it has been found by the writer that only five, or even four, Fourier terms for each cable are quite sufficient.

If $x_1 = x_3$, $x_2 = x_4$, and $p_1 = p_2$, the bridge becomes loaded symmetrically about its longitudinal centre line, and so $\beta_1 = \beta_2$ and $v_1 = v_2$, and consequently $a_i = b_i$. In such a case Eqs. 5.4, 5.5 become identical yielding

$$a_i = \frac{p_1 \left(\cos \frac{i\pi x_1}{L} - \cos \frac{i\pi x_2}{L}\right) - \beta_1 w \,(1 - \cos i\pi)}{\left(\frac{i\pi}{L}\right)^3 \cdot \frac{L}{2} \left[EI\left(\frac{i\pi}{L}\right)^2 + H_o \,(1 + \beta_1)\right]} \tag{5.7}$$

which is exactly the same equation as that given by Timoshenko for a single-cable bridge, (cf. Eq. 2.21 given before in Chapter II), a useful check.

It should be noticed that the torsional stiffness term GJ/b^2 will disappear if $a_i = b_i$, since it has opposite signs in the coefficients of each (as shown in both of Eqs. 5.4, 5.5).

* * *

As stated before, the foregoing analysis is based on knowing the values of h_1 and h_2, or alternatively the ratios β_1 and β_2. Similarly to the case of a single-cable bridge, β_1 and β_2 may now be obtained from the potential energy equations of both cables. The work done by the external loads on each cable can be equated to the change in the strain energy of the cable tension. This can be given, as in Chapter II, according to Timoshenko's method, (Ref. 1.14), for cables 1-1 and 2-2 respectively, as follows:

For cable 1-1:

$$\frac{H_o}{AE} \cdot \beta_1 L\left(1 + \frac{\beta_1}{2}\right)\left[1 + 8\left(\frac{D}{L}\right)^2\right] = \frac{16}{\pi}\left(\frac{D}{L}\right)\left(1 + \frac{\beta_1}{2}\right)\left(\Sigma \frac{a_i}{i}\right) \quad i = 1,3,5,\ldots$$

$$+ \frac{\pi^2}{4L}\,(1 + \beta_1)\left(\Sigma\, i^2 a_i^2\right) \quad i = 1,2,3,\ldots \tag{5.8a}$$

and for cable 2-2 :

$$\frac{H_o}{AE} \cdot \beta_2 L \left(1 + \frac{\beta_2}{2}\right)\left[1 + 8\left(\frac{D}{L}\right)^2\right] = \frac{16}{\pi}\left(\frac{D}{L}\right)\left(1 + \frac{\beta_2}{2}\right)\left(\Sigma \frac{b_i}{i}\right) \qquad i = 1,3,5,\ldots$$

$$+ \frac{\pi 2}{4L}\left(1 + \beta_2\right)\left(\Sigma\, i^2 b_i^2\right) \qquad i = 1,2,3,\ldots \qquad (5.8b)$$

The problem can be solved if Eqs. 5.6 and 5.8 can be solved together to give both the Fourier coefficients of the deflections of the two cables, a_i and b_i, and the parameters β_1 and β_2 of the increments of the two cable tensions.

* * * *

The solution was sought by iteration beginning with guessed β_1 and β_2 values, evaluating Fourier coefficients from Eqs. 5.6, and then getting better values for β_1 and β_2 using Eqs. 5.8, and so on. Unfortunately, this iterative procedure is not convergent, and the method for solving the single-cable bridge problem, (involving one Fourier series and one parameter β for the increment in the cable tension), is not at all directly applicable here to two sets of Fourier coefficients and two parameters β_1 and β_2 for the increments in the two cable tensions.

5.4 APPROXIMATE SOLUTION

5.4.1 Introduction

A simplified, but reasonably adequate, solution is presented here by the writer. It came from studies on the laboratory model.

Initially the increases in the cable tensions were measured on the laboratory model, and the parameters β_1 and β_2 evaluated and used in Eqs. 5.6 to solve for the deflections of both cables.

For a model, it was easy to measure β_1 and β_2, but for a real bridge, of course, not so. However, this led the writer to the recommended method.

5.4.2 The Procedure

Where torsion is involved, the method is to calculate β_1 and β_2, approximately, from a single-cable bridge analysis, considering that each lengthwise half of the bridge is carrying alone the entire load on its side (i.e. using half the flexural stiffness EI of the entire deck with each cable). Then these values of β_1 and β_2 are used in Eqs. 5.6 to get the vertical deflections of both cables.

It was found that a reasonable solution can be obtained using this procedure if only corrections due to tower movements are added. The procedure includes, already, the effect of the extensibility of the two cables, (between the towers), in evaluating the values of β_1 and β_2 as mentioned before in Chapter II. This method, although it uses approximate values for β_1 and β_2, showed very good agreement between the measured and the calculated deflections of both cables, for all loading conditions used by the writer, including some rather extreme ones.

5.5 APPLICATIONS

Several loading cases were applied to the laboratory model of the two-cable bridge to check the validity of the above procedure.

5.5.1 Flexural Loading, Examples F_1 and F_2

Firstly, however, and very much as a preliminary, in order to explore the properties of the model, two purely flexural loadings were applied. Here, of course, there is no torsion, and the cables undergo equal increase in the horizontal component of tension, i.e. $\beta_1 = \beta_2$.

A single-cable analysis is adequate,* using cable stiffness equal to the sum of the stiffnesses of the two cables, and deck stiffness equal to that of the entire deck. The solution is carried out exactly as in Chapter II.

The loadings as well as the calculated and the measured deflection curves are shown in Fig. 5.3, from which it is seen that the agreement is good between the calculated and the measured deflections for the two loading cases.

In Example F_1, the measured value of β was 0.235, and the calculated value was 0.249. The difference between the two values, (about 6%), represents only about 1% of the total (design) value of the horizontal component of the cable tension, $H = H_o + h = H_o(1 + \beta)$, which is practically very small.

In Example F_2, the measured value of β was 0.132, and the calculated value was 0.144. The difference between the two values, (about 9%), represents, again, only about 1% of the total (design) value of H, which is again very small for practical purposes.

* * * *

The above work was done, and is presented here, in order to prove the laboratory two-cable model for flexural loading. It is seen that the single-cable analysis is working well for the two-cable bridge under loadings causing flexure without torsion. The results are considered satisfactory, and give confidence in proceeding to torsional studies.

---

* See Eq. 5.7.

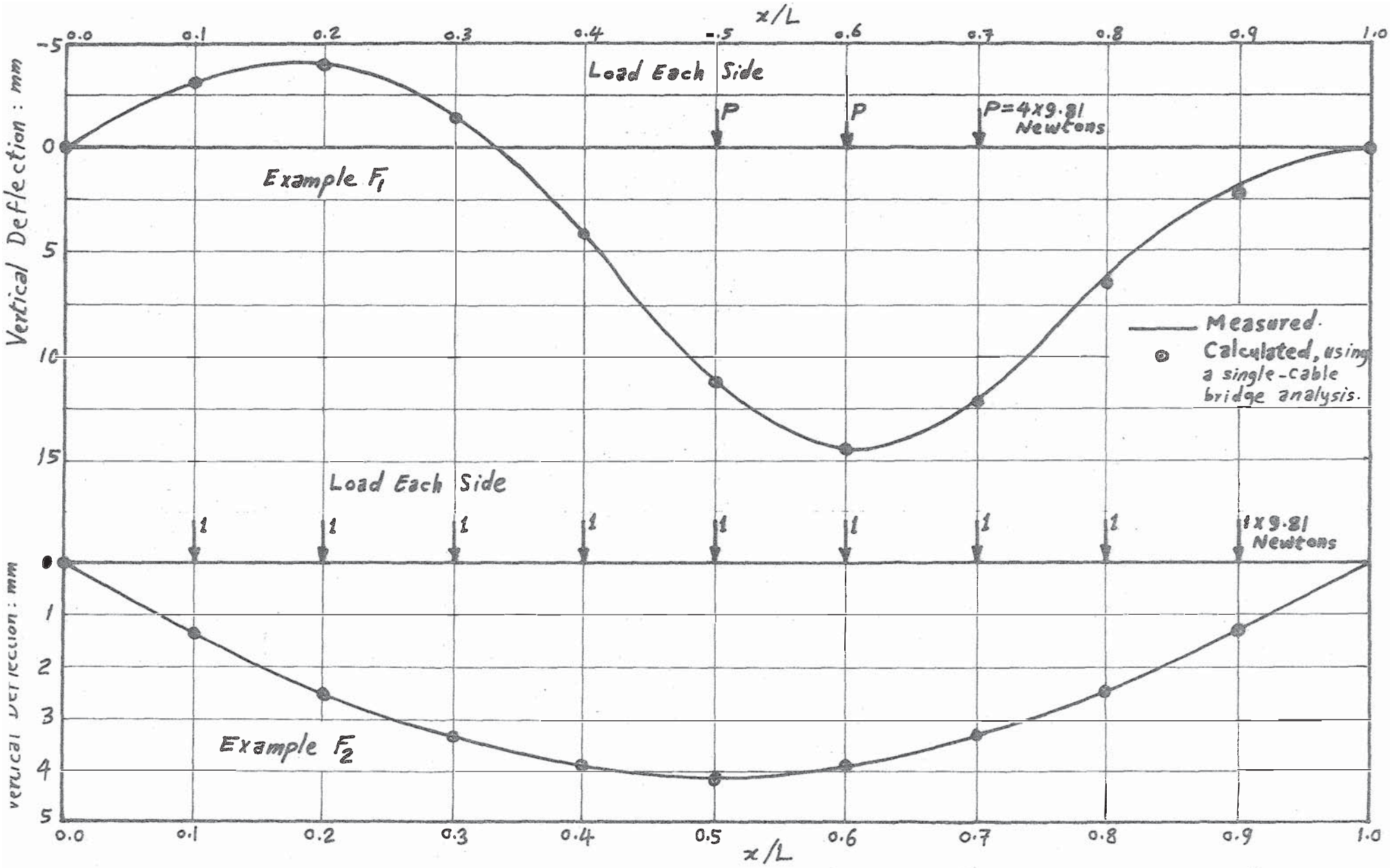

Fig. 5.3 .. Deflection Curves For Flexural Loadings, A Single-Cable Bridge Problem.

5.5.2 Torsional Loading, Examples T_1, T_2 and T_3

The torsional behaviour involves only the additional parameter of the torsional stiffness. (This was measured for a portion of the actual deck and agreed well with calculations,* so, no difficulty is expected in that regard.)

It is worth repeating here that we now have two different β values, one for each cable, and the recommended method for getting them, and also for evaluating the vertical deflections of both cables, has been stated in subsection 5.4.2.

Three torsional loading cases were applied to the bridge model as shown in Figs. 5.4, 5.5, and the bridge was analysed for each case of loading using this recommended method (of subsection 5.4.2). It can be seen, from the figures, that the calculated deflections for both cables compare reasonably well with measurements.**

The difference between the calculated and the measured values of the total (design) horizontal component of the tension in either of the cables, H, for any of the three loading conditions, does not exceed 3%. (Actually it ranges between 0.3% and 3.0%).

* * * *

An informative check is also available. The parameters β_1 and β_2 could be measured directly on the laboratory model and fed into Eqs. 5.6 to solve for the deflections of both cables. Here, of course, no corrections must be added to the calculated deflections because the measured β_1 and β_2 have already been influenced by both the cable extensibility and the tower movements. The results are shown, for interest, in Figs. 5.4, 5.5.

* * * *

Although it seems perhaps, at first, to be somewhat rough in concept, the recommended solution showed very good agreement between the measured and the calculated deflections of both cables. The reasons need consideration. It can be repeated that the approximation introduced is merely for the purpose of getting values for β_1 and β_2, to be inserted in Eqs. 5.6 resulting from energy. Now, firstly, if one of the β values, say β_1, is overestimated, (for example), the other one, β_2, will be underestimated.

---

* See appendix at the end of this chapter.

** To the calculated deflections, corrections are added due to tower movements only. (It has been stated in subsection 5.4.2 that the effect of the cable extensibility is already included in evaluating the values of β_1 and β_2.)

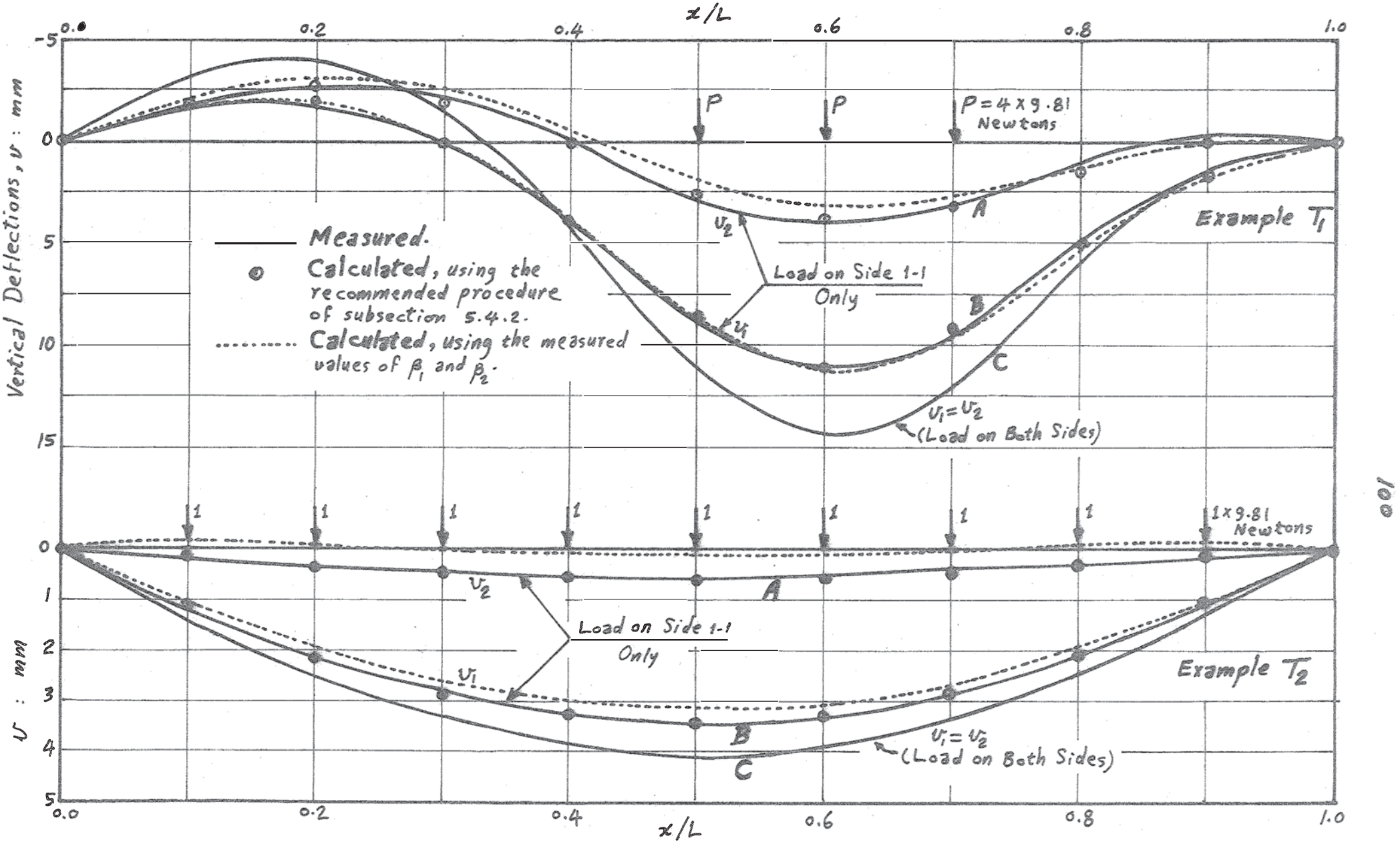

Fig. 5.4 — Deflection Curves For Torsional Loadings, Examples T_1 & T_2

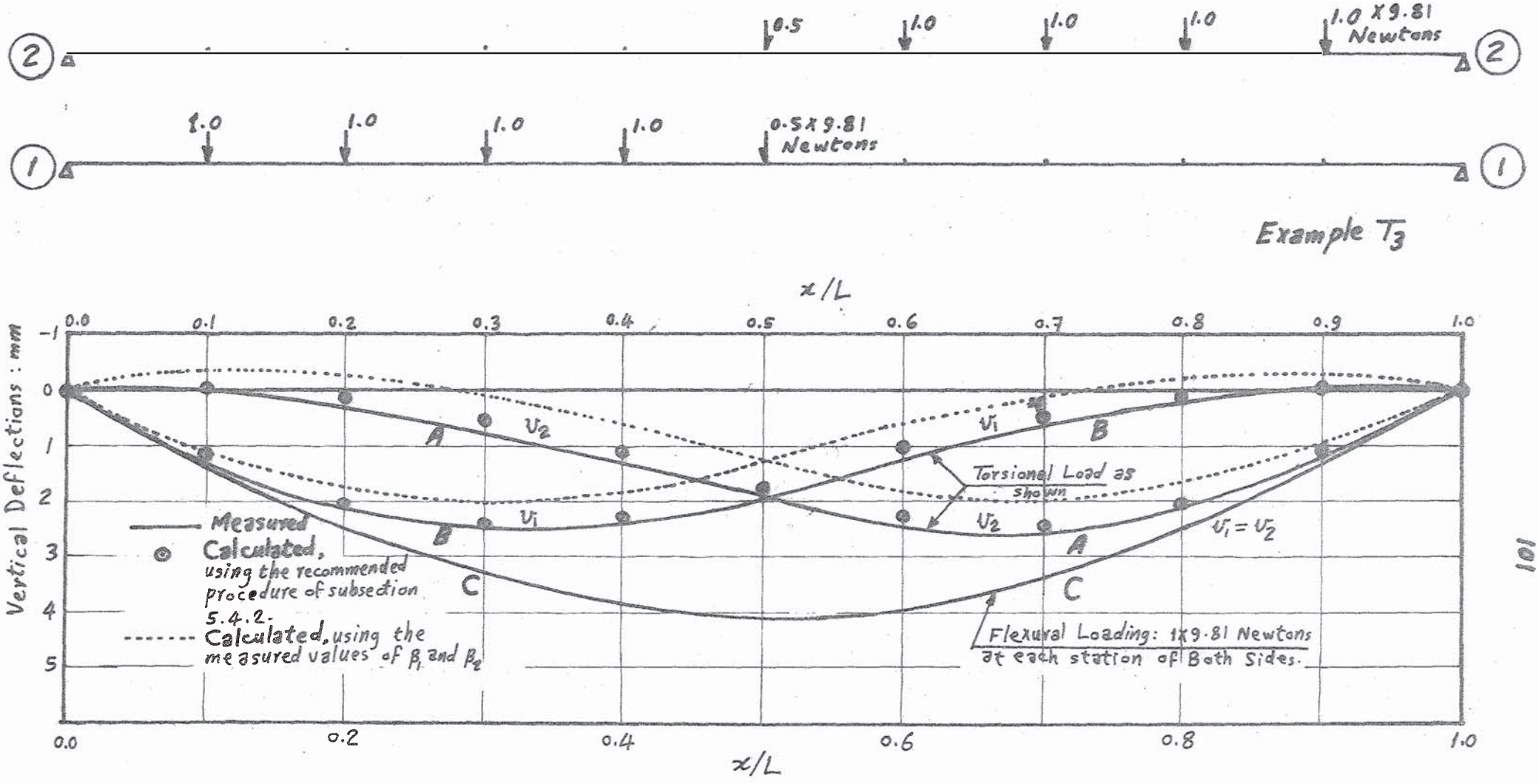

Fig. 5. 5 .– Deflection Curves for a Torsional Loading , Example T_3.

When the two values are used in Eqs. 5.6, the resulting deflections v_1 will be underestimated, while v_2 will be overestimated. (This may be clear from the simple Eq. 5.7). However, secondly, the added corrections due to tower movements, as given before in Chapter II, are proportional to the β values. Thus, because β_1 is an overestimate, the corrections to v_1 will be overestimated, while, because β_2 is an underestimate, those of v_2 will be underestimated. Thus the corrected deflections are reasonable as shown from the results of the analysis, because, from the foregoing, for example, if v_1 is initially underestimated then it receives a slightly overestimated correction, and vice versa for v_2.

5.6 THE PRINCIPLE OF SUPERPOSITION

As in the case of the traditional single-cable suspension bridge problems, and also suspension cables and nets in general, the principle of superposition may be applied without considerable error. Deflection measurements, (Figs. 5.4, 5.5), and calculations, (Fig. 5.6), support this conclusion when the resultant deflection curve is due to either flexural, (Figs. 5.4, 5.6c', 5.6c'"), or torsional, (Figs. 5.5, 5.6c, 5.6c"), loadings.

Measurments of the horizontal component of the cable tensions, H, Figs. 5.7, 5.8, for torsional and flexural loading cases, showed that the variation of H is nearly linear with the load, and that the principle of superposition holds also for H as in the case of the single-cable bridge, (cf. Fig. 2.8, Chapter II).

Fig. 5.9 shows that the variation of the deflections with the load is not exactly linear, but is nearly so. This is useful in the dynamic study of the two-cable bridge.

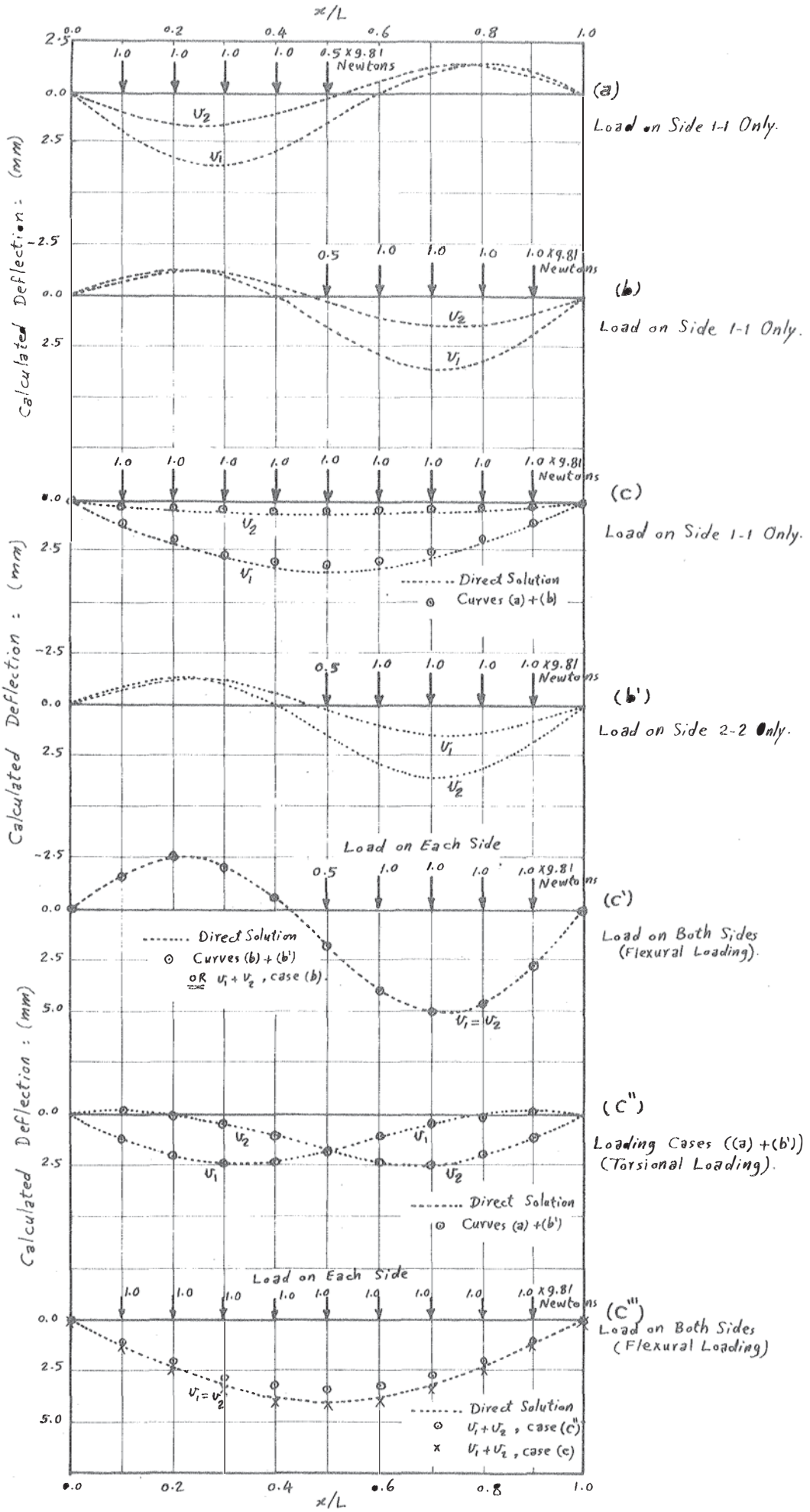

Fig. 5.6 – The Principle of Superposition.

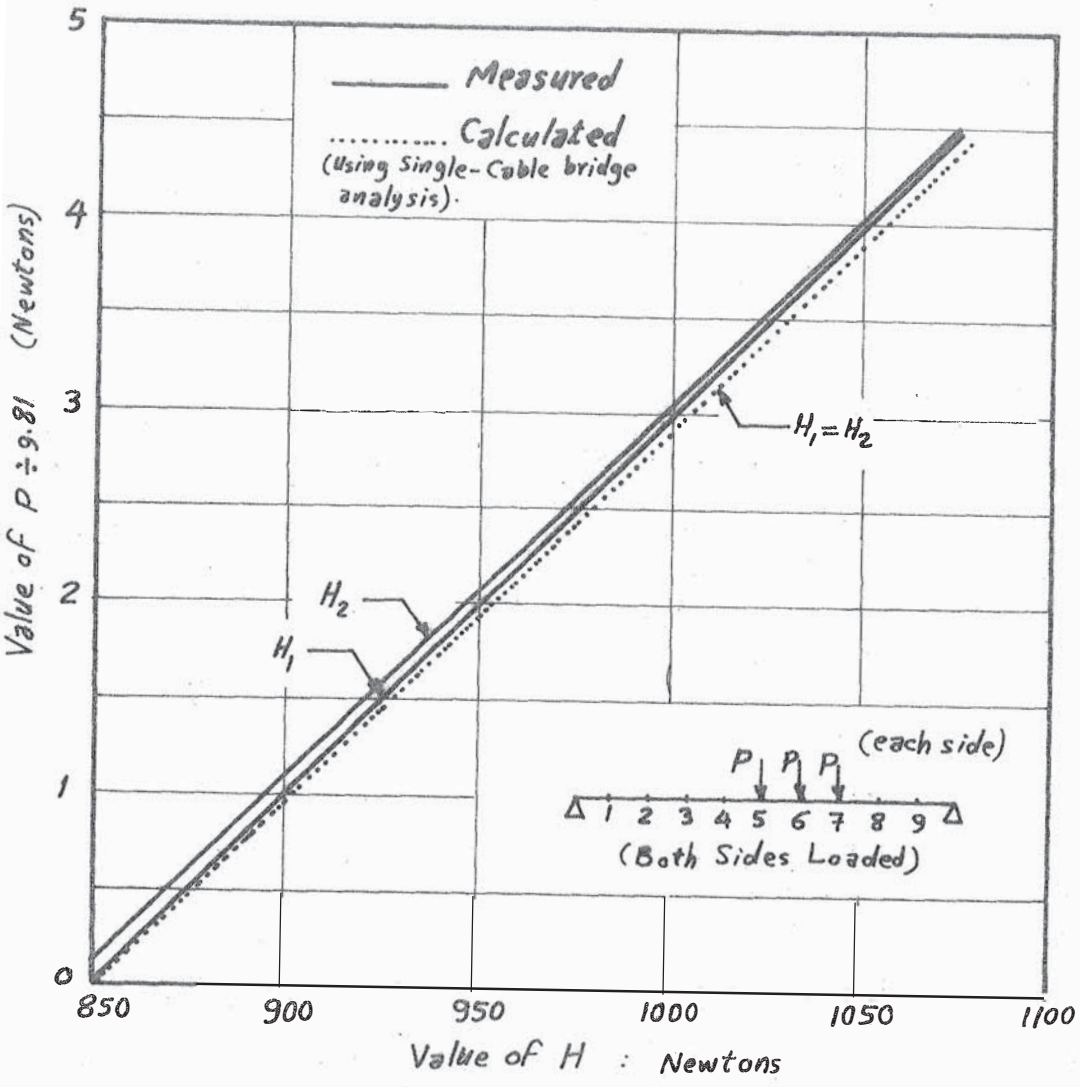

Fig. 5.7.— Variation of the Horizontal Compenent of the Cable Tension with Live Load.

Case of Purely Flexural Loading.

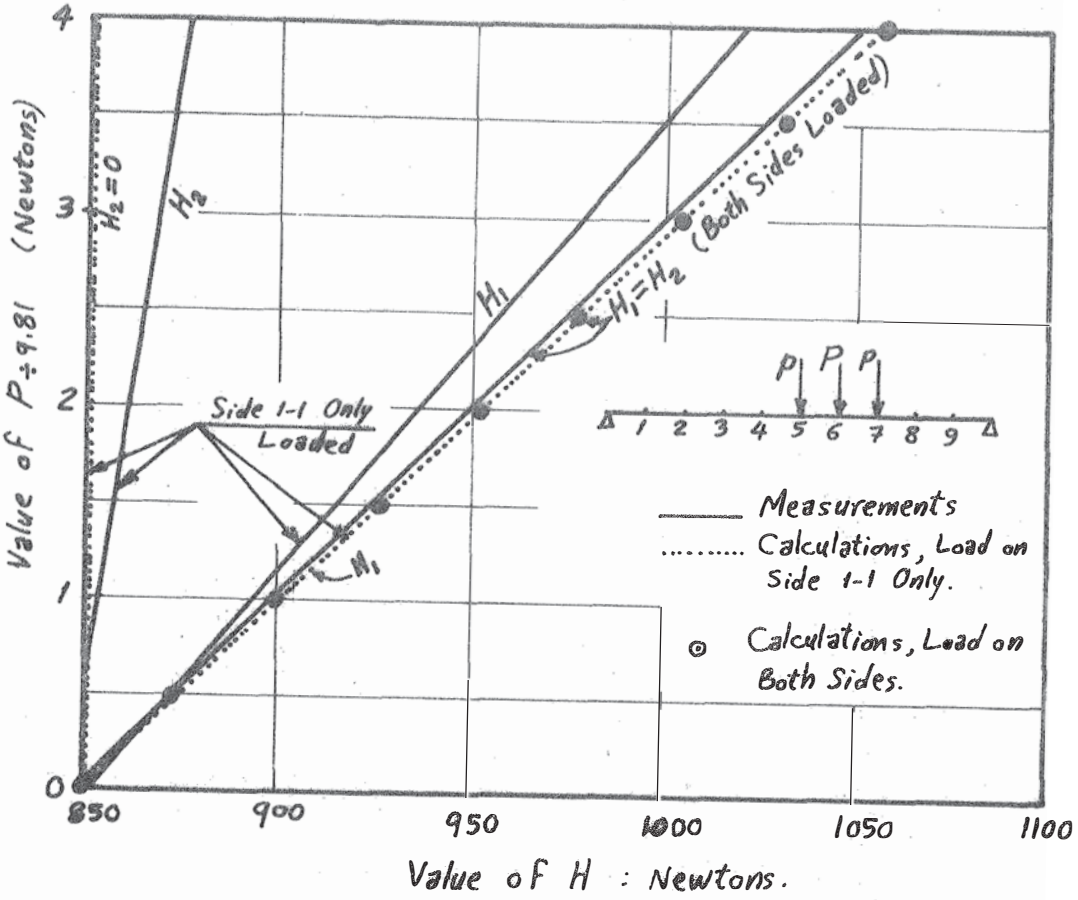

Fig.5.8 — Variation of the Horizontal Component of the Cable Tension with Live Load. (Two-Cable Bridge).

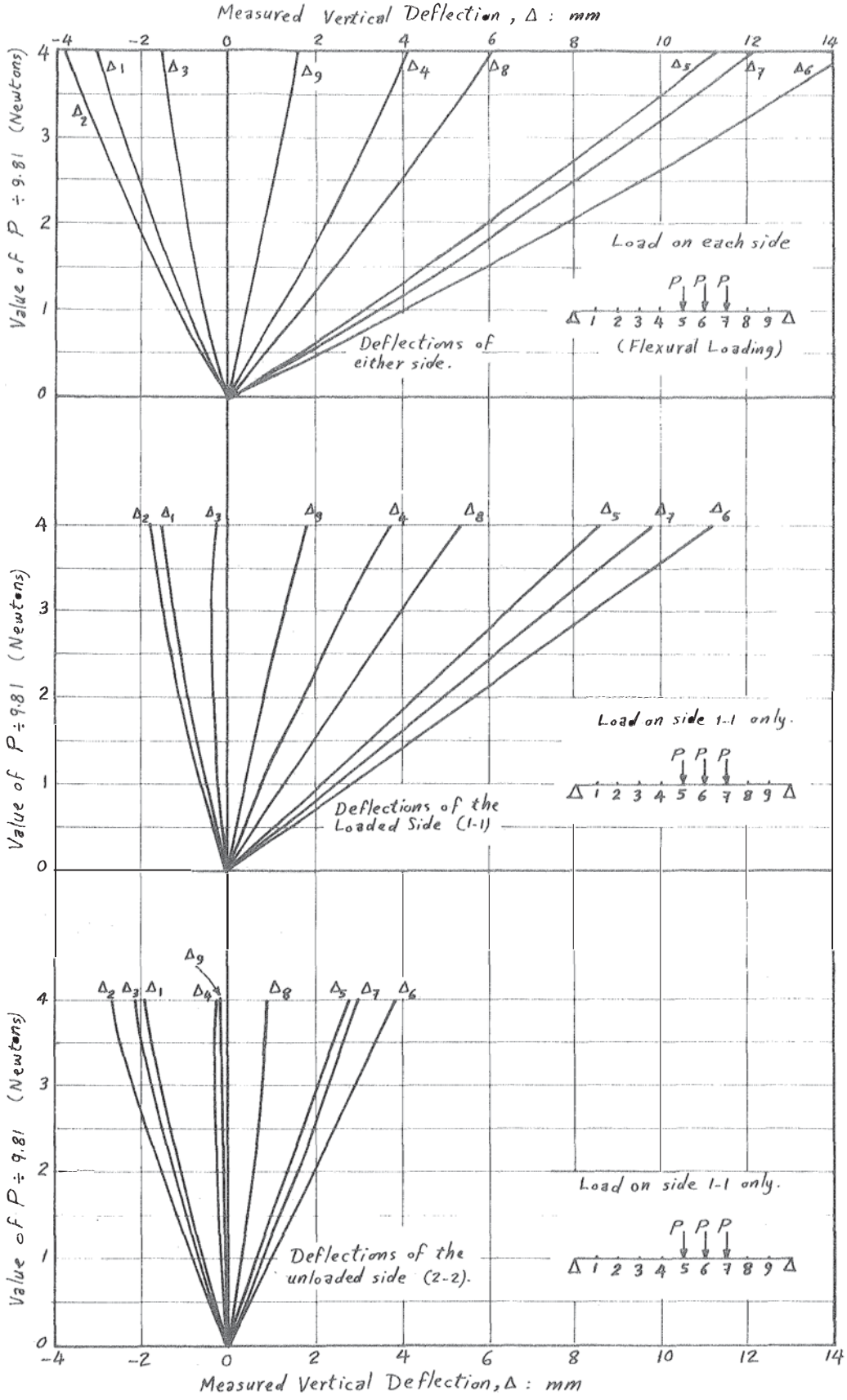

Fig. 5. 9. — Load ~ Deflection Curves for the Two-Cable Bridge.

APPENDIX TO CHAPTER V

A simple tension test was carried out in order to measure the modulus of elasticity in both bending and shear (E and G, respectively), as well as the Poisson's ratio μ for the deck material. The specimen was only 30 mm wide, but it had the same thickness as the model deck, (2 mm). Huggenberger tensometers were used to measure both the longitudinal and lateral strains, from which the following results were obtained:

$$E = 200 \times 10^3 \text{ Mpa},$$

$$\mu = 0.29,$$

$$G = \frac{0.5E}{1 + \mu} = 77.5 \times 10^3 \text{ Mpa}.$$

5.7 MEASURING THE TORSIONAL STIFFNESS

To measure the torsional stiffness of the deck, a specimen with the same width and thickness as the deck, (B = 0.250 m and t = 2 m), with a length = 0.500 m, was supported at three corners a, b, c, and loaded at the fourth one, d, as shown in Fig. 5.10. The vertical deflection Δ of the loaded corner was measured for different loads P. A graph between the torque acting on the specimen (= P.B), and the resulting twist (= $\Delta/B.\ell_s$) is shown in Fig. 5.10, which is obviously non-linear, (See Ref. 5.4). The first part of the graph, (for small twists), is nearly linear, the slope of which gives a reasonable value, for practical purposes, for the torsional stiffness, GJ $\simeq$ 56.6 N.m^2 (cf. $(1/3)B.t^3 . G$ = 51.67 N.m^2).*

5.8 MEASURING THE BENDING STIFFNESS

The bending stiffness of the deck was measured using more than one method. The above specimen was simply supported on a span = 0.45 m, and was loaded centrally and the central deflection was measured. This gives the bending stiffness, directly, as shown in Fig. 5.11.

The specimen was then loaded equally at the third points and the

---

* It is noticed from Fig. 5.10 that the specimen stiffens for higher twists, and this means that the bridge model will be more safe under higher twisting moments. Real bridges, however, are unlikely, at acceptable deformations, to have their decks enter upon the non-linear range of torque versus twist.

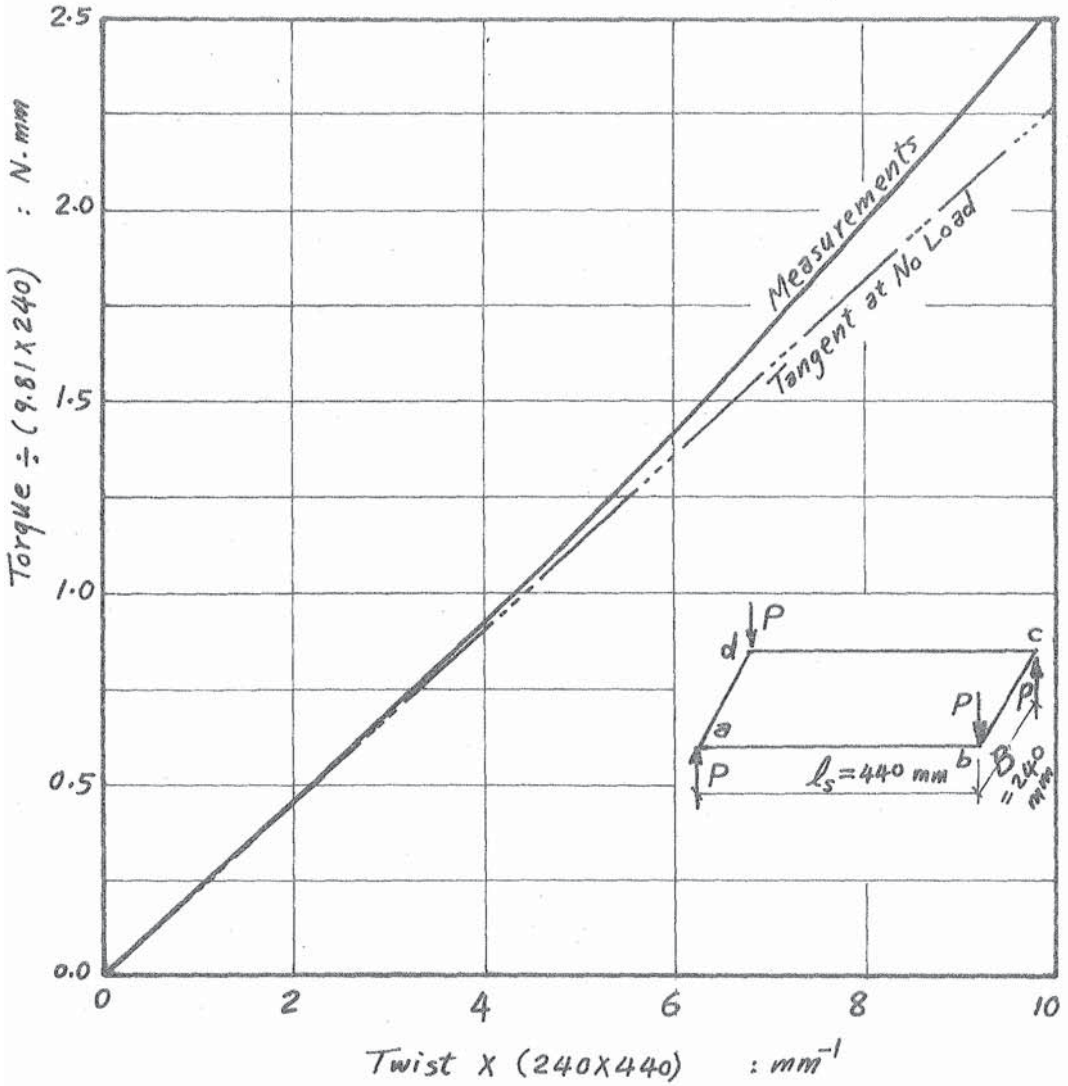

Fig. 5.10.—Torque ~ Twist for a Full-Width Specimen of the Two-Cable Bridge Deck.

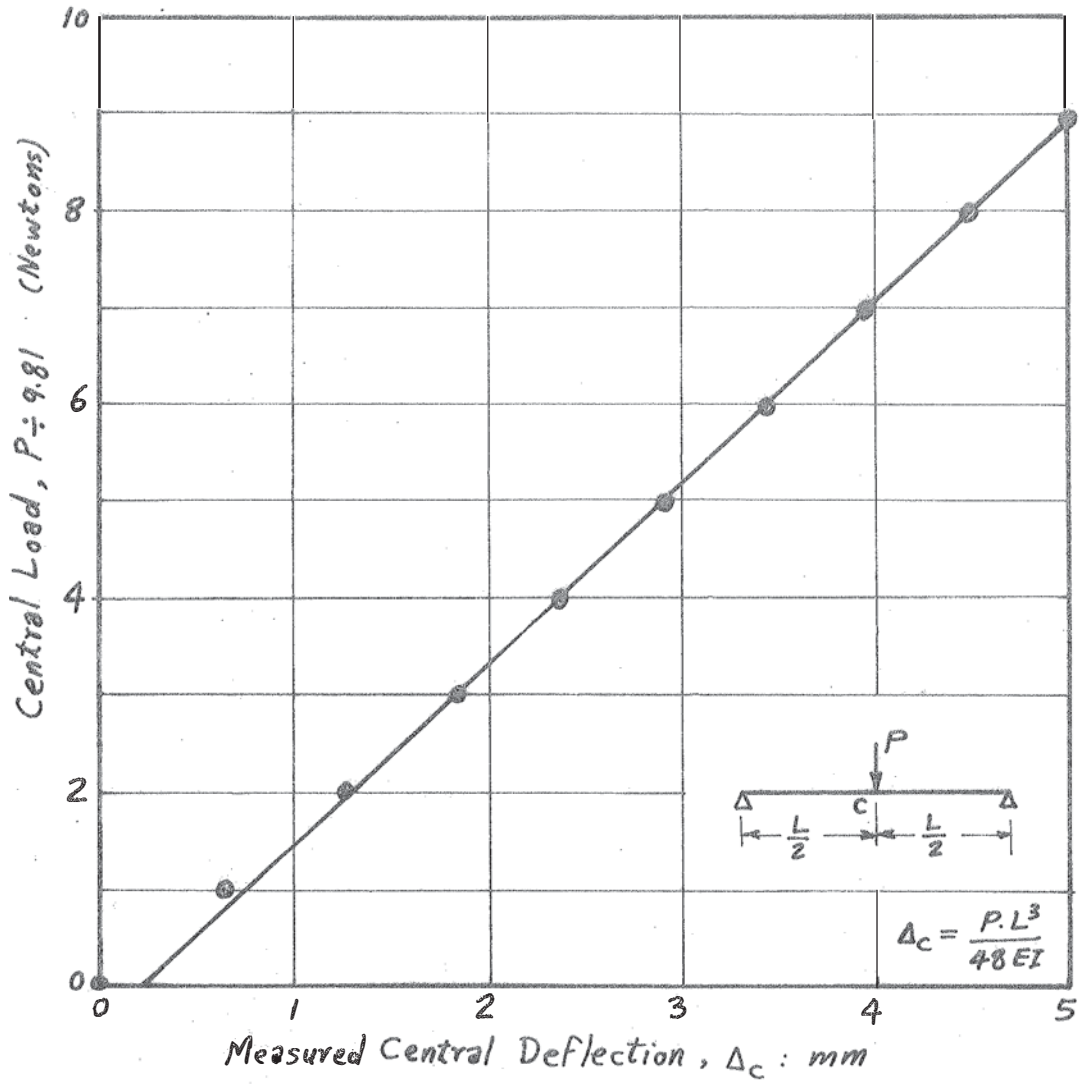

Fig. 5.11.— Central Load ~ Central Deflection for a Full-Width Specimen of the Two-Cable Bridge Deck.

deflections at the loaded points and the midspan, as well as the curvature* at midspan , were measured. Fig. 5.12 gives the load ~ deflection graph for this loading condition from which two values for the bending stiffness were calculated. M ~ K graph is shown in Fig. 5.13, from which a fourth value for EI was calculated.

An average value for the measured EI is about 35 $N.m^2$.

(cf. $E.\frac{B.t^3}{12(1-\mu^2)} = 36.43\ N.m^2$) ;

$$E.\frac{B.t^3}{12} = 33.33\ N.m^2 .$$

---

* The curvature was measured using the curvature meter, Fig. 5.13.

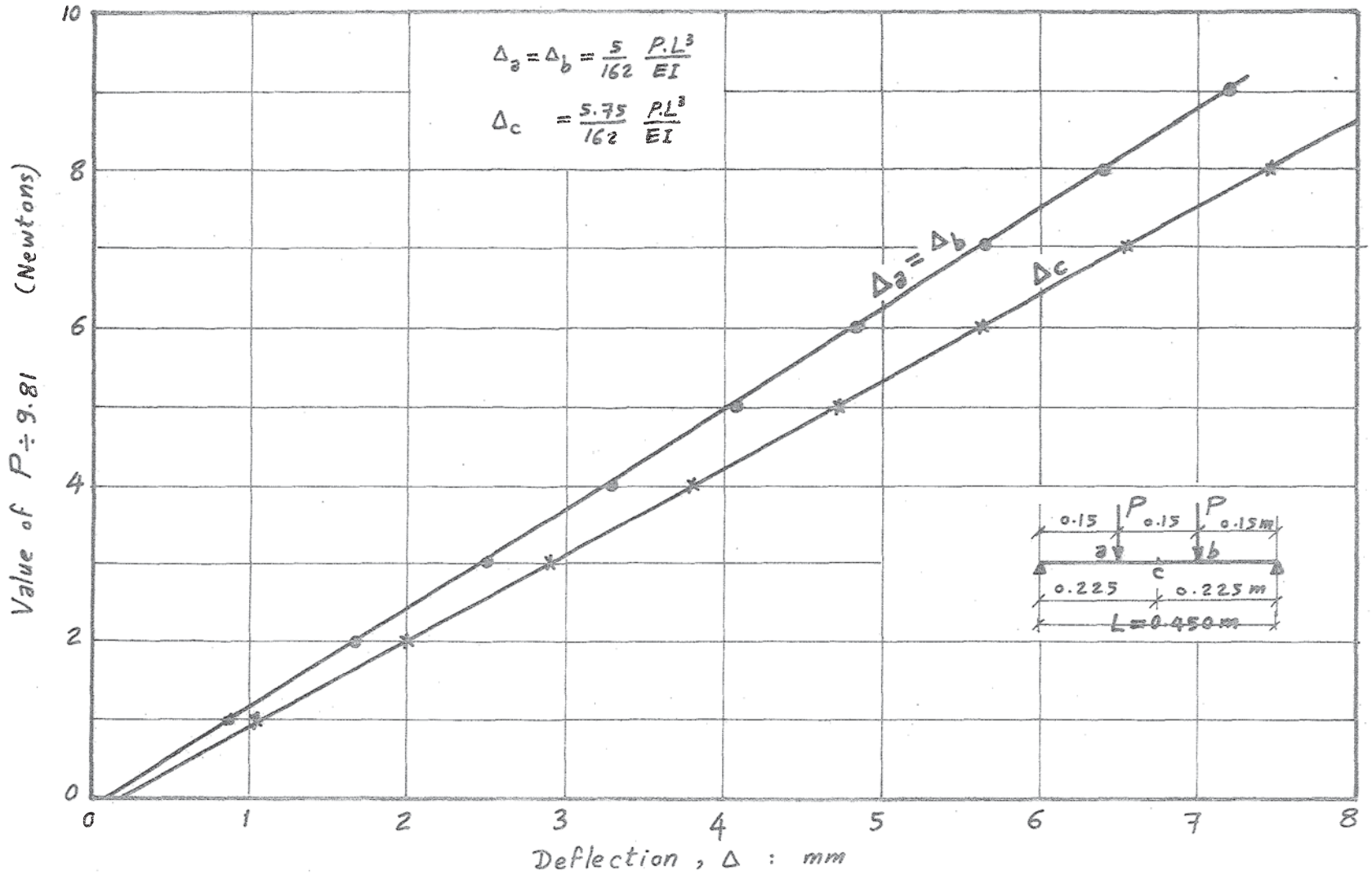

Fig. 5.12.- Load ~ Deflection Graphs for a Specimen of the Deck, (Full Width), of the Two-Cable Bridge.

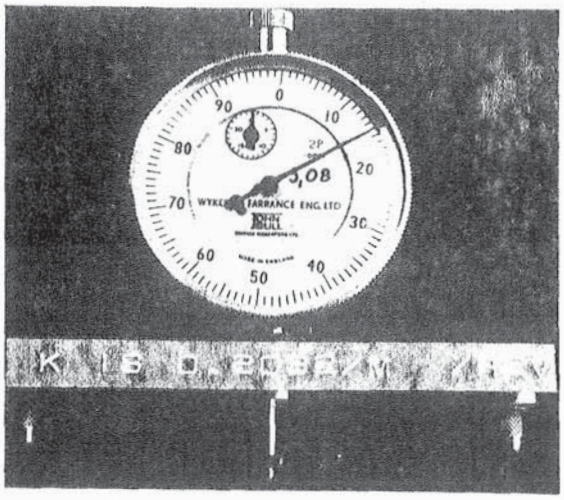

The Curvature Meter.

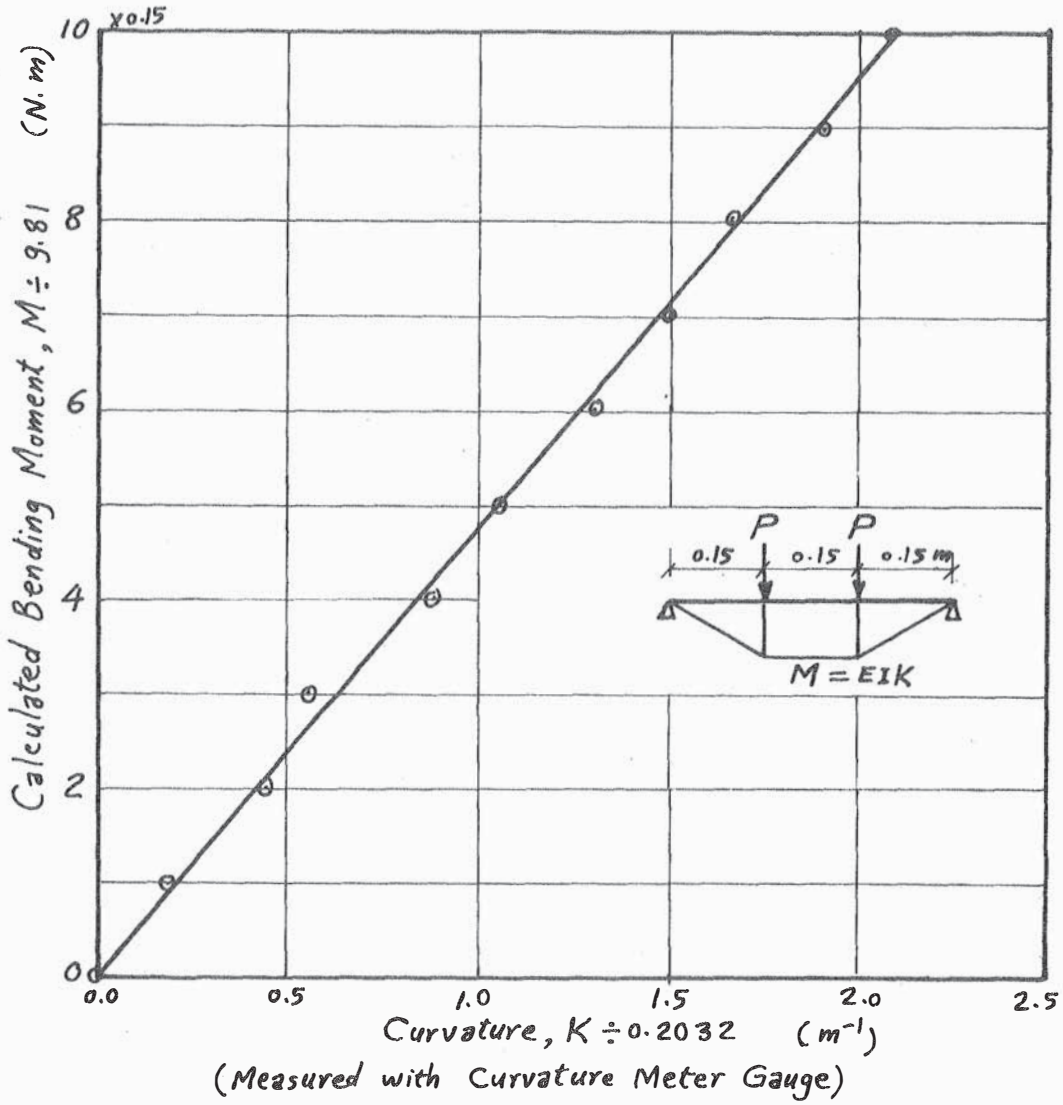

Fig.5.13.— M ~ K Graph for a Specimen of the Deck, (Full Width), of the Two-Cable Bridge.

CHAPTER VI

TWO-CABLE BRIDGE: DYNAMICS

6.1 INTRODUCTION

As in the case of the static study, there is not much published on the dynamic analysis of the two-cable bridge. Only one paper, (Ref. 6.1), on the topic, dealing with field tests on two existing bridges, could come to the hands of the writer. The foregoing eigenvalue analysis, presented by the writer in Chapter IV, is extended herein to get the flexural as well as the torsional modes and frequencies of vibration of the two-cable suspension bridge model. Some measurements were taken and showed good agreement with calculations.

6.2 NUMERICAL EXAMPLES

The vibrational modes and frequencies were calculated for the D.L. condition and also for the two L.L. conditions shown in Fig. 6.1. Measurements for the D.L. condition were taken for both the frequencies and the mode shapes to check the analytical results.

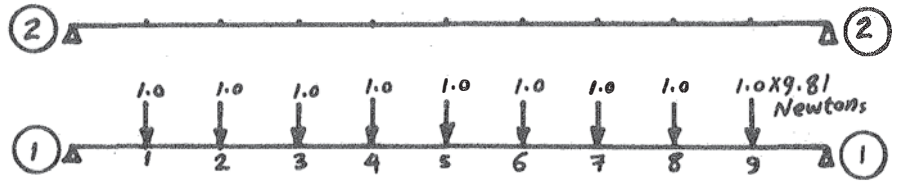

(a) Uniform load on one side only.

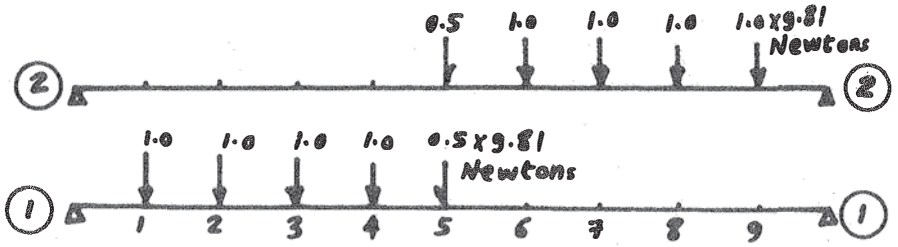

(b) Torsional load on both sides.

Fig. 6.1.- Two Torsional Loading Conditions.

The flexibility matrix was calculated for each loading condition using the secant to an influence load of 4 x 9.81 = 39.24 Newtons. The span of each cable was divided into ten equal segments, to give nine equidistant stations per cable.* Accordingly, the flexibility matrix of the bridge becomes 18 x 18. (See Appendix A4, "Singular Matrices".)

Due to the singularity of the flexibility matrix, only ten "reasonable"** vibrational modes could be obtained.

The flexibility matrix of the two-cable bridge is asymmetric due to the non-linearity of the structure. However, it is not very far from symmetric since the structure is not highly non-linear. An averaging procedure was subsequently carried out on the off-diagonal elements of the flexibility matrix of the D.L. condition to get rid of the complex eigenvalues and eigenvectors, but even then only the same ten "reasonable" vibration modes were obtained.

6.2.1 Reduction of Degrees of Freedom

This led the writer to think of reducing the order of the matrix to see what it gives. There are several methods for reducing the degrees of freedom of structures, called "eigenvalue economisation", Ref. 6.2, but the method presented herein by the writer has apparently never been used before. For a space structure with 18 joints, the usual number of degrees of freedom is 18 x 6 = 108. But for our simplified model of the suspension bridge, neglecting the hanger extensions and regarding the displacements of the 18 deck stations, (9 each side), to be identical with the corresponding joints of the two cables, the number of degrees of freedom can be reduced to half, i.e. 18 x 3 = 54. If we can go further and neglect the horizontal in-plane and out-of-plane displacements of the two cables, i.e. if we consider only the vertical deflections, the number of degrees of freedom is reduced again to 18 x 1 = 18.

The new reduction, introduced herein by the writer, is to imagine that the span is divided into a number of intermediate stations less than what it really is. For example, our model is divided by nine stations (each side) into ten segments, and now let us imagine reducing the number of stations from 9 to, say, 7, 5, 3, 1, corresponding to matrices of orders 14, 10, 6, 2 respectively. (In all cases the stations are horizontally equidistant, and the bridge is divided into equal segments, the number of

---

* The word equidistant, here, is related to the horizontal travel between each two successive stations.

** The word reasonable, here, refers to modes with low frequencies (not more than, say, 12 Hz).

which is equal to the number of stations per cable + 1, and the masses of all segments are assumed to be equal, each of which is lumped at its centre in the spanwise direction and divided equally between the two cables. When applying L.L., the total L.L. is independent of the number of stations and is distributed equally, (or otherwise), among the proposed number of stations.

The results of the obtained frequencies are shown in Table 6.1, and the mode shapes are shown in Figs. 6.2, 6.3, 6.4. It has been found that if the matrix order is 10, 14, or 18, not more than 10 "reasonable", (or useful), modes can be obtained, and the frequencies and the mode shapes are almost the same. This proved to be true for all the above-mentioned three loading cases. It is obvious, from Table 6.1 and Fig. 6.2, that the averaging procedure does not make any considerable change in the frequency of any of the ten modes.

When the order of the matrix is reduced to six, only the first six modes can be obtained. When the matrix order was further reduced to two, the first two frequencies could be obtained with adequate accuracy.

This is actually very important, since much time can be saved in finding the eigenvalues and the eigenvectors by using a matrix size just proper for the required number of modes, and also for defining the mode shape.

In this study, the number of stations per cable was always odd to provide a station at midspan, since the midspan is very important in defining many modes.

It is worthwhile to notice that, for any matrix order, half the obtainable modes are flexural and the other half are torsional. In other words, the number of each of the flexural and torsional modes is equal to the number of stations per cable. So, it is likely that for any number of stations, some flexural modes and an equal number of torsional modes will be obtained, with the advantage that modes with lower frequencies are obtained first. For example, if the number of stations per cable is four, the first four flexural and the first four torsional modes will be obtained.

This is actually very useful, not only in saving much time in solution, but also in making it possible to use smaller computers. For example, the laboratory-type digital computer Pdp-8, (using the Focal language), could not solve the 18 x 18 matrix which had to be solved by the Burroughs B6700/B7700, (using Fortran IV). However, the 14 x 14 matrix could just be solved by the Pdp-8 small computer, by dividing the Focal program into three separate programs because of the small capacity of that machine.

TABLE 6.1

Order of flexibility matrix	Number of modes obtained	Frequency, (in Hz), of Mode No.										Remarks
		1	2	3	4	5	6	7	8	9	10	
		Flexural	Flex.	Torsional	Flex.	Torsion.	Flex.	Torsion.	Flex.	Torsion.	Torsion.	
(i) D.L. Condition												
2	2		2.28	3.33								*
6	6	2.48	3.22	4.16	4.20	4.85		6.32				*
10	10	2.47	3.25	4.14	4.72	4.85	5.72	7.42	7.95	9.67	12.10	*
14	10	2.47	3.25	4.14	4.73	4.85	5.72	7.42	7.90	9.66	12.10	*
18	10	2.47	3.24	4.13	4.69	4.85	5.72	7.41	7.92	9.66	12.10	**
18	10	2.47	3.23	4.13	4.74	4.85	5.72	7.42	7.96	9.66	12.10	***
		2.56	3.15	3.88	4.13	4.75	5.34					measured
(ii) Torsional L.L. Conditions of Fig. 6.1												
(a) Uniform Load on One Side Only.												
2	2		2.20	3.19								*
6	6	2.45	3.13	4.16	3.81	4.70		6.12				*
10	10	2.45	3.16	3.97	4.53	4.71	5.63	7.20	7.75	9.39	11.80	*
14	10	2.45	3.20	3.99	4.52	4.71	5.63	7.20	7.73	9.35	11.80	*
18	10	2.46	3.19	3.99	4.50	4.72	5.63	7.20	7.74	9.40	11.77	**
(b) Torsional Load on Both Sides.												
6	6	2.45	3.10	3.92	3.78	4.68		6.08				*
10	10	2.45	3.17	3.96	4.53	4.55	5.63	7.17	7.68	9.42	11.80	*
14	10	2.46	3.13	3.94	4.37	4.65	5.63	7.17	7.67	9.41	11.70	*
18	10	2.46	3.09	3.92	4.28	4.67	5.63	7.16	7.67	9.42	11.73	**

* :Matrix as it is, (asymmetric), Jacobi's procedure for symmetric matrices used to get the eigenvalues and eigenvectors.

** :Matrix as it is, (asymmetric), procedure for unsymmetric matrices used.

***:Matrix is made symmetric by averaging the off-diagonal elements.

Note: Modes 1, 2, 4, 6, 8 are flexural modes, while modes 3, 5, 7, 9, 10 are torsional modes.

6.2.2 D.L. Condition

The first two modes, (which are both flexural), could easily be obtained experimentally, and their frequencies compare very well with the calculations. Because much work was carried out, in studying the single-cable bridge, on flexural modes, the writer does not find any necessity to measure any more flexural mode shapes here.

However, the frequencies of both the third and the fourth flexural modes, (modes 4 and 6, respectively), were also measured and showed reasonable agreement with calculations, (within 13% and 7%, respectively). Also, the mode shape of the fourth flexural mode, (mode 6), was measured, and good agreement was obtained.

Initially, to get the third flexural mode, (mode 4), in the laboratory, the vertical deflections of the bridge were restrained at $\frac{x}{L} \simeq 0.4, 0.6$, and to get the fourth flexural mode, (mode 6), the vertical deflection of the midspan was restrained. However, by some skill and care and much force with steady finger excitation, both modes 4 and 6 could, with practice, be obtained without any restraints.

To get the first two torsional modes, the longitudinal centre line of the bridge had to be restrained, (as far as possible), to avoid the mixture of modes, or the likelihood of the flexural modes to happen first, (because of the lower frequency of the first two flexural modes). The longitudinal centre line of the bridge was very lightly restrained at $(\frac{x}{L}) = 0.22, 0.5, 0.78$, and the first torsional mode, (mode 3), could easily be obtained and measured, showing good agreement with calculations. An additional restraint was then added at $\frac{x}{L} = 0.5$ on each side to prevent mode 3, and to facilitate getting mode 5, (second torsional mode), which could, thus, be obtained and also measured easily, showing good agreement with calculations. The two side restraints of the midspan were then removed and, with care, mode 5 could still be obtained and measured, a very pleasing result. It was certainly not expected, when the model was designed, that so many flexural and torsional modes of oscillation could be obtained, and measured in detail, so readily.

The use of the light restraints is to prevent the unwanted modes from coming in while counting oscillations. The restraints affect neither the frequency nor the mode shape of the wanted mode. With some skill and care, the number of restraints could be reduced,or completely eliminated. In a real bridge, there are, often, no restraints, and the excitation is usually due to wind force, and the mode which happens is, usually, the one whose natural frequency is equal to the frequency of the exciting force. Or, there may be a mixture of modes. But with our

laboratory model, suitable excitation was achieved with the finger, (because of its convenience, the frequencies being too small for mechanical devices which we had available), and skill is needed to excite the structure in the required natural mode, especially when two or more modes have close frequencies, (like modes 4 and 5 of Fig. 6.2, (frequencies are 4.69, 4.85 Hz, respectively)). Moreover, the frequencies of the model are much higher than the corresponding frequencies of a real bridge, a fact that makes it harder to excite and measure higher modes.

The procedure may be repeated and extended to measure the rest of the ten calculated modes, using more restraints and more exciting force, but the writer thinks that four flexural and two torsional modes are quite enough to measure in the laboratory, and it was with much gratification that these six modes were adequately covered.

Figs. 6.2 show the calculated vibration modes of the D.L. condition, (laboratory measurements are superimposed), from which it can be said that the number of the intermediate stations used in the analysis has, generally speaking, no remarkable effect on any of the frequencies or the mode shapes. The main thing is to decide how many modes are required, and how many stations are adequate to define each mode. It must be known also that the number of torsional modes obtained is always equal to the number of flexural modes, and each is, generally speaking, equal to the number of stations per cable. For some cases, the number of the useful modes may be less than the matrix order, (like the case of our laboratory model), and not more than, say, ten modes can be obtained, even if the matrix is 18 x 18 or greater.

* * * *

Suppose it is wanted to know the first two torsional modes and the first three flexural ones. In such a case, at least three intermediate stations can be used in the analysis so that three flexural modes can be obtained. In this case, also, three torsional modes will be obtained, more than the required number, (two).

If three flexural and four torsional modes are required, the number of stations per cable must be not less than four, i.e. the span must be divided, at least into five segments, and so on.

However, adequate accuracy can be obtained if the span is divided into six or eight segments (by five or seven stations per cable, respectively). This will give all the possible useful ten modes.

In all cases, modes 1, 2, 4, 6, 8 were found to be flexural, while modes 3, 5, 7, 9, 10 are torsional.

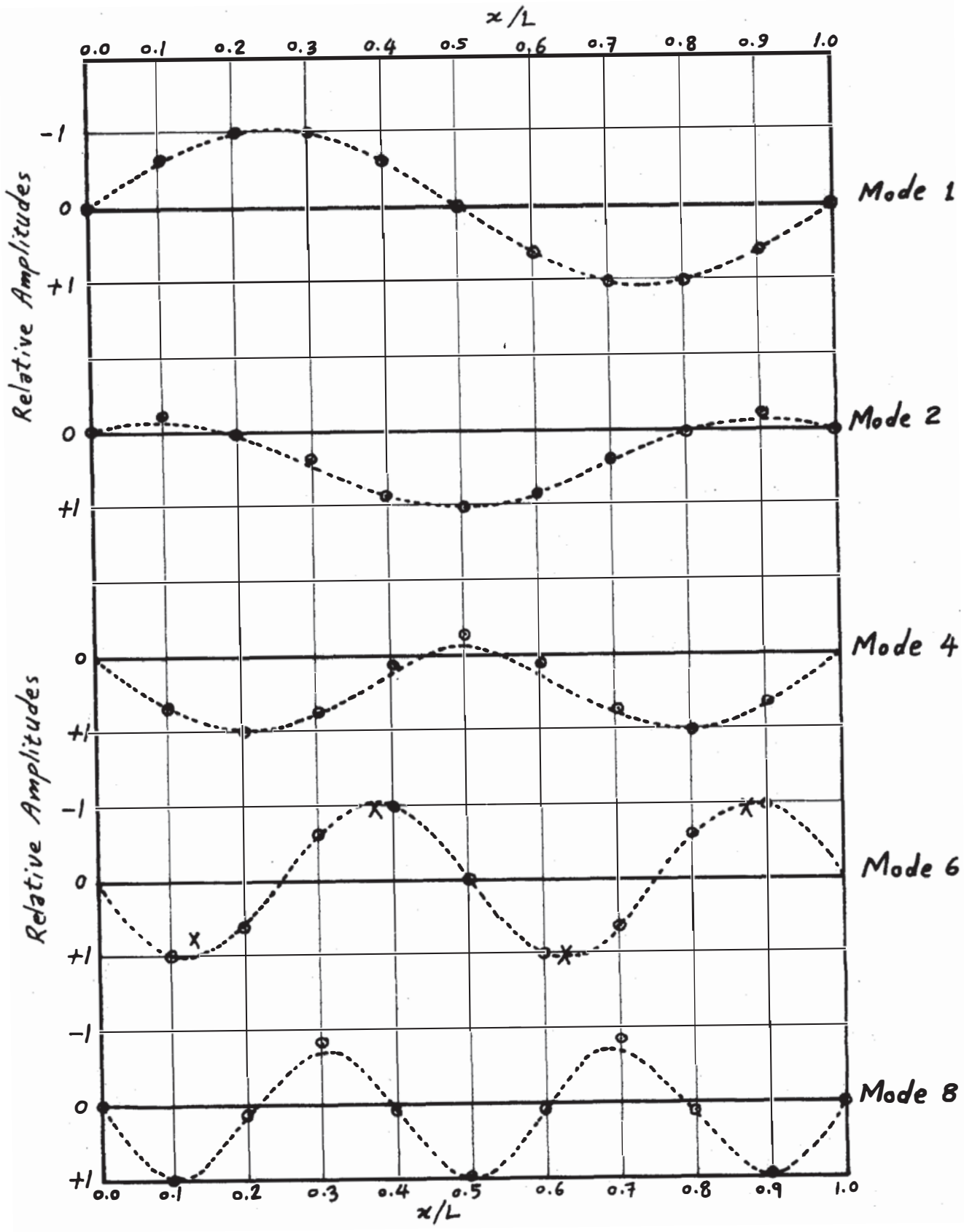

		Frequencies, Hz.				
		Mode 1	Mode 2	Mode 4	Mode 6	Mode 8
x	Measured.	2.56	3.15	4.13	5.34	
.....	Matrix as it is, (asymmetric).	2.47	3.24	4.69	5.72	7.92
o	Matrix made symmetric by averaging the off-diagonal elements.	2.47	3.23	4.74	5.72	7.96

Fig. 6.2.1. - First Five Flexural Modes, Dead Load Condition.

No. of Stations Per Cable = 9.

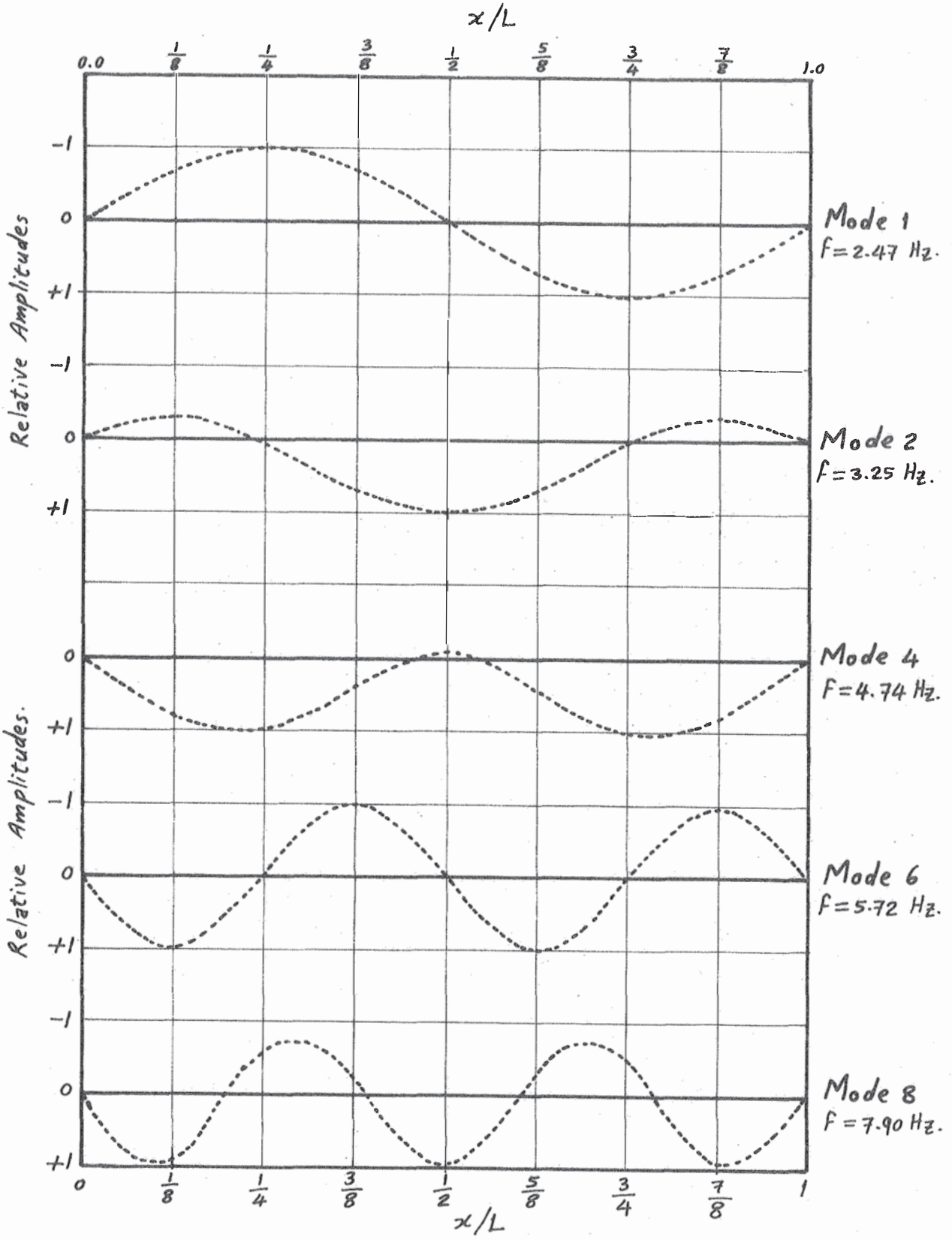

Fig. 6.2.2.- First Five Flexural Modes for the Dead Load Condition.

No. of Stations Per Cable = 7

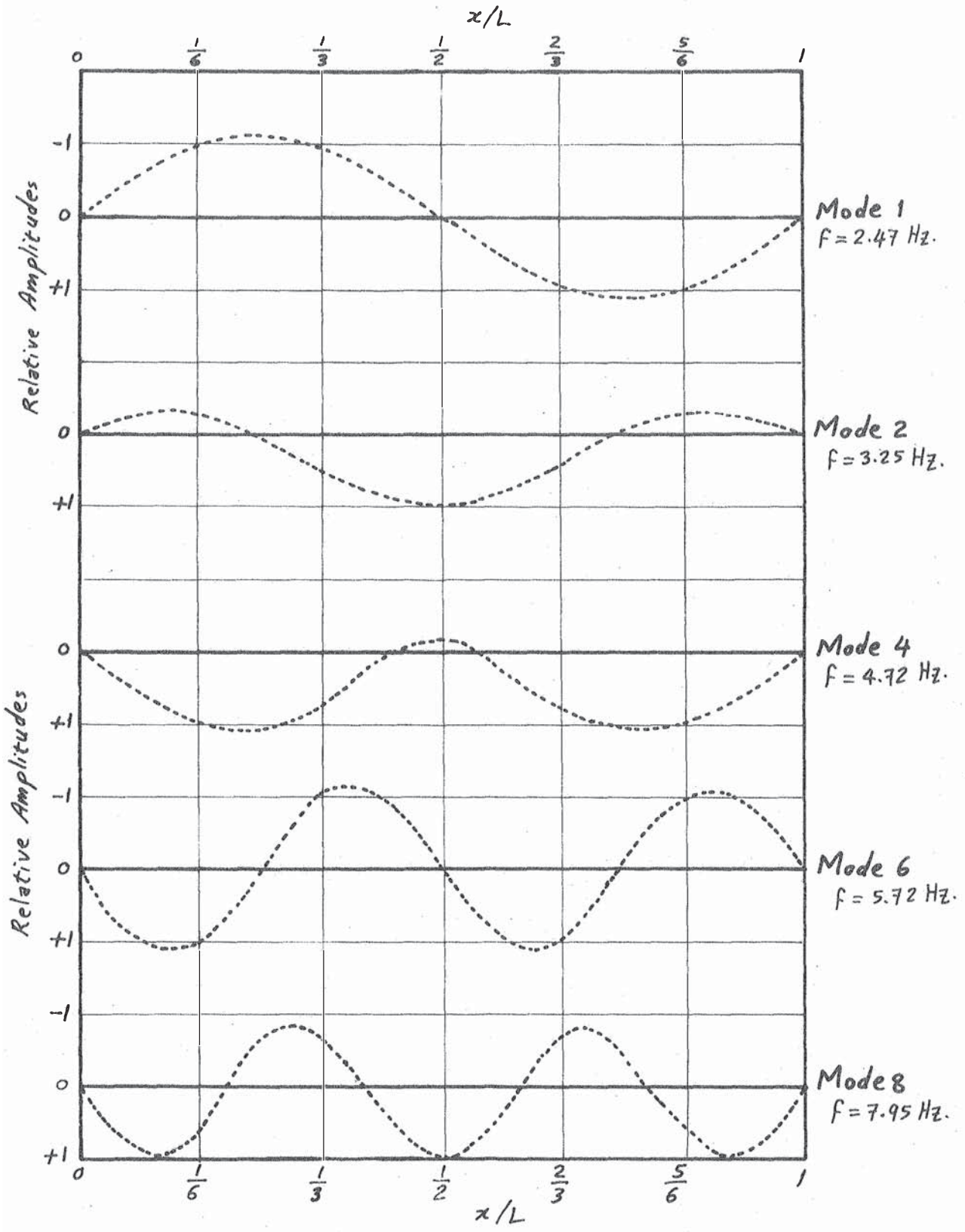

Fig. 6.2.3.- First Five Flexural Modes, Dead Load Condition.

No. of Stations Per Cable = 5

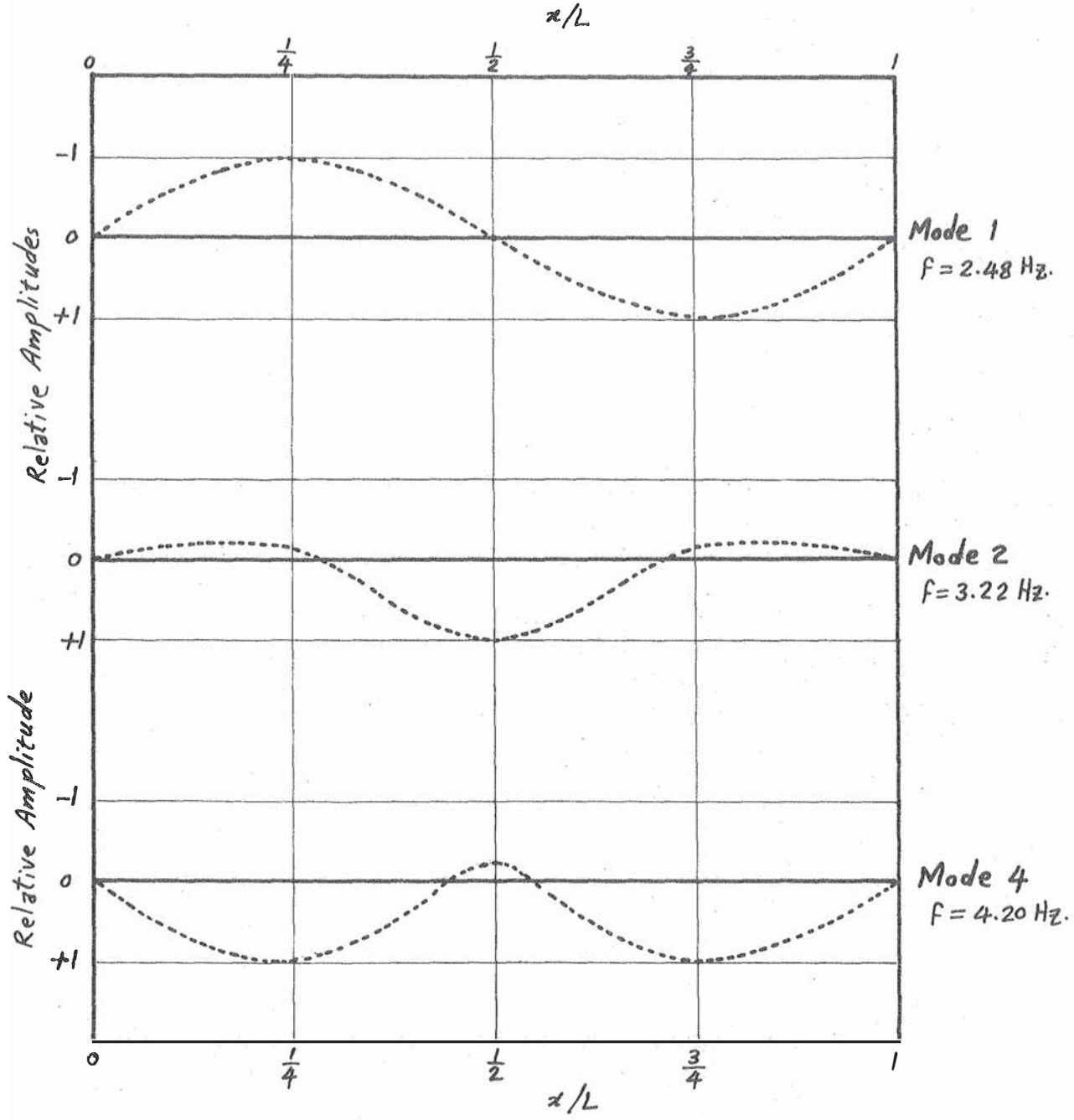

Fig. 6.2.4.- First Three Flexural Modes, Dead Load Condition.

No. of Stations Per Cable = 3.

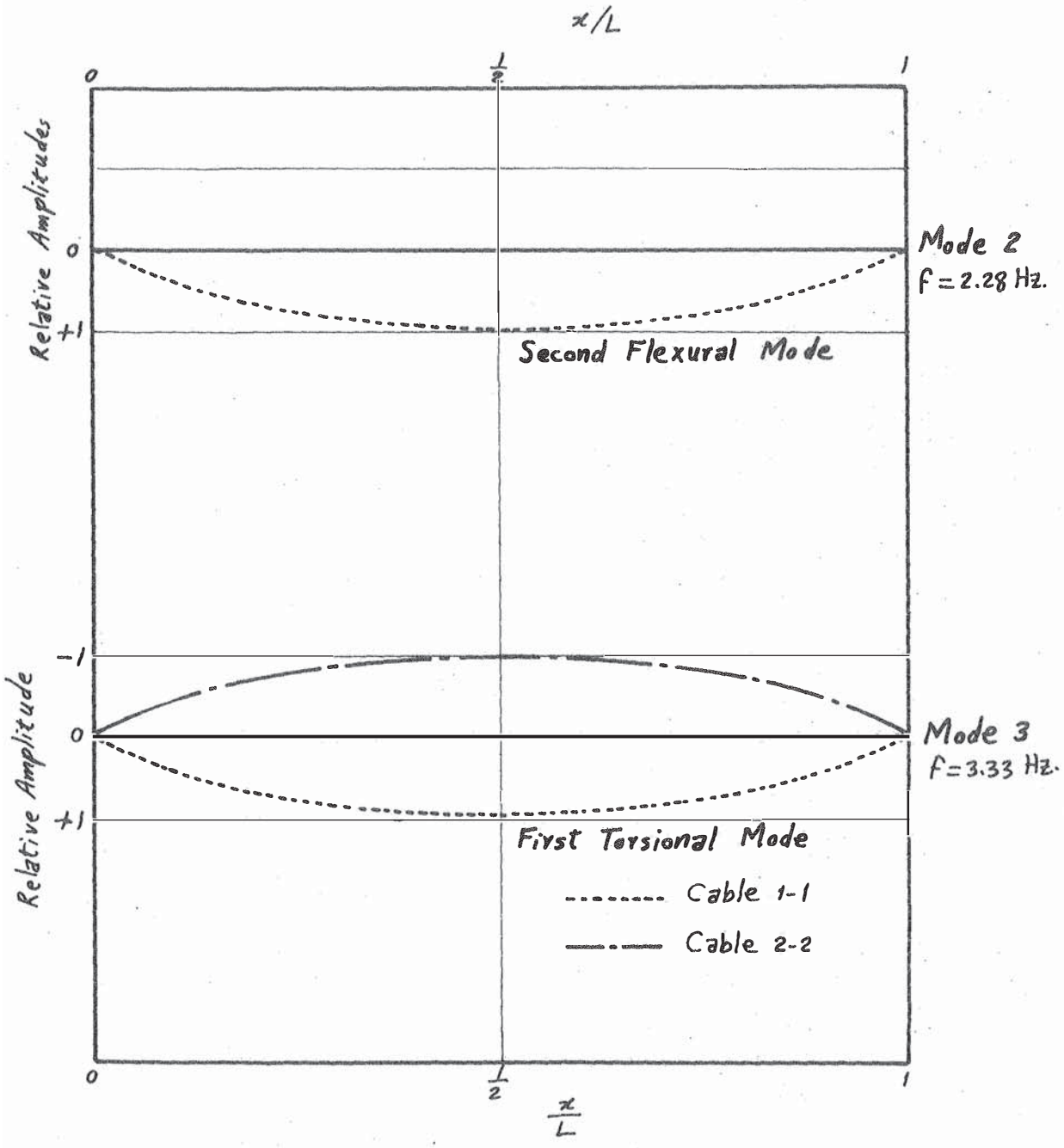

Fig. 6.2.5.— Flexural and Torsional Modes, Dead Load Condition.

No. of Stations Per Cable = 1.

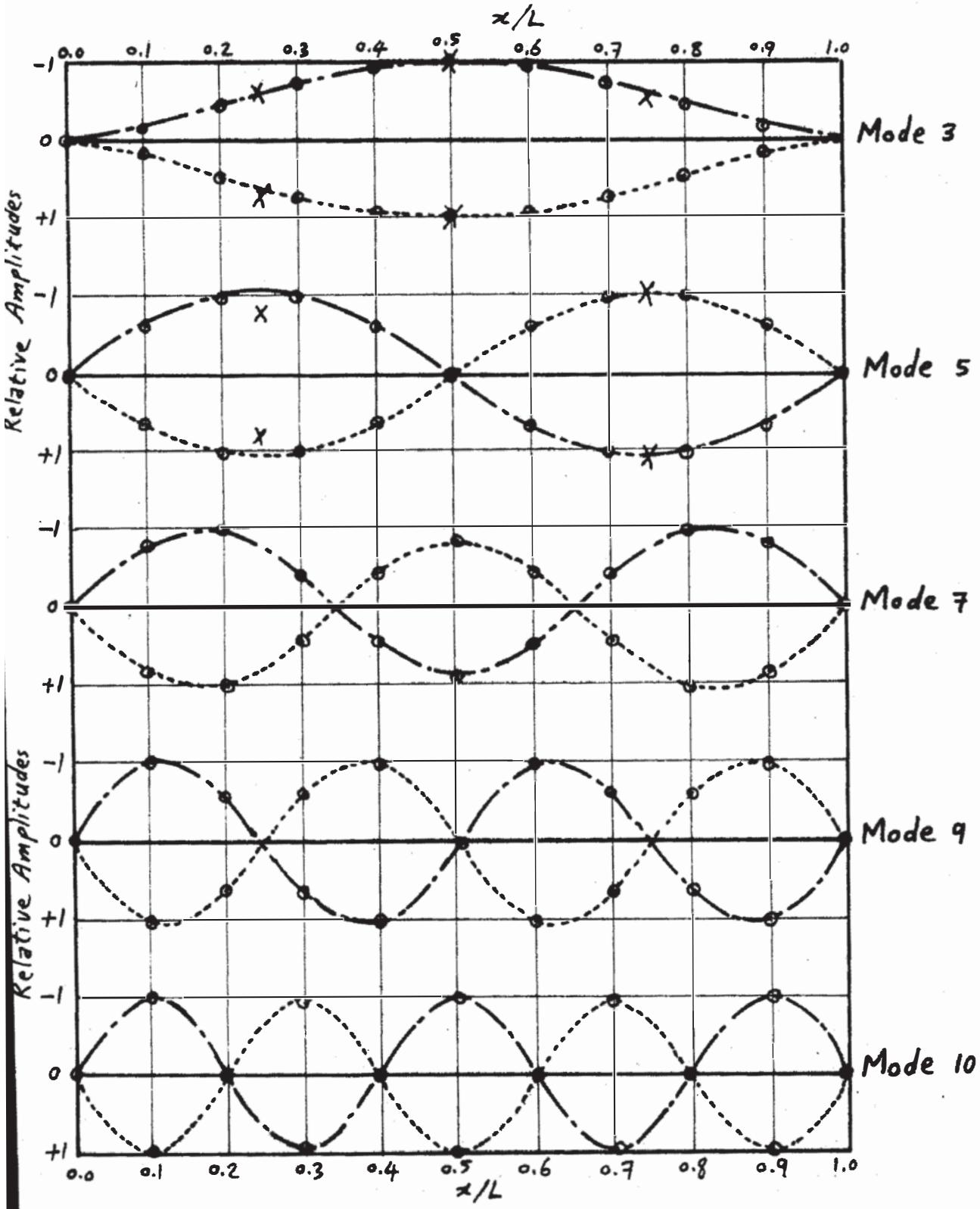

		Frequencies, Hz				
		Mode 3	Mode 5	Mode 7	Mode 9	Mode 10
x	Measured.	3.88	4.75			
.....	Cable 1-1 } Matrix as it is (asymmetric).	4.13	4.85	7.41	9.66	12.09
—·—	Cable 2-2 }					
⊙	Matrix made symmetric by averaging the off-diagonal elements.	4.13	4.85	7.42	9.66	12.09

Fig. 6.2.1 — First Five Torsional Modes, Dead Load Condition.

No. of Stations Per Cable = 9.

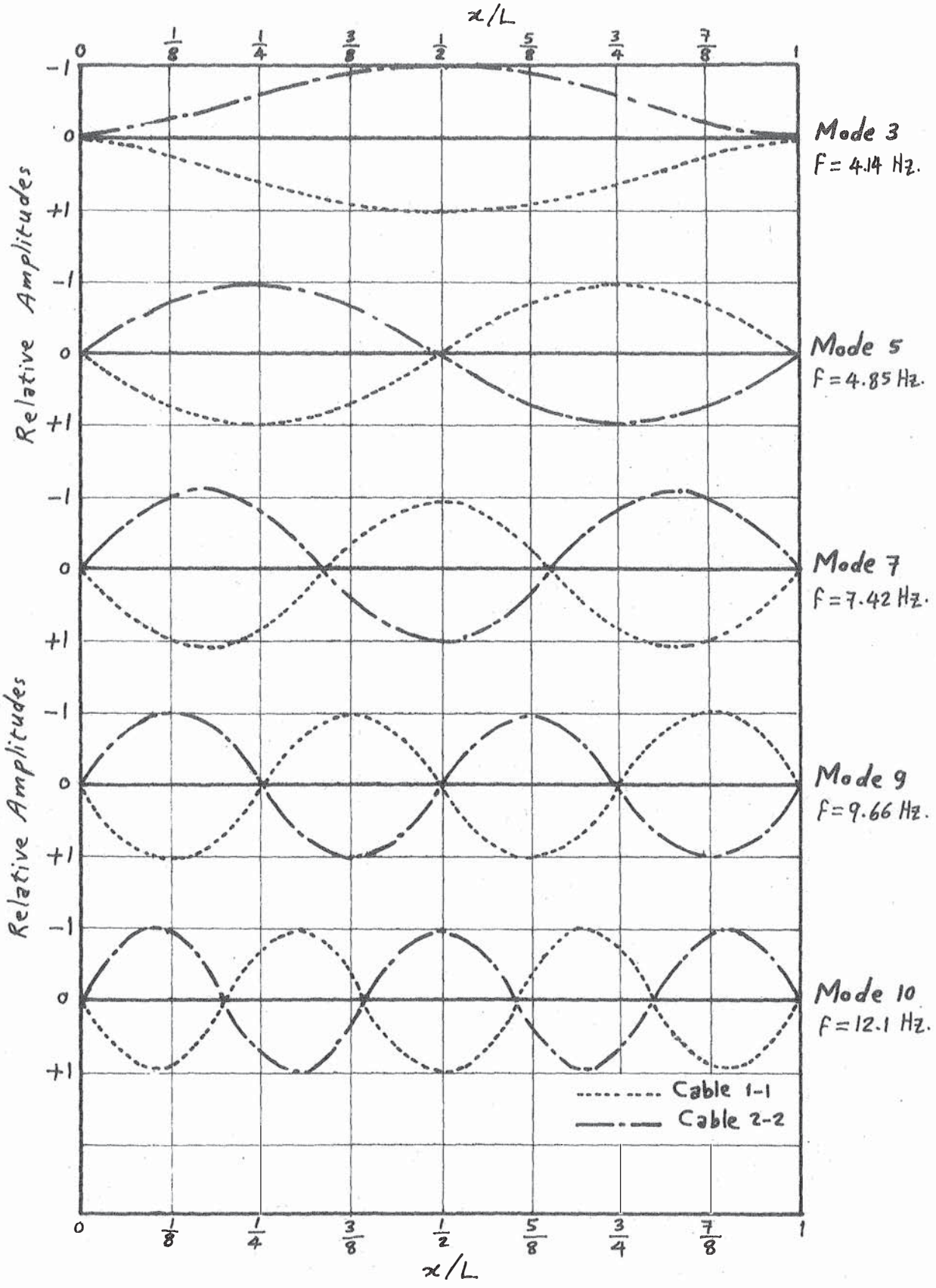

Fig. 6.2.2 — First Five Torsional Modes, Dead Load Condition.

No. of Stations Per Cable = 7.

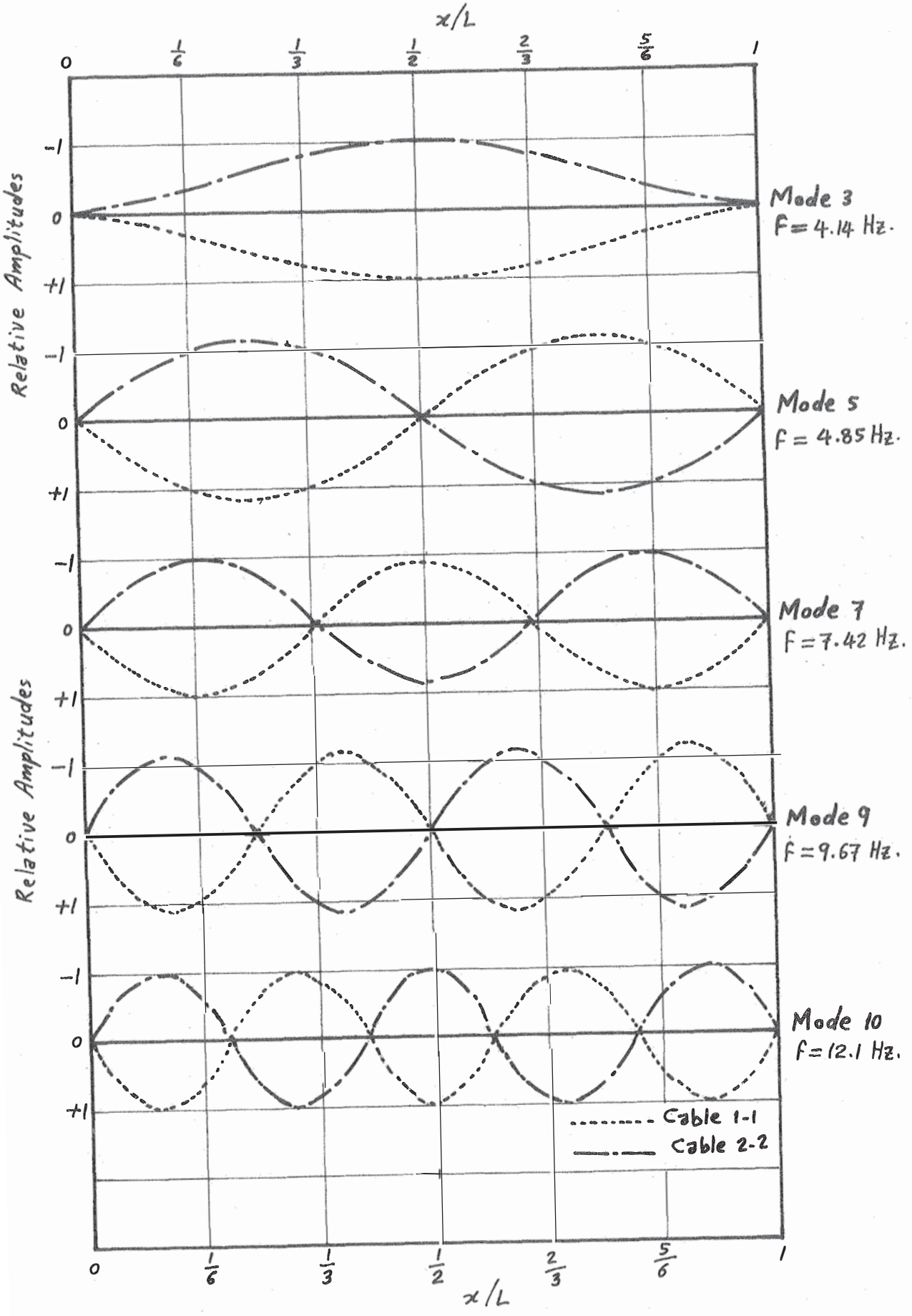

Fig. 6.2.3 - First Five Torsional Modes, Dead Load Condition.

No. of Stations Per Cable = 5.

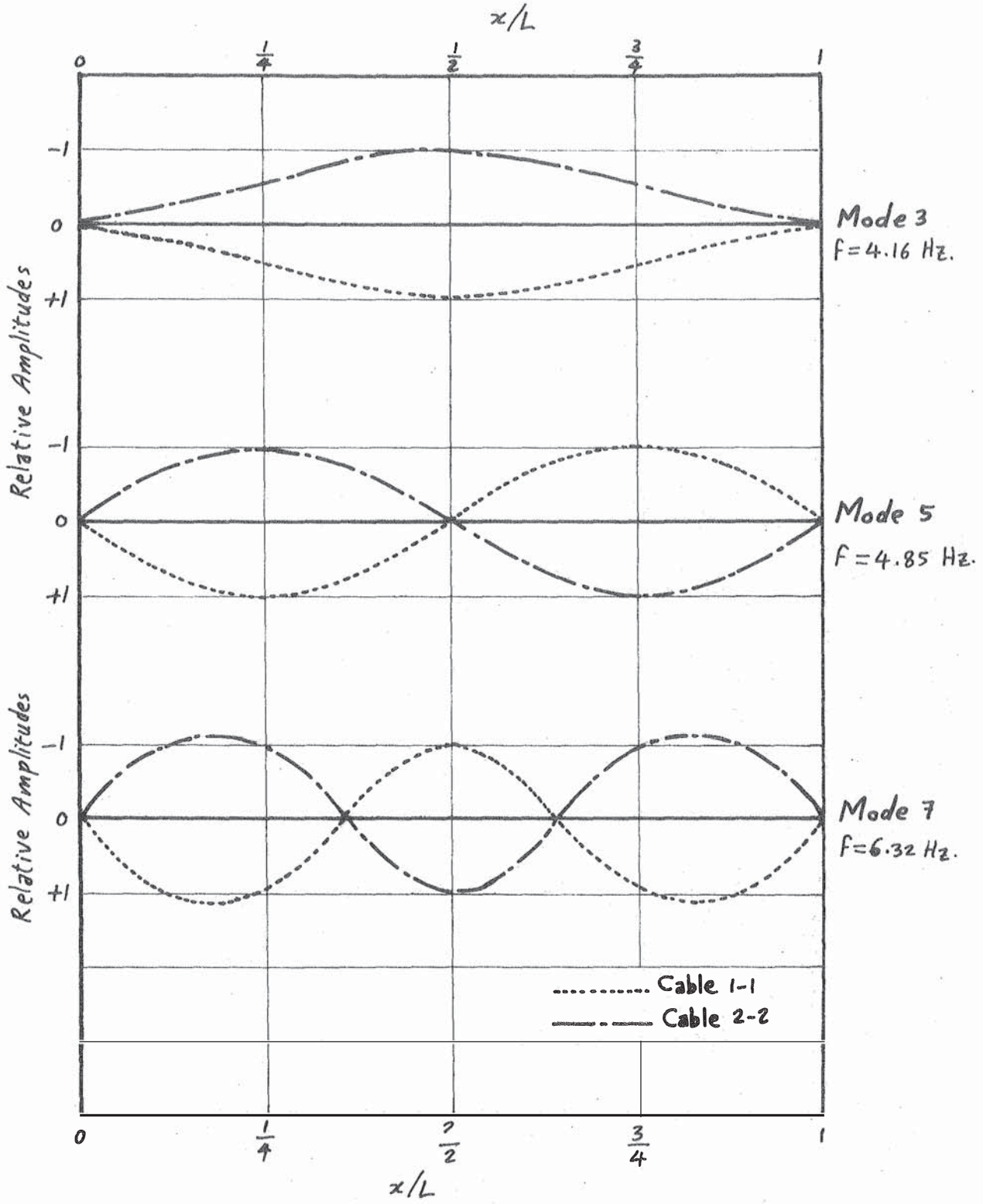

Fig. 6.2.4'.- First Three Torsional Modes, Dead Load Condition.
No. of Stations Per Cable = 3.

For the flexural modes, modes 2, 4, 8 are symmetric, while modes 1, 6 are antisymmetric. But for the torsional modes, modes 3, 7, 9 are symmetric, while modes 5, 10 are antisymmetric.

When only three intermediate stations per cable are used, three flexural and three torsional modes are obtainable, (modes 1, 2, 4 and 3, 5, 7, respectively). In other words, the sixth mode, here, is mode 7 of the case of a number of stations per cable more than three, (in order to get equal number of flexural and torsional modes). Similarly, if four stations per cable are used, the analysis will give modes 1, 2, 4, 6 as the four flexural modes, and modes 3, 5, 7, 9 as the four torsional modes and so on.*

It is obvious that the smaller the number of stations per cable, the lower will be the accuracy of the results. As mentioned above, five or seven stations per cable are more than enough, and will give all the five flexural and five torsional modes.

6.2.3 L.L. Condition (a) of Fig. 6.1

Suspension bridges must have suitable dynamic properties under live load. This topic appears to have received little or no attention. The implications of the results of the following study may be of considerable importance in design.

When the full span of one side only is uniformly loaded, there is no remarkable change in the resulting modes, regarding both their frequencies and shapes. A slight reduction is noticed in all the ten frequencies, and the amplitudes of the two cables become slightly different, (instead of being equal for the D.L. condition). For the "flexural" modes, it is noticed that the amplitudes of the loaded side are slightly greater than those of the unloaded side,** while for the "torsional" mode, the contrary happens, as shown in Fig. 6.3

The reduction in frequency when adding loads is expected, according to the rule which says that adding mass reduces the frequency. Also, the amplitudes of a loaded cable must be less than those of the unloaded one because cables, (and suspension structures in general), usually stiffen by loading. This justifies what happens to the "torsional" modes, but what happens to the "flexural" modes still needs some justification.

---

* If only one central station is used, (for each cable), only two modes will be obtained: the first (symmetric) flexural mode, (mode 2), and the first (symmetric) torsional mode, (mode 3). Here only symmetric modes are obtained since they can have non-zero amplitudes at mid-span, (unlike the antisymmetric modes).

** As it was previously noticed in the single-cable bridge, Chapter III.

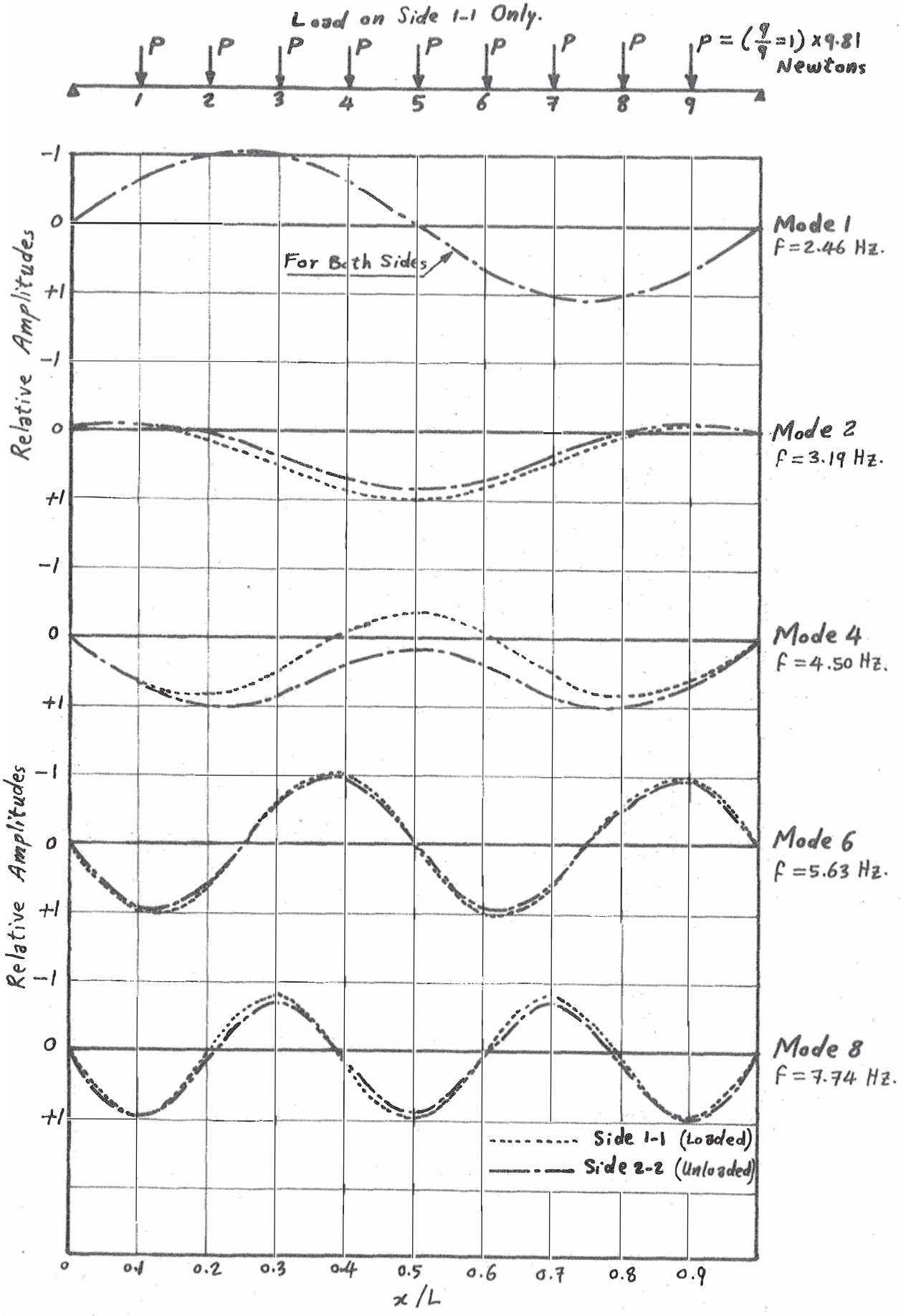

Fig. 6.3.1.—First Five "Flexural" Modes, Live Load as Shown.

No. of Stations Per Cable = 9.

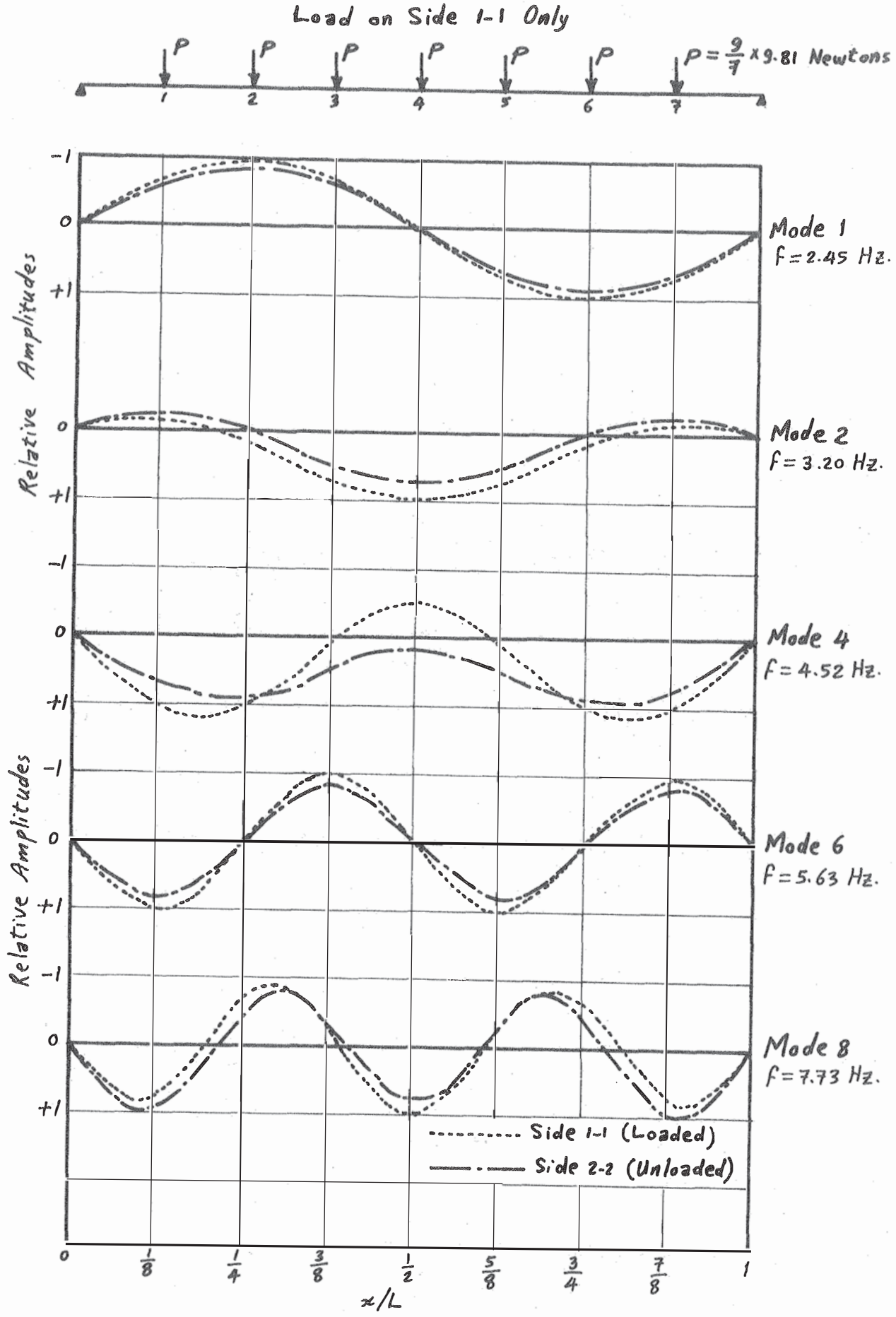

Fig. 6.3.2.– First Five "Flexural" Modes, Live Load as Shown.

No. of Stations Per Cable = 7.

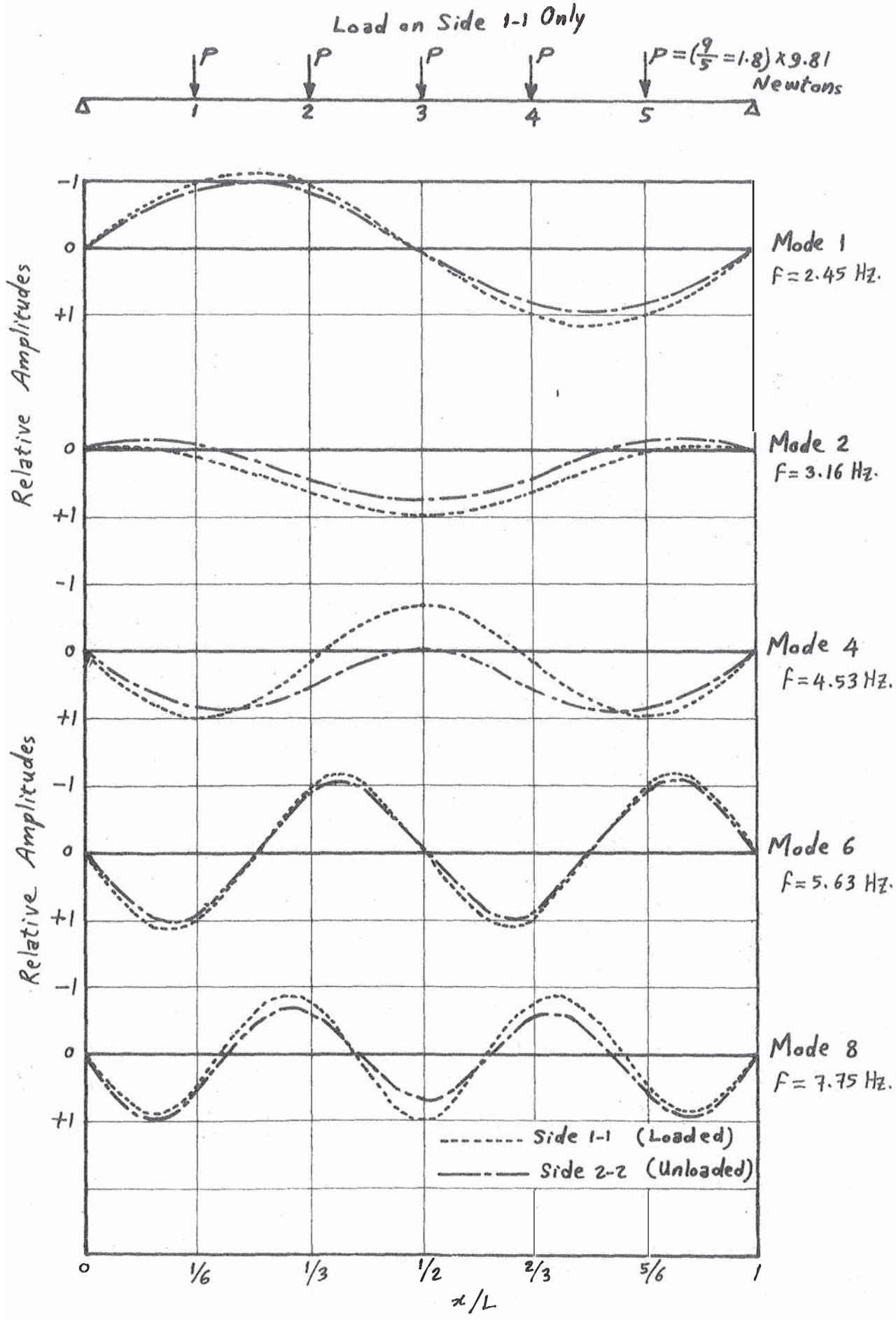

Fig. 6.3.3.- First Five "Flexural" Modes, Live Load as Shown.

No. of Stations Per Cable = 5.

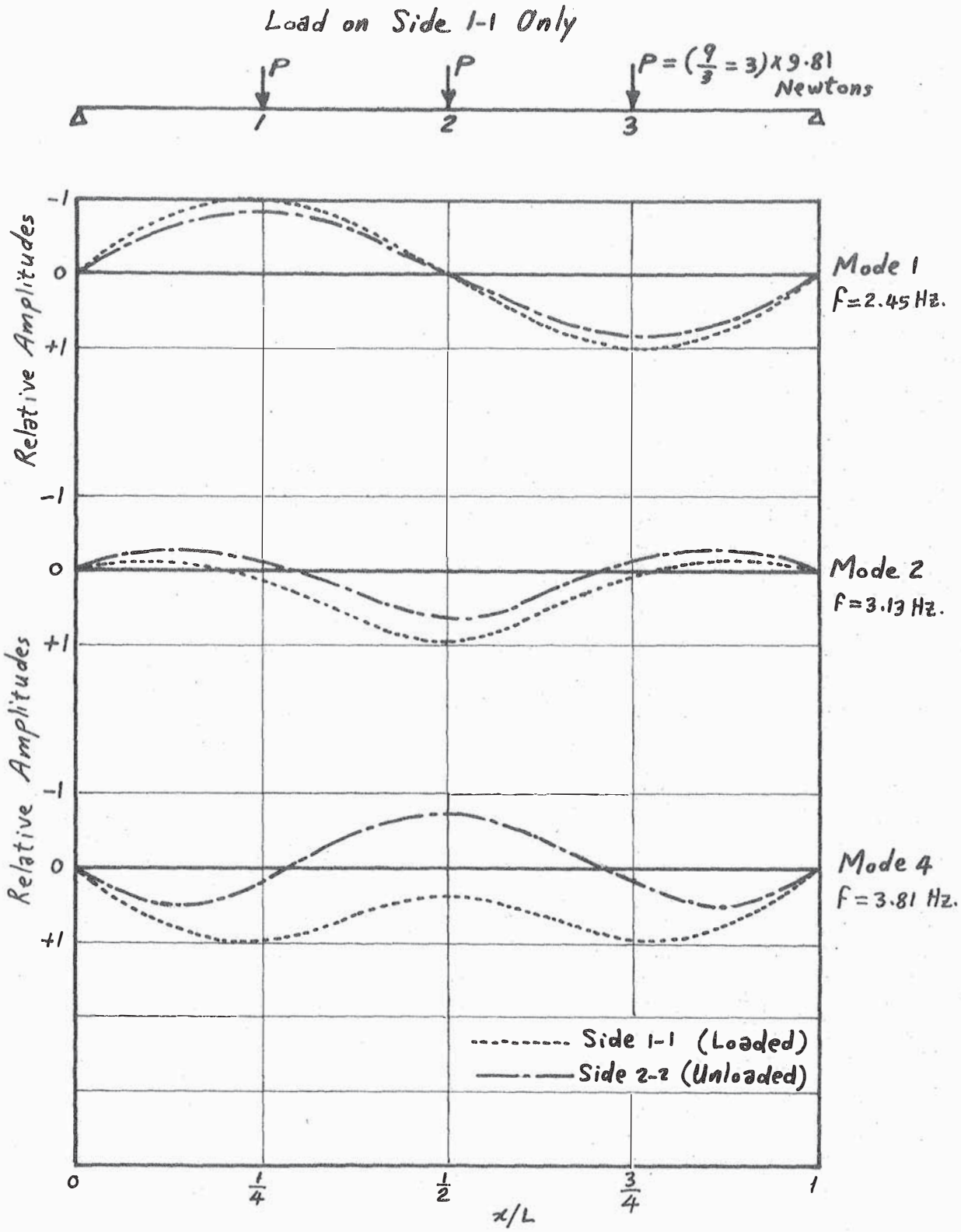

Fig. 6.3.4.— First Three "Flexural" Modes, Live Load as Shown.

No. of Stations Per Cable = 3.

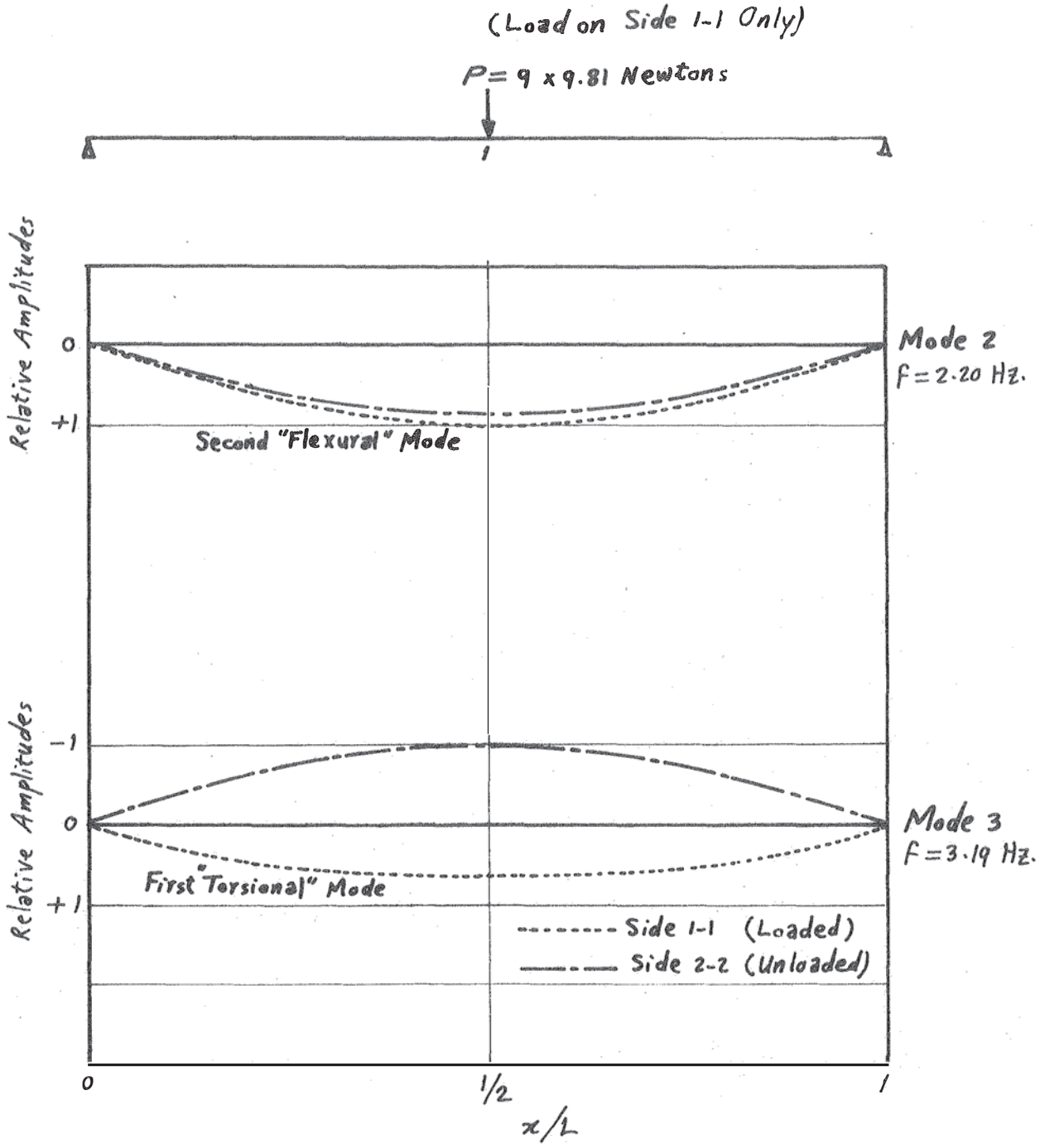

Fig. 6.3.5.- "Flexural" and "Torsional" Modes, Live Load as Shown.

No. of Stations Per Cable = 1.

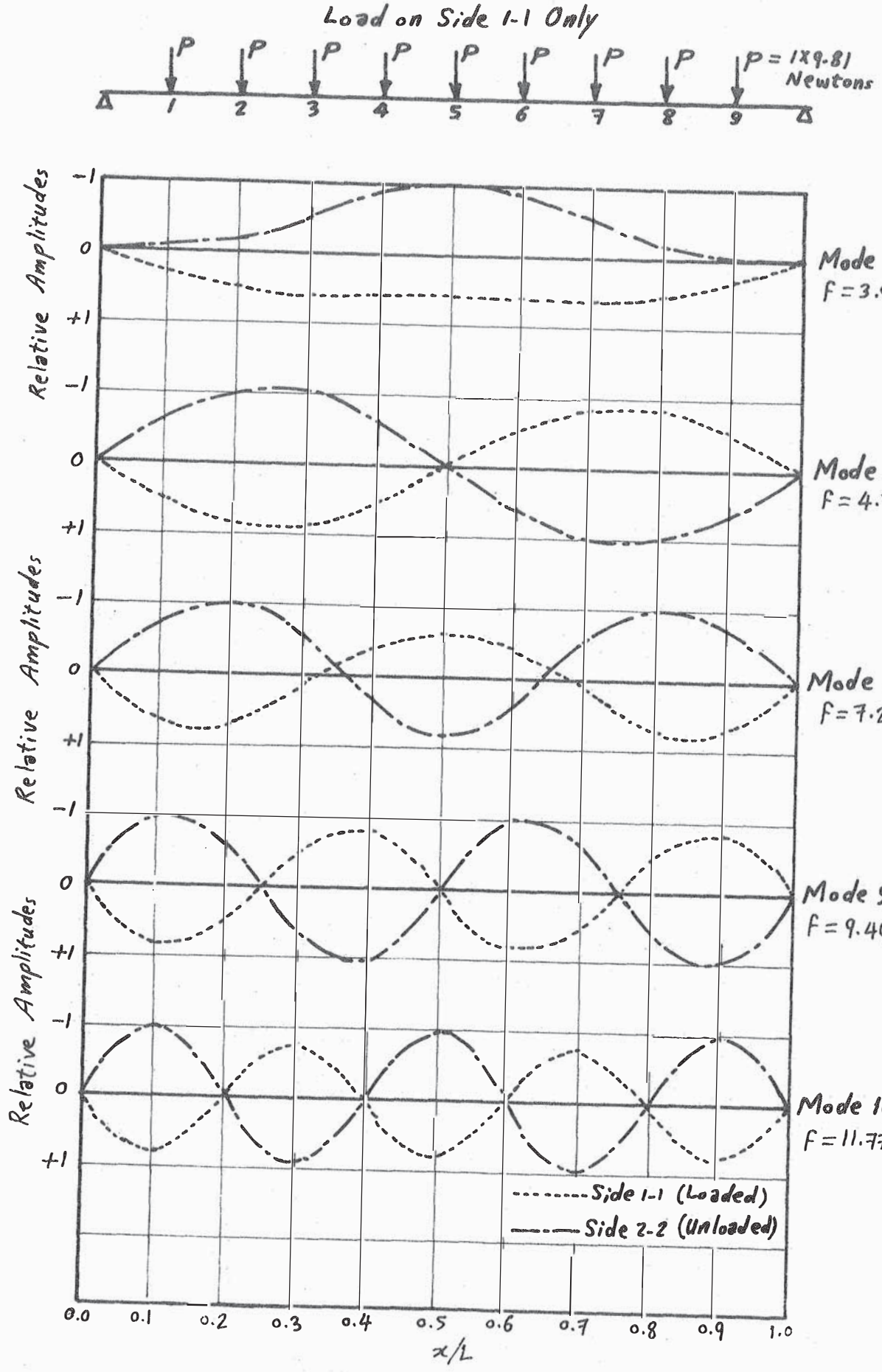

Fig. 6.3.1 — First Five "Torsional" Modes, Live Load as Shown.

No. of Stations Per Cable = 9.

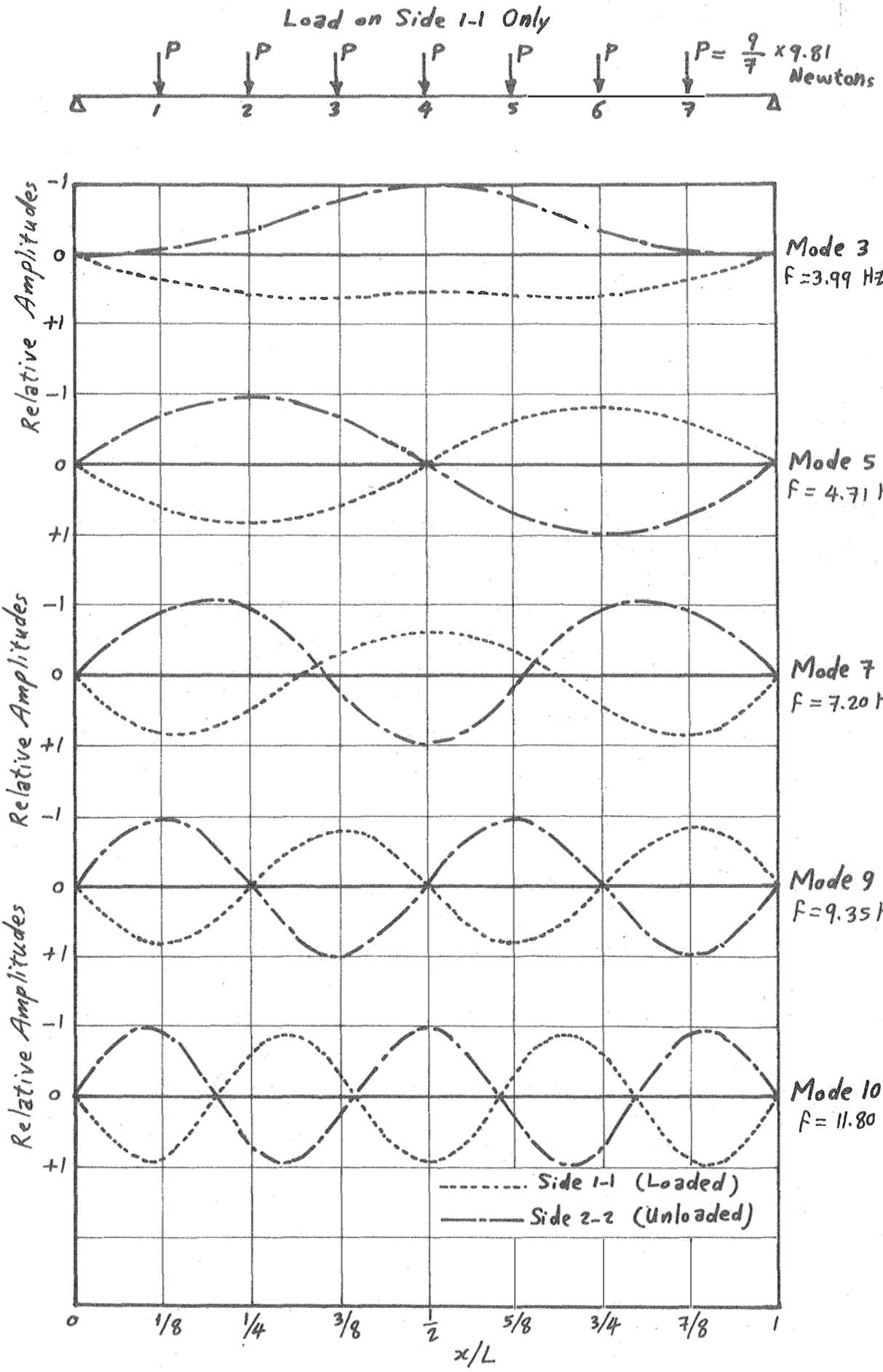

Fig. 6.3.2 — First Five "Torsional" Modes, Live Load as Shown.

No. of Stations Per Cable = 7.

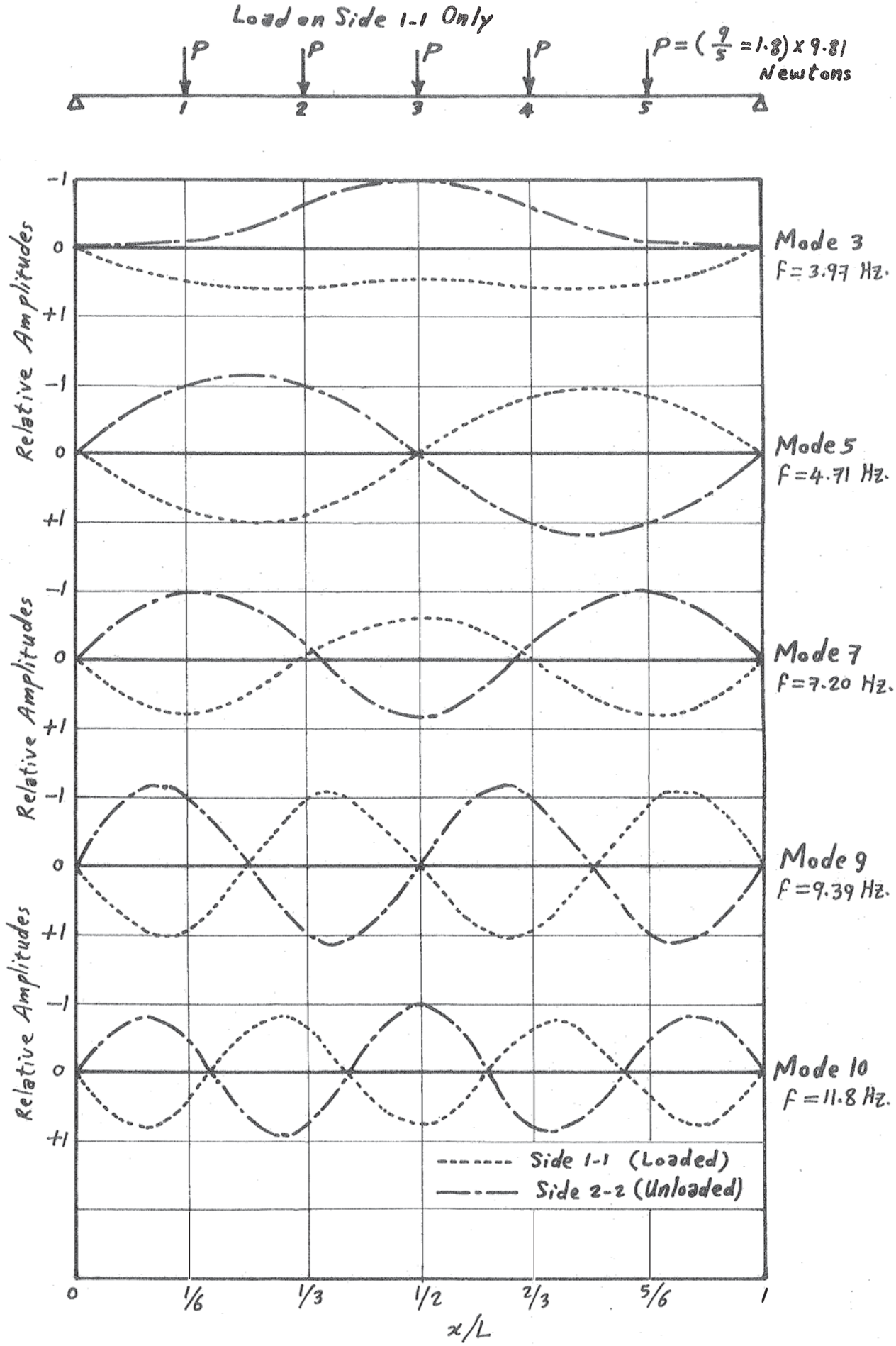

Fig. 6.3 .3`_ First Five "Torsional" Modes, Live Load as Shown.

No. of Stations Per Cable = 5.

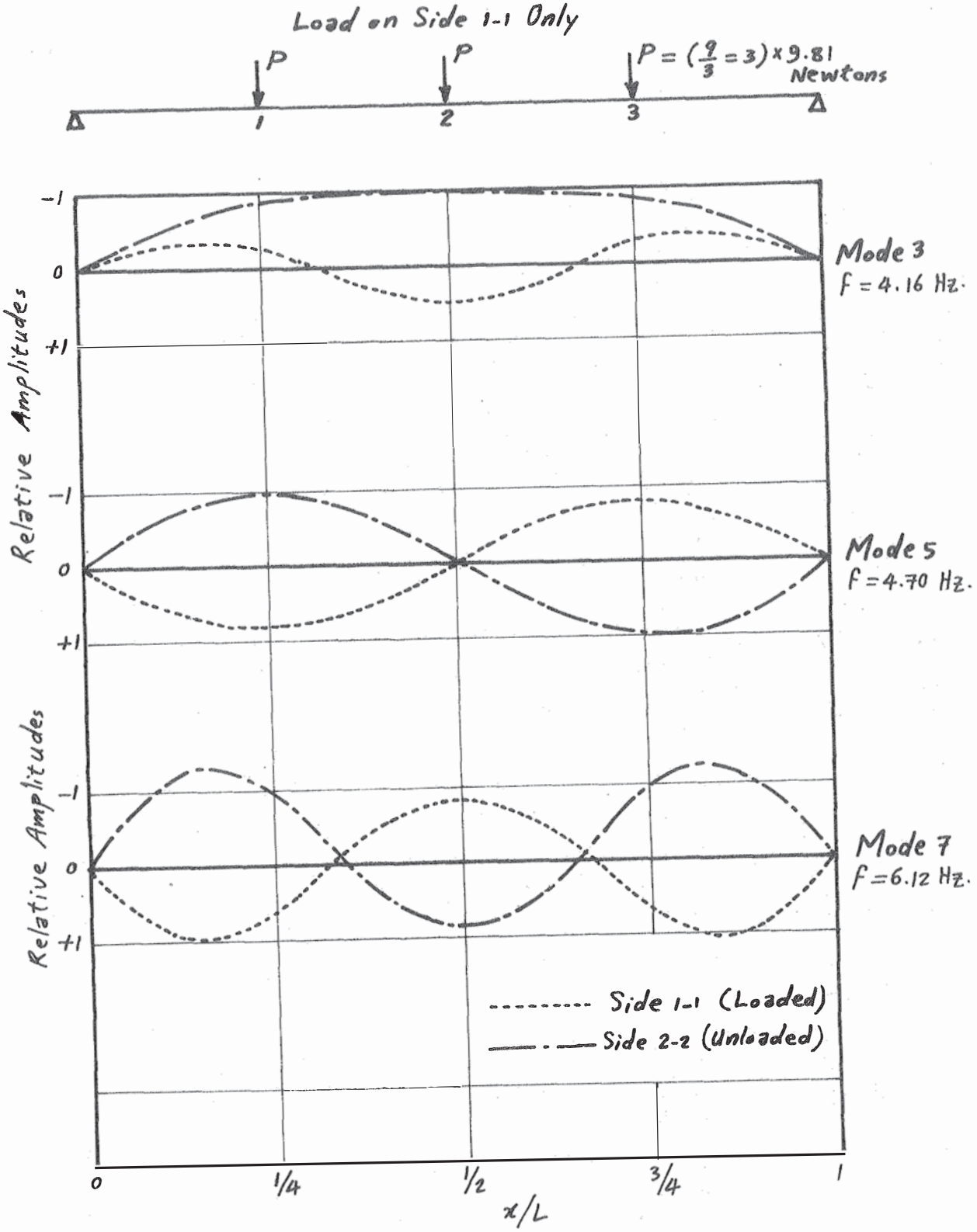

Fig. 6.3.4 – First Three "Torsional" Modes, Live Load as Shown

No. of Stations Per Cable = 3.

The terms "flexural" and "torsional" modes are not accuracte for L.L. conditions since neither of them is purely flexural or torsional, but each flexural mode contains some torsion, and vice versa. However, a mode which is mainly flexural can be said to be "flexural", and vice versa. This proved to be appropriate when compared with the D.L. condition.

6.2.4 L.L. Condition (b) of Fig. 6.1

When the same L.L. of the previous case was divided equally among the two sides in a torsional manner, such that the left half span of one side, 1-1, is uniformly loaded and the right half span of the other side, 2-2, is uniformly loaded, the frequencies reduced a bit further. The areas under any mode shape of both cables became absolutely equal, but with a reversed distribution.

For "flexural" modes, (i.e. modes which are mainly flexural with relatively little torsion), the amplitudes of the loaded half of each cable are greater than those of the unloaded half, (as in the previous loading condition, (a) of subsection 6.2.3, and as also happened in the single-cable bridge, Chapter III). The contrary happened to the "torsional" modes, Fig. 6.4.

This phenomenon is in agreement with what happened in the previous loading condition, (i.e. loading increases the amplitudes of the "flexural" modes and reduces those of the "torsional" modes).

The slight reduction of the frequencies in this case seems to be due to the reduction in the stiffness of the structure due to distributing the load on the two sides instead of applying it on one side only. This reduction in the stiffness is due to the non-linearity of the structure which makes the reduction in the stiffness of side 1-1 due to halving its load, more than the increase in the stiffness of side 2-2 due to transferring half the load from side 1-1 to side 2-2. This process results in an overall reduction in the stiffness of the entire bridge, and consequently a reduction in its frequencies.

(Note: Calculations and measurements of the flexibility matrix of the laboratory model of the single-cable bridge, for dead and live load conditions, showed that each flexibility coefficient for any live load, $(P/2)$, is greater than the average of the corresponding flexibility coefficients for both the dead load condition and the condition of twice the live load, P.)

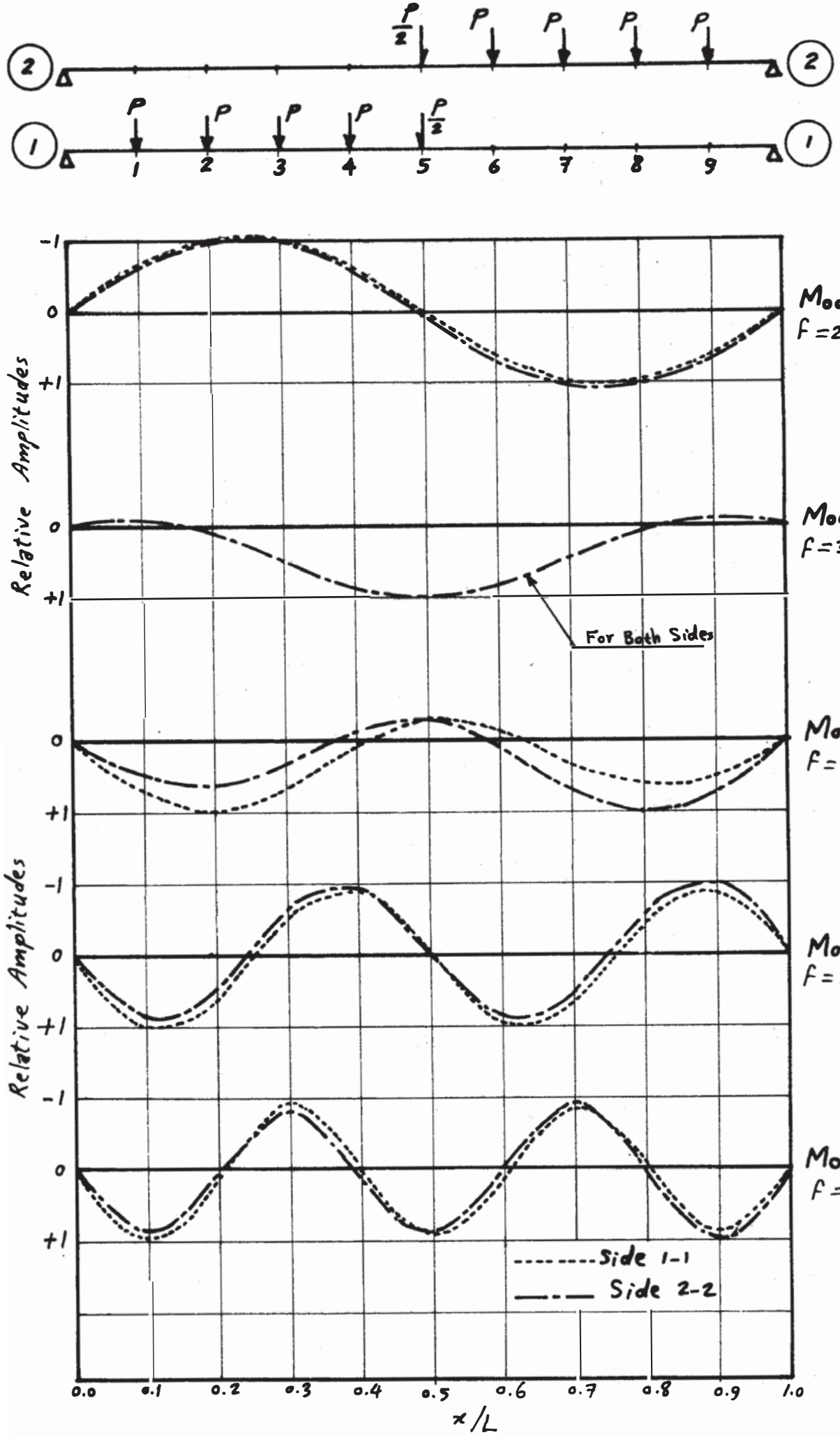

Fig. 6.4.1.– First Five "Flexural" Modes, Live Load as Shown.

No. of Stations Per Cable = 9 . P = 1 x 9.81 Newtons

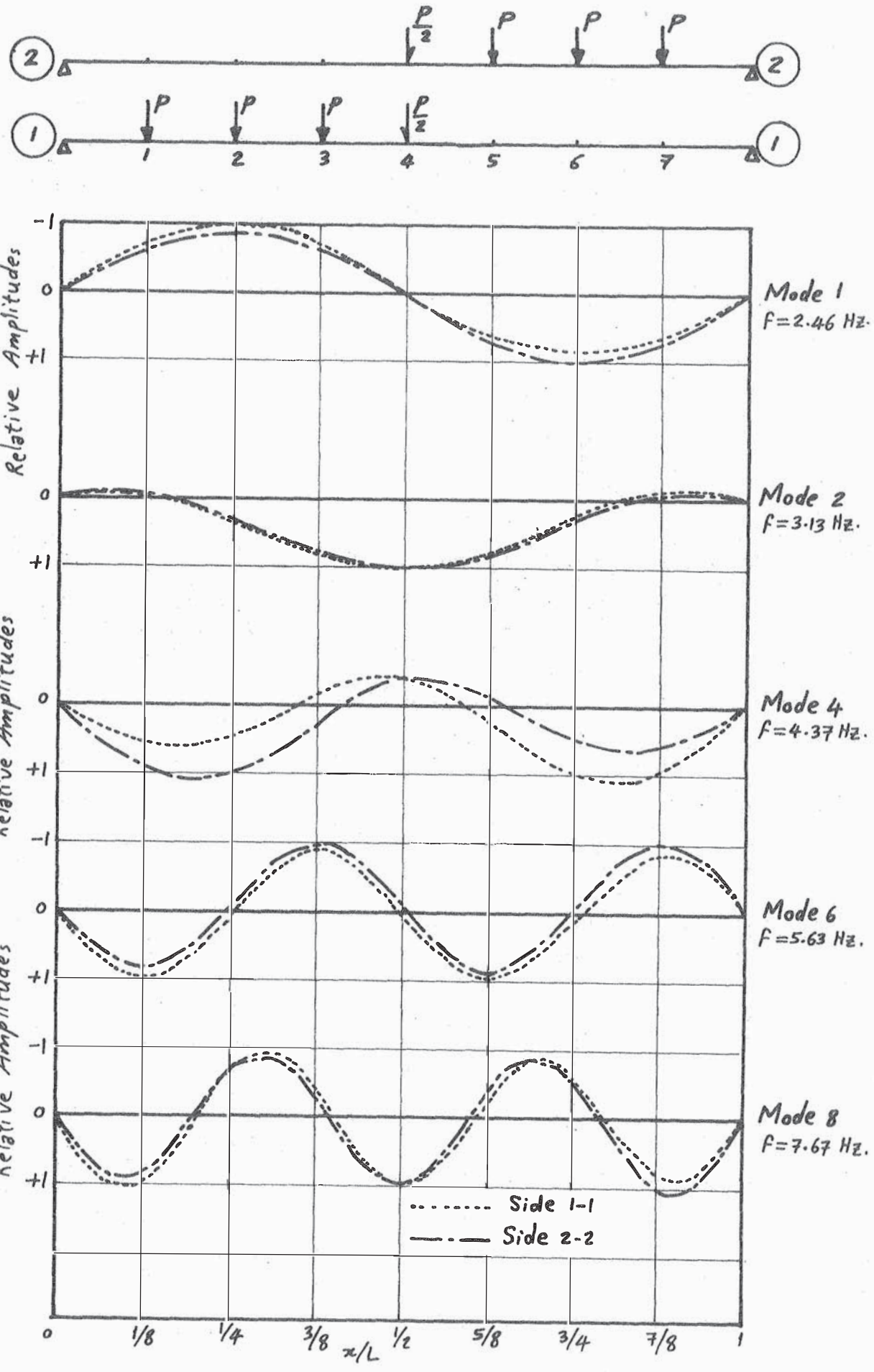

Fig. 6.4.2.- First Five "Flexural" Modes, Live Load as Shown.
No. of Stations Per Cable = 7, $P = \frac{g}{=} \times 9.81$ Newtons.

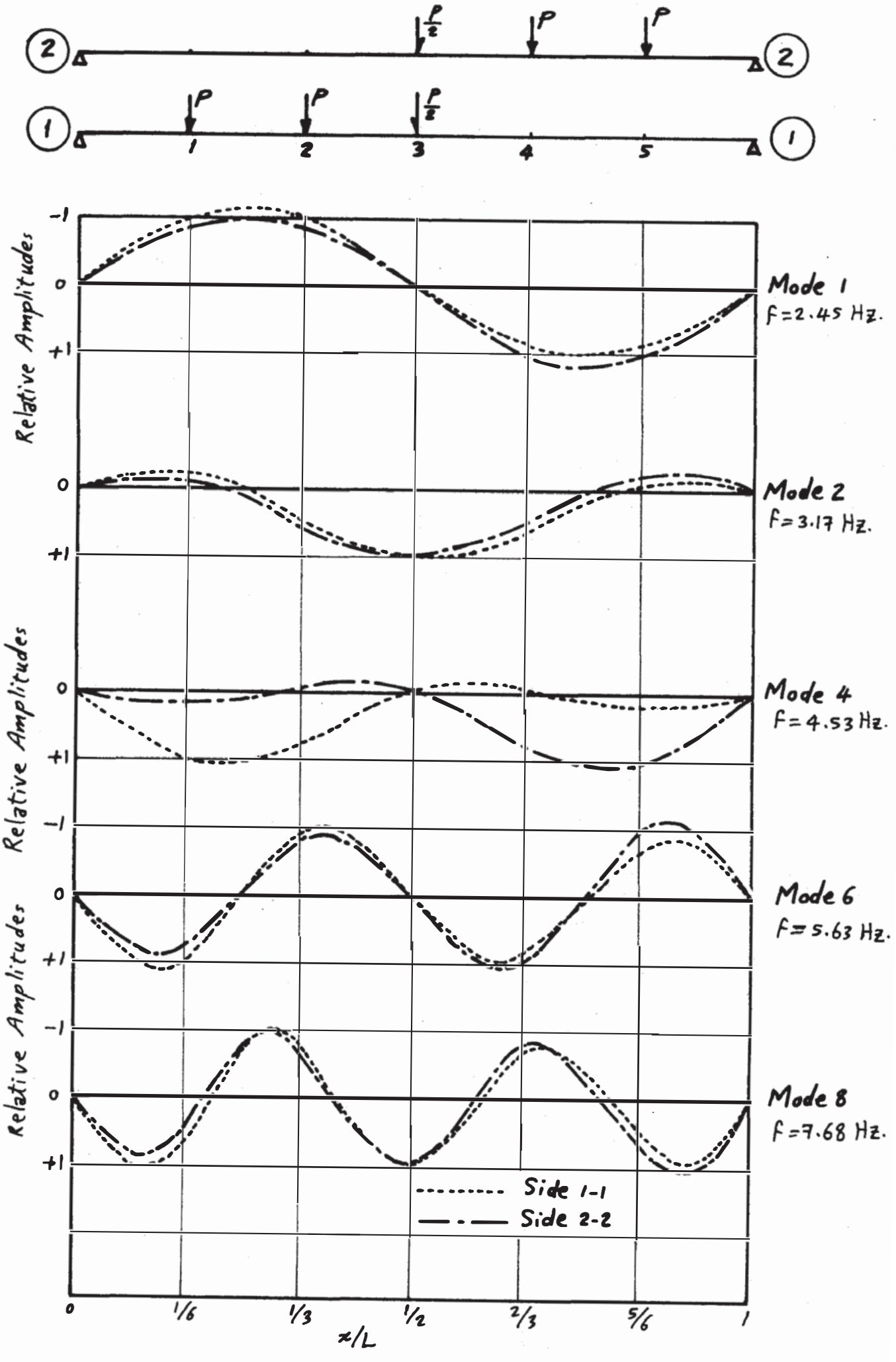

Fig. 6.4.3.— First Five "Flexural" Modes, Live Load as Shown.

No. of Stations Per Cable = 5 , $P = (\frac{9}{5} = 1.8) \times 9.81$ Newtons.

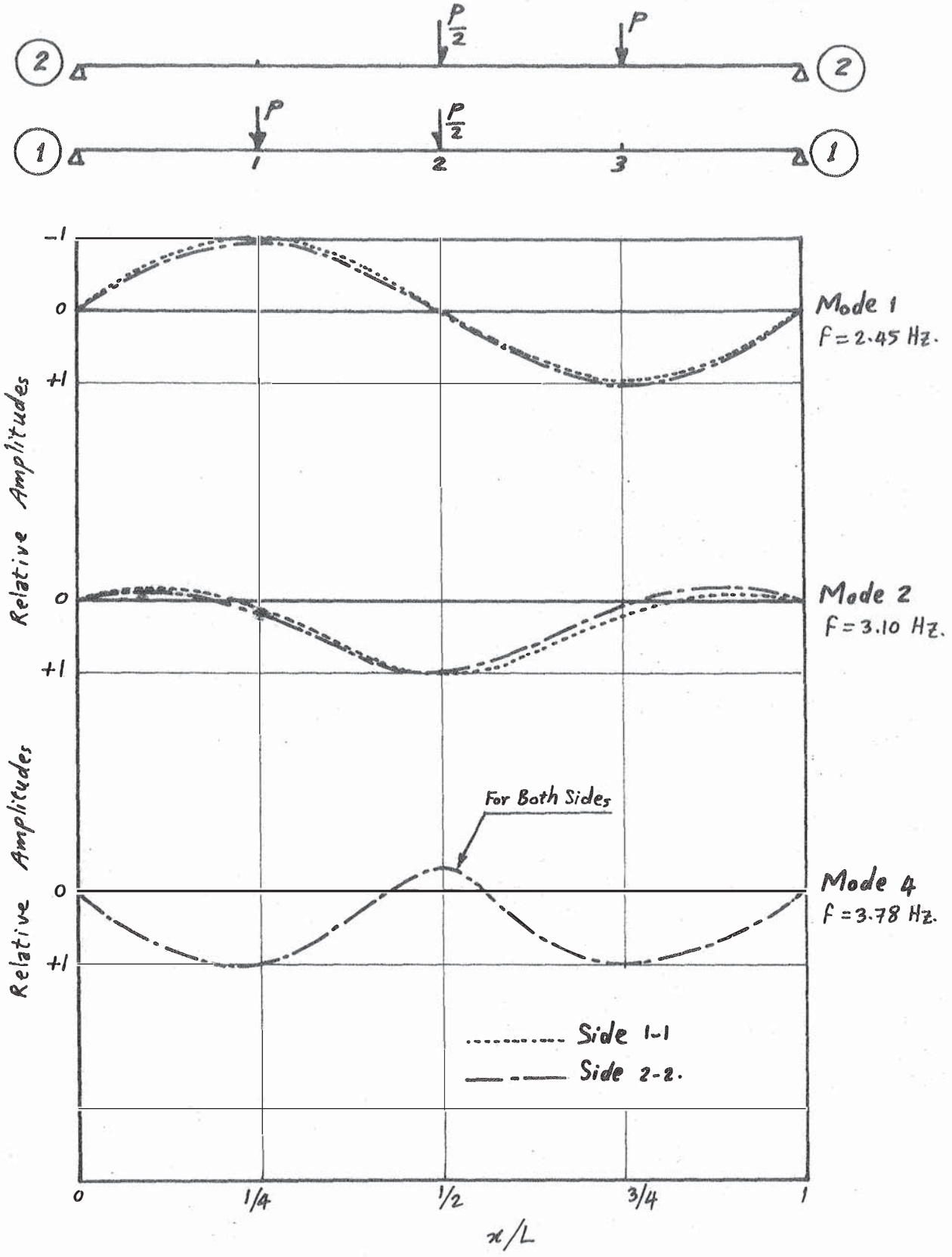

Fig. 6.4.4.- First Three "Flexural" Modes, Live Load as Shown.

No. of Stations Per Cable = 3 , $P = (\frac{9}{3} = 3) \times 9.81$ Newtons.

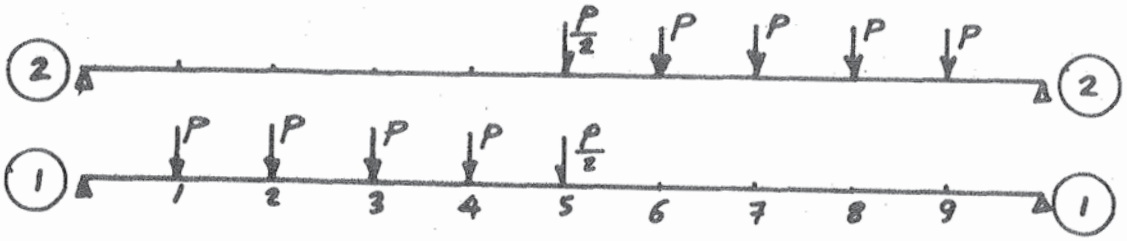

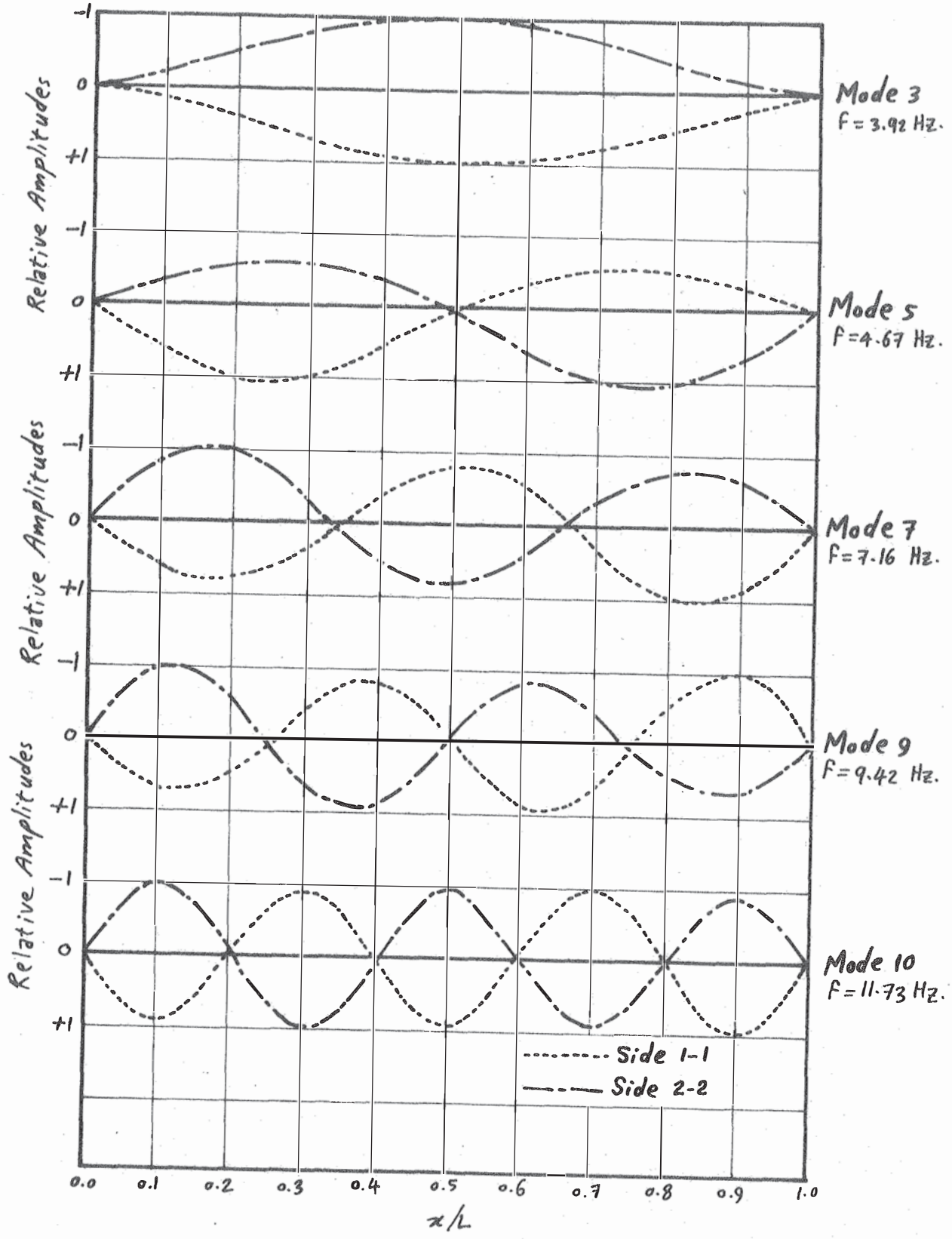

Fig. 6.4.1. – First Five "Torsional" Modes, Live Load as Shown.

No. of Stations Per Cable = 9 , P = 1x9.81 Newtons.

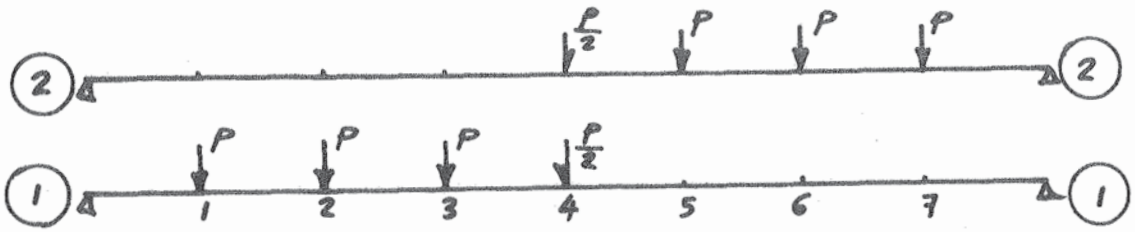

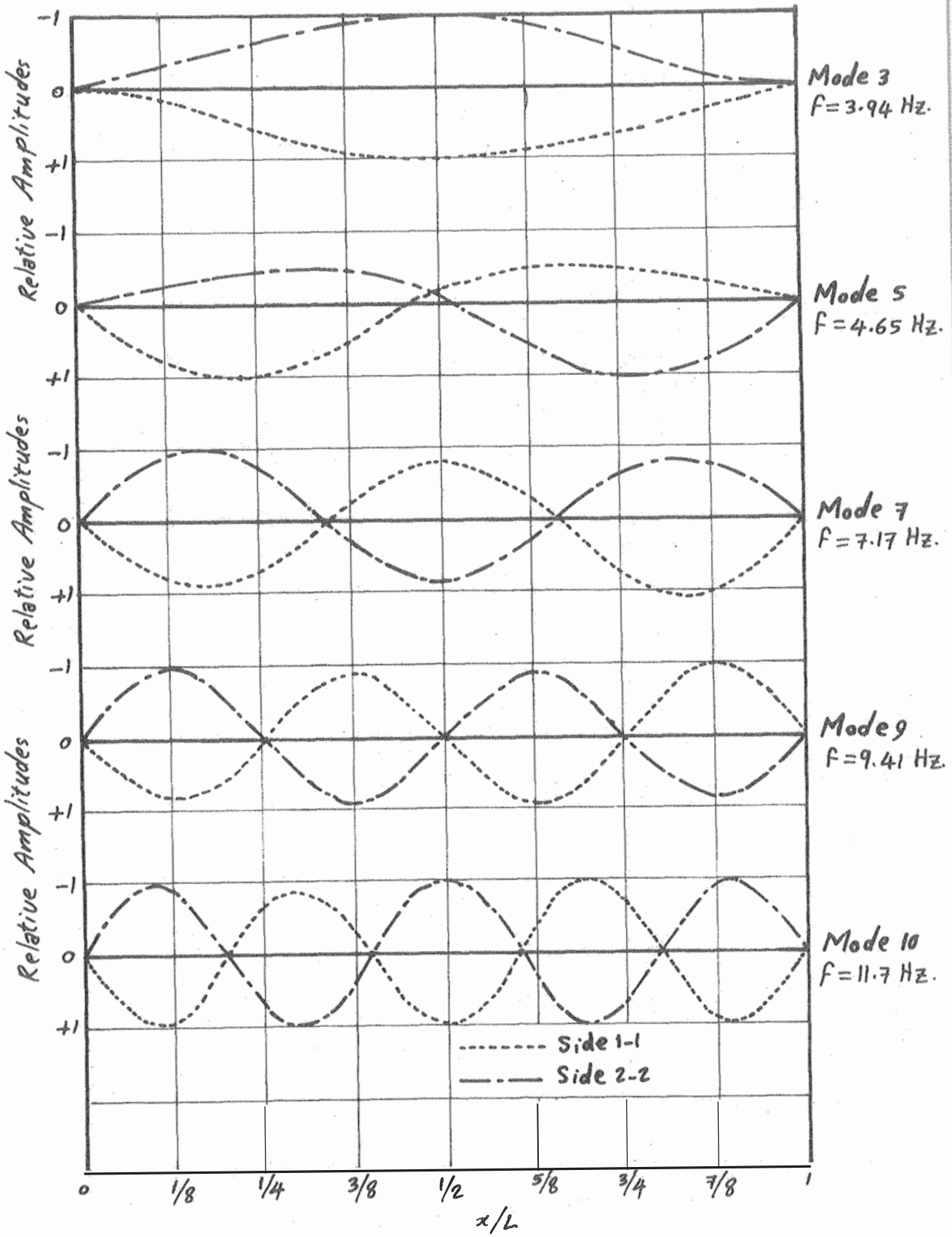

Fig. 6.4.2. – First Five "Torsional" Modes, Live Load as Shown.

No. of Stations Per Cable = 7, $P = \left(\frac{9}{7}\right) \times 9.81$ Newtons.

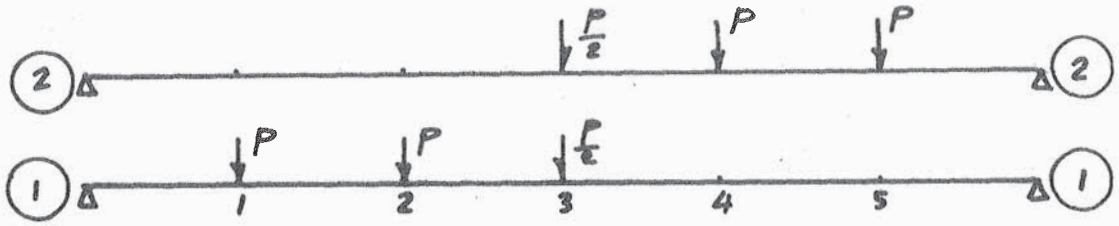

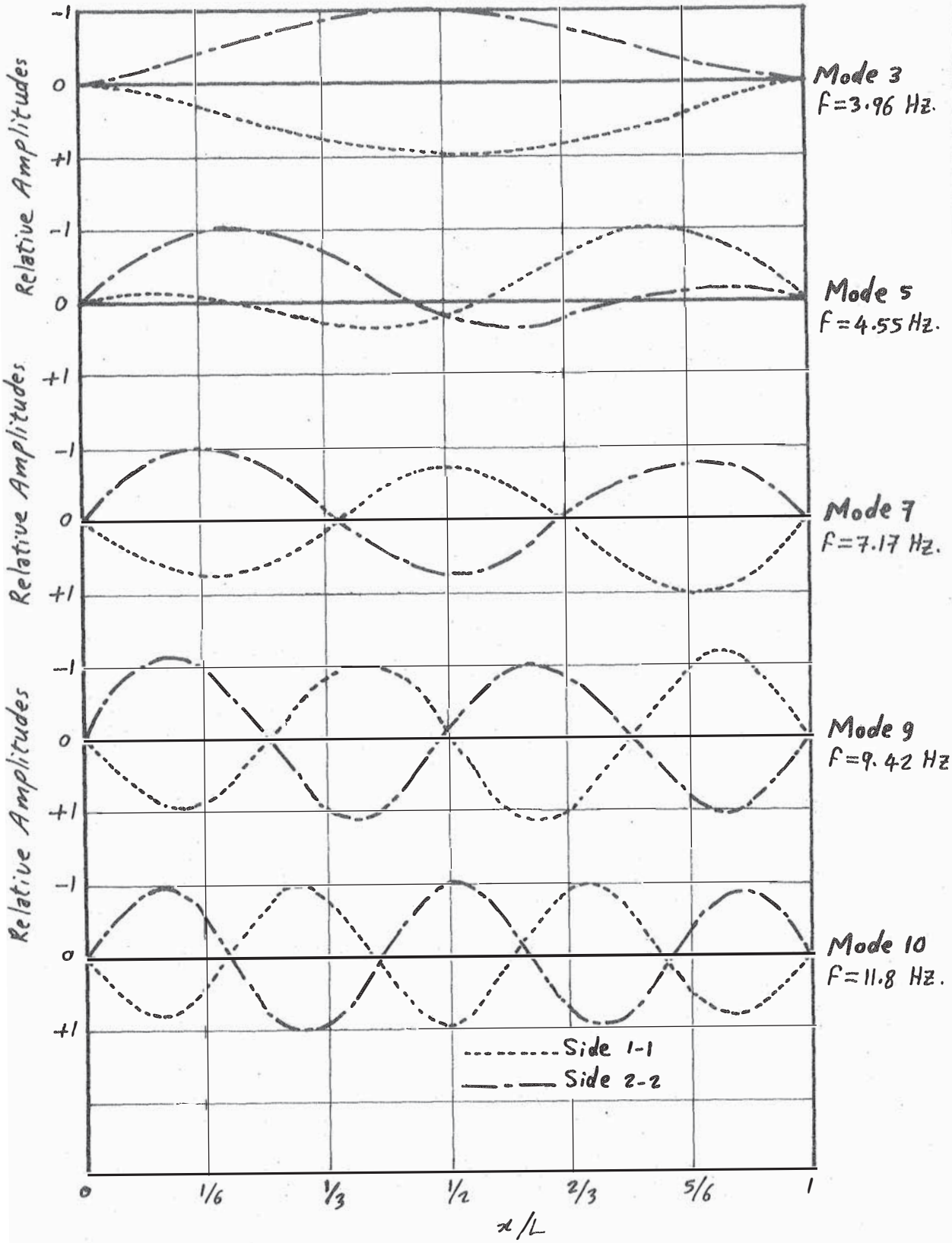

Fig. 6.4.3.– First Five "Torsional" Modes, Live Load as Shown.

No. of Stations Per Cable = 5 , $P = (\frac{9}{5} = 1.8) \times 9.81$ Newtons.

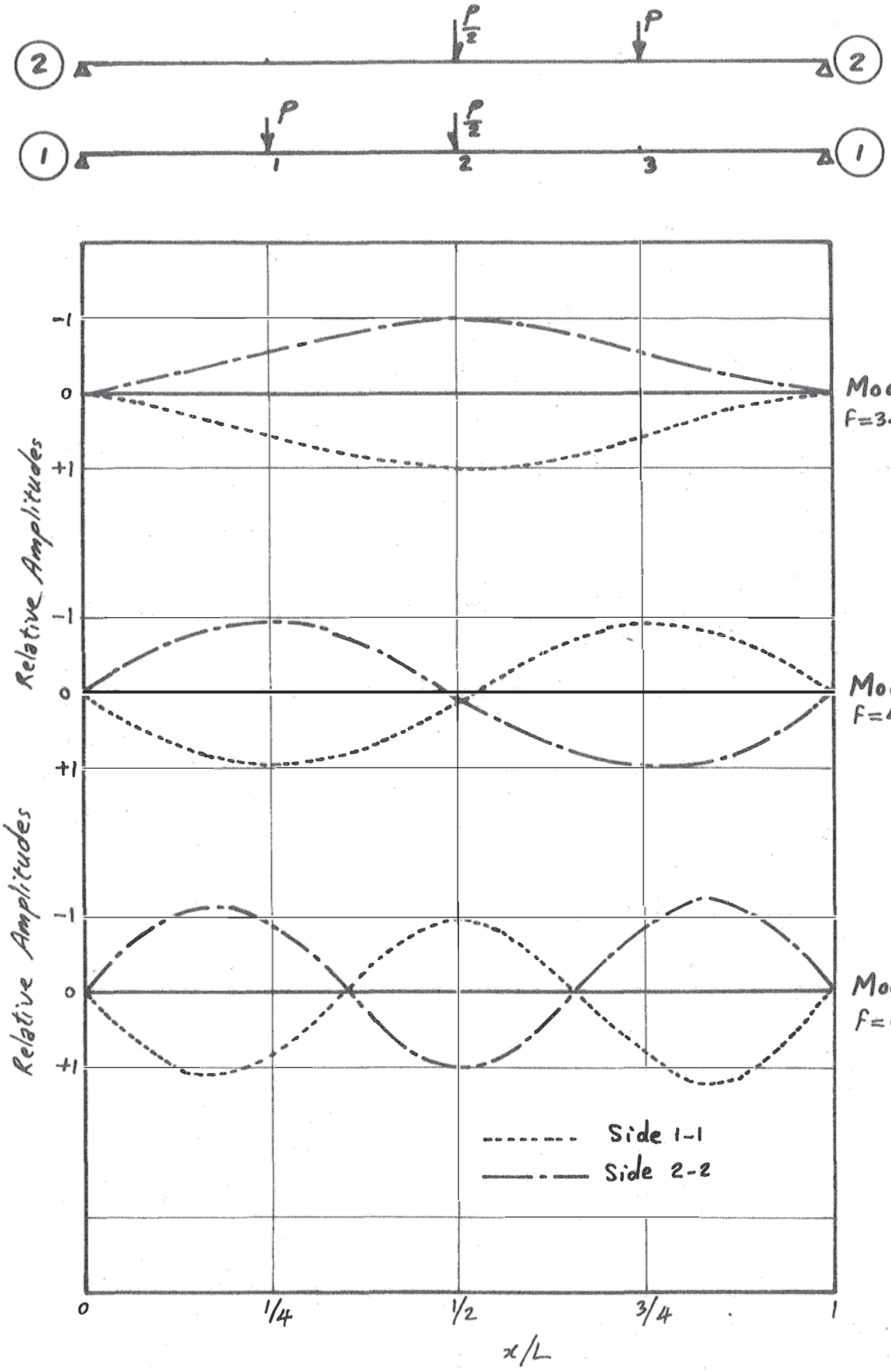

Fig. 6.4.4. – First Three "Torsional" Modes, Live Load as Shown.

No. of Stations Per Cable = 3, $P = (\frac{9}{3} = 3) \times 9.81$ Newtons.

6.3 COUPLING OF BENDING AND TORSION

For a system like the one shown in Fig. 6.5, the displaced position can be defined at any time using either of the following two methods:

(i) Using the vertical deflections v_1 and v_2, of sides (1) and (2) respectively; or

(ii) Using the translation X of the centre of mass, G, and the rotation θ of the line (1)-(2).

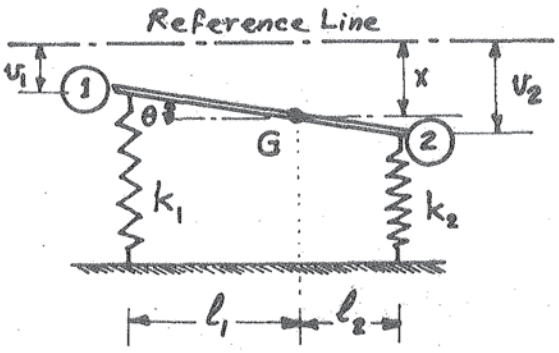

Fig. 6.5.- Coupling.

The first method is the one used by the writer in the dynamic analysis of the two-cable bridge. The method is very simple and easy, and can be used also for plates, shells, and complex space frames as well, using the finite elements procedure. It is quite sufficient, in order to define the mode, to know the necessary displacements of an adequate number of stations located properly on the structure. The flexibility coefficient, δ_{11}, for example, is simply the vertical deflection of side (1) due to a unit load acting vertically there.

The second method is perhaps a little more complicated. Here we have two kinds of influence coefficients: the first represents the translation X of the centre of mass G. It equals the vertical displacement of G due to a unit vertical load acting at G. The other influence coefficient represents the rotation θ of line (1)-(2). It is the angle of rotation due to a unit torque at G.

The equations of motion can be written as

$$m\,\ddot{x} = -k_1.v_1 - k_2.v_2 \qquad (6.1a)$$

$$I\,\ddot{\theta} = k_1.\,v_1.\ell_1 - k_2.v_2.\ell_2 \qquad (6.1b)$$

where m = mass of the system;

$\ddot{x} = d^2x/dt^2$ = acceleration of the centre of mass G;

k_1, k_2 = stiffness of springs (1) and (2), respectively;

$v_1 = (X - \ell_1.\theta)$, $v_2 = (X + \ell_2.\theta)$, are the displacements of sides (1) and (2), respectively;

I = mass moment of inertia;

$\ddot{\theta}$ = angular acceleration = $d^2\theta/dt^2$; and

t = time.

Substituting for v_1 and v_2, and rearranging, Eqs. 6.1 become

$$\begin{bmatrix} m.\ddot{x} \\ I.\ddot{\theta} \end{bmatrix} + \begin{bmatrix} \alpha_{11} & \alpha_{12} \\ \alpha_{21} & \alpha_{22} \end{bmatrix} . \begin{bmatrix} X \\ \theta \end{bmatrix} = \begin{bmatrix} 0 \\ 0 \end{bmatrix} \qquad (6.2)$$

where $\alpha_{11} = (k_1 + k_2)$; $\alpha_{12} = \alpha_{21} = (k_2.\ell_2 - k_1.\ell_1)$; $\alpha_{22} = (k_1\ell_1^2 + k_2\ell_2^2)$.

If $k_1.\ell_1 = k_2.\ell_2$, then $\alpha_{12} = 0$ and there will be no coupling between the angular and the linear motions. With zero coupling, a force applied to the centre of mass, G, produces only linear motion, while a torque applied to the system produces only angular motion, (Ref. 6.3, pp. 123-127).

In the case of a suspension bridge, for the D.L. condition, or for any flexural loading, $k_1 = k_2$, $\ell_1 = \ell_2$, and $v_1 = \pm v_2$, and this is the reason for getting uncoupled flexural and torsional modes.

If $v_1 = v_2 = X$, we have $\theta = 0$, Eqs. 6.1 become

$$m\ \ddot{X} = -2k_1.X \qquad (6.3a)$$

$$I\ \ddot{\theta} = 0 \qquad (6.3b)$$

This means that $\theta = \ddot{\theta} = 0$, and the system finishes up with only flexural motion, (as it is assumed that $v_1 = v_2 = X$). This will result in solving Eq. 6.3a for only the flexural modes, a case which can be solved using a single-cable bridge dynamic analysis, which saves much time.

If $v_1 = -v_2$, $X = 0$, Eqs. 6.1 become, after some algebra

$$m\ \ddot{X} = 0 \qquad (6.4a)$$

$$I\ \ddot{\theta} = -2k_1.\ell_1^2.\theta \qquad (6.4b)$$

This also means that $X = \ddot{X} = 0$, and the system finishes up with a pure torsional motion, (as it is assumed that $X = 0$, $v_1 = -v_2$). This will result in solving Eq. 6.4b for only the torsional modes.

Here, also, the stiffness matrix, $k_1 (=k_2)$, is the same as in Eq. 6.3a, i.e. for the single-cable bridge. $I = m.\ell_1^2/3$; $\ell_1 = b/2$ (= half the distance between the centres of the cables).

* * * *

This treatment can be followed for the D.L. condition or any flexural loading, in which pure flexural and pure torsional modes are obtainable, separately, by solving, independently, Eqs. 6.3a, 6.4b. If the stiffness matrix, k_1, is not existent or difficult to obtain, (as usually happens in suspension structures), the L.H.S. and the R.H.S. of both equations are premultiplied by the inverse $[k_1]^{-1}$, to use the flexibility matrix procedure, which is much easier, (in addition to avoiding the difficulty of k_1).

For any torsional loading, $k_1\ell_1 \neq k_2\ell_2$, and the flexural and torsional modes become impure, such that each "flexural" mode contains some torsion, and vice versa. In such a case, the terms "flexural" and "torsional" modes become no longer valid or applicable, since neither of them is purely flexural or torsional. But all the modes will be a combination of flexural and torsional components.

In this case, the solution can be obtained either by solving Eq. 6.2, or using method (i) mentioned above (early in this section), which uses the deflections v_1 and v_2 in the flexibility matrix.

* * * *

Eq. 6.2 can be rewritten in the form

$$\begin{bmatrix} m & 0 \\ 0 & I \end{bmatrix} \begin{bmatrix} \ddot{X} \\ \ddot{\theta} \end{bmatrix} + \begin{bmatrix} \alpha_{11} & \alpha_{12} \\ \alpha_{21} & \alpha_{22} \end{bmatrix} \cdot \begin{bmatrix} X \\ \theta \end{bmatrix} = \begin{bmatrix} 0 \\ 0 \end{bmatrix} \qquad (6.5)$$

In this case, the displacements X and θ are coupled by the off-diagonal term $\alpha_{12} = \alpha_{21} = (k_2\ell_2 - k_1\ell_1)$. If $k_1\ell_1 \neq k_2\ell_2$, a linear acceleration $\ddot{X}$ applied at G will produce both a linear displacement X and a rotation θ. Similarly, an angular acceleration $\ddot{\theta}$ applied to the bar will likewise cause both θ and X displacements. This type of coupling is called static coupling, distinguished by the off-diagonal terms of the stiffness matrix.

When $k_1\ell_1 \neq k_2\ell_2$, it can be seen that there is some point C, (Fig. 6.6), along the bar such that $k_1\ell_1' = k_2\ell_2'$. If the co-ordinate X is

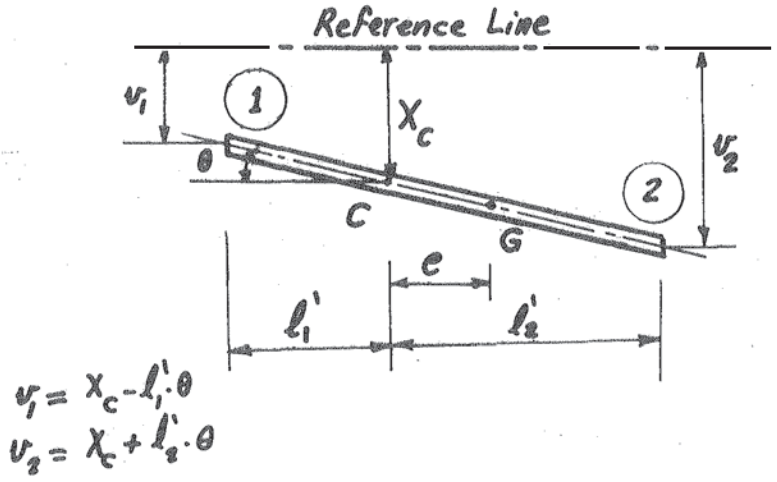

Fig. 6.6.- Co-Ordinate X Through Point C.

defined through point C, the equations of motion will have the form

$$m(\ddot{X}_c + e\ddot{\theta}) = -k_1 \cdot v_1 - k_2 \cdot v_2 \tag{6.6a}$$

$$I_c \cdot \ddot{\theta} + me\ddot{X}_c = k_1 \cdot v_1 \cdot \ell_1' - k_2 \cdot v_2 \cdot \ell_2' \tag{6.6b}$$

Rearranging and noting that $k_1\ell_1' = k_2\ell_2'$, (Ref. 3.1), these equations reduce to

$$\begin{bmatrix} m & m \cdot e \\ m.e & I_c \end{bmatrix} \begin{bmatrix} \ddot{X}_c \\ \ddot{\theta} \end{bmatrix} + \begin{bmatrix} \alpha_{11} & 0 \\ 0 & \alpha_{22}' \end{bmatrix} \cdot \begin{bmatrix} X_c \\ \theta \end{bmatrix} = \begin{bmatrix} 0 \\ 0 \end{bmatrix} \tag{6.7}$$

where I_c = mass moment of inertia for the bar about C; and

$$\alpha_{22}' = k_1(\ell_1')^2 + k_2(\ell_2')^2.$$

It is obvious that the coupling here is due to the term e which appears only in the off-diagonal elements of the mass matrix. This is called dynamic coupling. In this case, in order to displace the system only vertically, (i.e. in the X direction), it is required to apply both a vertical force at C and a torque as well. Similarly, to rotate the bar

through an angle θ, it is required to apply both vertical force through C and some torque simultaneously.

If the X-co-ordinate is chosen somewhere else, neither the mass matrix nor the stiffness matrix will be of the diagonal type. This means that both static and dynamic coupling will be obtained.

On the other hand, the co-ordinates may be chosen somehow such that both the static and the dynamic couplings can be eliminated. In such a case, both the mass and the stiffness matrices will be of the diagonal type. In this case, the co-ordinates are called the principal co-ordinates of the system, (Ref. 3.1). Here the equations of motion can be written in the form

$$\begin{bmatrix} m_{11} & 0 \\ 0 & m_{22} \end{bmatrix} \cdot \begin{bmatrix} \ddot{\Delta}_1 \\ \ddot{\Delta}_2 \end{bmatrix} + \begin{bmatrix} k_{11} & 0 \\ 0 & k_{22} \end{bmatrix} \cdot \begin{bmatrix} \Delta_1 \\ \Delta_2 \end{bmatrix} = \begin{bmatrix} 0 \\ 0 \end{bmatrix} \qquad (6.8)$$

where the displacements Δ_1 and Δ_2 are functions of X and θ. In this case, the natural frequencies will be given, directly, from the two uncoupled equations as

$$\omega_1 = \sqrt{k_{11}/m_{11}} \quad , \omega_2 = \sqrt{k_{22}/m_{22}} \quad .$$

6.4 CONTINUOUS MASS SYSTEMS

Beams, plates, and shells, and similar structures are continuous mass systems for which the mass matrix is not a diagonal matrix, but its off-diagonal elements are non-zeros. In our model, 92.5% of the D.L. is lumped at nine stations each side, for which a diagonal mass matrix becomes quite reasonable.*

For a real bridge, the dead weight is the self weights of the cables, hangers, joints, deck, flooring, etc., and it is not lumped at the hanger positions as in our model. But the big number of hangers** makes it appropriate to use a diagonal mass matrix without remarkable error. Also for other continuous mass systems, like beams, plates and shells, etc., the finite elements technique can make it possible to divide the system into segments with the mass of each acting at its centre of gravity, converting the system into a lumped mass system.

---

* Our model was solved as a lumped mass system, with 18 masses which form the diagonal of its 18 x 18 diagonal mass matrix. Using Eq. 6.3a the diagonal mass matrix reduces to 9 x 9.

** For a real suspension bridge, the number of hangers each side is usually of the order of 100.

CHAPTER VII

NOTES ON AERODYNAMIC INSTABILITY

These notes are intended to be a self-contained summary of existing published material on the topic, written for the structural designer whose knowledge of aerodynamics is small. The reader is advised to go through them critically, and to have in mind throughout the likely flexural and torsional modes of his suspension structure as calculated in Chapter VI.

7.1 INTRODUCTION

It has long been the practice to take static wind load into account using data derived from measurements made on models in wind tunnels. In the past, many bridge failures have been caused by the action of wind. Some of these have resulted from insufficient allowances for static wind pressures. Other bridges, adequately designed to withstand such pressures, collapsed by oscillations caused by steady winds. This dynamic action of wind is termed "aerodynamic instability".

The phenomenon of aerodynamic instability was recognized by engineers after the tragic failure of the Tacoma Bridge in 1940, and has been of vital importance in suspension bridge design ever since. Extensive work on the topic was started immediately after the disaster in the U.S.A. by Steinman, (Ref. 7.1), and F. Bleich, (Ref. 7.2), and others. This was followed in the U.K. by a similar extensive work by Scruton, (Refs. 7.3, 7.4), and Walshe, (Ref. 7.5), and others. The problem is still being investigated in the U.S.A., (Ref. 1.23), in Japan, (Ref. 1.24), and at the National Physical Laboratory in the U.K. as well, (Ref. 7.6).

Recent bridge structures have increased dimensions and flexibility and decreased dead weight and damping characteristics, (Ref. 1.23). Increased flexibility decreases the natural frequency of vibration, and reduction in dead weight reduces the rigidity of the structure and consequently produces a magnification of wind effects relative to the inertia of the structure. Also, modern fabrication techniques have decreased the ability of the structure to absorb energy by sliding friction between component parts, and thus less energy is required to initiate and maintain vibration.

It was shown, (Ref. 7.3), that the wind speeds capable of exciting oscillations are approximately proportional to the values of the natural frequencies. Hence, modern long-span, flexible suspension bridges, with their low natural frequencies, may be expected to be more vulnerable to aerodynamic action than other types of bridge.

The oscillations of structures excited by wind may be ascribed to the separation of the airflow around bluff structural shapes. The most common cause of wind-excited oscillations is vortex-excitation which tends to excite oscillations in a direction transverse to that of the wind-stream, and at wind speeds dependent on the natural frequencies of oscillation, (Ref. 7.4).

These oscillations may be prevented by sufficiently high structural damping, or by using streamlined cross-sections, or by both methods. The effect of wind can be greatly reduced by equalising the pressure above and below the deck. This issue will be discussed in detail in Sec. 7.8.

Most structural shapes are aerodynamically bluff, and the airflow separates from the surface to form a wide wake of turbulent air. The wind can cause oscillations in many ways, mostly attributed to separated airflow. The decay, maintenance, or growth of oscillations will depend on the balance of the energy taken from the airstream with that dissipated by structural damping.

A first step in the assessment of the tendency of a proposed structure to oscillate in wind is the determination of the natural frequencies and modes of oscillation and the structural damping. A method of getting the natural frequencies and modes has been described in Chapter VI. For structural damping, recourse must usually be made to an estimate based on observations of similar existing structures.

7.2 DEFINITIONS

In this section, an attempt is made to define the basic terms associated with the aerodynamic instability. The danger of definitions is, of course, that the terms are too limiting. Usually they relate to simple mathematical models of real behaviour, not to the real behaviour itself, and the designer must be aware of this.

(a) Self-Excited Vibration: Is an oscillatory motion where the alternating force that sustains the motion is caused or controlled by the motion itself. When the motion stops, the alternating force disappears.

(b) Forced Vibration: Is an oscillatory motion where the sustaining alternating force exists independently of the motion and persists even when the vibratory motion is stopped.

(c) Critical Wind Speed: Is the wind speed at which any disturbance will lead to oscillations with constant amplitudes. Below this speed movements will not develop, and if the structure is disturbed, the amplitudes reduce with time. Above this speed, any disturbance will lead to oscillations with increasing amplitudes. These amplitudes may continue to grow until structural failure occurs, or they are limited by non-linearities in the system, (e.g. aerodynamic forces are usually non-linear with amplitude), (Ref. 7.5). At the critical wind speed, the net damping, (aerodynamic + structural), becomes zero. (The aerodynamic damping is positive when the bridge is in still air but its value is influenced by the wind such that it becomes negative and numerically equal to the structural damping at the critical wind speed, (Ref. 7.3).)

(d) Critical Damping: Is that at which a structural system released from a displaced position will just return to its equilibrium state without passing through it.

Lesser damping is defined as a percentage of "critical", or as the "logarithmic decrement".

(e) Angle of Attack: Is the angle between the deck surface, (horizontal if not torsionally displaced), and the direction of the wind. It is usually considered positive when the wind is striking the section from the underside.

The geometric angle of attack, (Ref. 7.7), is the angle between the still deck surface and the airstream. The effective angle of attack is the angle between the deck surface and the direction of relative wind velocity, V_R. (V_R is the velocity of wind relative to the velocity of the centroid of the section, $\dot{X}$, during oscillation, see Fig. 7.1).

(f) Flutter: A dynamic instability of an elastic body in an air stream, (Ref. 7.8). This phenomenon happens at the critical (= flutter) wind speed.

Flutter may be classified into two main categories.

(i) Classical Flutter: This involves the combination, (or coupling), of both the torsional and flexural modes of the same general form, (Ref. 7.9). Flutter frequency is intermediate between the frequencies of the torsional and flexural natural modes.

Classical flutter usually means oscillation in which the direct aerodynamic dampings for motion in each single degree-of-freedom are positive, (so that when each single degree-of-freedom is isolated, the motion is damped by the wind). But when coupled motion occurs an instability can take place, (Refs. 1.24, 7.5).

Classical flutter is associated with small angles of attack, (Ref. 7.10).

Coupled oscillations occur when the ratio between the natural frequencies of the isolated torsional and flexural oscillations is very close to unity, (Ref. 7.3).

(ii) Stall Flutter: Is any flutter of a lifting surface in which the aerofoil sections are in stalled flow during at least part of each cycle of oscillation, (Ref. 7.8).

It involves a nearly pure simple harmonic motion and is a true instability in that the fluctuating flow and aerodynamic forces are generated by the oscillation and maintain it by supplying energy.

There is no upper wind-speed limit for a stalling instability, (Ref. 7.5), but it usually happens with large angles of attack, (more than 15°), (Ref. 7.10).

* * * *

Bisplinghoff, Ashley, and Halfman, (Ref. 7.8), argue that a single-degree-of-freedom flutter can happen. This is all right according to their definition of flutter as an aerodynamic instability. Accordingly, the catastrophic torsional oscillations of the Tacoma Bridge may be regarded as a single-degree-of-freedom flutter.

(g) Galloping: Is vibration at large amplitudes and low frequency, (Ref. 7.11). It is actually an example of stall flutter, and seems to be usually of the flexural instability type, (Ref. 1.24); once it is started, the disturbance is very persistent and continues with great violence, (Ref. 7.10), even if the wind stops. Some authors state that this means that it can be regarded as a free vibration, but the writer is unable to comment. Galloping is usually associated with transmission lines and the like.

This sort of instability happens if the lift slope is negative and numerically greater than the drag, (Refs. 7.5, 7.11). As with stall flutter, there is usually no upper wind-speed limit for galloping oscillations.

(h) Buffeting: Is a transient vibration due to aerodynamic impulses produced by the wake behind the structure, (Ref. 7.8).
Here, the forces are little affected by the motion and would be present even though the structure were infinitely rigid.

7.3 AERODYNAMIC FORCES

This brief section is included here to introduce the reader to some of the concepts used in flutter theory. Though incomplete it is hoped that it gives the structural engineer some idea of the sort of calculation that can be attempted. For simplicity, aerodynamic forces due to steady wind only will be considered. Classical flutter theory appears to consider only steady wind.

Fig. 7.1 shows a unit length strip of the deck of a suspension bridge.

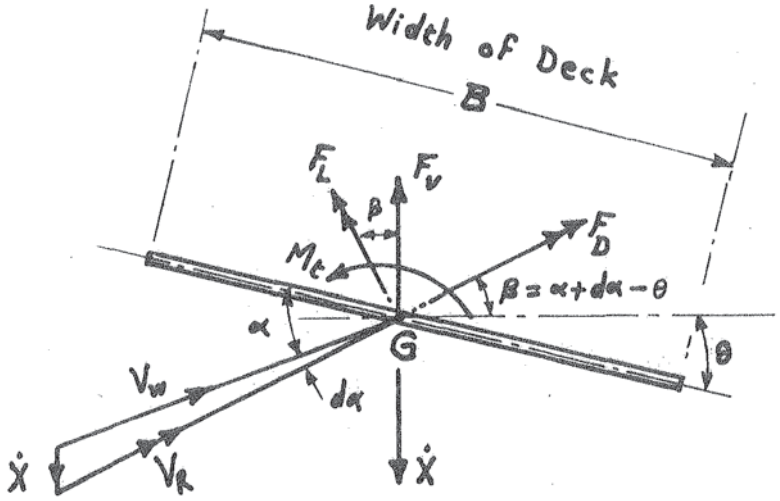

Fig. 7.1

Let the width be B, the cross-sectional area be A, and the centroid be at G at mid-width. Let the bridge be subject to a steady wind with velocity V_w in the direction shown in the figure. Under the effect of that steady wind, let the bridge be undergoing some mode of vibration with both torsional and flexural components. At any time, during one cycle of oscillation, let the angle of rotation of the section be θ, (from the horizontal), and let the velocity of the centre of gravity G be $\dot{X}$, (downward).

At that time, if the geometric angle of incidence of the wind is α, the effective angle of incidence, (between the relative velocity and the deck surface), will be $\alpha + d\alpha$. ($d\alpha$ is very much less than α since $\dot{X}$ is often very small compared with V_w.)

Here, the resulting wind force can be resolved into two components: the drag force F_D in the direction of the relative wind velocity V_R, and the lift force F_L in the perpendicular direction, where

$$F_L = C_L \cdot (\tfrac{1}{2}\rho V_R^2) \cdot A \tag{7.1a}$$

$$F_D = C_D \cdot (\tfrac{1}{2}\rho V_R^2) \cdot A \tag{7.1b}$$

in which C_L and C_D are non-dimensional lift and drag coefficients (respectively) that vary with α; ρ is the density of air; and the quantity $(\tfrac{1}{2}\rho V_R^2)$ is the aerodynamic pressure.

Also, there will be some aerodynamic twisting moment M_t on the deck where

$$M_t = C_T \cdot (\tfrac{1}{2}\rho V_R^2) \cdot A \cdot B \tag{7.1c}$$

in which C_T is a non-dimensional torque coefficient depending on α.

Consider first the lift and drag forces only. They will have a vertical component, F_v, where

$$F_v = F_L \cos\beta + F_D \sin\beta \tag{7.2}$$

If the rate of change of F_v with respect to β is positive, then the motion will be damped and the structure will be stable. But if $dF_v/d\beta$ is negative, then any motion will build up and helped by F_v, and the structure will be unstable. Thus, the structure will be flexurally unstable if

$$(dF_v/d\beta) < 0 \tag{7.3}$$

This reduces to *

$$(dF_L/d\beta) + F_D < 0 \tag{7.4}$$

---

* See Refs. 7.10, 7.11.

In other words, since the drag is always positive, this flexural instability, (perhaps galloping), will happen if the negative lift slope is numerically greater than the drag value. This can happen for values of α between 30° and 150°, (Ref. 7.10), Fig. 7.2.

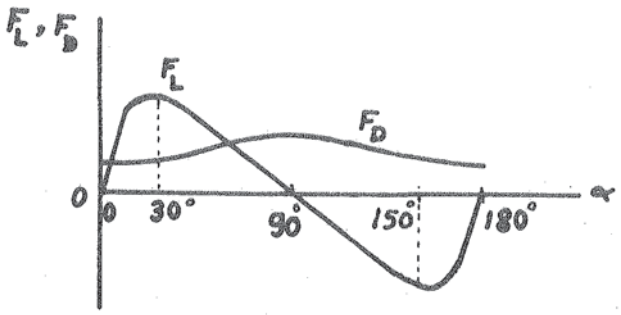

Fig. 7.2.- Lift and Drg Curves.

The foregoing discussion is based on the assumption that the horizontal oscillation (in plane of paper) is prohibited. In other words, it is assumed that the bridge is stable against oscillation in the direction normal to the plane of a cable.

Let us continue on that assumption, and let us take the aerodynamic torque into consideration. The resulting oscillation will be a coupled motion which has flexural and torsional components. Here, the equation of motion takes the form

$$[m][\ddot{X}] + [k][X] = [F] \tag{7.5}$$

where $[m]$ = 2 x 2 mass (and inertia) matrix;

$[\ddot{X}] = \begin{bmatrix} \ddot{X} \\ \ddot{\theta} \end{bmatrix}$ = acceleration column vector;

$[k]$ = stiffness matrix;

$[X] = \begin{bmatrix} X \\ \theta \end{bmatrix}$ = displacement column vector; and

$[F] = \begin{bmatrix} F_v \\ M_t \end{bmatrix}$ = column vector of aerodynamic exciting forces.

As mentioned before, the coefficients C_L, C_D, and C_T are functions of α, and consequently they are functions of θ which is a fraction of α. The values of C_L, C_D, and C_T are usually determined experimentally by a wind tunnel test.

It is to be noticed, here, that the aerodynamic forces F_v and M_t are functions of the torsional displacement θ only, but not the translational displacement X, though they do involve $\dot{X}$, because the velocity of the wind relative to the plate must be considered.

Eqs. 7.5 can be solved for the oscillation modes and frequencies. In the case of a real bridge, the span may be divided into n segments with known mass and inertia values, and the displacements will be (X_1, X_2, ..., X_n, θ_1, θ_2, ..., θ_n).

7.4 INSTABILITY OF THE COMPLETED BRIDGE

There has been a long history of undesirable oscillations and failures similar to those of the First Tacoma Bridge. The earliest modern records describe damage to the Menai Straights Bridge in 1826, 1836, and 1839, and the Brighton Chain Pier in 1836, (Refs. 7.3, 7.8).

Most of the bridges involved had stiffening systems that were abnormally weak in torsion. The dangerous vibration mode was first antisymmetrical torsional with a node at midspan.

Improved behaviour has generally been achieved by increasing the torsional stiffness and modifying the cross-sectional shape to reduce the instability of the air-loads which are developed.

* * * *

The stiffening system of the suspension bridge, generally, has many sharp corners and is anything but aerodynamically streamlined. As a result, the airflow over the bridge involves separation and formation of complicated vortex patterns, (Ref. 7.8).

Periodic shedding of vortices on alternate sides of the structure can give rise to an alternating transverse force, (in a direction normal to that of the wind). Airflow of this nature has been known to produce oscillations of bluff structures, and such oscillations occur over a range of wind speeds. These oscillations start at the critical wind speed and persist as the wind speed increases, (Ref. 7.5).

It is to be noticed that trouble occurs only if the frequency of the eddy-shedding coincides with one of the natural frequencies of the structure on which it acts. Then a resonance occurs which may be destructive, (Ref. 7.10).

* * * *

Vortices are formed, in the wake, at high wind speeds. The flow pattern appears to depend mainly on the value of Reynolds number R, (Ref. 7.11). For a wide range of values of R, the vortices are shed from the structure in a regular pattern, alternately clockwise and anticlockwise from either side, Fig. 7.3. This pattern is known as a "vortex street". The frequency of the eddy-shedding is called the Strouhal frequency, and the excitation due to this eddy-shedding is called Kármán vortex excitation.

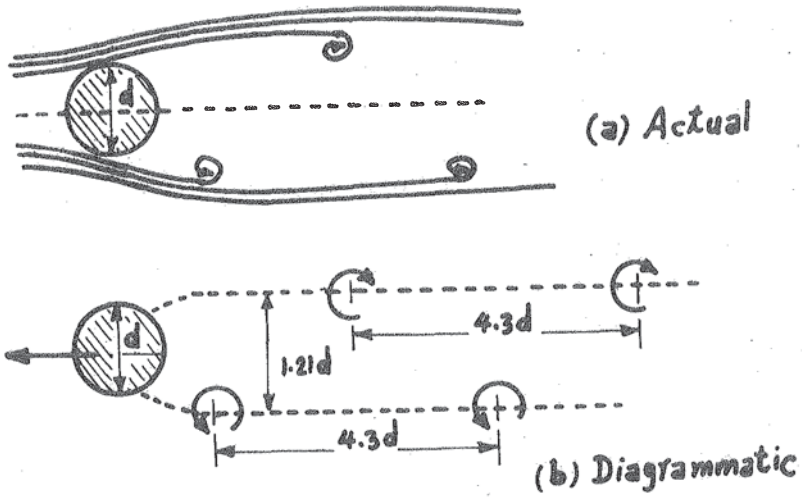

Fig. 7.3.- Kármán Vortices for a Cylindrical Body.

The frequency of vortex-shedding depends on wind speed, the cross-sectional shape, and Reynolds number, (Ref. 7.4). It is usually non-dimensionally defined by the Strouhal number, S_n, where

$$S_n = \frac{f.d}{V_R} \tag{7.6}$$

in which f = eddy-shedding frequency;

V_R = relative velocity of the cylindrical body, (or bridge section), with respect to the fluid; and

d = typical length = diameter of cylinder, (or width of bridge).

It was found that the Strouhal number S_n is constant for a cylinder, (about 0.20), and for other shapes it ranges between 0.14 and 0.30, (Ref.5.3). This Strouhal number S_n is, almost, the inverse of the reduced velocity V_r familiar to the British wind tunnel analysts, like Scruton, Walshe, and others, (Refs. 1.20, 7.3, 7.5). They write

$$V_r = \frac{V_w}{f.B} \qquad (7.7)$$

where V_w = wind velocity;

f = frequency of the bridge or its model, (for both sectional or full models); and

B = width of the bridge, (or model).

The eddy-shedding on alternate sides of the structure causes a harmonically varying force on the structure in a direction perpendicular to that of the stream, (Ref. 7.10). The intensity of this periodic force, F_K, is usually given in the form

$$F_K = [C_K.(\tfrac{1}{2}\rho V^2).A].\sin \omega t$$

where C_K = Kármán-force coefficient $\simeq 1.0$ for values of Reynolds number from 10^2 to 10^7 ;

ω = circular frequency = $2 f$; and

t = time.

This periodic force may cause the structure to vibrate in a direction normal to the flow direction.

This force is similar to the lift force F_L explained above. Thus, it may be expected here also, (in the case of vortex shedding), that there is also a "drag force" in the direction of the flow itself. This "drag force" also fluctuates and may cause the structure to oscillate in the direction of the flow. It is reported that piles can oscillate in the direction of a current of water as well as transversely.

* * * *

Small flexural oscillations of a span may be initiated by traffic, by wind gusts, or by the longitudinal component of the wind acting on the cambered span as an aerofoil, (Ref. 7.1). However, flexural oscillations have rarely proved dangerous though they can be a nuisance to traffic.

Most bridges which have failed have done so in torsional motion, (Ref. 7.5). Coupled flexural and torsional oscillation may lead to catastrophic response of the vibrating structure.

Conversely to galloping, a flexural oscillation with very high frequency and low amplitude could possibly cause the collapse of the structure due to fatigue, (by successive bending), (Ref. 7.10).

7.5 INSTABILITY DURING ERECTION

A more dangerous condition of instability may be during erection. The torsional frequency is reduced due to the joints not being made. As a result, the ratio of torsional to flexural frequencies approaches unity. This leads to the trouble of classical flutter, (due to the coupling of torsional and flexural oscillations, (Ref. 1.23)).

On the other hand, the aerodynamic excitation is proportional to the length of the suspended structure. But the contribution of the cables to the structural damping remains that of the full span. Thus, the control exerted on oscillations by structural damping would be expected to decrease as the length of the suspended structure increases. The ratio of the aerodynamic excitation to the structural damping is thus a maximum when the length of the suspended structure extends over the full span. Accordingly the conditions of stability, in that regard, would be the least favourable, (Ref. 7.5).

Reduced natural frequencies which might prevail during erection would reduce the critical wind speed, possibly, to a value within the range of natural winds. However, the critical wind speed can, almost, be doubled if temporary joints are made such that they can transmit torsional forces from one panel of the deck to the next, (Ref. 7.5).

* * * *

Instability during erection may be classified into the following four categories.

(i) Oscillation of the towers before cable erection.
(ii) Galloping of the cables before deck erection.
(iii) Oscillation of the deck before the final dead-load configuration is achieved.
(iv) Oscillation of (tubular) deck units during lifting from the water to their final loaction.

Remedies suggested for each of these instability phenomena will be presented in Sec. 7.8.

7.6 WIND TUNNEL TESTS

Extensive investigations, by testing models in wind tunnels, followed the collapse of the Tacoma Bridge. A very large wind tunnel was built at the University of Washington, in 1941, where a model for the Tacoma Bridge was tested and showed aerodynamic oscillations similar to those which had been observed on the prototype. In 1946, similar wind tunnel tests were started, at the National Physical Laboratory in England, to give guidance on the aerodynamic aspects of the design of the proposed Severn Bridge.

The object of model tests is to provide data from which the oscillatory behaviour of the full-scale bridge can be predicted. There are two types of models used. These are (1) full models; and (2) sectional models.

A full model is an aeroelastic model of the complete bridge. It is a geometrically similar model, and its elastic and inertial properties are scaled to produce, to prescribed scales, the natural modes and frequencies of the prototype. Thus, the oscillations of the model, caused by wind, occur at wind speeds and amplitudes which can be related to full-scale.

A sectional model is a geometrically similar copy of a short typical length of the suspended structure of the bridge. It is rigid but mounted on springs which represent the combined stiffness effects due to gravity, (cables), and elasticity of the full-scale bridge. The flexural and torsional motions of the bridge are simulated by vertical and pitching motions of the sectional model, (Ref. 7.5).

Generally, the wind-tunnel tests of the sectional models involved no more than the observation and measurement of the critical wind speeds and frequencies bounding the ranges over which oscillations were maintained by the wind. Occasionally, the damping rates of oscillations in the wind-stream were measured.

In the case of full models, critical wind speeds, frequencies, and oscillation modes as well, can be recorded. The effect of inclined winds, both horizontally and vertically, is simulated by inclining the model, (because the direction of the tunnel wind-stream cannot be varied).

However, it is clear that the full models are unsuitable for routine comparisons between different forms of suspended platforms, owing to the length of time required for construction and the high cost. Furthermore, a sectional model can be built with a greater scale that makes it possible to show the fine details which cannot appear in a full model with sufficient accuracy.

The results obtained with sectional and full models, (Ref. 7.3), led to the conclusion that sectional model tests were sufficient for reliable full-scale prediction. Nearly all the results showed very good agreement between the two methods of test, (sectional and full models). This

supports the conclusion that reliable predictions of the stability of proposed suspension bridges may be based on sectional-model tests only.

Tests may be carried with the full length and with a part of the length of the sectional model, to provide information on the influence of the length/width ratio of the model.

The disadvantage of the sectional model is that it does not give accurate values for the critical wind speeds and frequencies of oscillation. But for the purpose of comparison, at least, adequate results are obtained.

* * * *

The application of the results of model tests to prototype prediction requires a knowledge of the values of the structural damping for both model and prototype. There is as yet no reliable method for calculating these values for a proposed bridge. However, prediction of structural damping depends, to a great extent, on experience with similar existing structures, (Ref. 7.4).

7.7 TYPICAL RESULTS

Except where coupled motions are involved, the aerodynamic stability of a structure depends on the aerodynamic shape, the frequency of oscillation, and the structural damping. Oscillations may be prevented by modifications to one or more of these factors, (Ref. 7.4).

In the case of coupled motions, a new factor is involved; it is the natural frequency ratio for corresponding wave-forms of the torsional and flexural modes of vibration, (Ref. 7.3). It is only to be feared if the torsional stiffness is so low and the flexural stiffness is so high that they bring the natural frequency ratio close to unity, (Ref. 7.8). A coupled motion has a flexural and a torsional component, with a frequency distinctly different from the frequency of any of the natural modes of the system, (Ref. 7.2).

7.7.1 Shape

Both model and full-scale experience show that the stability of plate-girder-stiffened bridges compares unfavourably with that of truss-stiffened bridges, (Ref. 1.20). The results of the sectional-model tests are confirmed by full model tests. Truss-stiffened bridges are usually stable against flexural oscillations, and the tendency to instability in torsional oscillations, if any, can be corrected by suitable design of the suspended structure, (Ref. 7.3). Bridges stiffened by plate girders are liable to

both flexural and torsional oscillations, (Ref. 7.5). Their torsional flexibility and the continuous blocked area which they present bluff to the wind appears to render them very prone to instability.

The form of structural details such as handrails and roadway stringers have a marked effect on the stability. Models with plain decks, without stringers or handrails, proved to be unstable at both negative and positive angles of incidence, (but were stable at zero incidence), (Refs. 1.20, 7.3). Substantial improvements were effected by fitting stringers and handrailing which act as aerodynamic spoilers by shedding eddies, of mixed frequencies and directions, along the span. Such spoilers on the deck upper surface, (handrails), improve stability at positive angles of incidence, while those on the lower surface, (stringers), are effective for negative wind slopes.

A new concept is to adopt a shallow steel-plated hollow box section for the stiffening system. Such a form provides a high degree of torsional stiffness and yet is lighter and more economical to construct, (Ref. 7.5). The cross-section is somewhat streamlined, and it has been used successfully in the modern European long-span suspension bridges like the Severn, Bosporus, and Humber bridges. Here, the road-deck is provided by the top surface of the box.

7.7.2 Frequencies and Frequency Ratio

As mentioned in Sec. 7.1, a first step in the assessment of the tendency of a structure to oscillate in wind is the determination of the natural frequencies and modes of oscillation. Stability is promoted by a large ratio of the torsional/flexural natural frequencies of the structure, (Ref. 5.3). Thus, a primary object of the design should be to achieve a frequency ratio significantly greater than unity, (to avoid coupling), (Refs. 1.24, 7.3).

Increases in the torsional stiffness of both the deck and the towers increase the frequency ratio. A closed deck system has a relatively high torsional stiffness.

The flutter characteristics, (critical wind velocity and flutter frequency), of the whole suspension bridge are the same as those of an independent section of the bridge, (Ref. 7.2). Therefore, it may be concluded that this sort of coupled oscillations, (where flexural and torsional vibrations show the same vibration form), can be studied on sectional models, provided they have the same dynamic properties.

7.7.3 Damping

The damping rate for each natural oscillation depends on the structural damping, and on the damping forces due to the air, (aerodynamic damping), (Ref. 7.3). The aerodynamic damping is positive in still air but its value decreases with the increase of the wind speed, until it becomes negative* and numerically equal to the structural damping at the critical wind speed, (Ref. 7.3).

Structural damping derives from the capacity of the structure to dissipate energy during vibration, (Ref. 7.4). In actual structures, energy losses are due to internal hysteresis in materials, friction in sliding and fretting, and to aerodynamic resistance. Prediction of structural damping depends on experience of similar existing structures or on tests. The aerodynamic damping is dependent on the amplitude of oscillation, and the structural damping may also depend on the amplitude, (Ref. 7.4).

For oscillations of flexible suspension spans, the structural damping is represented by a varying logarithmic decrement of the order 0.002 to 0.130, (Ref. 7.1). It is sometimes expressed as a fraction of the critical damping, of the order 2% to 9%, (Ref. 7.12), for steel and concrete, respectively.** It is mainly caused by the girder, and its value for trusses is greater than that for plate girders, (Ref. 7.1).

It is perhaps worth repeating that at any wind velocity lower than the critical velocity, the structural (positive) damping is greater than the aerodynamic (negative) damping, (Ref. 7.1). As a result, any initial oscillation decreases and finally disappears, (Ref. 7.2). At the critical wind velocity, the motion is a steady state motion. Above the critical velocity, the aerodynamic damping, (negative), exceeds the value of the (positive) structural damping. The result is that the initial amplitudes increase steadily, (Ref. 7.2), until structural failure occurs, or it is limited by non-linearities in the system, (e.g. the aerodynamic forces are usually non-linear with amplitude), (Ref. 7.5).

7.8 CURING AND SECURING THE AERODYNAMIC BEHAVIOUR

Aeroelastic problems would not exist if the structure were perfectly rigid, (Ref. 7.8). Modern suspension bridges are very flexible, and this flexibility is responsible for the various types of aeroelastic phenomena.

Structural flexibility itself may not be objectionable. However, aeroelastic phenomena arise when structural deformations induce additional aerodynamic forces. These additional aerodynamic forces may produce

---

* Negative aerodynamic damping means that the wind feeds energy to the structure.

** Some designers, however, are not prepared to use these high damping values and say that damping is very much less.

additional structural deformations which will induce still greater aerodynamic forces. Unless these aerodynamic forces and the structural deformations are limited, the result will be a complete destruction of the structure.

In fact, securing the bridge against the aerodynamic instability is much better than curing an aerodynamically unstable bridge. Aerodynamic stability can be achieved by designing the suspended structure to withstand the aerodynamic conditions of the site.

7.8.1 Existing Bridges

Existing aerodynamically-unstable suspenion bridges can be cured by using stays from tower tops to intermediate points at the top of the deck, (to resist downward deflections of the antisymmetric torsional or flexural modes). This concept was used by John Roebling in some of his bridges, (Niagara, Cincinnati, and Brooklyn). As an alternative, stays may extend from the bottom of the tower, (at the road level), to intermediate points of the cable. The writer prefers this type as the stays are not affected by the tower-top movements. Instead, stays may extend from fixed points on the shore, or from the tops of the piers, to intermediate points at the bottom of the deck. The effect of these is a direct resistance to upward displacement, (or upward swing), of the points of attachment, and possibly an indirect and lesser resistance to downward displacement, (or downward swing), of the same points of attachment, (Ref. 7.1).

Transverse diagonal stays may be located between opposite suspenders in the transverse planes near the quarter points and other intermediate points of the span. The function of these stays is to prevent or resist out-of-phase, (i.e. torsional), oscillations, since the cable of each side is joined to the stiffening girder of the other side. Transverse horizontal struts between the cables may be used, (in conjunction with such transverse diagonal stays), in order to prevent the out-of-phase horizontal longitudinal movements of the cables, near the midspan, in the case of the first antisymmetric torsional mode. Such diagonal stays and horizontal struts do not help against vertical oscillations.

Another means of preventing the first antisymmetric torsional mode is by providing adequately proportioned centre stays in the planes of the cables. Their effect is to prevent the relative longitudinal motion of the cables and the suspended structure at midspan. Full effectiveness of the stays can be provided if they are given sufficient initial tension to prevent reversal of their stress in the cycle for any anticipated amplitude of oscillation, (Ref. 7.1).

Artificial damping devices may perhaps be installed to increase the absorption of the energy of undulations or oscillations, but there appears to be no proven methods. Of course, stay cables may provide damping as they are pulled about.

The addition of a second lateral bracing system at the level of the lower chords of the stiffening system, (in addition to the top bracing underneath the road deck), improves the torsional rigidity a great deal. This second bracing system raised the uncoupled natural frequency ratio, for the Golden Gate Bridge, from 1.25 to 1.96.

The rigidity of the suspension bridge is increased by its dead weight. The addition of the second deck to the George Washington Bridge raised the frequency ratio from 1.22 to 1.97. (This was possible because the bridge was initially designed to have a second deck to satisfy the future requirements of the increasing traffic.)

7.8.2 Proposed Bridges

New bridges are to be designed carefully to achieve an aerodynamically stable structure. Wind tunnel testing has now become essential on both sectional and full models of the bridge as well as some models of the towers. Experience from past research work and field observations on existing bridges must be made use of in order to get the most economic and aerodynamically stable structure. The aim is to secure the bridge against any possible aerodynamic forces that may arise on the site, so that complete safety is achieved with no need for any remedy.

Firstly, as has been emphasized in the foregoing notes, plate-girder stiffening systems compare unfavourably with open-truss systems. Truss-stiffened bridges are usually stable against flexural oscillations, and their tendency to instability in torsional oscillations can be corrected by suitable design of the suspended structure. Design features which have a corrective influence are, (Ref. 1.20):

(i) Separation of traffic lanes by open slots or gratings which permit easy flow of air through them. This helps in equalizing the pressure at the top and the bottom sides of the deck. Even if large eddies should form, no large pressure difference could be maintained, (Ref. 7.10).

Improvements are obtained by increasing the number and width of such slots, (or gratings). It may be suggested that the entire deck is covered by gratings, but it must be kept in mind that the dead weight of the deck helps in improving the rigidity of the structure, (Refs. 7.1, 7.3). It was found, (Ref. 7.1), that some 75% of the aerodynamic forces will be eliminated if vents over some 25% of the width of the bridge are provided.

(ii) Placing the road deck at the top of the stiffening system improves the stability. This makes it possible to install a double lateral system of bracing; one in the plane of the top chord and the other in the plane of the bottom chord of the stiffening trusses. This forms a four-sided closed section which ensures high torsional stiffness, (Refs. 7.3, 7.9). The result is an increase in the torsional frequencies and the frequency ratio, and consequently an increase in the critical wind velocity, and inhibition of flutter.

(iii) Sidetracks, (e.g. footpaths, cycle-tracks, etc.), mounted outside the stiffening trusses. They act as horizontal fins, (or wind-deflecting devices), since they reverse the aerodynamic effect otherwise produced, (Ref. 7.1).
Downward velocity of the windward girder plus horizontal velocity of the wind is claimed to contribute an upward pressure resultant opposing and damping the oscillation, (instead of a downward pressure resultant amplifying the harmonic motion).

(iv) Castellated handrailing, or other types of handrailing designed to break up the continuity of the airflow pattern. These act as aerodynamic spoilers, at the top of the deck, by shedding eddies and suppressing instability at positive angles of attack.

(v) Truss-type deck-stringers in preference to the plate girder type. If sufficiently deep, they considerably promote stability. They act as aerodynamic spoilers at the bottom surface of the deck and suppress instability at negative angles of incidence.

(vi) Lattice type wind bracing in preference to the plate girder type. The most favourable position for the top bracing is just underneath the roadway deck, where the spoiling effects are most pronounced, (Ref. 7.3). The most favourable position for the bottom bracing is at the level of the bottom chord of the stiffening trusses, so as to get the maximum possible torsional stiffness.

(vii) Stiffening truss chords of high width/depth ratio. The writer thinks that this increases the separation between the chord centre-lines, and consequently increases the stiffness of the two trusses. Moreover, it increases the separation between the top and the bottom bracing systems, and this increases the torsional stiffness. Also, the reduction of the depth of the chords reduces the aerodynamic (drag) forces due to the reduction in the area subject to horizontal wind forces.

* * * *

(viii) Since concrete has greater structural damping than steel, (about three times as much), (Refs. 7.4, 7.12), it may be preferable to use concrete towers. The large weight of concrete towers makes them more rigid, aerodynamically speaking. But this will have an adverse effect on the cost of the foundations. (It is noted that the Humber Bridge has concrete towers.)

However, in case of using steel towers, it must be noticed that riveting is better than welding or friction grip bolts, with respect to internal damping, (Refs. 7.4, 7.10, 7.11). During the erection of the towers, unfavourable wind effects may be avoided by leading wire cables, with inherent hysteresis damping capacity, from the tower tops to earth, (Refs. 7.4, 7.5).

(ix) To minimize the aerodynamic forces during erection, it is recommended not to construct the roadway deck, (nor the side-track decks), before the stiffening girders are complete, (otherwise significant aerodynamic forces may be applied to the incomplete structure), (Refs. 5.3, 7.5).

Floor forms in place before pouring a concrete deck may cause aerodynamic sensitivities even if the stiffening trusses are completed, (Refs. 7.1). The reason is the absence of the self weight of the roadway deck, and consequently a great reduction in the rigidity of the structure. In this case, a method of restricting instability is to attach elements having a non-linear response to deflection, (e.g. guy ropes), which inhibit resonance by modifying frequency as amplitude increases, (Ref. 7.4). However, it will be also useful if the floor forms are placed just before concreting, panel by panel.

(x) A cable anchor device at the main span is very effective in inhibiting the first antisymmetric torsional mode, (Ref. 7.9). Sometimes the cable is connected directly to the stiffening girder at midspan, (e.g. the Mackinac Bridge, (U.S.A.), and the Tancarville Bridge, (France)). The result is inhibiting the relative (out-of-phase) longitudinal movements of the cable centres.

(xi) Galloping of the cables, (especially before erecting the suspended structure), can be corrected by wrapping them to produce a smooth surface, (Ref. 7.4).

* * * *

(xii) Modern long-span suspension bridges have streamlined tubular decks. These aerofoil decks proved to be aerodynamically stable, especially when suspended by inclined hangers. The system of inclined hangers replaces all kinds of stays suggested by John Roebling in the last century, and then extended and confirmed by Steinman some 100 years

later, (Ref. 7.1). It also substitutes for the vertical hangers. During lifting of units, cross restraining wires, to the adjacent units, are adopted to prevent pitching and yawing oscillations of the units, (Refs. 7.5, 7.13).

Tests demonstrated the necessity of maintaining a high torsional stiffness during erection, (Ref. 7.5). This required the use of an interconnection device to transmit torsional stresses from one unit to the next. Tests also showed that in this case no advantage is gained by deck ventilation, (Ref. 7.5). But the high "aerodynamic efficiency" is related to the degree of "streamlining" of the cross-section, (Ref. 7.13).

CHAPTER VIII

NOTES ON THE DESIGN, ERECTION, AND ECONOMY OF SUSPENSION BRIDGES

8.1 INTRODUCTION

These notes are included here for the reader unfamiliar with the relevant design and construction methods. They form the context in which static and dynamic analysis must be viewed. It is hoped also that they help build up an appreciation of suspension bridges, so that the complexities of their aerodynamic behaviour, as summarized in Chapter VII, can be to some extent understood.

A little repetition occurs, from Chapter I, so that this chapter may be read separately.

The number of suspension bridges designed and erected in both the last and the present centuries, has been very great. As mentioned before, in Chapter I, primitive man built primitive suspension bridges in some parts of the world since prehistoric times. In modern times we use better materials and improved machinery, which have rendered possible the bridging of spans of a new order of magnitude.

The era of the modern suspension bridge is summarized by the following table:

Bridge	Clear Span (ft)	Year Completed
Brooklyn	1595.5	1883
George Washington	3500	1931
Golden Gate	4200	1937
Verrazano Narrows	4260	1964
Humber	4600 ft = 1410 m	(now being built)

In a paper in 1968, Fukuda,(Ref. 2.4) described a five-span bridge with a 1500 m span, tentatively designed for the crossing of the Akashi Straits in Japan. The main span here is about 100 m longer than that of the Humber bridge, but the writer is not sure whether this five-span bridge in Japan has been built or not.

As Steinman said, (Ref. 1.6), the decades immediately ahead will see the realization and the construction of other bridges of even greater spans. Also, there is a remarkable jump in reducing the time of construction. The construction of the Brooklyn Bridge took 13 years, while the Bosporus Bridge was opened to public traffic in 1973, only three years and three months after commencing its construction.

Another jump in suspension bridge design, construction and economy, is the great reduction in the depth of the stiffening system. Steinman's Mackinac Bridge, (completed in 1958), has the deepest suspended deck in the world, (38 ft), on a span of 3800 ft. This was reduced to only 10 ft deep tubular, (or box-girder), decks in both the Severn and the Bosporus Bridges, (in 1966 and 1973, respectively), over spans of nearly the same order. The Humber Bridge, (4600 ft span), has also a box deck only 15 ft deep (= 4.5 m). In 1966 the Tagus and the Severn Bridges were built (in Portugal and U.K., respectively), both with a span of the order of 3300 ft. The first has a truss deck 35 ft deep while the second has a tubular deck only 10 ft deep, (Ref. 5.3).

Experience in comparing alternative superstructure designs for Severn, Bosporus, and Humber, and studies for other suspension bridges of comparable span, indicates that for any given span within a range from 750 to 1500 m, (i.e. from 2500 ft to 5000 ft), and with a single-level deck, the all-welded aerofoil form of box girder with asphalted battle-deck floor, coupled with triangulated suspender system is of the order of 20% cheaper than the conventional open stiffening truss. And, with proper attention to certain details, it is at least equally aerodynamically stable, (Ref. 8.1).

* * * *

There is much written on the design, construction, and economy of suspension bridges. A complete book may not be sufficient to cover the topic. However, a brief discussion on the topic is presented in the following sections.

8.2 DESIGN OF SUSPENSION BRIDGES

Telford and Roebling were among the leaders of suspension bridge designers in the last century. The presentation of the deflection theory by Melan in 1888 has made a great revolution in the suspension bridge design ever since. It was the first non-linear theory of suspension bridges, and was further developed by Melan in 1906. It is still in use in suspension bridge design.

Other methods followed by other authors have been stated in Chapters I and II. Preliminary design methods were presented by many authors like Steinman, Hardesty and Wessman, and Pugsley, (Refs. 1.3, 1.7, 5.3).

The elastic theory was systematised and simplified by Steinman, (Ref. 1.7) for use in design by a series of charts giving girder bending and shears, etc. for a variety of bridge and loading conditions. Corrections were made after that to approximate the results to those of the deflection theory. Supplementary small adjustments for departures from the typical dip-span ratio, (1:10), dead-load to live-load ratio (w:p = 3:1), etc., were also given. This theory gives reasonable results for relatively short spans and stiff girders.

On the other hand, the method presented by Hardesty and Wessman in 1939 is relevant to relatively long-span suspension bridges with slender decks. This method suits modern suspension bridges where the cable is becoming the main carrying element. The method starts by studying the lengths of uniform live load that give maximum cable deflections at the quarter span points and at the centre. The method then assumes that the loading that gives these maximum deflections is identical with that giving maximum bending moments at the same points in the stiffening girder. The authors assume that the main cables and the hangers are inextensible, but they give various ways of refining the process, including allowances for the effects of cable extensibility due to load and temperature changes, and for the effects of side-span interaction.

In 1953 and 1962, Pugsley presented and extended his "elastic foundation analogy" method for both short and long-span suspension bridges. In this method the author treats the structure as an elastic deck supported on an elastic foundation provided by the cable. The main factor in his method is the relative stiffness of the bridge given by the ratio between the elastic stiffness of the girder to the gravity stiffness of the cable. This method is thus relevant to whether the cable, the girder, or both, are the main carrying element in the structure.

Another approximate method was presented earlier by Pugsley, using a flexibility coefficient approach, (Ref. 1.15). This method was applied in the analysis of our laboratory model of the single-cable bridge. It was also employed for the analysis of the erection stresses of both the Forth and Severn bridges. Reference can be made to Chapter II for more details on that method.

* * * *

All the above methods, and the majority of other methods presented for the analysis and design of suspension bridges, assume that the bridge is a plane structure. In other words, they do not include the torsional stiffness of the deck. However, a three-dimensional analysis of suspension bridges, taking into account the torsional stiffness of the deck, has been presented here in Chapter V, and utilised for both static and dynamic analyses. The method used by the writer in designing his laboratory model of the two-cable suspension bridge may be modified, extended, and used in designing real bridges.

* * * *

It should be noticed that, as is usual, the last element to be designed is the first one to be erected. This implies that the anchorages and the tower foundations, which are to be erected first, must be designed last.

Before going further, let us specify the major elements to be designed, and the major design decisions. These are: (1) spans' arrangement; (2) structural system; (3) cross-section; (4) dip-span ratio; (5) cable construction; (6) hanger arrangement; (7) stiffness and proportions of the stiffening system; (8) tower arrangement; and (9) foundations and anchorages.

Each of these will be discussed briefly in the following subsections.

8.2.1 Spans' Arrangement

For a real bridge, the main span is chosen according to the crossing and the geology of the site, as well as economical considerations. This means that there is not much choice regarding the main span. The side-main span ratio may also be dictated by the foundation requirements. However, this ratio ranges for existing long-span suspension bridges between 0.17, (George Washington), and 0.50, (Mackinac). This ratio largely determines the slope of the cable as it meets the deck near the anchorage, thus affecting the anchorage design. Also, shorter side spans tend to make the tension in the backstays much greater than in the main cable, (Ref. 1.7).

In the case of a side-main span ratio of 0.5, this slope would be zero if the backstays are loaded and each has a length equal to half the length of the cable in the main span. For the George Washington Bridge, the straight backstays have a slope of nearly 45° to the horizontal, which is the highest backstay slope in the world.

8.2.2 Structural System

This is related, (Ref. 5.3), to loaded or unloaded backstays, self-anchored or external anchorages, whether the cable is connected directly to the stiffening girder at midspan, etc.

If the side spans are unloaded, the horizontal component H_o of the cable tension due to dead load remains constant. If they are loaded, H_o will vary from one span to the other if the towers are rigid, or if the cables are anchored at the tower tops, (Refs. 1.26, 2.3 - 2.5). If the cables rest on movable saddles at the tower tops, as is usual, or if hinged or rocker towers are used, (Ref. 1.7)*, or if the towers are flexible, H_o can be taken as the average of H_o values in the different spans, (Ref. 1.13)**.

In a self-anchored suspension bridge, a strut is built, (usually at deck level), between the two anchorages, which relieves them of any horizontal pull, (Ref. 1.4). Obviously, the deck itself may be designed and made use of to carry, in thrust, that horizontal pull. When the deck carries the horizontal thrust, in addition to the traditional bending, shear, (and torsion), its cross-section will increase, and this possibly means more aerodynamic stability. Whether this is advisable is a matter of the relative safety and economy of providing separate anchorages versus self-anchoring. The former is usually the more economic; certainly so, it appears, for long spans.

---

* The Florianopolis Bridge is the first large American suspension bridge built with rocker towers. It was completed in 1926 (in Brazil) with a main span of 1114 ft. Other examples of suspension bridges with rocker towers are the Elizabeth Bridge at Budapest, Hungary, (built in 1903 with 951 ft span), and the self-anchored suspension bridge over the Rhine at Cologne, Germany, (built in 1915 with a span of 605 ft).

** This is the reason for adopting a dip-span ratio for the side spans much smaller than that for the main span, in order to equilibrate the cable under full dead load, (Ref. 1.7). We have $H_o = wL^2/(8D)$, and if w is assumed to be nearly constant over the main and side spans, (L^2/D) must be identical for both the main and side spans, in order to maintain H_o constant all through. This means that the dip-span ratios for the main and side spans are to be proportional to the span lengths. Or, in other words, the ratio between the sags of the different spans is to be equal to the square of the ratio between the span lengths.

The main cable is usually arranged to pass some small distance above the stiffening girder at midspan. This clearance causes a direct increase in the tower heights and in the lengths of all hangers. If this clearance is small, in the case of vertical hangers, the horizontal displacements of the central zone of the main cable may lead to significant inclinations of the central short hangers. When these central short hangers become remarkably inclined, the horizontal component of the cable tension will not become constant any more, but it will vary throughout the span. And this may need significant alterations and modification in the design. There is also the danger of fatigue of the central hangers and their connections to cable and girder, or indeed, also, the danger of these hangers being simply overloaded.

In some bridges the cable is connected directly to the stiffening girder at midspan. This connection can transmit horizontal forces to the cable. Thus, the horizontal component of the cable tension may alter across this point. Examples of this type are the Mackinac Bridge in U.S.A., (3800 ft span) and the Tancarville Bridge in France, (1995 ft span). The cables of the Tancarville Bridge were connected to the deck at midspan in order to help in achieving a large ratio between the frequencies of torsional and flexural vibrations, (Ref. 5.3).

8.2.3 Cross-Section

This includes (a) roadway arrangement; (b) type of stiffening girder; and (c) cable spacing.

(a) Roadway Arrangement

The width of the bridge depends on the requirements of the traffic over the bridge. Usually a suspension bridge has a single deck, but in some cases, where the traffic intensity is considerably high, two decks are used. Examples of double-deck suspension bridges are George Washington and Verrazano Narrows Bridges, both built by Ammann in the U.S.A. Both these bridges are among the largest suspension spans in the world.

However, the addition of a second deck, or the increase in the self weight of the single deck, as well as the allowance for a heavy traffic over the bridge; all these factors improve the aerodynamic stability of the structure.

(b) Type of Stiffening Girder

The stiffening girder may take the form of two trusses, two plate girders, or a box, (tubular), section.

The plate-girder decks are not common in suspension bridges. They were used in the First Tacoma Bridge in the U.S.A. in 1940, (2800 ft span), and the Rodenkirchen Bridge in Germany in 1954, (1240 ft span). The latter is still existing but the first one, as is well known, collapsed only four months after its opening for public traffic. The main disadvantage of the plate girder deck is the great lateral wind pressure on the solid webs, and the very low torsional stiffness. Indeed, it can possibly be said fairly, at this stage, that the failure of Tacoma was the result of low torsional stiffness which evolved naturally as an economic solution to an over-stylized or over-simplified method of design of a real suspension bridge as if it were a single-cable bridge.

The trussed deck has been used efficiently for a long time. But recent investigations showed that for long-span suspension bridges with a single-level deck, the all-welded aerofoil form of box girder is of the order of 20% cheaper than the conventional open stiffening truss, and that it is at least equally aerodynamically stable. Modern long-span suspension bridges, like the Severn, Bosporus, and Humber, have been built using the tubular deck system, for the sake of both economy and aerodynamic stability.

(c) Cable Spacing

The cable spacing plays an important part in the torsional behaviour of a suspension bridge. It has been shown in Chapter V that the parameter GJ/b^2 is involved in getting the deflections of both cables, (as in Eqs. 5.6). Furthermore, the torsional stiffness GJ is, in practice, approximately proportional to the spacing, b, between the two cables.

The cable spacing affects, tremendously, the lateral bending stiffness of the deck spanning between the towers and loaded horizontally by wind. In other words, the lateral deflections, (or oscillations), due to lateral wind forces, are greatly dependent on the spacing between the cables.

The First Tacoma Bridge was designed to have a theoretical maximum lateral deflection of 21 ft at full wind pressure, but its actual maximum lateral deflection at midspan never exceeded 4 ft, even during the gale which destroyed it, (Ref. 1.6). (The wind speed during that gale was only one third of the maximum design wind speed!) The bridge was the most flexible of all modern suspension bridges.* It had a width-span ratio, L/b, of 1:72

---

* This lateral slenderness, however, was not a factor in the failure of the bridge.

which is much smaller than that of any other bridge built before or after. This width-span ratio for existing bridges ranges between 1:56, (Mackinac Bridge, built in U.S.A. in 1958 with 3800 ft span), and 1:13, (Alvsborg Bridge, built in 1966 with 1370 ft span). Generally, the ratio ranges between about 1:50 and 1:40 for long spans and about 1:15 and 1:25 for short spans. For the Humber Bridge, (now under construction), however, the ratio reduces to 1:64.

8.2.4 Dip-Span Ratio

A typical dip-span ratio for the main cable is about 1:10. Until the first few decades of this century, the economic cable dip-span ratio was recognised as varying from 1:10 to 1:8, (Ref. 8.2). For modern long-span suspension bridges, the ratio varies from 1:12 to 1:10. Generally it is noted that the ratio is smaller, (i.e. smaller sag), for the longer spans. This is useful, actually, because the smaller the sag the shorter will be the hangers and the towers. But the reduction of the sag causes an increase in the horizontal component of the cable tension. However, the governing factor has been, always, economy.

It was shown by Pugsley, (Ref. 1.3, p.30), that the cable flexibility is directly proportional to the sag. A reduced sag, thus, increases the cable stiffness and hence the total stiffness of the structure. This leads to higher natural frequencies, and a reduced tendency to aerodynamic oscillations.

8.2.5 Cable Construction

There are three common types of cable construction.

(a) Parallel Wires, Individually Spun in Site

This method was first invented and patented by John Roebling in 1841 and has since been used on almost all the major suspension bridges.

(b) Structural Cables

A structural strand is an assembly of wires formed helically around a centre wire in one or more symmetrical layers. A structural cable is composed of several strands laid helically around a core, (Refs. 2.8, 8.3, 8.4).

Structural cables have been used in many, relatively, short span suspension bridges. The largest bridge using spiral strands at present in service is the Tancarville Bridge, built in France in 1959, with a main span of 1995 ft.

(c) Parallel Wire Cables with Prefabricated Strands

In this case, parallel wires are preassembled in the shop into bundles or strands. This type was used in the main cables of the Newport Bridge, (Refs. 8.5, 8.6). The bridge has a main span of 1600 ft and was completed in 1968. Tender figures for the cost of this bridge showed a saving of 17.5% for the completed cables, as compared with the conventional spun cable,* (Ref. 5.3). The primary objective in using strands rather than wires is to reduce the erection cost and time.

* * * *

In all the above three cable types, the individual wires are galvanized,** and the final cable is bound into a unit and covered with a protective coating. The major disadvantage of the spiral strand is that bearing between the wires reduces, a great deal, the allowable stress and the modulus of elasticity.

8.2.6 Hanger Arrangement

There are two main types of hangers: (1) vertical hangers, and (2) inclined hangers.

In the case of the conventional vertical hangers, the horizontal pull in the cable is constant, but when inclined hangers are used it is not so. Inclined hangers were used in both the Severn and the Bosporus Bridges. The main advantage of inclined hangers is to increase the damping properties, (in addition to a slight increase in the stiffness of the structure). This system is relevant to tubular decks where the hanger slopes can be maintained nearly constant by varying their spacings. But in the case of a truss, the uniform spacing of the hanger connections causes varying hanger slopes with consequent difficulties in avoiding slackness in the hangers at the midspan.

* * * *

Sometimes, inclined hangers may be inserted from the tops of the towers to the deck, in addition to the conventional vertical hangers. This arrangement was used by John Roebling in some of his bridges in the last century.

---

* It should be noted that "spinning" refers to Roebling's method of running out thin parallel wires to form a cable. No twisting is involved. There is nothing in common with spinning wool, by twisting, to form a thread.

** The steel is high tensile and fairly notch-sensitive. However, designers apparently do not fear the dangers of hydrogen embrittlement.

8.2.7 Stiffening System: Proportioning

About the year 1910, authorities recommended, for the stiffening trusses of suspension bridges, a minimum depth-span ratio of 1:40. This recommendation of minimum depth-span ratio, however, was later reduced to the range from 1:90 to 1:50 for spans between 2000 and 3000 ft, (Ref. 1.6). Nearly a generation later, the ratio could be greatly reduced to 1:168 in the Golden Gate Bridge, (in 1937, span = 4200 ft), then to 1:178 in the Verrazano Narrows Bridge in 1964.

In one jump, and using a tubular deck, the ratio could nearly be halved two years later, (in 1966), by building the Severn Bridge with a depth-span ratio of 1:324. The ratio was slightly reduced further in the Bosporus Bridge in 1973 to 1:358. The Humber Bridge, which is now being built, will have a ratio of 1:313.

This makes false the claim that the vertical slenderness of the First Tacoma Bridge, (depth-span ratio = 1:350), was a main factor in its failure.

What seems to be obvious is that the use of the aerofoil form of box girders, instead of the traditional truss decks, for long span suspension bridges, made it possible to reduce the depth-span ratio down to about one-eighth of what was recommended about half a century earlier. Future decades may perhaps witness further reductions in the depth-span ratio and further increases in spans, with the development of the materials and methods of construction.

8.2.8 Tower Arrangement

Under the dead load condition, the towers are assumed to be vertical carrying only central vertical loads. Let us assume also that the cables are fastened at the tower tops.

Under vertical live load on the bridge deck, the tower tops move in the spanwise direction due to the extension of the backstays. If these vertical live loads are not symmetrical about the longitudinal centre line of the bridge, the towers will also twist. Additional tower deflections in the spanwise direction occur also due to the longitudinal wind pressure on towers. Also the towers will deflect laterally due to the lateral wind pressure on the entire bridge, (including the towers).

This means that the towers are designed to carry the following loads:

(i) Vertical reaction from the cable of both the main and the side spans.
(ii) Self weight acting vertically, (central).
(iii) Horizontal wind force in the spanwise direction.
(iv) Horizontal wind force in the lateral direction.

If the backstays are loaded, i.e. if the deck in the side spans is supported from the backstays, additional horizontal spanwise force, equal to the difference between the horizontal cable pull in the main and side spans, will act at each tower top.

Deflections of the tower tops due to all the horizontal forces will cause the large vertical loads to become eccentric, producing bending moments and stresses. Also the twist of the towers, due to torsional loadings on the bridge, may be increased by these horizontal forces and by tower top movement.

8.2.9 Foundations and Anchorages

The design of the foundations and anchorages of suspension bridges is beyond the scope of this thesis. However, a few notes are given.

It is essential to design the foundations for the towers sufficiently large and massive to be immovable in case of impact from floating objects, (Ref. 8.7), or collision by ships. The pier top is set so that the steelwork of the tower is clear of splashing by salt water.

The safety of a suspension bridge depends upon the security of the anchorages, (Ref. 1.7). The anchorages are usually designed to resist a very high pull from each cable, at some slope above the horizontal. Overturning moments at the top of each anchorage are usually high. There are two types of anchorages:

(i) Tunnelled anchorages, where its weight, (submerged), plus the weight of the overburden would be sufficient to prevent its being drawn against the friction on its base. This system was used in the Forth Bridge, (Ref. 5.2). Sometimes the anchorage is into rock.

(ii) Gravity type anchorages, where each cable is anchored into a solid block of mass concrete, the two blocks being joined by a massive cross-wall at the rear, (Ref. 8.8). In this case, the pull in each cable is counteracted by the weight of the mass anchorage. This type was used in the Severn Bridge.

It appears that designers consider it sufficient that the resultant of the cable pull on the gravity anchorage and its self weight and the superimposed load should make an angle with the vertical less than the angle of friction of the soil under the anchorage, (Ref. 1.7).

If the gravity anchorage is resting on rock, the toe pressure must not exceed the allowable foundation pressure, so that the anchorage can be safe against settlement. The heel pressure must not be less than about half the toe pressure to minimize the tilting or overturning of the anchorage.

* * * *

The foregoing notes and comments on published work treat the suspension bridge more or less as a plane, or two-dimensional, structure. The fact that suspension bridges are three-dimensional, however, must be considered. The major distinction is the behaviour of the bridge under torsional loadings. This requires taking the torsional stiffness of the girder into consideration. The problem has been tackled herein by the writer in Chapter V, and carefully checked against the behaviour of the three-dimensional laboratory model. This model was also designed by the writer taking into account the torsional stiffness of the deck.

In the following subsection, the method of designing the laboratory three-dimensional model is extended to suit the design of real bridges.

8.3 SUMMARY AND FURTHER NOTES ON THE DESIGN

As previously said, a designer usually needs:
(i) a preliminary design method which must be clear, short and quick, and possible on a small computer; and (2) a final design method which must be accurate enough and reliable, and usually relevant to the use of big computers.

In fact, all the available methods, for both preliminary and final design of suspension bridges, are not designing methods, but they are actually methods of analysis. The authors always design the bridge as if it is existing with all its dimensions and details known in advance!

The following preliminary design procedure is suggested by the writer:

1. The main span, L, is chosen first according to the crossing and the geology of the site and other factors. The lengths of the side spans are decided according to the foundation requirements, etc.
2. The dip-span ratio, D/L, for the main cable is then chosen. For spans of the order 3000 ft (or over), a ratio of 1:11 or 1:12 is reasonable, while for shorter spans (2000 ft or less), a ratio of 1:9 or 1:10 is more appropriate.
3. Now comes the step of estimating the intensity of the dead load, w_1, per unit area.* Unfortunately there is no rule, until now, for giving an estimate for the dead load of suspension bridges. However, a survey of some of the existing bridges may help.
   Modern long-span suspension bridges with tubular slender decks have apparently less self weight than those with the conventional stiffening trusses. Each of the Severn and the Bosporus weighs about 0.5 tonne/m^2. The Forth Bridge, which is the lightest bridge with stiffening trusses, weighs about 0.65 tonne/m^2.

---

* The width of the bridge, here, is regarded as the spacing between the centres of the two cables, b.

The George Washington Bridge (with two decks) has a self weight of about 1.8 tonne/m^2. This means an average of about 0.9 tonne/m^2 for each deck. The Tancarville Bridge (built in France in 1959 with a span of 1995 ft) weighs more than 1 tonne/m^2, (stiffening trusses 17.6 ft deep were used). The Chesapeake Bay Bridge, built in the U.S.A. in 1952 with 1600 ft span, weighs about 0.77 tonne/m^2.

In short, for spans of the order 3000 ft (or over), a dead weight of about 0.6 tonne per square metre (of the area of the deck between the planes of the two cables), is reasonable. For shorter spans (2000 ft or less), this self weight of the bridge may be taken as 0.8 tonne/m^2.

4. The cable spacing, b, is chosen according to the relevant width-span ratio, and also to satisfy the reasonable bridge width for the expected traffic. The intensity of the dead load per unit length of the bridge, w, is then obtained as the product of the width, b, between the two cable centres and the weight w_1 per unit area of the deck (between the planes of the two cables).

5. The sum of the horizontal pull in the two cables, $2H_o$, is given by $2H_o = wL^2/8D$.

6. If the live load is about 30% of the dead load, as is usual, this means that the increment, h, in H_o due to live load will be about $0.3\ H_o$. This means that the design value for $H = H_o + h$ will be about $1.3\ H_o$.

7. If the backstays are unloaded, then the main cables will have their critical sections at the side spans. If they are loaded, however, the cables are designed to carry the maximum possible tension (at the position of maximum cable slope with the horizontal). Usually, the tension at any section in the main span does not exceed 110% of the horizontal pull; (for a dip-span ratio of 1:10, maximum cable tension equals 1.077H). Knowing the working stress of the cable material, the required cross-section can be obtained.

8. The non-dimensional stiffness factor $S^2 = EI/2H_oL^2$ may be given some trial value. Values of this parameter, for some of the existing bridges are shown on Fig. 2.5. A moderate value, for one of the long-span suspension bridges with stiffening trusses, is that of the Forth Bridge ($= 4.3 \times 10^{-3}$). Modern bridges with tubular decks, like the

Severn, Bosporus, and Humber, usually have slender decks, for which the parameter S^2 may have a value less than 1×10^{-3}.

Once S^2, and the modulus of elasticity, E, for the deck material become known, the moment of inertia, I, of the deck can be obtained.

9. The depth of the deck is then determined, as in subsection 8.2.7. That is, for stiffening trusses, a depth-span ratio of 1:120 - 1:180 is reasonable, while for tubular decks, a ratio of 1:300 - 1:360 is adequate.

Once the depth becomes known, the top and the bottom chords of the deck section can be calculated, to give the required moment of inertia.

10. The torsional stiffness of the deck is then checked, using, as suggested by the writer, the non-dimensional parameter $(GJ/EI).(L/b)^2$. Unfortunately, there is not enough information available about that parameter. Its value for only one existing bridge (the Forth Bridge) could be obtained (= 190). For our laboratory model of the two-cable bridge this value is 250.

However, the deck section can be designed according to step 9, and its torsional stiffness can easily be computed.

(Note: usually $G \simeq 0.4E$, for steel decks).

* * * *

A preliminary design has been described above, and the main components of the bridge, mainly the cable and the deck cross-section, could be designed. This can be followed by a preliminary analysis, for that proposed design, (as given before in Chapters V and VI), to get the stresses in and the deflections of the main cables, the deck, the towers, and the hangers, etc. Also, the vibration frequencies and modes can be obtained.

The dimensions of the bridge may then be altered if needed, and the self weight can be re-estimated. The bridge can then be analysed again, and the above procedure may need to be repeated until satisfactory results are obtained.

Note: It would be very useful if designers, besides checking aerodynamic stability of the bridge, could give some indication of its fatigue life. (Some comments on the importance of this appear in Chapter III. The main danger appears to be fatigue in connections.) The analytical tools appear to be available, but their application would need considerable development. More knowledge is needed of the damping properties of suspension bridges and of transient excitation by wind.

8.4 CONSTRUCTION AND ERECTION OF SUSPENSION BRIDGES

The order for the erection of a suspension bridge is (i) foundations and anchorages; (ii) towers; (iii) cables; (iv) suspenders; and (v) deck.

8.4.1 Construction of Piers and Anchorages

(a) Piers

Each pier is usually solid concrete and sufficiently long to support the bases of the two tower legs. The pier tops are usually reasonably set above the water level so that the towers, (especially if made from steel), are clear of splashing by salt water.

Piers may be built, as a non-tidal operation, inside temporary steel cofferdams up to high tide level. Alternatively, a perimeter concrete wall is built to enclose the base concrete. This perimeter wall forms a cofferdam so that the internal portions can be carried out as a non-tidal operation. The external wall is divided into a series of vertical elements, the size being such that concreting can be started at low tide and the level of wet concrete rises at a rate greater than that of the water outside. In this way the maximum use is made of each tidal period, (Ref. 8.7).

(b) Anchorages

The procedure followed in building the piers can also be used for the anchorages. The external surfaces of the anchorages are usualy tanked with asphalt to ensure watertightness.

The anchorage block is perforated by steel tubes concreted in place through which prestressed HT steel screwed rods are passed to secure steel slabs to the upper face. The strand shoes are attached to these slabs, and the spaces between the strands are sealed, (Ref. 8.8).

Usually it is impossible to paint the strands effectively in the tapering spaces between the strands, as they leave the splay saddle. The protection of the wires is thus regrettably reduced to the galvanizing alone, (Ref. 5.2).

8.4.2 Erection of Towers

The tower bases, and some limited height of the towers, are usually set by a derrick boat. Later, the creeper derrick is connected to the tower legs. If the legs of the towers are not vertical, hammerhead derricks are used (between the tower legs) instead of the creeper derricks, as in the San Franciso-Oakland Bridge built in U.S.A. in 1936, (Ref. 8.6).

The towers are usually built of structural steel, although stone, concrete, and timber have been used, (Ref. 1.7). The Humber Bridge will have concrete towers.

When the tower legs are fabricated steel cells, internal diaphragms, access ladders, and hoist supports are assembled, (Ref. 8.9).

Diagonal bracing or cross girders are usually erected between the tower legs to ensure the torsional stiffness of the towers. The main saddles are built up, perhaps, in mild steel plates and assembled and welded in jigs. The cable grooves are formed by welding in layers of plate, and the grooves are ground smooth. Strand spacers are welded in, (Ref. 8.10).

8.4.3 Construction of Cables

A temporary footwalk system for cable spinning is constructed for each cable to enable men to adjust the wires as they are erected to form the cables and subsequently to compact and wrap them. These footbridges (or catwalks) are located about four ft below the level where the cables are to be, and extended from anchorage to anchorage across the waterway (or the gorge). The footwalks of the two cables are interconnected by crossbridges to prevent any overturning due to wind.

On days of high wind and gales no wire might be spun at all. This makes advantageous the method of preassembled strands used in the Newport Bridge, where the shop fabrication of the strands in good working conditions saves a great deal of the erection cost and time. But, unfortunately, this method is relevant for only short span suspension bridges, (not more than 2000 ft).

On a good day, however, more than 500 miles of wire can be spun, (Ref. 8.9), using a spinning wheel. In the Forth Bridge, eight wires were spun at a time, (Ref. 5.3).

When completed, the cables are squeezed, by hydraulic jacks, at intervals throughout their length into a compact and approximately circular formation. After compaction, the cables are tightly bound with temporary galvanized steel straps at about 1 m spacings. The cables are then carefully measured along their length, and permanent cable bands are bolted in position, (at the hanger positions).

The last major operation on the cables is wrapping them round from end to end between the cable bands with galvanized wires under tension. The temporary straps round the cables are removed ahead of the wrapping and a coat of red lead paste is applied to it. Alternatively, a plastic covering for the cables, (essentially a glass-reinforced acrylic-resin system), was developed and used for the second time on the Newport Bridge. It promises long life, does not require painting, and is less expensive than wire wrapping, (Ref. 8.11).

On completion of the cable wrapping, the catwalks are dismantled, (Ref. 8.10).

8.4.4 Erection of Suspenders

Suspenders (or hangers) are then pinned to the cable bands. On the erection of the deck, they are also pinned to the deck suspender lugs. Sometimes, hangers are formed of wire ropes looped over the cable bands. However, single strands formed of larger wires are more resistant to corrosion and less liable to damage at road level, (Ref. 8.8)

Before erection, the hangers are laid up in some Metalcoat, and, after erection, a further coat of this material is also applied.

8.4.5 Erection of the Deck

The scheme should aim to balance the dead-load distribution along the span, so as to minimize the distortion of the cables during erection. Usually, the erection proceeds, simultaneously, from the two towers outwards, using traveller derricks.

A deflection model, however, may be built to obtain some information, in advance of the calculations, relating to cable and deck deformations during erection. Such a model for the Severn Bridge, (Ref. 8.10), showed that erection should be started in the centre of the main span outwards and that this span could be completed without counter balancing erection in the side spans. The erection of the two side spans together can follow after the completion of the main span. (This is for the case of loaded backstays.)

Whether the deck is tubular or of the truss type, it is not possible to close the transverse joints until about half the main span is erected, (Refs. 1.7, 8.9, 8.10). Thus, temporary joints made with grip bolts and sufficiently flexible to permit bending along the axis of the bridge are devised. The reason for this is that the main cables have to stretch some 0.3% between the anchorages as the deck is erected and its dead weight comes on to them.

When using stiffening trusses, the roadway may be made of reinforced concrete or orthotropic steel plates. On the other hand, the top plate of a tubular deck acts as an orthotropic steel plate. In either case, a wearing surface of mastic asphalt is laid over a layer of hot rubber/bitumen compound. Tubular decks offer clear advantages in painting and surfacing, compared to stiffening trusses.

All external surfaces of steelwork and any internal surfaces which might be subjected to atmospheric corrosion are grit-blasted, zinc-sprayed, and then given two, three, or four coats of paint, (Ref. 8.9). In the Newport Bridge, (Ref. 8.11), all the exposed steel of the superstructure, as well as the concrete roadway, were coated with a two-component epoxy compound. This coat reduces maintenance cost and protects the concrete from damage due to deicing salts.

* * * *

Throughout construction, safety measures for the workmen are considered of prime importance. During erection of the suspended structure, safety nets are usually provided under three panels of each of the working fronts. Samples of these nets are tested by dropping a weight shaped like a man's body at different places from heights up to 30 ft, (Ref. 8.9). Experience has shown that men work more quickly and freely on structural steelwork if safety nets are provided beneath them. A safety boat must be always in attendance in the waterway.

8.5 ECONOMICS OF SUSPENSION BRIDGES

The great majority of bridge designers believe that the most economic structure is the one for which the first cost of construction is a minimum. (Ref. 8.12). But, actually, the most economic structure is the one which will do the work required of it for as long a time as necessary, safely, and with the least possible expenditure for operation, maintenance, and repairs, all these being obtained with the smallest practicable initial cost of construction.

A suspension bridge is usually cheaper than any other bridge type for exceedingly long spans, or at the crossing of a gorge or a river of great depth and swift current where it would be too expensive to build piers in the stream, (Ref. 8.13).

Usually, suspending the stiffening girder from the backstays is not economic, if it is practicable to build a trestle approach, (Ref. 7.13). And even if it is not, it may be better to substitute short spans for the trestle supporting them, at intervals, on piers. The only case in which it is economic to use loaded backstays appears to be when there is deep water beneath the side spans as well.

8.5.1 Economics of the Stiffening Girder

With regard to the stiffening girder, the first economic point to consider is that the deck and the floor system should always be made as light as the ruling conditions will allow, because the heavier the floor the greater the load on the cables, (Ref. 8.13), though of course dead load is an aid to stability. The weight of the stiffening girder is a direct function of the live load since the dead load is entirely carried by the main cables (through the suspenders). As stated before, recent investigations showed that for long-span suspension bridges with a single deck, the aerofoil form of box girder is about 20% cheaper than the conventional stiffening trusses, and that it is at least equally aerodynamically stable, (Ref. 8.1). A box girder is also much easier than the trusses in painting and maintenance. Complete segments (or panels) of the tubular deck can be prefabricated in shop or on shore, and then floated and lifted to the required position. This process is easier and quicker than assembling truss members on site over the safety nets and in bad weather. Stiffening plate girders are of course to be avoided. A double-deck suspension bridge may be adopted if the traffic is too heavy for a single deck.

8.5.2 Economics of the Cables

Eye-bar cables were used in the past in the suspension bridge construction for a long time. The longest eye-bar suspension bridge in the world is the Florianopolis Bridge, built in Brazil in 1926 with a span of 1114 ft. About the middle of the last century John Roebling patented the use of the wire cables instead. In the competitive bidding of the George Washington Bridge at New York (in 1927), the wire design had a favourable margin of $2 million, indicating that the eye-bars cannot of course compete with wire cables for extremely long spans, (Ref. 1.7). It is very interesting to note that eye-bars were considered so recently as the late 1920's.

In the construction of the typical parallel-wire cables of John Roebling, the wires are placed wire by wire, in the field, where a travelling wheel pulls one or more loops or bights of wire from one end of the bridge to the other. This process is known as "air spinning". For convenience, the wires for large cables of this type are sometimes assembled initially in small bundles, known as strands.

The idea of avoiding the laborious wire-spinning process has teased the imagination of designers and contractors in the suspension bridge field for many years. One method of accomplishing this goal, (Ref. 8.5), was developed and reduced to practice during the late 1920's and early 1930's. In this method the "parallel-strand cable" consisted of a group of prefabricated, machine-made helical strands.

The urge still remained to develop prefabricated parallel-wire strands. A workable method was eventually reached, and the parallel-wire strands could be achieved successfully in the Newport Bridge in 1968, (span - 1600 ft).

Parallel-wire strands are better than helical-wire strands because of less weight for equal load carrying capacity, (Ref. 8.14). Similarly, parallel strand cables made up of helical strands are better than helical-strand cables for the same reason. For long spans, the conventional air spinning of the individual wires is more economic.

8.5.3 Economics of Towers

The towers are usually built of structural steel, especially for long-span suspension bridges. However, reinforced concrete towers have been used for smaller bridges. The longest suspension bridge with concrete towers is the Tancarville Bridge, built in France in 1959, with 1995 ft span and 404 ft high concrete towers.* (The steel towers of the Severn Bridge are 445 ft high). The latest suspension bridge with concrete tower is the Bordeaux Bridge, built in France in 1967, with 1292 ft span and 344 ft concrete towers, (Ref. 5.3). Stone and timber towers were also used in the past in suspension bridge building, (Ref. 1.7).

As was previously mentioned, the height of towers depends on the dip-span ratio of the main cables. This means that the cost of the towers depends not only on the unit price of the towers' material and erection, but also on the dip-span ratio of the main cables. The general trend these days is to reduce the tower heights (by reducing the cables' sag), and to use structural steel or even somewhat high-tensile steel to get light-weight towers. For economy in the construction of the towers (and the piers), the sidetracks are supported outside the cables, (Ref. 7.3).

---

* The Humber Bridge (4600 ft span) will have concrete towers 536 ft high.

8.5.4 Economics of Piers and Anchorages

There are three general cases of governing conditions to consider for the sake of economy of foundations, (Ref. 7.13):

(i) Foundations on bed rock.

(ii) Foundations on piles.

(iii) Foundations on clay or similar material without piling.

If the bed rock is fairly close to the surface, it will be advisable to found upon it. But otherwise it will be cheaper to put in shallow foundations, obtaining the necessary supporting power either by piling or by spreading the base. If piles are to be used, they may be friction or bearing piles, depending on the depth of the bed rock.

The piers are the foundations of the towers, and so they are also affected by the dip-span ratio of the main cables. In other words, a reduction in the cables' sag will lead to a corresponding reduction in the piers' costs as it reduces the towers' heights and costs as well.

* * * *

On the same bases, the costs of the anchorages increase by the reduction of the cables' sag, (due to the resulting rise in the cable tensions).

The maximum of economy in the gravity type anchorages, if the site is rocky, is obtained by making both the weight of the anchorage block in its rear, and the foundation area in the front, as large as practicable, (Ref. 8.13). The first expedient tends to increase the resisting moment against overturning, and the second to reduce the intensity of bearing at the toe of the face, where, of course, it is greatest. These anchorages are thus, for the sake of economy, long and narrow, low in the front and high in the rear. Also a separate anchorage is provided for each main cable. These individual anchorages are connected in the front below the ground so as to increase the base area. They are also joined in the rear by a great wall above the ground in order to increase the weight there.

If the site is clayey or something similar, tension and compression piles are, perhaps, to be used to support the anchorages. Piles should obviously be driven as closely together as practicable near the front of the anchorage, and spread somewhat near the rear.

8.6 SUGGESTIONS

8.6.1 Steel Stress-Ribbon Concept

This is a new unusual concept in suspension bridge construction, (Ref. 8.15). In this concept, the suspension bridge is built with central sags of less than 2% of the span length using currently available materials and technology.

This returns the suspension bridge structure to the primitive fashion, where the roadway is put directly on the main cables. The only difference here is that the deck shares the axial forces with the high tensile cables. This means that there are no hangers. There are here also no towers, but the stress-ribbon is anchored to stiff abutments at the ends.

Recent studies reported in the press suggest that highway bridges with a span length of up to 2000 ft are practically and economically feasible using the stress-ribbon concept. The study was based on the use of high tensile steel wires for the cables, and structural steel plates for the deck.

At sites where long high pipeline crossings are required, the stress-ribbon structure offers some important advantages. The pipe itself forms the deck, and advantage can be taken of its unused longitudinal tension capacity. The pipe is erected on high tensile steel cables attached to the anchorages and pretensioned to a reasonable stress level.

The writer thinks that the cross-sectional area of the pipe is much more than that of the cables. Thus, if the pipe can be made of high tensile steel or any other high quality steel, the cables can then even be dispensed with, and the entire load can be carried by the high tensile steel pipe. The same may perhaps be done with the highway suspension bridges, where the cables can be dispensed with and the entire load can be carried by a high tensile steel deck. In this case the deck will be functioning in both bending and axial tension, as well as in torsion (in case of torsional loadings).

* * * *

The steel stress-ribbon bridge gains its high stiffness from the very high axial tension which is caused by the low sag. The success of the stress-ribbon structure depends on the existence of sound rock at the anchorage points. A typical sequence of steps in the construction of a stress-ribbon suspension bridge would be as follows:

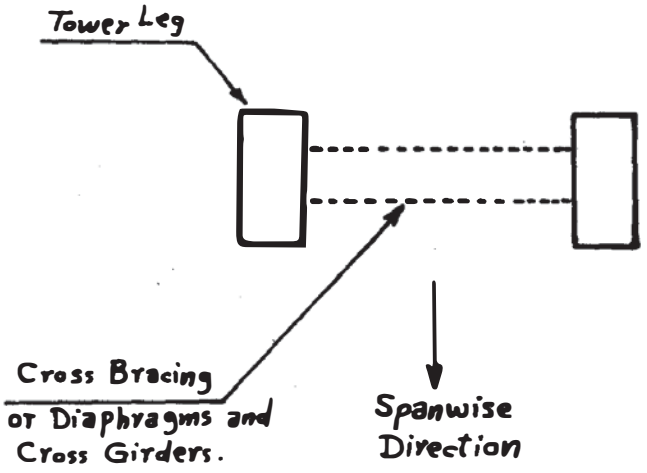

Fig. 8.1.- Typical Cross-Section of a Modern Steel Tower.

(a) Construct tensioning anchorages at each abutment.

(b) String high tensile steel tendons between the abutments and tension them.

(c) Erect and join steel deck segments, directly supported on the tendons.

(d) Adjust the tension forces in the deck and the tendons to their optimum levels.

* * * *

Cost savings of up to about 40% in special applications are said to be possible using the stress-ribbon concept.

There are a few bridges of this type built recently, in the last decade, in both Europe and Japan, (Ref. 8.16). The first of these is the Bircherweid Bridge (in Switzerland), built in 1967 with 131 ft span. The latest bridge of this type is the Rhone Gent-Lignon Bridge, built in 1971 with 426 ft span. The Freiburg Bridge, built in Germany in 1969 with three spans, approximately 131 ft each, has a prestressed concrete slab deck.

8.6.2 A New Shape for the Towers

The typical cross-section of a tower leg comprises one or more hollow rectangular cells made of structural steel. The two legs of each tower are placed such that the greater dimension of the section of each leg is in the spanwise direction of the bridge, (Refs. 5.2, 7.6, 8.8). A typical cross-section of a modern suspension bridge tower is shown in Fig. 8.1.

To improve the aerodynamic stability of the tower, (in the spanwise direction), the writer suggests perforated tower legs, the holes in both legs are to be made in the side of the greater dimension (to minimize the effect of lateral wind). It is to be noted that for the longitudinal wind, the tower with its two legs and bracing web members, in between, acts as a vertical truss, or vierendeel.

The idea of perforated towers came to the writer from designing many of the concrete and steel towers for transmission lines in 1968-1971 in Egypt and other Middle East countries. This idea is in agreement with the conclusion which prefers the open stiffening truss to the stiffening plate girder with solid web, (see subsection 8.2.3).

Typical cross-section, elevation, and side view, for the suggested tower are shown in Fig. 8.2.

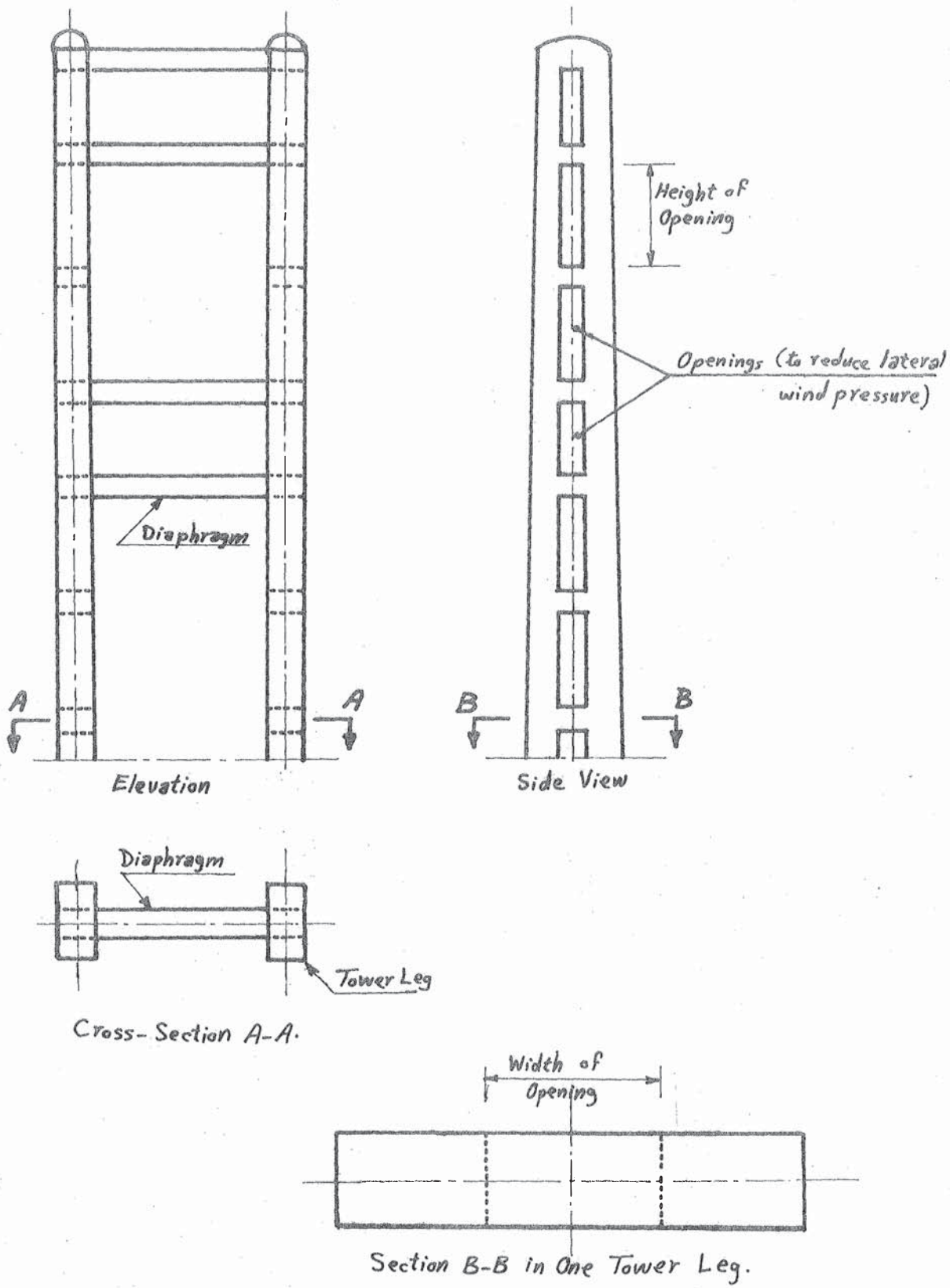

Fig. 8.2.- Arrangement of the Suggested Aerofoil Perforated Tower.

CHAPTER IX

CONCLUSIONS AND RECOMMENDATIONS

A summary of the work presented in this thesis has been given in the preface. The general conclusions and recommendations of the analytical and experimental investigation are set out below.

STATICS OF THE SINGLE-CABLE BRIDGE

(i) The increase in the horizontal component of the cable tension, h, due to any L.L. is almost linearly proportional to the intensity of that live load.

(ii) The stiffness of the bridge increases by increasing the L.L. intensity.

(iii) If the Deflection Theory is to be used in analysing a suspension bridge, the integration constants must be obtained in terms of the dimensions and properties of the bridge in order to avoid any ill-conditioning that may arise from evaluating them in terms of one another.

(iv) Timoshenko's Energy Method showed the best agreement with measurements on our laboratory model while the Deflection Theory gave reasonable agreement but with less accuracy. The reason is perhaps an over-estimate in evaluating h when using the Deflection Theory. Pugsley's Flexibility Method, and Charlton's Energy Method give nearly the same result showing an overestimate of the deflections everywhere in the span.

(v) The extensions of the hangers are not considerable and can be ignored without any significant error. In other words, the deflection curve of the deck can be considered identical with that of the main cable.

DYNAMICS OF THE SINGLE-CABLE BRIDGE

(i) The iterative procedure is reasonable for a preliminary design where only the first few modes of vibration are wanted. For this purpose, it is relevant to use the flexibility matrix of the vibrating structure since the iterative procedure then converges first to the lowest mode.

(ii) Since suspension structures are non-linear, it is recommended that the flexibility matrix be evaluated for each loading condition separately. It was noticed that suspension structures stiffen by loading, and this results in a reduction in the magnitudes of the flexibility coefficients as the L.L. increases.

(iii) Rayleigh's quotient gives an upper bound to fundamental frequency. This estimate for the fundamental frequency approaches the correct frequency value as the guessed mode shape approaches the correct fundamental mode shape.

(iv) Similarly to the displacements due to static loading, the displacements of a vibration mode under a loaded zone are greater than those of the unloaded zone, Fig. 9.1.

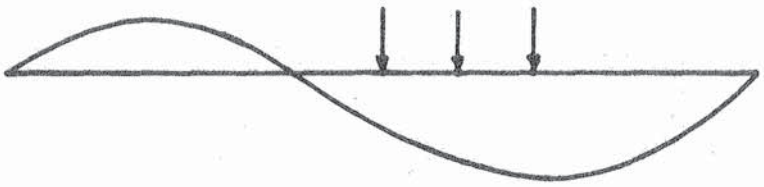

Fig. 9.1.- Fundamental Mode.

(v) The fundamental frequency increases as the L.L. increases, while the contrary appears to apply to the second frequency.

DYNAMICS OF SUSPENSION CABLES AND NETS

(i) For the suspension cables, as in suspension bridges, any increase in the fundamental frequency, (due to L.L.), is always associated with a reduction in the second frequency, and vice versa.

(ii) Experimental observation, and symmetry and antisymmetry, can be made use of to simplify the analytical solution of the dynamic problems of suspension cables and nets, and suspension bridges as well. A great reduction in the order of the frequency and mode equations can thus be achieved.

STATICS OF THE TWO-CABLE BRIDGE

(i) The energy procedure presented herein is recommended for solving the problem of three-dimensional suspension bridges taking the torsional stiffness of the deck and the effect of torsional loading into consideration. The method is approximate, but it is recommended for design purposes, both statically and dynamically.

(ii) The principle of superposition can be applied to two-cable bridges, without considerable errors, in both the vertical deflections and cable tensions.

(iii) The torsional stiffness of the deck of a suspension bridge increases with the increase of the torsional loads. In other words, the bridge stiffens, both in flexure and in torsion, as the load increases.

DYNAMICS OF THE TWO-CABLE BRIDGE

(i) The energy method of the static analysis of two-cable bridges, presented herein, can be used successfully in evaluating the flexibility matrix for the dynamic analysis.

(ii) A new method for reducing the number of degrees of freedom is presented. The structure can be dynamically analysed by assuming that it has a reduced number of "joints", if the mass and the flexibility matrices are accordingly modified. No remarkable error was found when the number of "joints" was halved.

(iii) Whether the flexibility matrix is made symmetric, (by an averaging procedure), or used as it is, (asymmetric), in a procedure of finding the eigenvalues and eigenvectors of symmetric (or asymmetric) matrices, the results are not remarkably different.

(iv) The dynamic analysis and the method of eigenvalue economization presented herein for suspension bridges are applicable to, and recommended for, many other structures, including lumped and continuous mass systems.

AERODYNAMIC STABILITY

(i) The flexibility matrix procedure is very usefully applicable to aerodynamic problems. The equation $[m][\ddot{X}] + [k][X] = [F]$ can be premultiplied by the flexibility matrix, $[k]^{-1}$ in order to facilitate the solution. A real structure can be divided into n segments with known mass and inertia values, and the displacements (X_1, X_2, ..., X_n; θ_1, θ_2, ..., θ_n) can be determined for all modes of vibration.

Alternatively, the displacements may preferably have the form $(X_1, X_2, \ldots, X_n ; Y_1, Y_2, \ldots, Y_n)$, where the X's are the displacements of one side, and the Y's are those of the other.

To the author's knowledge, and most surprisingly, this very important suggestion has not apparently been made before. It seems almost impossible to believe that the latest papers on flutter handle structural aspects by differential equations only.

This procedure is recommended for other structures as well, (e.g. aircraft wings). (Note that damping is not included in the above equation and that it can be introduced if required.)

(ii) For flutter calculations on suspension bridges it must be strongly emphasised that what matters is the relative natural frequencies of flexural and torsional modes of similar shape. It is desirable that structural designers learn how to do flutter calculations.

For a modern suspension bridge, there is a possibility of a heavy live load on one side of the bridge (due to stoppage of traffic, for example) for a period of time. Designers may be well-advised to carry out the necessary relevant checks for stability against flutter under live load.

(iii) The structural damping is greatly increased by the construction of the deck, but the aerodynamic forces also depend on the existence of the deck. It is thus desirable to design the cross-section of the deck such that any oscillation caused by aerodynamic forces will certainly damp out.

DESIGN OF SUSPENSION BRIDGES

A procedure for the design of suspension bridges is presented in section 8.3, and it is recommended for the design of real suspension bridges.

APPENDIX A1: REFERENCES

CHAPTER I

1.1 Needham, J., "Science & Civilisation in China", Vol. IV:3, Cambridge University Press, 1971, pp. 184-210.

1.2 Hopkins, H.J., "A Span of Bridges", David & Charles: Newton Abbot, 1970, pp. 174-236.

1.3 Pugsley, A., "The Theory of Suspension Bridges", Arnold, London, 2nd edition, 1968.

1.4 Shirley-Smith, H., "The World's Great Bridges", Phoenix House, London, 2nd edition, 1964.

1.5 Straub, H., "A History of Civil Engineering", English Translation (from German) by E. Rockwell, The M.I.T. Press, Massachusetts, 1964.

1.6 Steinman, D.B., and Watson, S.R., "Bridges and Their Builders", Dover, New York, 1957.

1.7 Steinman, D.B., "A Practical Treatise on Suspension Bridges", Wiley, New York, 1929.

1.8 Johnson, J.B., Bryan, C.W., and Turneaure, F.E., "Modern Framed Structures", Part III, Wiley, New York, 9th edition, 1916.

1.9 The Statics of Bridges, Civil Engineer and Architect's Journal, Aug. 1862, pp. 236-237.

1.10 Melan, J., (Translated by D.B. Steinman), "Theory of Arches and Suspension Bridges", Chicago, 1913.

1.11 Godard, T., "Theory of Suspension Bridges with Stiffening Girders", Minutes of Proceedings of ICE with other Abstracted Papers, Vol. CXIX, 1895, Edited by J. Forrest, pp. 417-419. Translated and Abstracted from Annales des Ponts et Chaussees, Aug. 1894, p. 105.

1.12 Atkinson, R.J., and Southwell, R.V., "On the Problem of Stiffened Suspension Bridges and its Treatment by Relaxation Methods", J.ICE, No. 5, March 1939, p. 289.

1.13 Johnson, J.B., Bryan, C.W., and Turneaure, F.E., "Modern Framed Structures", Wiley, New York, Part II, 10th edition, 1929, Chapter V.

1.14 Timoshenko, S., "The Stiffness of Suspension Bridges", Trans. ASCE, Vol. 94, 1930, p. 377.

1.15 Pugsley, A.G., "A Flexibility Coefficient Approach to Suspension Bridge Theory", J.ICE, Vol. 32, 1949.

1.16 Crosthwaite, C.D., "The Corrected Theory of Stiffened Suspension Bridges", J.ICE, Vol. 27, 1946.

1.17 Bowen, C.F.P., and Charlton, T.M., "A Note on the Approximate Analysis of Suspension Bridges", The Structural Engineer, Vol. 45, 1967.

1.18 Charlton, T.M., and Drakeley, B.K., "Approximate Analysis of Suspension Bridges: A Study in Rational Approximate Analysis - Synopsis", The Structural Engineer, Vol. 53, April 1975.

1.19 Van der Woude, F., Gregory, M.S., and Hegab, H.I.A., Discussion of Ref. 1.18, Correspondence 2, The Structural Engineer, Vol. 53, Sept. 1975.

1.20 Scruton, C., "An Experimental Investigation of the Aerodynamic Stability of Suspension Bridges", 3rd Congress (Liège), International Association for Bridge and Structural Engineering, Zürich, 1948.

1.21 Frazer, R.A., and Scruton, C., "A Summarised Account of the Severn Aerodynamic Investigation", NPL/Aero/222, Feb. 1952.

1.22 Walshe, D.E., and Rayner, D.V., "A Further Aerodynamic Investigation for the Proposed River Severn Suspension Bridge", NPL/Aero/1010, March, 1962.

1.23 Gade, R.H., Bosch, H.R., and Podolny, W., "Recent Aerodynamic Studies of Long Span Bridges", J. Struct. Div., ASCE, Vol. 102, July 1976.

1.24 Nakamura, Y., and Yoshimura, T., "Binary Flutter of Suspension Bridge Deck Sections", J. Eng. Mech. Div., ASCE, Vol. 102, August 1976.

1.25 Sih, N., "Torsion Analysis for Suspension Bridges", J. Struct. Div., ASCE, Vol. 83, November 1957.

1.26 Fukuda, T., "Multispan Suspension Bridges Under Torsional Loading", Proc. Japan Society of Civil Engs., No. 242, October 1975.

1.27 Van der Woude, F., "Analysis of Suspension Bridges using Energy Principles", The Structural Engineer, Vol. 54, April 1976.

CHAPTER II

2.1 Poskitt, T.J., "Structural Analysis of Suspension Bridges", J. Struct. Div., ASCE, Vol. 92, February 1966.

2.2 Saafan, S.A., "Theoretical Analysis of Suspension Bridges", J. Struct. Div., ASCE, Vol. 92, August 1966.

2.3 Fukuda, T., "Analysis of Multispan Suspension Bridges", J. Struct. Div., ASCE, Vol. 93, June 1967.

2.4 Fukuda, T., "Multispan Suspension Bridges Under Lateral Loads", J. Struct. Div., ASCE, Vol. 94, January 1968.

2.5 Fukuda, T., "Analysis of Longitudinally Loaded Suspension Bridges", J. Struct. Div., ASCE, Vol. 94, April 1968.

2.6 Brotton, D.M., "A General Computer Programme for the Solution of Suspension Bridge Problems", The Structural Engineer, May 1966.

2.7 Jennings, A., and Mairs, J.E., "Static Analysis of Suspension Bridges", J. Struct. Div., ASCE, Vol. 98, November 1972.

2.8 Hegab, H.I.A., Discussion of "Effective Modulus of Twisted Wire Cables", J. Eng. Mech. Div., ASCE, Vol. 102, December 1976.

2.9 von Kármán, T., and Biot, M.A., "Mathematical Methods in Engineering", McGraw-Hill, 1940, Chapter VII, Section 5.

2.10 Gregory, M.S., "Introduction to Extremum Principles", Butterworths, London, 1969.

Reference is also made to Refs. 1.3, 1.7, 1.9, 1.10, 1.12 - 1.15, 1.17-1.19, and 1.27.

CHAPTER III

3.1 Thomson, W.T., "Vibration, Theory and Applications", Allen & Unwin, London, 1973.

3.2 McMinn, S.J., "Matrices for Structural Analysis", Spon, London, 1962.

3.3 Prentis, J.M., and Leckie, F.A., "Mechanical Vibrations", Longman, London, 1963.

3.4 SAA Steel Structures Code, Australian Standard CA1, Standards Association of Australia, 1968, Appendix B, pp. 81-94.

Reference is also made to Refs. 1.6, 1.14, and 2.10.

CHAPTER IV

4.1 Hegab, H.I.A., "Theoretical and Experimental Analysis of Suspension Roofs", M.Sc. Thesis, Ain Shams University, Cairo, Egypt, 1972.

4.2 Saafan, S.A., "Theoretical Analysis of Suspension Roofs", J. Struct. Div., ASCE, Vol. 96, February 1970.

4.3 Thornton, C.H., and Birnstiel, C., "Three-Dimensional Suspension Structures", J. Struct. Div., ASCE, Vol. 93, April 1967.

4.4 Shore, S., and Bathish, G.N., "Membrane Analysis of Cable Roofs" Space Structures, edited by R.M. Davies, Blackwell Scientific Publications, Oxford, 1967, pp. 890-906.

4.5 Skop, R.A., and O'Hara, G.J., "The Analysis of Internally Redundant Structural Cable Arrays", N.R.L. Report 7296, Naval Research Laboratory, Washington D.C., September 1, 1971.

4.6 Max Irvine, H., "Analytical Solutions for Prestressed Cable Nets", J. Eng. Mech. Div., ASCE, Vol. 102, February 1976.

4.7 Heale, D.G., Reddy, D.V., and Subramonian, N., "Analysis of Layered Pretensioned Cable Networks by Finite Difference Calculus", Proc. Int. Conf. on Tension Roof Structures, The Polytechnic of Central London, April 1974.

4.8 Subramonian, N., and Reddy, D.V., "Frequency Analysis of Cable Networks Using Finite Difference Calculus", J.App.Mech., Trans. ASME, Vol. 41, Series E, March 1974, pp. 293-294.

4.9 West, H.H., Geschwindner, L.F., and Suhoski, J.E., "Natural Vibrations of Suspension Cables", J. Struct. Div., ASCE, Vol. 101, November 1975.

4.10 Max Irvine, H., Discussion of Ref. 4.9, J. Struct. Div., ASCE, Vol. 102, June 1976.

4.11 Sarrazin, M.A., Roesset, J.M., and Whitman, R.V., "Dynamic Analysis of Cable Systems", J. Struct. Div., ASCE, Vol. 98, July 1972.

4.12 Ralston, A., "A First Course in Numerical Analysis", McGraw-Hill, 1965.

Reference is also made to Refs. 1.14 and 1.18.

CHAPTER V

5.1 Irvine, H.M., "Torsional Analysis of Box-Girder Suspension Bridges", J. Struct. Div., ASCE, Vol. 100, April 1974.

5.2 "Forth Road Bridge", Institution of Civil Engineers, 2nd print, 1967.

5.3 O'Connor, C., "Design of Bridge Superstructures", Wiley-Interscience, 1971, Chapter 8.

5.4 Gregory, M.S., "The Bending and Shortening Effect of Pure Torque", Australian Journal of Applied Science, Vol. 11, No. 2, pp.209-216, 1960.

Reference is also made to Refs. 1.14, 1.25, and 1.26.

CHAPTER VI

6.1 McLamore, V.R., Hart, G.C., and Stubbs, I.R., "Ambient Vibration of Two Suspension Bridges", J. Struct. Div., ASCE, Vol. 97, October 1971.

6.2 Clough, R.W., and Penzien, J., "Dynamics of Structures", McGraw-Hill, 1975, pp. 235-243.

6.3 Thomson, W.T., "Mechanical Vibrations", Prentice-Hall, 2nd edition, 1964.

Reference is also made to Ref. 3.1.

CHAPTER VII

7.1 Steinman, D.B., "Rigidity and Aerodynamic Stability of Suspension Bridges", Proc. ASCE, Vol. 69, Nov. 1943, pp. 1361-1397.

7.2 Bleich, F., "Dynamic Instability of Truss-Stiffened Suspension Bridges Under Wind Action", Proc. ASCE, Vol. 74, Oct. 1948, pp. 1269-1314.

7.3 Scruton, C., "An Experimental Investigation of the Aerodynamic Stability of Suspension Bridges with Special Reference to the Proposed Severn Bridge", Proc. ICE, Vol. 1, March 1952, pp. 189-222.

7.4 Scruton, C., and Flint, A.R., "Wind-Excited Oscillations of Structures", Proc. ICE, Vol. 27, Apr. 1964, pp. 673-702.

7.5 Walshe, D.E., "A Résumé of the Aerodynamic Investigations for the Forth Road and the Severn Bridges", Proc. ICE, Vol. 37, May 1967, pp. 87-108.

7.6 Brown, W.C., and Parsons, M.F., "Bosporus Bridge, Part I: History of Design", Proc. ICE, Vol. 58, Feb. 1975, (Part 1), pp. 505-532.

7.7 Williams, D., "Theory of Aircraft Structures", Arnold, London, 1960.

7.8 Bisplinghoff, R.L., et al, "Aeroelasticity", Addison-Wesley, 1955.

7.9 Hedefine, A., and Silano, L.G., "Newport Bridge Superstructure", J. Struct. Div., ASCE, Vol. 97, Nov. 1971.

7.10 Den Hartog, J.P., "Mechanical Vibrations", McGraw-Hill, 4th ed., 1956.

7.11 Warburton, G.B., "The Dynamical Behaviour of Structures", Pergamon Press, 1964.

7.12 Marécos, J., et al., "Field Observation of Tagus River Suspension Bridge", J. Struct. Div., ASCE, Vol. 95, Apr. 1969.

7.13 Morely, G.W., et al., Discussion of Ref. 7.5, Proc. ICE, Vol. 38, Dec. 1967, pp. 781-783.

Reference is also made to Refs. 1.20, 1.23, 1.24, and 5.3.

CHAPTER VIII

8.1 Sir Ralph Freeman (of Freeman Fox and Partners), "Two Design Factors Which Gave Economy", Bosporus Bridge Pamphlet, New Civil Engineer Special Supplement.

8.2 Waddell, J.A.L., "Bridge Engineering", Vol. I, Wiley, 1st ed. 1916.

8.3 Scalzi, J.B., and McGrath, W.K., "Mechanical Properties of Structural Cables", J. Struct. Div., ASCE, Vol. 97, Dec. 1971.

8.4 "Cable-Suspended Roof Construction State-of-the-Art", by the Sub-Committee on Cable Suspended Structures of the Task Committee on Special Structures, of the Committee on Metals of the Structural Division,J. Struct. Div., ASCE, Vol. 97, June 1971.

8.5 Birdsall, B., "Main Cables of Newport Suspension Bridge", J. Struct. Div., ASCE, Vol. 97, Dec. 1971.

8.6 Dwyer, J.W., "Fifty-Year Development: Construction of Steel Suspension Bridges", J. Construction Div., ASCE, Vol. 101, March 1975.

8.7 Gowring, G.I.B., and Hardie, A., "Severn Bridge: Foundations and Substructure", Proc. ICE, Vol. 41, Sept. 1968, pp. 49-67.

8.8 Sir Gilbert Roberts, "Severn Bridge: Design and Contract Arrangements", Proc. ICE, Vol. 41, Sept. 1968, pp. 1-48.

8.9 Shirley-Smith, H., "Supply and Erection of the Main Superstructure", The Forth Road Bridge, ICE, 2nd print, 1967.

8.10 Hyatt, K.E., "Severn Bridge: Fabrication and Erection", Proc. ICE, Vol. 41, Sept. 1968, pp. 69-104.

8.11 Hedefine, A., and Mandel, H.M., "Design and Construction of Newport Bridge", J. Struct. Div., ASCE, Vol. 97, Nov. 1971.

8.12 Waddell, J.A.L., "Bridge Engineering", Vol. II, Wiley, 1st ed. 1916.

8.13 Waddell, J.A.L., "Economics of Bridgework", Wiley, 1921.

8.14 Hedefine, A., and Silano, L.G., "Newport Suspension Bridge", Civil Engineering, Vol. 40, No. 8, Aug. 1970.

8.15 Wheen, R.J., "Steel Stress-Ribbon Concept - Will it Save Money?", Civil Engineering, ASCE, May 1976.

8.16 Tang, M.C., "Stress-Ribbon Bridge in Freiburg, Germany", Civil Engineering, ASCE, May 1976.

Reference is also made to Refs. 1.3, 1.4, 1.6, 1.7, 1.13, 1.15, 1.26, 2.3 2.5, 2.8, 5.2, 5.3.

APPENDIX A4

A4.1 Selby, S.M., "Standard Mathematical Tables", The Chemical Rubber Co., 19th ed. 1971, pp. 123-124.

A4.2 Bell, S.W., and Matley, H., "Mathematics for Higher National Certificate", Cambridge University Press, Vol. II, 2nd ed., 1963, pp. 404-407.

Reference is also made to Refs. 1.3, 1.15, 1.17, 1.18.

APPENDIX A2: NOTATION

A	:	Cross-sectional area of the bridge deck;
AE	:	Effective cable stiffness;
a_i, b_i	:	Fourier coefficients of vertical deflections;
$[a_{ij}]$	:	Flexibility matrix of the cable;
B	:	Total deck width, (two-cable bridge);
b	:	Width between centres of cables, (two-cable bridge);
C, C'	:	Integration constants;
C_L, C_D, C_T	:	Non-dimensional lift, drag, and moment coefficients, respectively;
c	=	$\sqrt{(H_o + h)/EI}$;
D	:	Central dip of the main cable;
δD	:	Change in the central dip of the main cable due to cable extensibility and tower movements = $\delta D_1 + \delta D_2$;
ds	:	Elemental length of the cable;
EI	:	Bending stiffness of the deck;
$[F]$	:	Exciting-force column vector;
F_L, F_D	:	Lift and drag forces, respectively;
f	:	Frequency in Hertz;
GJ	:	Torsional stiffness of the deck, (two-cable bridge);
H	:	Horizontal component of cable tension, (D.L. + L.L.);
H_o	:	Value of H for D.L. only, i.e. L.L. = 0;
h	:	Increment in the horizontal component of cable tension due to L.L., (single-cable bridge);
h_1, h_2	:	Values of h for cables 1-1 and 2-2, respectively, (two-cable bridge);
I	:	Mass moment of inertia;
$[I]$	:	Identity matrix;
K	:	Curvature of the deck $\simeq d^2v/dx^2$;
K_{xy}	:	Twist of the deck, (two-cable bridge);
$[k]$	:	Stiffness matrix of the vibrating system;
$[k]^{-1}$	:	Flexibility matrix of the vibrating system = $[\delta_{ij}]$;
L	:	Span length;
ℓ	:	Length of main cable, (D.L. condition);
δL	:	Shortening of the span due to tower movements = $\delta L_1 + \delta L_2$;
$\delta \ell$	:	Extension of the main cable due to h;

M : Final B.M. in the deck for any loading condition;

M_t : Twisting moment in the deck, (two-cable bridge);

m_o : B.M., due to L.L., on the girder when treated as isolated and simply supported at its ends;

$[m]$: Mass matrix of the vibrating system;

$[m]^{-1}$: Inverse of the mass matrix;

$[0]$: The zero matrix;

P : Point-load;

p : Intensity of L.L. on the single-cable bridge;

p_1, p_2 : Intensities of L.L. on sides 1-1 and 2-2, respectively, (two-cable bridge);

q : Intensity of L.L. portion carried by the cable, (single-cable bridge);

q_1, q_2 : Intensities of L.L. portions carried by cables 1-1 and 2-2, respectively, (two-cable bridge);

R : Reynolds number;

$[s_{ij}]$: Stiffness matrix of the cable only = $[a_{ij}]^{-1}$

t : Time;

T_i : Tension in hanger i due to L.L. only;

U : Potential (or strain) energy;

u : Horizontal deflection of a point on the cable;

u_{ij}, v_{ij} : Horizontal and vertical deflections, respectively, of point i on the cable due to a point-load acting at j;

V : Vertical deflection of a point on the girder;

V_w : Wind velocity;

V_R : Relative wind velocity;

V_r : Reduced wind velocity = $V_w/f.B$);

v : Vertical deflection of a point on the cable;

v_i : Vertical deflection of point i on the cable;

v_1, v_2 : Vertical deflections of cables 1-1 and 2-2, respectively, (two-cable bridge);

w : Intensity of D.L. on the bridge;

W_i : Tension in hanger i due to D.L. only;

x, y : Horizontal and vertical co-ordinates of a point on the cable, with the left end of the cable as the origin;

x_1, x_2 : Start and end, respectively, of L.L., p, of the single-cable bridge (or p_1 on side 1-1 of the two-cable bridge), measured from the left end of the span;

x_3, x_4 : Start and end, respectively, of L.L., p_2, on side 2-2 of the two-cable bridge, measured from the left end of the span;

$[X]$: Column vector of displacements;

$\dot{X}$: Velocity of vibrating system = dX/dt;

$[X]_o$: Guessed (or assumed) mode shape;

$\ddot{[X]}$: Column vector of accelerations = $\frac{d^2}{dt^2}[X]$;

β = h/H_o;

β_1, β_2 = h_1/H_o, h_2/H_o, respectively;

θ : Angular rotation of a section;

$\ddot{\theta}$: Angular acceleration of a section;

λ : Eigenvalue;

μ : Poisson's ratio for the deck material;

ρ : Density of air;

ω : Angular frequency; and

ω_i : Angular frequency of the normal mode $[X]_i$.

APPENDIX A3: ABBREVIATIONS

ASCE	:	American Society of Civil Engineers;
D.E.	:	Differential equation;
D.L.	:	Dead Load;
Hz.	:	Hertz = cycle per second;
ICE	:	Institution of Civil Engineers, (U.K.);
L.H.S.	:	Left hand side;
L.L.	:	Live Load; and
R.H.S.	:	Right hand side.

APPENDIX A4: SINGULAR MATRICES

A4.1 MATHEMATICAL DEFINITIONS

A singular matrix is defined by either of the following two definitions which have the same meaning.

(i) A square matrix [A] is called singular if there exists a vector [X] $\neq$ [0] such that [A][X] = [0], or [A$'$][X] = [0], where [A$'$] is the transpose of [A]. Note that [X] $\neq$ [0] if a single element of [X] is unequal to zero, (Ref. A4.1). This means that a singular matrix has no inverse.

Proof:

Let [A][X] = [B] (A4.1)

If [X] = [0], therefore [B] will be equal to [0], whatever [A] is.
If [X] $\neq$ [0], then we may write

$$[X] = [A]^{-1} \cdot [B] \tag{A4.2}$$

A non zero solution [X] can be obtained, from Eq. A4.2, if [B] $\neq$[0] and if the inverse $[A]^{-1}$ exists.

Eq. A4.2 is similar to Eq. A4.1. If [B] = [0], therefore, [X] will be equal to [0], provided that $[A]^{-1}$ exists. But if [B] = [0], [X] $\neq$ [0], this means that Eq. A4.2 is not true, and, consequently, this means that $[A]^{-1}$ does not exist. Thus, if [A][X] = [0] while [X] $\neq$ [0], therefore, [A] will have no inverse and is called singular.

(ii) A square matrix [A] is called singular if its determinant $|A|$ is zero, (Ref. A4.2). It is obvious, here, that the matrix has no inverse. This is because

$$[A]^{-1} = \text{adj}[A] \div |A| \tag{A4.3}$$

where adj[A] is the adjoint of the matrix [A]. Thus, if $|A| = 0$, then the inverse $[A]^{-1}$ becomes unobtainable.

* * * *

If we have a system of simultaneous equations as in Eq. A4.1, the solution can be obtained as in Eq. A4.2 if $[A]^{-1}$ exists. If $[A]^{-1}$ does not exist, or in other words if $|A| = 0$, then the process of solution breaks down. In practice this means that the equations are not independent. One, or more, can be obtained from the others.

A4.2 COROLLARY

"Any rectangular matrix is also called singular".

This is because the rectangular matrix can be made square by the inclusion of one, or more, rows (or columns) of zeros. Having at least one row (or column) of zeros, a matrix becomes certainly singular.

Engineers are more likely to think in the terms that a rectangular matrix means: number of equations $\neq$ number of unknowns.

A4.3 APPLICATION TO STRUCTURES

In the study of structures, it is common to use either the flexibility matrix or the stiffness matrix. In some structural systems, the stiffness matrix is given or easily obtainable, but often the flexibility matrix is very much easier to obtain, for most structures. For suspension structures, in general, it may be impossible to obtain the stiffness matrix due to the singularity of the flexibility matrix.

The singularity of the flexibility matrix of a suspension structure may be concluded if any of the following phenomena is noticed.*

(a) The computation procedure may fail to find the matrix inverse if the determinant of the matrix is zero.

(b) If the computational procedure is not accurate, or the matrix itself has some impurities, or due to the accumulation of the round-off errors, or any other errors that are likely to happen during the inversion process, a silly inverse may be obtained with very big elements which seem to be very far beyond the capacity of the structure and the possibility of happening.

(c) Sometimes all, or most of, the elements of the inverse have an opposite sign to what is expected. This impossible solution means that such inverse is not acceptable (or reliable), and, so, the original matrix is considered to be singular (with no inverse).

---

* All these cases were met by the writer in the study of Chapters III, IV.

The first case, case (a), was met by the writer when the flexibility matrix for both the D.L. and L.L. conditions of the single-cable bridge (Chapter III), was evaluated and sought to be inverted in one program. Here, the inversion process stopped once a division by a zero pivot was met.

The second case, case (b), was met when the above flexibility matrices were punched on the punch tape in the E-Format* using one program, and then were sought to be inverted by a separate program for matrix inversion. This shows, in spite of using the E-Format in storing the matrices, how the accumulation of the very small round-off errors can give non-zero pivots in place of zeros. Fortunately, the obtained inverses were so funny that they could not be believed.

In the dynamic study of the suspension nets, Chapter IV, the third form of singular flexibility matrix was met. The flexibility matrix of the net model was measured and fed to the computer. All the elements of the inverted matrix had a negative sign, while it is expected, for example, that the influence load at any joint will produce, no doubt, a deflection in the same direction at the loaded joint (at least).

* * * *

In all these cases, corrections to the calculated deflections were added to include the cable(s) extensibility (and the tower movements in the case of the single-cable bridge). However, Charlton, (Ref. 1.17), in his potential energy method, used the stiffness matrix (of the cable only) which was obtained by inverting the flexibility matrix. Charlton's method is based on Pugsley's influence coefficients, (Ref. 1.15), for inextensible cables, but when corrections, due to cable extensibility and tower movements, are added, the flexibility matrix proves also to be singular for some cases, (see below).

Charlton could not get the stiffness matrix of the cable directly but, rather, he had to invert the flexibility matrix, which is easy to obtain. It seems to the writer that the stiffness matrix for an inextensible cable is meaningless, and that it is not likely to exist. This is because the number of equations is more than the number of unknowns by one (i.e. the actual flexibility matrix is rectangular, and consequently singular according to the corollary of Section A4.2). Furthermore, for an inextensible cable, the occurence of any deflection at any joint is accompanied, no doubt, by deflections at all (or at least some of) the other joints of the cable. This contradicts at once the characteristics of the stiffness matrix, and makes it obviously not existent. This will be clarified by a following example, (Section A4.4).

---

* i.e. each element in the matrix has the form of a decimal and exponential parts (eg. 0.325×10^{-11}).

The existence of the stiffness matrix for extensible cables also seems to be questionable. This matter was investigated by the writer. The flexibility matrix of the single-cable bridge was calculated for the D.L. condition assuming a number of equidistant stations of 9, 8, 7, ..., 3, 2 to get a matrix of the order 9, 8, 7, ..., 3, 2 respectively. Each time corrections due to cable extensibility and tower movements were included. The matrix was singular when its order was 9, 8, 7, 6, but it could be inverted properly when the number of stations was reduced down to five or less, (until two). This means that our single-cable bridge model cannot have more than five modes of vibration.* The same result was obtained when the deck was removed, (i.e. considering the cable only). This is, again, due to the singularity of flexibility matrices with higher order.

Thus it can be seen that the flexibility matrix for a single-cable bridge (or for the cable only) is not certainly singular if the cable extensibility is considered, and that the number of possible vibration modes may be less than or equal to the matrix order (which is equal to the number of stations). But if the cable is inextensible, the flexibility matrix is certainly singular (if its order is equal to the number of stations), and in this case, the number of possible modes will be certainly less than the number of stations to which the span is divided.

A4.4 Examples

Fig. A4.1 shows the two-stations' inextensible wire system (0-1-2-3). According to all the previous work of Pugsley, Charlton, and others, (Refs. 1.15, 1.17, 1.18), and according to the writer's work presented herein (Chapters III, IV, VI)**, the system has two degrees of freedom if only vertical deflections are considered. But, actually, it is a single-degree of freedom system. The system's shape can be identified at any time and for any loading condition if only one component of the joint deflections becomes known (or calculated), either analytically (from the geometry of the system) or graphically (using the three circular arcs C_3, C_0, C_2' (the suffix refers to the centre of the arc)).

Thus it has only one degree of freedom and its flexibility matrix is 1 x 1, and accordingly it has only one mode of vibration with only one

---

* The number of possible modes is equal to the order of the largest possible non-singular flexibility matrix.

** In his study in these chapters, the writer took the cable extensibility into account.

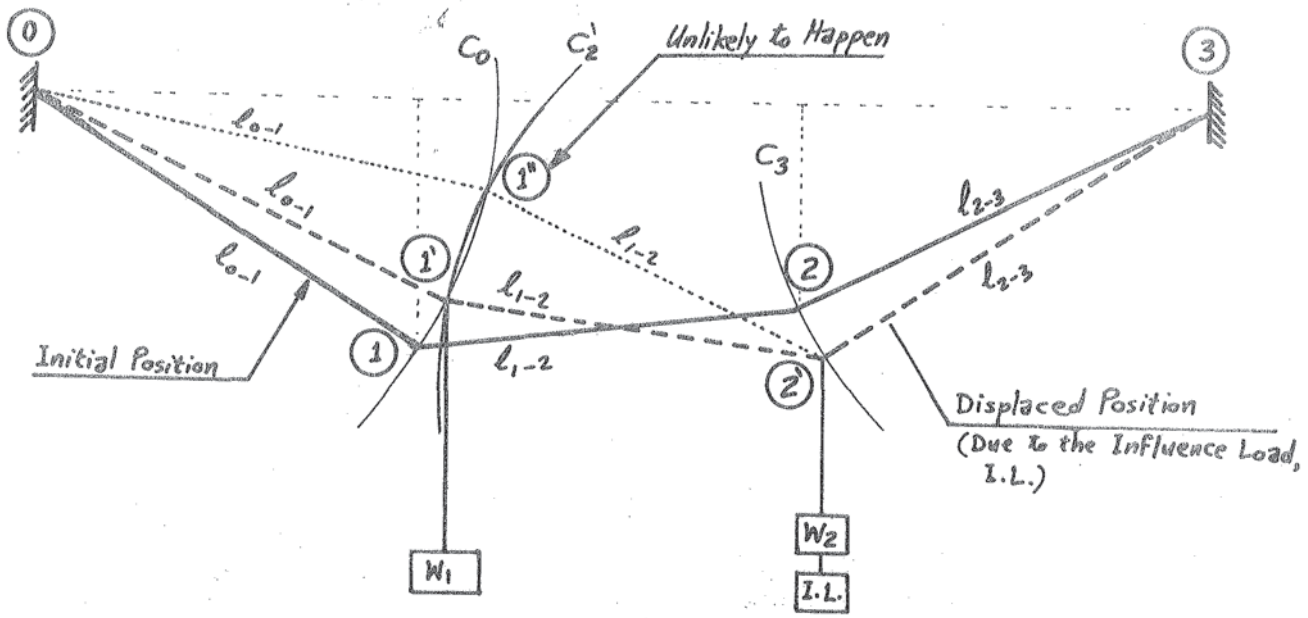

Fig. A4.1.

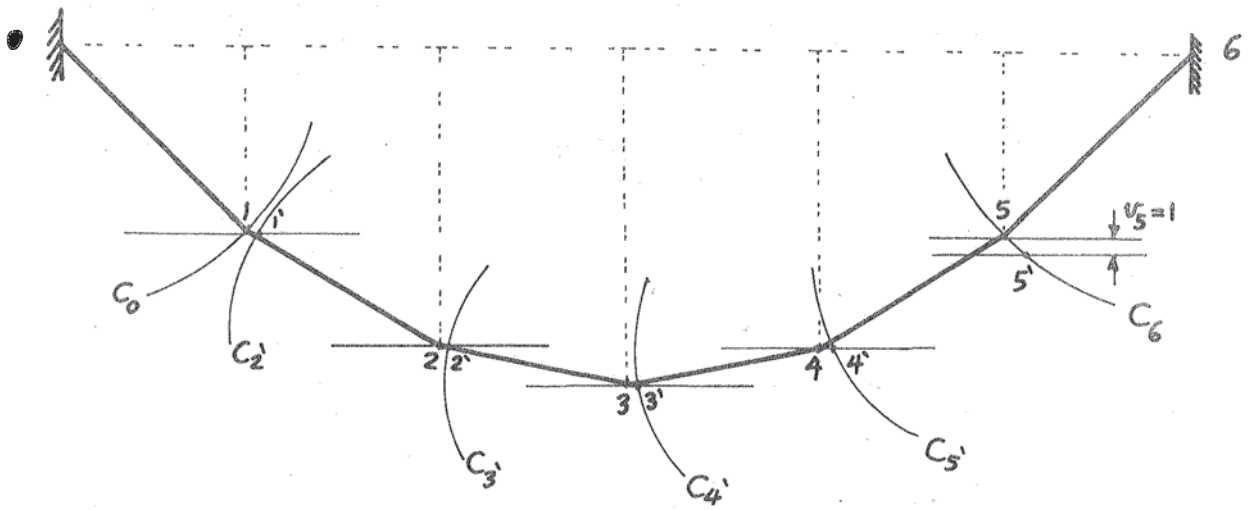

Fig. A4.2.

natural frequency. Once the displacement of (say) joint (2) is given, the mode shape becomes completely defined. If the flexibility matrix is written as 2 x 2 it must be reduced to 1 x 1 by writing the deflection of (say) joint (1) in terms of the deflection of joint (2). This means that the matrix 2 x 2 represents two equations in only one unknown, and two equations in one unknown means, simply, a rectangular matrix which is necessarily singular according to the corollary of Section A4.2.

Thus, a 2 x 2 flexibility matrix for the inextensible system of Fig. A4.1 is singular and has no inverse, i.e. there is no 2 x 2 stiffness matrix for that system. This is clear from investigating the displaced position of the system due to an influence load, I.L. A unit (vertical) deflection at joint (2) will certainly be accompanied by some (vertical) deflection at joint (1), whatever the loads acting at joints (1) and (2) are. It can never happen that the deflection of either of the joints has some value while the other joint is held in place or restrained against vertical deflections.

We can get a 1 x 1 stiffness matrix by inverting the 1 x 1 flexibility matrix or by evaluating (if possible) the (vertical) load required at (say) joint (2) to produce a unit deflection at the same joint and in the same direction, regardless of what deflections will happen at the other joint, (1).

* * * *

Similarly, the 9 x 9 flexibility matrix of Pugsley and Charlton (Refs. 1.3, 1.15, 1.17, 1.18) for the nine stations' inextensible cable is merely singular since it represents only eight independent variables, while the ninth one may be evaluated as a function of these independent eight. This means that the flexibility matrix must be only 8 x 8 and then it can be inverted to give an 8 x 8 stiffness matrix.

This can be demonstrated using, as a simplificiation, Fig. A4.2 which represents a five-stations' inextensible cable. If the number of the degrees of freedom or the order of the flexibility matrix is equal to the number of stations, the flexibility matrix would be 5 x 5. But it is clear that the deflections of four joints only are quite sufficient to obtain the deflected shape for any loading condition, while the deflection of the fifth joint is obtainable by the intersections of two circular arcs whose centres are the far ends of the two segments intersecting at that joint.

Thus we have only four unknowns, and if we write for them five equations, the 5 x 5 matrix becomes singular. The correct solution is therefore obtained using a 4 x 4 flexibility matrix, whose inverse will also be a 4 x 4 stiffness matrix.

The 5 x 5 stiffness matrix cannot exist at all because, starting from the right (for example), a unit vertical deflection can be applied at joint (5) while joints 4, 3, 2 can be prevented from vertical displacements, but joint (1) will have some vertical deflection if the arcs C_0 and C_2' intersect somewhere. If the two arcs do not intersect, this means, physically, that a unit vertical deflection at (5) is too much for the cable to undergo, and, if it happens, the cable will break somewhere to allow for that gap between the two arcs C_0 and C_2'. The mathematical meaning of this phenomenon is that the 5 x 5 stiffness matrix will never exist.

If the two arcs C_0 and C_2' intersect somewhere, this means that joint (1) will undergo some vertical deflection, and that we can get a 4 x 4 stiffness matrix regardless what deflections will happen at the fifth joint (joint (1) in this case). If the two arcs C_0 and C_2' do not intersect, the result will either be a singular structure or a singular 4 x 4 flexibility matrix (i.e. the 4 x 4 stiffness matrix is also not existent.

A4.4.1 Numerical Examples

Consider the symmetric flexibility matrix

$$[A] = \begin{bmatrix} 2.5 & -3 \\ -3 & 3.6 \end{bmatrix}$$

which is singular.

This matrix may be obtained for a system with two degrees of freedom, or for a suspension structure with two joints (or two stations). The system will have two eigenvalues (one of which is zero), and two eigenvectors. The solution is

$$\lambda_1 = 0, \quad \begin{bmatrix} X_1 \\ X_2 \end{bmatrix}_1 = \begin{bmatrix} 1.2 \\ 1.0 \end{bmatrix} ; \text{ and}$$

$$\lambda_2 = 6.1, \quad \begin{bmatrix} X_1 \\ X_2 \end{bmatrix}_2 = \begin{bmatrix} -1.0 \\ 1.2 \end{bmatrix} .$$

As is usual when the flexibility matrix is used in the dynamic analysis, if the eigenvalue λ is a function of $(1/\omega^2)$, then f_1 will be infinity, where f_1 is the frequency corresponding to λ_1. This frequency is to be cancelled, and the other one only is considered reasonable.

If, due to non-linearity, the matrix is slightly asymmetric, e.g.

$$[A_1] = \begin{bmatrix} 2.5 & -2.9 \\ -3.1 & 3.6 \end{bmatrix}$$

which is not exactly singular, but not very far from singularity, (determinant = 0.01), in this case the solution becomes

$$\lambda_1 = 0.0016, \quad \begin{bmatrix} X_1 \\ X_2 \end{bmatrix}_1 = \begin{bmatrix} 1.16 \\ 1.0 \end{bmatrix} \quad ; \text{ and}$$

$$\lambda_2 = 6.0984, \quad \begin{bmatrix} X_1 \\ X_2 \end{bmatrix}_2 = \begin{bmatrix} -1.0 \\ 1.24 \end{bmatrix}$$

which is not very far from the first solution when the matrix was symmetric and singular. In this case, the matrix $[A_1]$ could be inverted to give

$$[A_1]^{-1} = \begin{bmatrix} 360 & 290 \\ 310 & 250 \end{bmatrix}$$

which seems to be silly, and not reliable.

This means that an averaging procedure (to make a matrix symmetric), or any other approximation, may slightly alter the mathematical properties of the matrix, such that it seems to become non-singular while, really, it is singular.

In this example, the first frequency is not infinity, but it is so large that it cannot be trusted (here it is about 61 times the second frequency). The mode shapes are not affected much by these approximations.

The idea may become more clear by considering the 3 x 3 symmetric

flexibility matrix

$$[A] = \begin{bmatrix} 2 & -0.5 & 0 \\ -0.5 & 2.5 & -3 \\ 0 & -3 & 3.79 \end{bmatrix}$$

which is also singular.

The solution gives, as expected, three eigenvalues and three eigenvectors. One of the eigenvalues is zero (with infinite frequency) and is rejected, while the other two are "reasonable" and give reasonable frequencies. The solution is

$$\lambda_1 = 0, \quad \begin{bmatrix} X_1 \\ X_2 \\ X_3 \end{bmatrix}_1 = \begin{bmatrix} 1.0 \\ 4.0 \\ 3.17 \end{bmatrix}$$; and this mode is rejected since its frequency is infinity;

$$\lambda_2 = 6.24, \quad \begin{bmatrix} X_1 \\ X_2 \\ X_3 \end{bmatrix}_2 = \begin{bmatrix} 1.00 \\ -8.48 \\ 10.38 \end{bmatrix}$$; and

$$\lambda_3 = 2.05, \quad \begin{bmatrix} X_1 \\ X_2 \\ X_3 \end{bmatrix}_3 = \begin{bmatrix} 1.00 \\ -0.10 \\ -0.17 \end{bmatrix}$$.

In general, if the (n x n) flexibility matrix is singular, it will have, at least, one zero eigenvalue (which is to be rejected due to infinite frequency), and not more than (n - 1) "reasonable" eigenvalues and eigenvectors will be obtained. In some cases, due to several approximations, or due to the accumulation of the round-off errors, the determinant of the flexibility matrix may be very small instead of zero. In this case, one of the eigenvalues will also be very small (giving very high frequency) which can, here also, be rejected.

This means that the variables are not independent of each other, but some of them can be obtained in terms of the others. If the correct number of variables is used, the resulting matrix will become non-singular and all the eigenvalues (and eigenvectors) will be acceptable.

A4.5 CONCLUSIONS

The general conclusion out of the foregoing discussion is that for a nine stations' inextensible cable, the flexibility matrix must not be larger than 8 x 8. In other words, the stiffness matrix also (if it exists) will not be larger than 8 x 8.

The question now is: Are the 9 x 9 flexibility matrices given by Pugsley and Charlton (Refs. 1.3, 1.15, 1.17, 1.18) singular or not?

Charlton answered this question by inverting his 9 x 9 flexibility matrix to get a 9 x 9 stiffness matrix, and he used the latter in an approximate analysis (using stationary potential energy) and got reasonable results out of that.

This needs some justification. Perhaps the reason is the long list of approximations set out by Pugsley and Charlton. Pugsley linearised the problem by using the tangent coefficients, and he used an approximate method in evaluating the increase, due to L.L., in the horizontal pull in the cable, h. This is in addition to some other approximations used by him to simplify the analysis. The same approximations were made by Charlton except that he used the secant flexibility coefficients instead of the tangent flexibility coefficients. Furthermore, he made the matrix symmetric by averaging its off-diagonal elements. He then went further and used the Fourier series approximation in his energy analysis.

Finally, the writer wants to point out that the use of extensible cables (or, in other words, taking the cable extensibility into consideration) makes the problem different. The movement of each joint will not be restricted by a circular arc. But it will be possible (theoretically and experimentally) to locate all the joints in position * by aid of the influence vertical loads (and some horizontal loads), provided these loads are within the safe carrying capacity of the system.

In other words, the writer, by considering the cable extensibility, did not fall in error by taking the order of the flexibility matrix of each structure, equal to the number of its joints. (Note that the vertical deflections only are dealt with).

However, the flexibility matrices of the single-cable bridge and the suspension nets proved to be singular. Also, the flexibility matrix of the two-cable bridge gave some complex eigenvalues and eigenvectors. But all the matrices could be measured, and they actually were measured. This shows that the three structures, themselves, are not in any sense singular, and that the singularity, perhaps, arises from the methods of solution, somehow.

---

* One joint will have a unit vertical deflection (and perhaps some horizontal displacement) while all the other joints will have no vertical deflection (but they may have some horizontal deflections). This is for each column of the stiffness matrix.

ABSTRACT

A historical review of the construction and erection of suspension bridges, and of the literature on them, is presented. Suspension bridges are often analysed as plane structures, as if a bridge has only one cable supporting a narrow deck with no torsional stiffness and no torsional stresses. The statics and dynamics of a laboratory model of such a single-cable bridge are investigated both experimentally and analytically, followed by a short chapter on the dynamics of suspension cables and nets.

A real suspension bridge has usually two or more cables supporting a deck with some width and some torsional stiffness, and undergoes torsion. A laboratory model for a two-cable bridge was designed and built. A method for the static analysis of such a two-cable bridge is derived and used for both the static and dynamic analyses of the model. Measurements of the static deflections and natural frequencies and modes of vibration of the model showed good agreement with calculations.

A chapter comprising some notes on the aerodynamic instability of suspension bridges is also included.